The University of Nottingham

UNITED KINGDOM · CHINA · MALAYSIA

ROLE OF INTERFERON REGULATORY FACTOR 5 (IRF5) IN THE REGULATION OF T HELPER CYTOKINES

Ashwinder Kaur

A thesis submitted to the University of Nottingham for the degree of

Doctor of Philosophy

October 2020

This thesis is dedicated to my family for their love and support

Abstract

Interferon regulatory factor 5 (IRF5) has a diverse role in the induction of pro-inflammatory cytokines and chemokines downstream to various signalling pathways contributing to the pathogenesis of various autoimmune and inflammatory diseases. Using *Irf5* knockout mice under different experimental settings, studies have reported that IRF5 plays a crucial role in T helper (Th) polarization. Previous studies have shown that IRF5 has a potential role in regulating Th2 cytokine production, particularly Interleukin-13 (IL-13). Sequence analysis human *Il13* promoter showed the presence of the IFN sensitive response element (ISRE) motif, the region that IRFs can recognize through their helix turn helix nucleotide domain. As a transcription factor, IRF5 has been shown to recognize and bound to this region to regulate the expression of its targeted genes. Based on these findings, we were intrigued to examine the transcriptional role of IRF5 in regulating the expression of human IL-13 and assess the modulation of IRF5 in regulating the expression of Th1 and Th2 associated cytokines.

Two of the predominant transcriptionally active IRF5 isoforms, IRF5 variant 4 (IRF5v4) and variant 5 (IRF5v5) were used in this study. To evaluate the binding of the IRF5 to *Il13/ISRE* region, DNA pulldown assay was performed using protein lysates extracted from HEK 293T cells transfected with either IRF5v4 or IRF5v5 in the presence or absence of the Toll-like receptor (TLR) adaptor protein, Myeloid

differentiation primary response 88 (MyD88) expression. The ectopic MyD88 was included to mediate activation of IRF5 spliced isoforms. The transactivation of *Il13* promoter activities by IRF5 spliced isoforms were examined through dual luciferase reporter assay. To do so, HEK 293T cells were transiently transfected with varying concentrations and combinations of IRF5v4 or IRF5v5 in the presence or absence of MyD88. The human *IL13* promoter driven by firefly luciferase reporter vector and Renilla luciferase control vector were included for dual luciferase reporter activities. To evaluate the modulation of IRF5 spliced isoforms in regulating Th1 and Th2 cytokines, stably expressing IRF5 isoforms were generated in Jurkat cells, a human T cell line. Cells were stimulated with a combination of Phorbol-12-myristate 13-acetate (PMA) and Ionomycin for evaluating cytokines expression by reverse transcription polymerase chain reaction (RT-PCR) and secretion by enzyme-linked immunosorbent assay (ELISA).

Based on the DNA pulldown assay, our findings showed that both activated IRF5 spliced isoforms can bind to the oligonucleotide corresponding to *Il13/ISRE*. In luciferase reporter assay, our results showed that both IRF5v4 and IRF5v5 can transactivate *Il13* promoter activation, however, their activities were suppressed when higher MyD88 concentrations were tested. By using semi-quantitative RT-PCR, we demonstrated that stable expression of IRF5v4 and IRF5v5 in Jurkat cells modulated Th1 and Th2 associated cytokines in response to co-stimulation of PMA and Ionomycin. Upon stimulation, overexpressed IRF5v5 showed upregulation of IFNγ

and downregulation of IL-4 and IL-13 gene expression. On the other hand, IRF5v4 showed induction of IL-13 but inhibition of IL-4 gene expression. In protein level, IRF5v4 had a diminished level of IFNγ secretion. Interestingly, both IRF5v4 and IRF5v5 were shown to augment IL-2 expression in gene and protein levels. Moreover, IRF5v4 and IRF5v5 were able to secrete moderate amounts of IL-10 in comparison to control cells. In conclusion, our findings provided useful insight into IRF5 spliced isoforms' involvement in inducing human *Il13* promoter activity as well as the differential regulation of the expression of Th1 and Th2 cytokines in the human T cell line.

List of Figures

List of tables

List of abbreviations and symbols

ADAP	Adhesion and degranulation promoting adaptor protein
AICD	Activated induced cell death
APCs	Antigen presenting cells
AP-1	Activator protein-1
BCL6	B cell lymphoma protein 6
BP	Base pair
BSA	Bovine serum albumin
CBP	CREB binding protein
CD	Cluster of differentiation
CMV	Cytomegalovirus
CSN	COP9 signalosome
CXCL	Chemokine ligand
DAG	Diacylglycerol
DAMPs	Danger associated molecular patterns
DBD	DNA binding domain
DCs	Dendritic cells
DMSO	Dimethyl sulfoxide
DN	Double-negative
DNA	Deoxyribonucleic acid
DNAse	Deoxyribonuclease
DNTP	Deoxy nucleotide triphosphates
ECL	Enhanced chemiluminescence
ETPs	Early thymic progenitors
EDTA	Ethylenediaminetetraacetic acid
ELISA	Enzyme- linked immunosorbent assay
Ex	Exon
FasL	Fas ligand

GATA3	GATA binding 3 protein
Gads	Grb2-related adaptor downstream of Shc
GEF	Guanine triphosphate (GTP) exchange factor
GFP	Green fluorescence protein
GM-SCF	Granulocyte macrophage colony stimulating factor
Grb2	Growth-factor receptor-bound protein-2
GTP	Guanine triphosphate
HLA	Human leukocyte antigen
Hlx	Homeobox transcription factor
HDAC	Histone deacetylase
HEK	Human embryonic kidney
HIV	Human immunodeficiency virus
HRP	Horseradish peroxide
HSV	Herpes simplex virus
HTLV	Human T cell leukaemia virus
IAD	IRF associated domain
IBD	Inflammatory bowel disorder
IFN	Interferon
IFNγ	Interferon gamma
IKKβ	IκB kinase beta
IL	Interleukin
IP$_3$	Inositol triphosphate
IRF	Interferon regulatory factor
IRAK1	Interleukin-1 receptor-associated kinase 1
ISRE	IRF sensitive response element
ITAMs	Immune-receptor tyrosine-based motifs
ITK	IL-2 induced tyrosine kinase
KAP	KRAB associated protein
LAT	Linker for activation of T cells

L.donovani	*Leishmania donovani*
MAPK	Mitogen-activated protein kinase
MHC	Major histocompatibility complex
mRNA	messenger RNA
MS	Multiple Sclerosis
MyDD	Myeloid differentiation primary response
NDV	Newcastle disease virus
NES	Nuclear export signal
NF-κB	Nuclear factor kappa B
NFAT	Nuclear factor activated T cells
NK	Natural killer
NLS	Nuclear localisation signal
NOD	Nucleotide oligodimerisation
PAMPs	Pathogen associated molecular patterns
PCR	Polymerase chain reaction
PGK	Phosphoglycerate kinase
PIP2	Phosphatidylinositol biphosphate
PKC	Protein kinase C
PLCγ1	Phospholipase Cγ1
PMA	Phorbol 12-myristate13-acetate
PRRs	Pattern-recognition receptors
PVDF	Polyvinylidene fluoride
RA	Rheumatoid Arthritis
RIG	Retinoic acid-inducible gene
RIPA	Radioimmunoprecipitation assay
RUNX3	Run related transcription factor 3
RNA	Ribonucleic acid
RNAse	Ribonuclease
RSV	Rovs sarcoma virus

RT	Reverse transcription
SSc	Systemic sclerosis
SDS	Sodium Lauryl sulphate powder
SLE	Systemic Lupus Erythematosus
SNP	Single nucleotide polymorphism
STAT	Signal transduction and activator of transcription factor
SV	Simian Vacuolating virus
Taq DNA polymerase	Thermus aquaticus DNA polymerase
TAK1	Transforming growth factor-beta activated kinase 1
TBK1	TANK-binding kinase 1
T-bet	T box expressed in T cells
TCR	T cell receptor
Tfh	Follicular T helper
TH	T helper
TMB	Tetramethylbenzidine
TLR	Toll like receptor
TNF	Tumour necrosis factor
TRIM	Tripartite motif
TSPs	Thymic seeding progenitors
v	Variant
WT	Wildtype
YFP	Yellow fluorescence protein
ZAP	Zeta-chain associated protein kinase

Acknowledgement

Firstly, I am grateful to Almighty God for blessing me with the strength and determination throughout my journey of Ph.D.

I would like to express my gratitude to my supervisor, Dr. Fang Chee Mun for providing me the opportunity to pursue a Ph.D. at the University of Nottingham with fully funded scholarship. I am very thankful for his continuous support, guidance, and patience throughout my research and thesis writing. I am indeed fortunate to have such a kind-hearted supervisor. Also, I would want to express my sincere appreciation to my co-supervisors at the University of Monash; Professor Dr. Chow Sek Chuen for his insightful conversations that have helped me enhanced my knowledge in cell biology and allowing me to work in his laboratory and Dr. Lee Learn Han for his kind assistance with handling the purchases and formalities associated with the research funding grant. I would also like to take this opportunity to express my gratitude to my undergraduate lecturer, Dr. Yam Wai Keat for her encouragement and inspiration for pursuing my doctoral studies.

I am extremely thankful and indebted to Dr. Le Cheng Foh for his technical assistance and for sharing his expertise whenever I am in difficulty. Special thanks to Poh Boon Min (Trista) for helping me enhance my skills in molecular cloning during the early phase of my studies. I would also like to thank my lab colleagues Koh May Zie, Loh Fei Kean, Shahadat Hossan, Tham Shiau Ying, Chan Won Ting for helping

Table of Content

Chapter 1

1 Introduction

1.1 Overview

An effective host defense system depends on prompt recognition and response against invaders. Thus, the immune systems produce various cells and molecules that communicate with each other via signaling pathways that are coordinated by gene regulatory networks. This gene regulatory network is controlled by transcription factors, chromatin modifiers, miRNA, and long noncoding RNAs (lncRNAs) that activate or repress their target genes in determining cell fate or effector state [1]. One of the transcription factors that have been extensively studied for their crucial role in regulating gene networks in the immune system is the Interferon Regulatory Factors (IRFs). The IRFs play crucial roles in the regulation of immune responses and oncogenesis [2]. In addition, the IRFs family possesses a turn-helix-turn motif that recognizes and binds to DNA consensus, known as the IFN sensitive response element (ISRE) which can be found in the promoters of many genes that are involved in immune responses [3].

The immune responses and pathogenesis of certain diseases are known to correlate with the balance of T helper (Th) 1 and Th2 responses [4,5]. For instance, an imbalance of Th1/Th2 responses, with Th1 bias is linked to autoimmune diseases such as Systemic Lupus Erythematosus (SLE) and Rheumatoid Arthritis (RA). On the

other hand, Th2-dominated responses are associated with allergic diseases such as asthma. Interestingly, many IRFs have been found to be involved in Th differentiation. For instance, IRF1, IRF2, and IRF8 are mainly involved in Th1 differentiation [6,7]. Meanwhile, IRF4 that shares several similar biological activities with IRF5 is proven critical for Th2 cell development [6,7]. Both IRF4 and IRF5 is involved in MyD88-dependent- TLR signaling and they were found to interact with each other in the induction of proinflammatory cytokines and type I interferons [8]. Furthermore, both transcription factors were shown to directly regulate B lymphocyte-induced maturation protein-1 (Blimp1), the master regulator of plasma cells' differentiation [9,10].

Accumulating data from several labs have shown that IRF5 is a critical mediator in the development of Th1 responses associated with the pathogenesis of various diseases including autoimmune, metabolic, and infectious diseases [11–13]. Conversely, studies have also demonstrated that IRF5 play role in inducing Th2 responses [14,15]. Strikingly, most studies have attributed IRF5 in regulating Th1/Th2 responses by altering the functions of antigen presenting cells (APCs) (e.g., macrophages and dendritic cells) rather than IRF5 intrinsic properties in T cells. This was because early studies reported that expression of IRF5 is barely detected in T cell [16]. Nonetheless, recent studies have detected elevated IRF5 expression in parasitic and virally infected T cells [17,18]. Moreover, its involvement in inducing apoptosis in CD4^{+} T cells during chronic parasitic infection has been recently been highlighted

[19]. However, to date, the role of T cell-intrinsic dependent on IRF5 in modulating the expression of Th cytokine remains uncertain.

Previously a study has demonstrated that IRF5 was important for controlling the severity of airway allergic inflammation mediated by IL-13 [20]. The cytokine, IL-13 is primarily made by the Th2 subset of CD4 T cells but many other cells like basophils, mast cells, epithelial cells, and nuocytes also produce IL-13 [21]. Besides the role in antibody production, TLR-mediated activation of B cells can also produce cytokines [22]. In relation to this, preliminary data from our group found that B cells of *Irf5*^{-/-} mice showed impairment in TLR-mediated induction of IL-13 as compared to normal B cells (data not shown). Thus, suggesting a potential role of IRF5 in regulating IL-13 production. As a pleiotropic cytokine, IL-13 plays critical roles in mediating allergic, inflammatory, and autoimmune diseases [23]. Interestingly, TLR7 activation which could activate IRF5 has been linked to enhancing allergic sensitization with an increase in the numbers of the airway and tissue eosinophils, mucus-producing cells, and antigen-specific production of IL-13 [24,25]. Sequence analysis of human *Il13* promoter showed the presence of the ISRE motif that is recognised by IRFs for binding. The ISRE motif located in the 5' upstream region (-450 to-430 nucleotides) from the transcription start site. Based on these findings, we were intrigued to examine the role of human IRF5 in regulating IL-13 cytokine expression and other Th1 and Th2 associated cytokines.

In humans, the *Irf5* gene exists as multiple spliced variants that give rise to at least nine isoforms [11,13,16]. Out of these nine isoforms, four are known as the functional isoforms (variant (v)-1, v3, v4, v5, and v6), the rest are either transcriptionally inactive or lack certain functional elements, resulting in mutant IRF5 [16,26,27]. We utilised the predominant functional IRF5 spliced isoforms; IRF5v4 and IRF5v5 in this study [28,29]. The IRF5v4 is among the first to be cloned variant and it exhibit similar characteristics to another spliced variant, IRF5v3 in terms of identical deletion pattern in exon6 encodes identical polypeptide sequences as well as their functions [16,30]. In addition, IRF5v4 is widely characterised in early studies in defining IRF5 roles in regulating type 1 interferons in response to viral infection [31,32]. Meanwhile, IRF5v5 contains full genomic sequences with no deletion within its exon 6. Of note, the amino acid sequences of human IRF5v5 and murine IRF5 are highly homologous (87% similarity), and the most obvious difference between human IRF5 and murine IRF5 is the deletion of five amino acids within murine IRF5 protein [33]. Unlike human IRF5 that exists as multiple isoforms due to alternate splicing, murine IRF5 is predominantly expressed in full length and only a single splice variant has been detected at a very low level in the bone marrow [33]. In this regard, there is a high probability of both human IRF5v5 and murine IRF5 to share similar activities. Besides that, both IRF5v4 and IRF5v5 were found to be involved in ubiquitination, a post-translational process that is critical for the nuclear translocation and target gene regulation of IRF5 [34]. Given that, IRF5 has been reported to display differential functions depending on its isoforms, we were intrigued whether these IRF5 spliced variants could possibly function differently in our experiments [16].

4

In the initial phase of the project, we investigated whether human IRF5 could bind to the ISRE motifs on the human *Il13* promoter and transactivate its expression. Subsequently, we assessed the role of IRF5 in regulating IL-13 expression as well as other cytokines associated with Th1 (IFNγ, IL-2) and Th2 (IL-4, IL-5, IL-10) in Jurkat cells upon PMA and Ionomycin stimulation. Results obtained from these investigations will shed some light on understanding the contribution of IRF5 in regulating Th responses, in a T cell-intrinsic manner.

1.1.1 Aims of project

The aims of this project described in this thesis are:

1. To investigate the transcriptional role of IRF5 in regulating expression of IL-13

2. To investigate the role of IRF5 in regulating expression of Th1 and Th2 associated cytokines

1.1.2 Objectives of project

The specific objectives of this project described in this thesis are:

1. To examine whether IRF5v4 and IRF5v5 can bind to functional elements (ISRE) located within human *Il13* promoter through DNA pull-down assay

2. To examine the direct effect of IRF5v4 and IRF5v5 regulation in transcriptional the activity of the human *Il13* promoter using a reporter assay

3. To generate stably expressing IRF5v4 and IRF5v5 in Jurkat cells by lentiviral transduction

4. To measure mRNA levels of Th1 (IFNγ, IL-2) and Th2 (IL-4, IL-5, IL-10, and IL-13) cytokines in stably expressing IRF5v4 and IRF5v5 in Jurkat cells upon PMA and Ionomycin stimulation by semi-quantitative RT-PCR

5. To measure cytokines secretion of Th1 (IFNγ, IL-2) and Th2 (IL-4, IL-5, IL-10, and IL-13) in stably expressing IRF5v4 and IRF5v5 in Jurkat cells upon PMA and Ionomycin stimulation by ELISA

1.2 Literature review

1.2.1 Overview of gene expression

Most living organisms have their genetic materials carrying the blueprint of life in the form of deoxyribonucleic acid (DNA) contained within a genome. The genome comprises a subset of coding DNA sequences, also known as genes that specify RNA or protein, and the vast majority of non-coding DNA sequences that play crucial regulatory roles in gene expression [35]. Gene expression is a series of molecular events of processing genetic information. In the central dogma of molecular biology, the flow of information regards as DNA transcribed to RNA (copy), and then RNA is translated (read) to protein [36,37]. However, there is an exception to some viruses which store their genetic material in RNA and convert their RNA to DNA via reverse transcription. Of note, not all genes encode proteins as the end product. Some genes also encode for non-coding RNA, such as small nucleolar RNAs (snoRNAs, including ribosomal RNA and transfer RNA), micro-RNA (miRNA), small interfering RNAs (siRNAs), and long- non-coding RNA (lncRNA) that play a diverse role in cellular processes [37,38].

In multicellular organisms, what makes a cell unique from each other is what and when a set of genes are expressed differentially ("turn on" or "turn off"), which determines the specific production of proteins and RNA, dictating the morphology and the function of the cell. Interestingly, the number of genes alone does not reflect the complexity of organisms, for the reason that humans share a similar number of genes with other organisms [39,40]. Instead, the number and size of non-coding DNA

sequences correlate with the complexity of organisms, and variation in these non-coding sequences contributes to diverse phenotypes between individuals and species [41]. In this regard, only about 2% of the human genome comprises genes, while the rest consists of non-coding DNA sequences that are responsible for different regulatory processes [39,40]. Gene expression drives biological processes; thus, the control of this mechanism is ascertained to ensure proper cellular functions. Regulation of gene expression is highly sophisticated as it involves many elements such as protein, RNA, and their complexes interacting with gene and the regulatory DNA sequences in a complex network [42]. The requisite control is established through every stage of gene expression from transcription to RNA processing and in the case of protein-coding genes; it involves the regulation of translation and post-translation. Herein, the processes of gene expression and their regulation are summarised as follows.

1.2.1.1 Transcription and post-transcription

Transcription is the process of synthesising RNA transcript from a DNA template, catalysed by enzyme RNA polymerase (RNA Pol). Prokaryotes utilise a single type of RNA Pol. In contrast, eukaryotes have three prominent RNA Pol, namely RNA Pol I, Pol II, and Pol III, that mediate the synthesis of ribosomal RNA (rRNA), messenger RNA (mRNA), and small RNAs including transfer RNA (tRNA) respectively [43,44]. Transcription is activated when DNA binding proteins, typically known as transcription factors in eukaryotes and the sigma factors in bacteria, recognise and bind to DNA sequences on the promoter [45,46]. Promoter comprises of regulatory

DNA sequences extending upstream and downstream of the transcription start site. In eukaryotes, the regulatory DNA sequences of a gene consist of multiple binding sites that are characterised based on their location and function (core and proximal promoter, distal regulatory sequences; enhancers, insulators, silencer) [35,45,47]. Transcription factors bind to these regulatory regions to modulate transcriptional activity. Moreover, binding of transcription factors in cooperation of cofactors to distal regulatory elements mediates DNA looping the formation, bringing the distal region to the closer proximity of the promoter for interactions during transcription [38,47–49]. Therefore, in a given time and space, multiple interactions of transcription factors and cofactors with the DNA regulatory elements in response to surrounding signals can give rise to several patterns of gene expression.

Unlike in prokaryotes, where the transcription factor can readily bind to the promoter region, this process is much sophisticated in eukaryotes due to the organisation of the genome. In most prokaryotes, DNA contained within a single chromosome in the nucleoid, and some of the prokaryotes, such as bacteria, carry an extra circular DNA known as a plasmid, distinct from the chromosomal DNA [45]. Conversely, in eukaryotes, most DNA is coiled and packaged into linear chromosomes placed within the nucleus. Moreover, the eukaryotes genome is condensed into chromatin, composed of nucleosomes that wrap DNA around histone proteins [42,45]. The packaging of chromatin can influence the accessibility of DNA sequences for transcription factors and other molecules to bind to the regulatory elements and regulate transcription [42,46,50]. For instance, tightly packed chromatin

arrangements render the accessibility of DNA sequences for transcription and accommodate repress genes (heterochromatin) while loosely packed chromatin is readily accessible and transcriptional active (euchromatin) [35]. In this regard, many factors such as chromatin-modifying and remodelling enzymes, epigenetic modifications, transcriptional proteins, and non-coding RNAs can alter the chromatin structure leading to activation or repression of gene transcription [37,42,46,50–52]. Also, DNA can be folded in the three-dimensional structure bringing active genes together to the centre of the nucleus as well as regulatory sequences into a closer proximity for interaction to modulate gene activity, thus portraying the complex gene-regulatory mechanism in eukaryotes [52].

In the context of protein-coding genes in eukaryotes, transcription factors (known as general transcription factors) bind to enhancer region and recruit RNA Polymerase II, along with other proteins (mediators) to the core promoter region, forming a complex to initiate transcription [53,54]. Here, the use of different promoters (alternative promoter) on the gene can result in different messenger RNA (mRNA) transcripts thereby; implying one gene can produce more than one transcript allowing distinct pattern gene expression [41]. Once RNA Pol II has successfully constructed a stable transcript, the transcription factors and mediator assist the enzymes in escaping from the promoter to proceed with the elongation phase, where the pre-mRNA strand is synthesised and terminated upon receiving the appropriate signal [53–55]. Following transcription, the pre-mRNA strand is subject to several post-transcriptional modifications such as capping of the 5' and polyadenylation of 3'

end as well as splicing of the mRNA before transporting to the cytoplasm for protein synthesis [51]. The 5'capping of the mRNA mediates initiation of the translation process, whereas the polyadenylation of 3' (poly (A) tail) provides stability and facilitates the nuclear export of mRNA. RNA splicing involves the removal of introns (non-protein coding sequences) from the pre-mRNA strand and splicing of exons (protein-coding sequences) to generate a mature transcript [56]. The splicing can be done more than one way in a process called alternative splicing to create multiple transcripts coding more than one polypeptide (isoform) [56].

1.2.1.2 Translation and post-translation

The translation is a process of interpreting protein-coding region in mRNA transcript for the generation of amino acids in proteins. This process initiated when mRNA bind to ribosome, followed by specific recognition of the codons (specify amino acids) by tRNA that is mediated by enzyme aminoacyl-tRNA synthetases for polypeptide synthesis [43,57]. Control of protein synthesis can be achieved by modulating the initiation factors, initiation rate, lifetime, and stability of mRNA, by numerous factors such as the regulatory sequences of the mRNA (5' and 3' untranslated region), RNA binding proteins, and non-coding RNAs such as miRNA and siRNA [41,51,57,58]. In the context of post-translational regulation, the polypeptide chains undergo several modifications such as covalent or enzymatic addition of functional groups to the amino acids, for instance, phosphorylation, glycosylation, acetylation [59,60]. These post-translational modifications are essential for protein folding, stability,

conformation, subcellular compartments, signal transduction, and, also, regulate biochemical processes such as enzymatic activity [59,60].

1.2.1.3 Importance of gene regulation

Genes exemplify switches that can be turned on and off in response to numerous factors, thus denoting when and what level of RNA transcripts and proteins generated. Gene expression is fundamental of biological processes that govern the structure and function of cells in an organism. Hence, gene expression is tightly controlled to ensure balanced homeostasis and survival of an organism. A slight change in gene expression can lead to drastic changes in the functions of cells. Indeed, misregulation of gene expression is associated with detrimental consequences resulting in diseases [38]. In this regard, the immune system which is the host defence mechanism is controlled by transcription factors and other elements that activate or repress their target genes in determining cell fate or effector state to ensure effective immune responses [1].

1.2.2 The human immune system

The immune system consists of a dynamic network of cells, proteins, tissues, and organs that communicate with each other to provide effective defence responses. Immune responses involve recognition of any "non-self" substances including pathogens, foreign or modified particles that present in the host body, resulting in activation of cascade complex events are known as the inflammatory process to get rid of the non-self-substances [61]. Following the inflammatory process, the immune systems initiate restoration mechanisms involving a series of cellular and molecular events that mitigate the restoration of tissue homeostasis and resolution of the inflammatory process [62]. On that note, immune responses are tightly regulated involving various mechanisms to ensure normal homeostasis. When there is an imbalance of the immune system activity, it can lead to diseases such as autoimmune, chronic inflammatory, and cancer that can potentially be life-threatening [63]. In general, the immune system can be subdivided into two forms of protection known as innate and adaptive immune responses that work closely together to provide effective host defences.

1.2.2.1 Innate immunity

Innate immune response acts as the first line of defence. It is also known as a non-specific defence mechanism that responds immediately upon recognising a diverse array of microbial or "danger" signals due to changes in the homeostasis via the pattern recognition receptors (PRRs) such as Toll-like receptors (TLRs), Nucleotide oligodimerization domain (NOD) -like receptors (NLRs) and Retinoic acid-inducible

13

gene 1 (RIG-1)-like receptors (RLRs) which recognise pathogen-associated molecular patterns (PAMPs) and danger-associated molecular pattern (DAMPs) [64]. These recognition systems elicit distinct cellular responses depending on nature of stimuli and responding cells. The major roles of innate responses involve; a) prevent the entry of any foreign substances b) initiate complement pathway for getting rid of pathogens, c) generation of local inflammatory responses, d) induce phagocytosis and cytotoxicity activities, e) facilitate wound healing and tissue repair and, f) activation of adaptive immune responses through APCs [61,65–67].

The components of the innate immune system consists of physical and chemical barriers, immune cells and soluble factors that orchestrate rapid immune responses [68]. The physical barriers include epithelial layers of skin and the mucosal membrane that protect the external environment and exposure to foreign substances, including pathogens [68]. Any breakdown or defect in the physical barrier increases the susceptibility of infection and leads to the activation of immune responses. Chemical barriers consist of anti-microbial proteins and peptides, such as defensins that are permeable to microbes and induce their cell death [68]. Thus, physical, and chemical barriers both play a crucial role in preventing the entry of foreign substances and infection. In the case when pathogens breach protective physical and chemical barriers, they are combated through innate immune cells and soluble proteins. Upon recognition of foreign molecules via the PRRs, innate cells are activated following a cascade of signalling pathways that activate transcription factors and other proteins to

regulate the gene expression of various soluble factors to mount defence responses against the pathogens [68,69].

One of the key soluble factors of immune responses is cytokines. Cytokines are peptides that act as mediators in cell communication and signalling. The role of cytokines is not isolated for innate immune responses, as they also play vital roles in adaptive immune responses. Cytokines are broadly classified based on their nature of immune responses and often have overlapping functions [67]. Most cytokines are primarily but not exclusively produced by leukocytes termed as interleukin (IL) [70–72]. Interleukins can amplify their production in an autocrine or paracrine manner, as well as induce or inhibit the production of other cytokines. They bind to their receptors on the cells that produce them (autocrine) or other cells (paracrine) and modulate transcriptional program in determining the cells' fate [70]. A distinct subset of cytokines named chemotactic cytokines or chemokines is predominantly involved in trafficking activation of leukocytes to inflammatory sites [67,72,73].

With respect to immune cells, the cells are developed from hematopoietic stem cells within the bone marrow [74]. As these cells mature, they can be differentiated into two main lineages, myeloid progenitor cells (neutrophils, basophils, eosinophils, monocytes, macrophages, mast cells, and dendritic cells) and lymphoid progenitor cells (B cells, T cells, and innate lymphoid cells) [74]. Some of the primary innate immune cells include the granulocytes that contain granules sacs containing enzymes and inflammatory proteins (neutrophils, basophils, eosinophils, and mast cell) [74].

15

Among these cells, neutrophils are the most abundant leukocytes whose primary function in host defence is to patrol and guard the immune system against invaders [67,74]. While basophils and eosinophils are responsible in defence against helminth and allergic-related diseases through the degranulation process [70,74]. Mast cells primarily reside in the tissues rather than in the circulatory unlike the other granulocytes [70]. Mast cells play important roles in triggering inflammatory response as well as participate in wound healing [74]. Meanwhile, another group of innate cells; monocytes, macrophages, and dendritic cells belong to the mononuclear phagocyte system that plays multiple roles during inflammation [75]. Monocytes circulate in the circulatory with a rather short life span and may differentiate into tissue macrophages or dendritic cells depending on the surrounding stimuli [67,75]. Both macrophages and dendritic cells are also known as the APCs, as they capable of processing and presenting foreign proteins-based molecules (antigens) to lymphocytes [70,76]. In terms of protection against virally infected cells and tumour cells, another innate cell known as Natural killer cells are well known for their function in killing infected and transformed cells that managed to escape T cell recognition [74].

1.2.2.2 Adaptive immunity

The adaptive immune response is highly specific as it involves recognition of antigen (foreign agents and particles) via the receptors bound to the surface of B lymphocytes and T lymphocytes which are unique to different antigens [73]. This second defence mechanism is a contingent of the innate immune system and initiated in the later onset of infection. It provides great defence responses against persistent infection and

16

importantly possesses immunological memory [65,73]. In the event when the same or closely related antigens are encountered, the immunological memory program is activated, and the adaptive immune system provides rapid and enhanced protection. The adaptive immunity is broadly divided into humoral-mediated immune responses and cell-mediated immune responses which are coordinated by B cells and T cells, respectively [71,73]. Humoral mediated immune responses involve the production of antibodies by B cells against soluble antigens such as extracellular microbes and toxins. On the contrary, cell-mediated responses involve activation of effector T cells such as cytotoxic T cells that kill intracellular microbes and tumour cells, which are inaccessible to antibodies and Th cells that produce cytokines for modulating the function of other immune cells to mount against the antigens.

The principal cells involved in the adaptive immune response are APCs, B, and T-lymphocytes [73]. The APCs refer to the specialised cells that internalise and process antigen, concomitantly presenting the antigen as peptide within Major histocompability complex (MHC, also known as human leukocyte antigen, HLA, the term designated for humans) on their cell surface [66,73]. There are two types of MHC complexes. MHC class I is expressed on all nucleated cells and present peptide antigens derived from intracellular antigens (e.g., viral proteins, autologous proteins, and tumour antigens) [71,73,77]. On the contrary, MHC class II expression is predominantly restricted to APCs, and present peptide antigens synthesized from extracellular antigens (e.g., extracellular microbes, toxins, and allergens). Examples of prominent APCs are DCs, macrophages, B cells, and thymic epithelium [77].

Antigens processed by dendritic cells are displayed on their MHC class I and class II can activate naïve T cells into cytotoxic T cells (CD8^{+}) or Th cells (CD4^{+}) subsets respectively [65,76,77]. Macrophages and B cells can also serve as APCs by presenting antigens to T cells during diverse types of immune responses [76]. A subset of DCs known as follicular dendritic cells can present antigens to B cells during the establishment of the humoral immune response [70].

As mentioned previously, B cells and T cells are the lymphocytes that developed from lymphoid lineage originated from the hematopoietic stem cells (HSCs) that share the same common lymphoid progenitors with innate lymphoid cells (ILCs) (e.g., NK cells). These lymphocytes undergo complex maturation by which they express surface receptors that dictate their functions and phenotypes. Upon recognition and binding of the antigen-specific to their surface receptors, B and T cells undergo activation, proliferation (clonal expansion), and differentiation to effector cells and memory cells [61]. Unlike B and T cells, innate lymphoid cells are not clonally expressed for specific antigens and they serve the innate defence system [73]. B cells comprise of several subsets that are classified based on their ontogeny and anatomical location they reside in [78]. For example, B1 and B2 B cells are associated with antibody productions and regulatory B cells (Bregs) which are important for suppressing autoimmune and inflammatory responses. The developmental and maturation process of B cells involves structural and functional rearrangement of their receptors that take place within the bone marrow [79]. B cells express membrane-bound immunoglobulin (Ig) receptors on their surface and produce

soluble antibodies of the same antigenic specificity of the receptor. Mature B cells (express membrane-bound IgM and IgD) migrate to peripheral lymphoid organs or lymph nodes via the circulatory where they encounter with antigens for the establishment of humoral immunity [78,79]. Depending on the nature of antigens encountered and the subset of B cells involved, B cells can be activated either with the involvement of activated Th cells that express CD40L and the cytokines produced by them (T-dependent B cell activation) or without the involvement of Th cells (T-independent B cell activation) which is usually facilitated by TLR stimulation [79,80].

Following the activation of B cells, the B cells undergo clonal expansion and differentiate into plasma cells that produce IgM and IgD type antibodies that are designed to mount against specific antigens [78]. In addition, most of the B cells become effector cells, plasma cells whereby further interaction with other stimuli such as cytokines in the local microenvironment, the plasma cells capable of producing different classes of antibodies other than IgM and IgD, (IgA, IgG, and IgE) through the process called Ig class switching [78,79]. Some of the B cells become memory cells that preserve the "information" for those successful antibodies generated against the antigen and provide robust protection if the same antigens are encountered [79]. The functions of antibodies are to neutralise virulence factors of antigens, enhance activation of the complement pathway and phagocytes to eliminate the antigens [61,68,73]. However, antibodies can also contribute to the pathogenesis of autoimmune diseases due to the disrupted mechanism of self-tolerance leading to the generation of autoantibodies because of B cells reacting against self-antigens

(particles of host body) [78]. Unlike B cells that can recognise antigens in the extracellular spaces, T lymphocytes have restricted specificity for antigens as they recognise and respond to surface-bound antigens that are displayed on the MHC of APCs.

1.2.2.3 T cells

1.2.2.3.1 T cell development

T lymphocytes are known as thymus-derived lymphocytes. These cells are developed from thymic seeding progenitors (TSPs) derived from lymphoid progenitors which originated from the bone marrow [81,82]. These TSPs develop into early thymic progenitors (ETPs) and undergoes several stages of differentiation, selection, and eventually maturation by interacting with the microenvironment of the thymus to produce functional T cells (Figure 1.1) [81−83]. In early development, ETPs lack of co-receptors CD4 and CD8; denoted as double-negative (DN) populations [81]. These DN cells consist of four major subsets (DN1-DN4), categorised based on surface markers expressed on the cells. These DN cells undergo several differentiation processes involving the gene rearrangement of T cell receptor (TCR), producing a diverse repertoire of receptors capable of recognising a wide variety of antigens [81,82,84]. The TCR consists of a linked heterodimer of αβ or γδ chains associated non-covalently with the invariant transmembrane, the CD3 complex that plays a crucial role in signal transduction [82,85]. Most circulatory T cells (~95%) express αβ TCR that recognises antigen peptide complexed to MHC molecules displayed on

APCs, and small of a population of T cells (~5%) express γδ that recognise antigens that are not associated with MHC molecules [73,74].

Following the αβ gene rearrangement segment, the developing T cells (thymocytes) undergo checkpoints for evaluating the competency of TCR. At this stage, the cells begin to express CD4 and CD8 co-receptors resulting in double-positive cells and go through the selection process by interacting with the self-peptide-MHC complex [81,82,85]. The selection process involves three steps; non-selection, positive selection, and negative selection [85]. Thymocytes that exhibit non-functional TCR as they failed to recognise and bind to the self-peptide-MHC complex are not selected and eliminated through apoptosis. Thymocytes with TCR that bind to restricted self-peptide-MHC complex, either to MHC I or MHC II in intermediate strength (neither too strong nor too weak) are positively selected for maturation and commitment to single-positive CD8$^+$ (cytotoxic) or CD4$^+$ (helper) T cells lineages, respectively. Negative selection involves removing those thymocytes whose TCR bind to the self-peptide-MHC complex strongly, as the auto-reactive interaction can lead to detrimental auto-immune responses. The matured CD4$^+$ and CD8$^+$ T cells are regards as functionally naïve T cells as they are yet to encounter their cognate antigen [86]. After maturation, these cells migrate into peripheral lymphoid organs, where they encounter their cognate antigens and go through clonal expansion before differentiating into either effector or memory cells. Activated effector cells are short-lived, and some cells may survive to become long-lived memory cells [83].
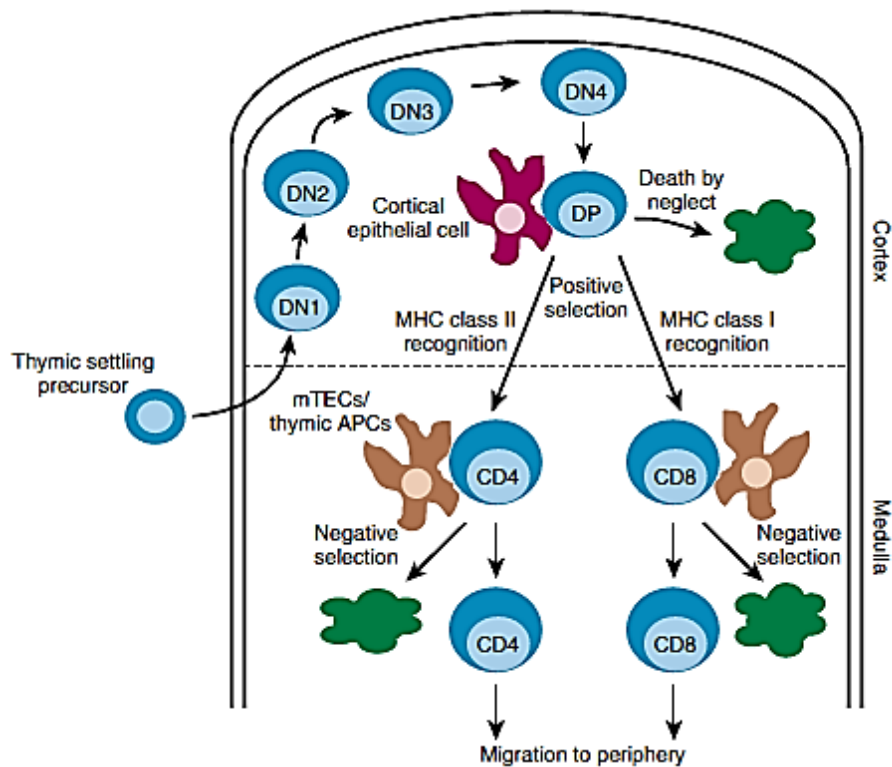
Figure 1.1 T cells development in the thymus.

Thymic settling precursor also known as thymic seeding progenitors (TSPs) originated from the bone marrow enters the corticomedullary junction. The TSPs develop into double-negative (DN) thymocytes and undergo differentiation involving the gene arrangement of T cell receptor (TCR). The developing αβTCR thymocyte gets through checkpoints and upregulate CD4 and CD8 coreceptors resulting in double-positive cells (DPs). The DPs interact with self-MHC complexes presented by cortical epithelial cells to access the competency of TCR prior to committing to either single positive CD4$^+$ or CD8$^+$ T cells. Those cells with ineffective TCR are not selected and undergo death by neglect (apoptosis). The DP thymocytes that bind to self-MHC molecules adequately are positively selected. The autoreactive single positive CD4$^+$ T and CD8$^+$ T cells that bind strongly to the self-MHC presented by thymic antigen presenting cells (APCs) or medullary thymic epithelial cells are eliminated through negative selection. Positively selected cells are released into the periphery. Illustration is adapted from Carty et.al [77].

1.2.2.3.2 T cell activation and signalling cascade

1.2.2.3.2.1 Activation

Effective activation of naïve T cells involves at least three signals; via TCR, co-stimulatory molecules, and cytokines [72,85]. Activation of naïve T cells first occurs through the engagement of TCRαβ with antigen peptide-MHC complex presented by APCs such as DCs (signal 1). As mentioned earlier, CD4$^+$ T cells recognise antigen peptide-MHC class II whereas CD8$^+$ T cells recognise antigen peptide-MHC class I. In the simplest term, the earliest event of T cell proximal signalling begins with association of TCR-CD3 complex with either CD4 or CD8 coreceptor, leading to activation of three major families of protein kinases; Src family (lymphocyte-specific protein tyrosine kinase; Lck), Syk family (zeta-chain associated protein kinase; ZAP-70) and Tec family (IL-2 induced tyrosine kinase; ITK) (Figure 1.2) [87–90].

The Lck phosphorylates CD3 subunits on the immune-receptor tyrosine-based motif (ITAMs), creating a docking site for binding of zeta-chain associated protein kinase (ZAP-70) to the TCR-CD3 complex [88–91]. Following this, Zap-70 gets activated and promotes phosphorylation of hematopoietic-specific adaptor proteins; transmembrane adaptor protein linker for activation of T cells (LAT) and cytosolic adapter protein Src homology 2 (SH2) domain-containing leukocyte phosphoprotein of 76 kDa (SLP-76) [88,90,91]. Accordingly, phosphorylation of these two adaptor proteins establishes the assembly of other adaptor proteins, kinases, and regulatory subunits forming a multi-molecular subunit complex (signalosome) of the proximal signalling [88,90,91]. For example, phosphorylated LAT leads to the binding of

23

adaptor proteins; growth-factor receptor-bound protein-2 (Grb2) and Grb2-related adaptor downstream of Shc (Gads). Grb2 recruits Son of Sevenless (Sos), a guanine triphosphate (GTP) exchange factor (GEF) for activation of GTP binding protein Ras that mediate mitogen-activated protein kinase (MAPK) pathway [77,88]. On the other hand, Gads associate with phosphorylated SPL-76 that is involved in recruiting other signalling mediators such as Vav1 (a GEF), adhesion and degranulation promoting adaptor protein (ADAP) and protein kinase of the Tec family, Itk and non-catalytic tyrosine kinase (Nck) [77,88,89]. The Vav1 is responsible for initiating signal for actin polymerization, involved in cytoskeletal reorganisation through the activation GTPase RAC, while ADAP and Nck are essential for inducing integrin signalling [88,90,91]. Also, Vav1 is also involved in stimulating transcription factor, FOS, and JUN [91]. By virtue of the association between Itk and SPL-76, the membrane-bound phospholipase Cγ1 (PLCγ1) is brought closer proximity to Itk, leading to activation of PLCγ1 which initiates a cascade of distal signalling [88,90].

Activated PLCγ1 hydrolyses membrane lipid phosphatidylinositol biphosphate (PIP$_2$), producing second messenger inositol triphosphate (IP$_3$) and diacylglycerol (DAG) [77,89,90]. The IP$_3$ involves in Ca^{2+} mediated signalling pathway, by which sustained Ca^{2+} influx influence the activation of transcription factor; Nuclear factor of activated T cells (NFAT) translocation into the nucleus to bind on the promoter of genes and work in cooperation with other transcription factor such as activator protein 1 (AP-1). On the other hand, the DAG mediated pathway involves a member of protein kinase Cθ (PKCθ) that initiates activation of transcription factor, nuclear

factor κB (NF-κB), and Ras guanyl nucleotide releasing protein (RasGRP) that regulate Ras/MAPK pathway. Like Grb2 and SOS, RasGRP activate Ras, which in turn activate downstream components of MAPK pathway involving extracellular signal regulated kinase (ERK) that contributes to activation of transcription complex consisting of activator protein-1 (AP-1), FOS, and JUN. The net outcome of these cascades of signalling is the activation of transcription factors NFAT, AP-1, and NF-κB, which coordinate activation of various gene programmes, involved in T cells proliferation, survival, and effector functions.
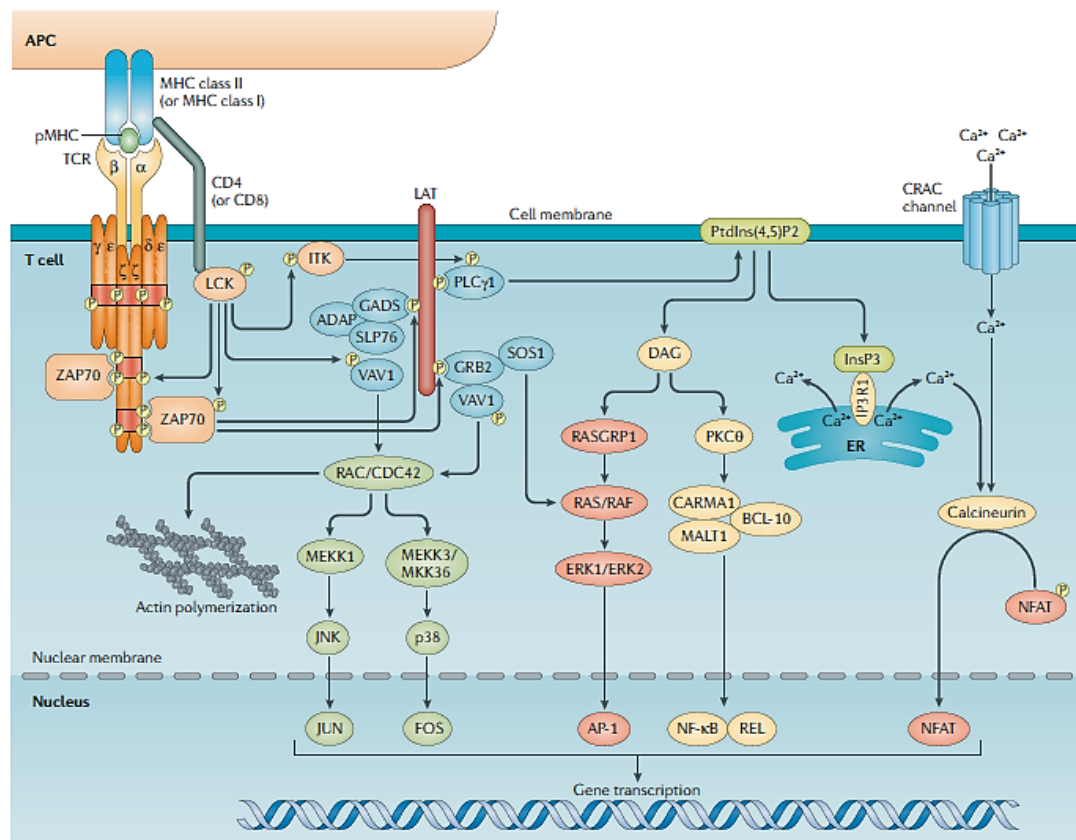
Figure 1.2 Overview of the major T cell receptor (TCR) signalling pathways.
Engagement of TCR and peptide- MHC complex on antigen presenting cells (APCs) triggers association of TCR-CD3 complex with either CD4 or CD8 coreceptor, leading to activation of three major families of protein kinases (represented in the orange colour); Src family (lymphocyte-specific protein tyrosine kinase; Lck), Syk family (zeta-chain associated protein kinase; ZAP-70) and Tec family (IL-2 induced tyrosine kinase; ITK). Activation of Lck on the immunoreceptor tyrosine-based activation motifs (ITAMs) creates docking site for binding of ZAP-70. Activated ZAP-70 in turn phosphorylates the transmembrane adaptor protein linker for activation of T cells (LAT) resulting in the assembly of multiple adaptor proteins and regulatory subunits (LAT signalosome, represented in the blue colour). Activation of the elements of the signalosome leads to activation of distal signalling; the Ca^{2+} calcineurin pathway, DAG mediated pathway and Rac pathway. The Ca^{2+} calcineurin pathway promotes translocation of nuclear factor of activated T cells (NFAT). Whereas diacylglycerol (DAG) mediated pathway activates transcription factor, nuclear factor κB (NF-κB) and activator protein 1 (AP-1). GTPase Rac-dependent pathway contributes to actin polymerization and activation of transcription factors FOS and JUN. Illustration is adapted from Gaud et.al [91].

1.2.2.3.2.2 Co-stimulatory signalling

Engagement of TCR alone results in unresponsiveness called anergy [92]. Therefore, T cell activation is mediated by various surface receptors, including co-stimulatory receptors (signal 2). Among all the co-stimulatory molecules, CD28 present constitutively on all naïve T cells, and their expression is enhanced upon activation [93]. Other co-stimulatory are expressed and upregulated upon activation, for example CD40L [93]. Costimulatory CD28 on activated T cells bind to B7-1 (CD80) and B7-2 (CD86) on APCs [89,90]. Upon binding, tyrosine residue of CD28 within its cytoplasmic tail is phosphorylated, resulting in recruitment of phosphatidylinositol '-hydroxyl kinase (P13K). Notably, TCR stimulation also activates PI3K through the binding of phosphorylated LAT to the p85 subunit of P13K [90]. However, TCR stimulation alone is insufficient as full activation of PI3K is dependent on co-stimulatory molecule, CD28 [90]. The PI3K converts PIP_2 to triphosphate (PIP_3) which mediates phosphorylation of Akt (a protein kinase B). Activated Akt, in turn, phosphorylates multiple proteins associated with the regulation of metabolic and survival activity of proliferating T cells [87,94]. Besides, CD28 also interacts with multiple downstream proteins such as Grb2, Vav and ITK that are activated by TCR/CD3 complex, thereby augmenting T cell activation signalling [87,92]. Furthermore, several lines of investigations have reported that CD28 signalling play unique biochemical events independent of TCR signalling such as post-translational modification of proteins involved in downstream signalling, an epigenetic modification that alters gene expression for transcription as well induces alternative splicing in T cells [92].

1.2.2.3.2.3 Surface markers

During T activation, several changes in surface molecules take place such as upregulation of regulatory proteins, receptors of co-stimulatory, co-inhibitory, adhesion, and chemokine that can be recognised as phenotypic surface markers [93]. One of the early and common T cell activation markers upregulated is CD69. The CD69 is an early T cell activation marker that is essential for retaining T cells in the lymph node to receive sufficient signal for proliferation and differentiation [93]. In addition to that, CD25 (IL-2Ra) expression is also upregulated whose function is to enable binding of IL-2 to activate IL-2-STAT5 signalling pathway [93]. As a result, the event leads to robust T cell proliferation. Nonetheless, the stimulatory activities of T cells are suppressed through a counterbalance mechanism to prevent over-activation of T cells. This is done by upregulation of CTLA-4 expression, a co-inhibitory molecule that competes with CD28 for binding B7 proteins to inhibit TCR-induced cellular activation, [95]. And program cell death mechanism via upregulation of death receptor and ligands (Fas/FasL and TNFα/TNF) [96,97].

1.2.2.4 General Principles of T helper differentiation

Once CD4$^+$ T cells are appropriately activated via signal 1 and signal 2 and undergo clonal expansion in lymph nodes, they receive instructions from specific cytokines (signal 3) within the local environment which directs them for differentiation before migrating to the inflammatory site to perform their effector functions. The CD4$^+$ T cells can differentiate into various effector T cells subsets such as Th1, Th2, Th9, T17, follicular Th cell (Tfh), induced T-regulatory (iTreg) and regulatory type 1 cell (Tr1) depending on the cytokine signalling and transcription factors involved [98]. Cytokines are essential players in Th differentiation as they act via different STAT signalling pathway in activating master transcriptional regulators that determine different subsets of the effector CD4$^+$ T cells [98–101]. The master transcriptional regulators dictate effector CD4$^+$ T cells subsets by several ways; a) activate the expression of lineage genes by binding to the promoter and enhancer regions, b) repress the genes of alternative lineage, c) influence epigenetic modifications of the cytokine locus favouring gene expression of specific subset [100,102]. Of note, Th differentiation can also be influenced by co-stimulatory molecules, depending on the strength of TCR stimulation [103–105]. For example, weak TCR stimulation favours Th2 development in association with CD28, and intense stimulation promotes Th1 development in association with CD28 and other co-stimulatory such as OX40L and CD40L.

Each of these Th subsets produces distinct cytokines and elicits specific effector functions. The signature cytokines; IFNγ, IL-4, and IL-17A define Th1, Th2 and Th17 cells, respectively [99]. The signature cytokines of particular subset can amplify their production via positive feedback mechanism and inhibit the cytokine production of the alternative subset by cross-regulation, driving Th differentiation to a dominant subset (polarisation) [99,106]. Noteworthy, Th1, Th2, and Th17 subsets can produce the same cytokines; IL-2, IL-6, IL-10, IL-21, granulocyte-macrophage colony-stimulating factor (GM-CSF), and tumour necrosis factor α (TNFα) [99]. In general, Th1, Th2, Th9 and Th17 cells provide protection roles in the clearance of the pathogens that they can combat [102,107,108]. Meanwhile, Tfh cells are essential for interacting with B cells within germinal centres for humoral mediated immunity [102,108]. Whereas, regulatory T cells are essential for the maintenance of immunological self-tolerance, downregulate pro-inflammatory responses, and preventing autoimmune diseases [107–109]. Of note, when the regulatory role of keeping the immune system in balance is disrupted, it causes over-activation of Th1, Th2, Th9, and Th17 which provide cytokines milieu, contributing to pathogenic responses implicated with the pathogenesis of immune-mediated diseases. For example, Th1 and Th17 cells are involved in pathogenesis of autoimmune diseases such as SLE, RA, inflammatory bladder disease (IBD), multiple sclerosis (MS), and type 1 diabetes [110,111]. Meanwhile, Th2 and Th9 cells contribute to inflammatory allergies such as asthma, chronic rhinosinusitis, and atopic dermatitis [112–114]. Besides this, it must be stressed that although Th subsets secrete specific cytokines that define their subsets and characteristics, these Th cells have the capacity for

plasticity [99,101]. In other words, they can be reprogrammed to alter their phenotype for expressing cytokines characteristic of other Th cells when the situation requires. Besides, signature cytokines and master transcriptional regulator of a particular subset can be expressed in other subsets, implying the existence of heterogeneity within the Th subsets [99,101,102,109]. These concepts, therefore, provide useful insights into the complex heterogeneity of Th cells seen human immunological diseases.

1.2.2.4.1 T helper 1 (Th1) cells

The Th1 cells are traditionally defined by their production of IFNγ and IL-2. In addition to these cytokines, Th1 cells can produce lymphotoxin α, tumour necrosis factor (TNF) and granulocyte-macrophage colony stimulating factor (GM-CSF) as well as chemokine receptors (CXCR3A, CCR5) which facilitate recruitment of Th1 cells to inflammatory sites [115,116]. During infection, Th1 cells play a crucial role in eliciting the cytotoxic response that is involved in pathogen clearance. For instance, Th1 cells enhance the activity of macrophages, NK cells, CD8^{+} T cells, and group 1 innate lymphoid cell partly through IL-12 and IFNγ for mediating cellular immunity by killing infected intracellular bacteria and viruses [77,100,117]. Also, Th1 cells are responsible for promoting B cells to produce for Ig class to produce IgG2a antibodies that facilitate the clearance of virus and extracellular bacteria [77,117]. Furthermore, Th1 cells is involved in creating pro-inflammatory cytokines milieu causing a pathogenic response that leads to chronic inflammation and tissue destructions in autoimmune diseases [111,118].

The mechanism of Th1 development is widely established. For instance, during infection, intracellular pathogens elicit innate immune responses that trigger the release of IL-12, IL-18 and type I interferons that promote CD4^{+} T cells differentiation to Th1 effector cells [102,108,116]. Among these, IL-12 is predominant in generating Th1 cells [119]. The cytokine, IL-12 induces NK cells to produce IFNγ [98,108]. As Th1 signature cytokine, IFNγ plays an important role in driving Th1 differentiation through its positive feedback mechanism [98,108]. The reason being, IFNγ interacts with the intracellular transcription factor known as signal transducer and activator of transcription 1 (STAT1) to activate expression of T-bet (T-box expressed in T cells), the master transcription factor, which in turn bind to *Ifng* promoter and induce IFNγ production. As a result, this establishes the amplification loop of T-bet and IFNγ expression. At the same time, IL-12 Rβ2, the receptor for IL-12 is upregulated. The role of IL-12 comes to play when IL-12 in the local environment binds to IL-12Rβ2 and activate STAT4 signalling; an additional pathway that induces T-bet expression, thus further enhancing IFNγ production [98,108].

Besides that, T-bet play a crucial role in Th1 development by binding to *Ifng* locus and inducing chromatin remodelling favouring to Th1 differentiation [99]. Importantly, T-bet cooperates with its partner the run-related transcription factor 3 (Runx3) to suppress the expression IL-4 and GATA binding protein 3 (GATA3), the two important regulators for driving Th2 development [98]. Furthermore, other transcription factors such as a homeobox transcription factor (Hlx) and IRF1 are known to enhance IFNγ production, by acting downstream of T-bet [98,102].

32

Remarkably, T-bet can interact with a transcription factor B cell lymphoma 6 protein (BCL-6), in antagonistic manner [98,113,120]. For example, in the early stage of Th1 differentiation T-bet act as a negative regulator of BCL-6. However, in a later stage, BCL-6 binds to T-bet and suppresses its expression to inhibit Th1 over-activation, thus highlighting the counterbalance mechanism regulating Th1 polarization. It is important to note that, although the induction of T-bet and IFNγ and subsequent induction of IL-12Rβ2 are known as the defining factors that endow Th1 differentiation, participation of IL-2 has shown to play a crucial role in T differentiation. This is because multiple studies have shown that IL-2 contributes to IFNγ production by positively regulating T-bet and IL-12Rβ2 expression, hence in this aspect lack of IL-2 would result in impaired Th1 differentiation [121].

1.2.2.4.2 T helper 2 (Th2) cells

The Th2 cells are typically characterised by their signature cytokines IL-4, IL-5, and IL-13 [102,114]. In addition to these cytokines, Th2 cells also known to produce IL-9, IL-10, IL-25, and amphiregulin [98]. In terms of chemokines, they are known to produce the CCR4 chemokine receptor [101]. Also, these cells provide the necessary cytokine environment to elicit diverse immune responses to mount against extracellular parasites and allergens. For example, IL-4 stimulates B cell-Ig class switching to produce IgG1 and IgE antibodies; IL-5 activates eosinophils. Meanwhile, IL-13 acts on epithelial and smooth muscles and both IL-4 and IL-13 elicit alternative activation macrophage phenotypes [77,99,108,122]. However, overproduction of the

Th2 cytokines is implicated in the pathological features of allergic diseases and asthma [77,99,108] .

The main cytokine that drives Th2 differentiation is IL-4, which can be provided by many innate immune cells. For example, during parasitic infection, cells from the local environment, as epithelial cells and thymic stromal lymphopoietin, produce Th2 inducing cytokines such as IL-25 and IL-33 could activate innate immune cells like basophils, ILCs, and dendritic cells to produce IL-4 to drive Th2 differentiation [77,108,114,115]. As a result, IL-4 acts on STAT6 transcription factor, causing phosphorylation of the STAT6, which subsequently induces GATA3 expression, the master transcription factor for Th2 development [98,101,108,114]. The GATA3 enhances its own expression through positive feedback loops and together with its partner; basic helix-loop-helix transcription factor Dec2 drive Th2 differentiation [106,123]. Moreover, GATA3 is responsible for the activation of IL-4, IL-5, and IL-13 which are all located on the same gene locus [101,114,123]. As aforementioned earlier that the master transcription factor of Th1 cells, T-bet is capable of inducing chromatin remodelling, in a similar manner, GATA3 can act on the promoter of the gene of Th2 cytokines and induces chromatin remodelling to activate the Th2 cytokines genes [98,114,120]. Importantly, to maintain Th2 populations, GATA3 inhibits IFNγ production, by blocking IL-12/STAT4 signalling pathway, which is required for Th1 differentiation [123].

Another important transcription factor in Th2 development is IRF4. It functions as a crucial regulator that is important for maintaining Th2 polarizing state via various mechanisms such as a) GATA3 and IRF4 together form complex with chromatin organizer special AT-rich binding protein (SATB1), binding on the Th2-related cytokines genomic loci to promote the gene expression of Th2 cytokines, b) IRF4 also cooperate with NFAT2 to induce IL-4 expression and lack of IRF4 have shown impairment of Th2 development, c) enhance growth factor independent 1 (Gif1) expression which is important for promoting Th2 cell expansion [98,120,124]. In addition to IRF4, c-Maf (a basic leucine zipper transcription factor) is also known to play a crucial role in Th2 differentiation. The c-Maf acts directly on *Il4* promoter through collaboration action of Jun-B and Dec-2 transcription factors, thus promoting Th2 polarisation [98,125].

It is noteworthy to mention that, although IL-2 is known to contribute to Th1 differentiation as described earlier, it is also shown to play a critical role in Th2 differentiation. This is broadly due to STAT5 activation which is dependent on IL-2, contributing to upregulation of IL-4 expression. The reason being, STAT5 induces chromatin accessibility of *Il4* locus in a different region than GATA3 and subsequently binds to *Il4* key regions to induce IL-4 expression, therefore highlighting a different pathway for IL-4 production independent of GATA3 [114,121,122]. In this case, it reflects that IL-2 plays a crucial role in early Th2 differentiation, by being the source of IL-4 production because GATA3 alone cannot produce IL-4 [98]. Interestingly, studies have identified that Notch signalling; the

35

conserved cell signalling pathway with pleiotropic functions also participate in Th2 differentiation by upregulating GATA3 and IL-2 expression, which is crucial in driving Th2 polarisation as described above [122]. In addition to IL-2, another cytokine IL-6 can also enhance Th2 differentiation by at least two mechanisms; a) upregulating NFAT2, a transcription factor which involved in transcription of IL-4 and b) inhibit Th1 differentiation by interacting with suppressor cytokine signalling 1 (SOSC-1) to block STAT1 activation which is downstream to IFNγ signalling [98].

1.2.2.5 Key regulators involve in the signalling of T helper differentiation

The immune system protects against invaders such as microbial pathogens, toxic agents, and as well as transformed malignant cells. The crosstalk between innate and adaptive immunity ensures an effective host defence system, mediated by various cells and molecules that work dynamically. In terms of T cells, upon activation naïve CD4+ T cells acquire the ability to differentiate into several subsets including Th1 and Th2 cells that are mediated by specific cytokine signalling and transcription factor. The positive key regulators involve in Th1 differentiation are T-bet, IFNγ/STAT1, and IL-12/STAT4; meanwhile for Th2 differentiation is GATA3 and IL-4/STAT6. Of note, besides the master transcription factor, several other transcription factors such as the RUNX3, Hlx, IRF1, Dec2, IRF4, NFAT, Gif-1, c-Maf, and Jun-B are known to cooperate with the subset specific master transcription factor that collectively involved in establishing Th1/Th2 differentiation. Although certain cytokines expressions and transcription factors of T helper subsets are exclusive to each subset, they can still in present in both states and fine-tune the Th

cells capabilities for polarization when the situation requires. This can be exemplified clearly by IL-2, which is important for both Th1 and Th2 differentiation. Collectively, the immune cells orchestrate a complex network made of transcription factors in cooperation with other proteins involved in cytokine signalling which subsequently influences the chromatin state of the targeted genes, resulting in activation or repression of the genes, thereby eliciting the required immune responses in a given state.

1.2.3 Interferon Regulatory Factor (IRF) family

1.2.3.1 Overview of IRF family

As introduced earlier (section 1.2.1.1), transcription factors are one of the key players during gene expression as they facilitate when and what gene is "turn on or off" by binding to DNA sequences, acting as co-activator or co-repressor of the gene in response to various signals [126]. Structurally they comprise of two domains: a) DNA binding domain that recognises and bind to DNA sequences, b) activation (effector) domain which interacts with cofactors or other transcription factors [35,127,128]. Some of them also have additional domain (signal-sensing domain) that binds to ligands to modulate their activity in response to environmental cues [35,127]. Transcription factors are categorised into several groups based on their DNA binding domain structures and their interaction with DNA sequences [127–129]. Some of these transcription factors are known as general transcription factors, which are ubiquitous and essential for initiating transcription in the protein-coding gene [126,128]. Other transcription factors are either constitutive or inducible and are specific to certain cell types and stages of organism development [126,128]. Several of these transcription factors function as master transcriptional regulators in controlling signal responses and specifying the lineage of cells [38,126]. In addition, transcription factors play a crucial role in interacting with histone proteins which influence chromatin state and establish the environment that allows interactions for activation or repression of gene transcription [52,127]. One group of transcription factors that have been extensively studied for their crucial role in regulating gene

networks in the immune system is the IRFs which possess the turn-helix turn motif [130].

The first IRFs member, IRF1 was initially identified as a factor that binds to the upstream regulatory region of the human interferon (IFN) β gene and induced its expression [131]. Over the past decades, the family of IRFs has been expanded to ten members, to which IRF1 to 9 are found in mice and human, whereas IRF10 is only found in chickens [2]. Also, several viral IRFs that interact with cellular IRFs have been identified [132]. All IRFs consists of two domains, the N-terminal (DNA binding domain) and C-terminal (regulatory domain) (Figure 1.3). The N-terminal binding domain is enriched with five tryptophan repeats that are well conserved among all IRF. This region recognises a DNA consensus, known as ISRE found in the promoters of type 1 IFN, IFN-inducible genes, and many other genes that are involved in immune responses [3]. On the other hand, the C-terminal consist of the IRF association domain (IAD), that is responsible for homo- and heteromeric interaction with other family members or transcription factor [130,133]. IRFs functions are not limited to regulating innate, and adaptive immune responses as these transcription factors also play a crucial role in regulating type 1 IFN induced by viruses and pathogens, involved in the cell cycle, apoptosis, and oncogenesis [[2,3,130,133]. Some of these IRFs are also involved in regulating immune cell development and functions [2,6,7,134].
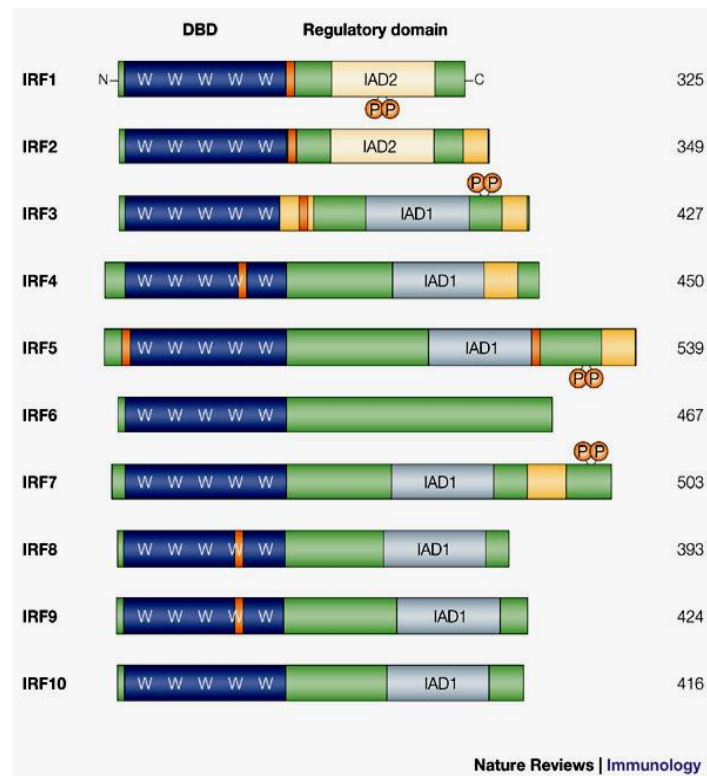
Figure 1.3 Structure of Interferon Regulatory Factors (IRFs).
DNA-binding domain (DBD: blue) and regulatory domain (green). The DBD of all IRFs are defined by 5 tryptophan (W) residues that are separated by 10-18 amino acids. All IRFs, except IRF-6 contain IRF-association domain (IAD) of either type 1 (grey) or type 2 (pale yellow). Some IRFs contain a repression domain (s) (yellow and nuclear-localization signal (s) (orange). For IRF-1, -3, -5 and -7, activity depends on phosphorylation as shown with the attached phosphate groups on the regulatory domain. The size of each IRF in number of amino acids is also indicated. (C, carboxyl terminus; N, amino terminus). The illustration is adapted from Lohoff et.al [7].

1.2.3.2 Roles of IRFs in T helper differentiation

Over the years, many IRFs have been found to be involved in Th differentiation either by modulating the functions of APCs or directly altering the transcription of cytokine genes of Th cells [7]. The IRF1 is a crucial factor in promoting Th1 differentiation and its absence results in predominant Th2 responses as best characterized using experimental mice disease model. For example, IRF1 deficient mice ($Irf1^{-/-}$) were

vulnerable to *Leishmania major* (*L. major*) and *Listeria monocytogenes* (*L. monocytogenes*) because the host could not control the parasitic infection due to a lack of Th1 responses which is needed for protection against the intracellular parasitic infections [135,136]. In contrast, *Irf1*^{-/-} mice were shown resistant towards *Nippostronglyus brasiliensis* (*N. brasiliensis*) due to biased Th2 response, which is essential for the expulsion of the worms (29). The impairment of Th1 response observed in the *Irf1*^{-/-} mice were mainly due to the defects in multiple cell types such as CD4^{+} T cells and NK cells as well as APCs (macrophages and dendritic cells) that are associated in IL-12, a Th1 cytokine that drives Th1 differentiation [135–139]. Like *Irf1*^{-/-} mice, *Irf2*^{-/-} failed to mount Th1 response due to impaired IL-12 production by macrophages thereby was susceptible to *L. major* [140]. Consistently, Elser et al. reported that IRF1 and IRF2 act as transcriptional repressor of IL-4, thereby attenuating Th2 responses and assisted IFNγ in inducing Th1 response [141]. Likewise, *Irf8*^{-/-} mice showed failure in Th1 driven response, which correlated with the defect in IL-12 p40 production [142]. Collectively, IRF1, IRF2, and IRF8 directly participated in Th1 differentiation predominantly by regulating the production of IL-12, the Th1 signature cytokine.

On the other hand, IRF4 is critical for Th2 cell development. Mice lacking IRF4 showed to be able to mount Th1 immune response against *L. major* but the Th2 development was found impaired [143]. Also, CD4^{+} T cells of *Irf4*^{-/-} mice were unable to differentiate into Th2 cells and displayed impaired production of Th2 cytokines; IL-4, IL-5, and IL-13 [144]. Moreover, overexpression of IRF4 in human Jurkat cells

activated the expression of Th2 cytokines in response to mitogenic stimulation [145].

Consistently, in absence of IRF4, IL-4 failed to induce Th2 cytokine, instead induced Th1 response by upregulating IFNγ and TNF expression, thereby implying the importance of IRF4 in Th2 differentiation [146]. In accordance with the role of IRF4 in Th2 differentiation, Honma et al. reported that IRF4 plays a dual role in distinct stages of CD4$^+$ T cells [147]. Furthermore, IRF4 was shown to inhibit Th2 cytokine production in naïve CD4$^+$T cells but induced Th2 cytokine production in effector/memory CD4$^+$ cells. However, IRF4 function is not only restricted to Th2 cell differentiation, since several studies have shown that IRF4 is vital in generating Th9, Th17, and Tregs cells [6]. Taken together, IRF4 can differentially control the Th subsets and act as a Th modulator. Another member of the IRFs family, IRF5, is also known to play some role in Th differentiation. Since IRF5 is the focus of this thesis; the following sections consist of a detailed description of IRF5 and findings on its role in regulating T cells and Th differentiation.

1.2.4 Interferon regulatory factor 5 (IRF5)

1.2.4.1 Overview of IRF5

The IRF5 was first identified in antiviral responses and induction of type I interferon production [31]. It is now well established that IRF5 has a diverse role in the induction of pro-inflammatory cytokines and chemokines downstream to various signalling pathways contributing to the pathogenesis of various autoimmune and inflammatory diseases [11,13,148]. An early study showed that $Irf5^{-/-}$ mice were unable to secrete proinflammatory cytokines such as IL-6, IL-12 and TNFα, consequently $Irf5^{-/-}$ mice showed resistance towards lipopolysaccharide (LPS)-induced endotoxic shock [149]. Also, IRF5 lacking myeloid cells showed similar impairment in the proinflammatory cytokines following various TLRs stimulation [149].

Constitutive expression of IRF5 has been detected in lymphoid tissues such as spleen and peripheral blood lymphocytes [31]. In the latter, IRF5 expression is mainly found in B cells and barely in T cells and NK cells. A higher level of IRF5 expression has been found in other immune cells such as monocytes and macrophages but relatively lower in dendritic cells [16,150]. Other factors, such as viral infection and IFNα stimulation, could enhance the expression of IRF5 [16,18]. Notably, expression IRF5 was found to be absent or downregulated in most cancer cell lines [150]. This indicates the inclination of IRF5 for gene deletion or epigenetic silencing in these malignancies [151−153]. The importance of IRF5 in regulating immune cells

functions and its expression dysregulation in the pathogenesis of immune system disorders is summarised in Table 1.1

Table 1.1 Summary of IRF5 role in regulating immune cells functions.
The table is adapted from our published review [13].

Cells	Role of IRF5 in immune cells
B cells	• Involves in B cell activation and proliferation. • Regulates Blimp-1 expression. • Loss of IRF5 in B cells lead to defect in plasma cell differentiation. • Exhibit differential regulation of autoantibody and IgG classes in non-autoimmune and autoimmune murine models.
Monocytes	• Increased expression and activation in SLE patients • Involves in recruitment of Ly6C^{high} monocyte subsets to inflammation site in pristane-induced mice • Induces IFNβ production in response to TLR8 mediated sensing of *S.aureus.* • Involves in proinflammatory cytokine production in response to TLR8 signalling
Macrophages	• Master regulator for both human and murine M1 macrophages. • Induces proinflammatory cytokines associated with M1 phenotypes. • Specific marker for M1 macrophages. • Plays role in profibrotic inflammation. • Repressor of IL-10 and TGFβ1 expression. • Elevated level of IRF5 expression is associated with diseases where inflammatory macrophages play role in disease progression.
Dendritic cells	• Involves in type 1 IFN production in TLR7 and TLR9 mediated stimulation. • Contributes in IFNβ production in response to microbial infections. • Involves in production of proinflammatory cytokines. • Involves in recruitment of plasmacytoid dendritic cells to inflammation site in pristane-induced mice.
T cells	• Malignant T cells expressed mutant IRF5 transcripts as a protective mechanism for survival. • Plays pivotal role in T proliferation and activation in lupus induced mice. • Serves as repressor of T-bet gene in CD4^{+} T cells in SSc murine model. • Modulates T helper responses by altering function of antigen presenting cells (macrophages, dendritic cells) and influencing the cytokine production for T helper differentiation.

1.2.4.2 Gene structure of IRF5

In humans, *Irf5* gene is located on chromosome 7q32 within a region where imprinted genes associated with haematological malignancies was reported. Whether IRF5 is imprinted or associated with any disorder is yet to be established [28,31]. The *Irf5* gene consists of 9 exons, and its first non-coding exon consists of four different exons (Ex) promoters (1A, 1B, 1C and 1D) as a result of alternative splicing of the promoter (Figure 1.4a) [28,154]. The start codon ATG is in Ex2 hence the use of different first exons would not result in an altered protein sequence [16,154]. Early studies demonstrated that Ex1A is constitutively active and harbours an IRF element (IRFE) binding site and can be stimulated in virus-infected cells by other IRF family [16]. Interestingly, Ex1A has the highest translation efficiency among all other exons and most of the IRF5 variants are derived from this promoter [11,154]. On the other hand, Ex1C has the ISRE binding site, which allows the binding of IFN stimulated gene factor 3 (ISGF3) complex following IFN stimulation [16]. Besides that, several transcription factors binding sites on IRF5 promoters have been identified in promoter analysis studies using ChIP-Seq datasets [154]. For instance, Ex1A and Ex1D have a putative binding site for PU.1 and NF-κB which increased expression of IRF5 upon activation by imiquimod a TLR7 ligand. Further studies on how the other transcription binding factors regulate IRF5 expression will provide insights into the mechanism of IRF5 transcriptional regulation.

Alternative splicing of precursor mRNA of the IRF5 gene can give rise to multiple transcripts variants. Early studies reported by Mancl et al. identified nine

IRF5 transcripts with distinct cell-type-specific expression, regulations, and functions [16]. These transcripts differ in their first exons, in Ex6, and missing some parts of other exons (Figure 4b). The Ex6 confers a 30-base pair (bp) in frame insertion-deletion and an alternative splicing 48bp downstream of the canonical splice junction [11,155]. These polymorphic regions are localised within the domain rich in proline (P), glutamic acid (E), serine (S) and threonine (T) (PEST) associated with IRF5 protein stability [11,28,155] and some of the IRF5 isoforms have been reported to alter the degradation of IRF5 protein [156]. For example, IRF5 v2 and v3 with altered PEST domain structure (missing first 48 nucleotide encoding PEST region) showed resistance towards E3 ubiquitin ligase TRIpartite Motif, (TRIM) 21 whereas TRIM21 degraded v1 and v5 with not much of altered PEST structure following TLR7 stimulation [156]. The TRIM21 protein is known as a negative regulator of the IRF family and mediates ubiquitination that leads to degradation and eventually termination of signalling following TLR stimulation [156]. The resistance to TRIM21-induced degradation could result in enhanced expression and activity of IRF5 that could potentially lead to the development of certain diseases. To date, 17 known variants of human IRF5 have been reported, and there is a possibility of identifying more variants since there may be numerous ways to splice IRF5 in response to different stimuli [157]. In murine, IRF5 is predominantly expressed in full length and only a single splice variant has been detected at a minimal level in the bone marrow [33]. Notably, the murine IRF5 is highly homologous to human IRF5v5, with the striking difference of 5 amino acid deletion in MuIRF5. Collectively, the diversity

of human IRF5 splicing reflects the complexity and differential functions of this gene

in comparison to the murine model.
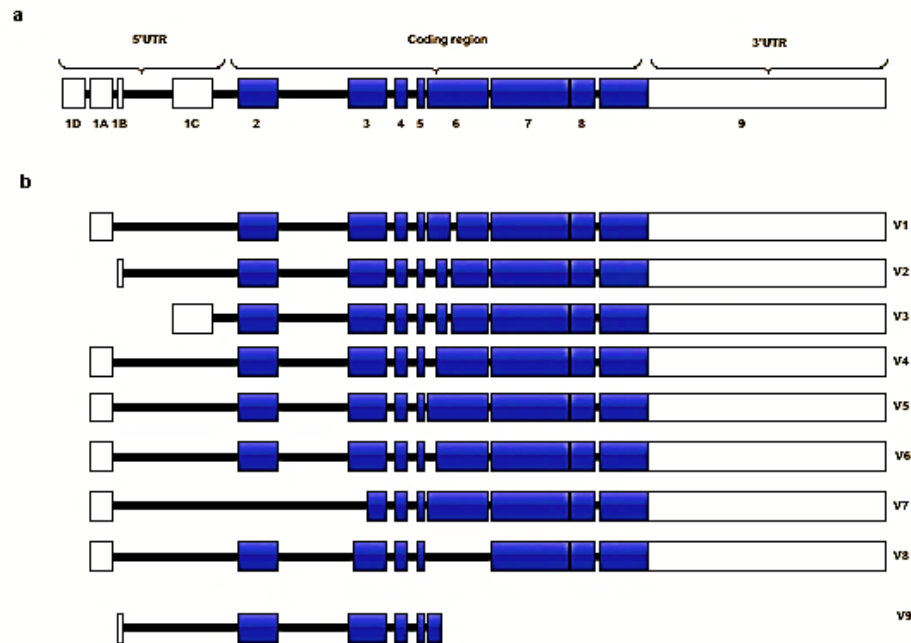
Figure 1.4 Schematic diagrams of human *Irf*5 gene and its variants
Blue boxes represent exons are proportional to length and lines are introns reduced in size 10:1. (a) Full length of human IRF5 gene, with four possible exon promoters of the non-coding exon 1; Ex1A, 1B, 1C, and 1D as represented in white box. (b) Utilization of different first exons and alternative splicing that give rise to nine distinct transcripts. Most variants are derived from Ex1A, except for V2 that begins with Ex1B and V3 with Ex1C, respectively. The deletion pattern in Ex6 is indicated by the open space or the difference in length of the represented box. All exons are present in all variants except for V7 (missing of Ex2), V8 (missing of Ex6) and V9 (missing of Ex5 and some part of Ex6 and other exons onwards due to the presence of early stop codon). This figure is adapted from our published review [13].

1.2.4.3 Polymorphisms of IRF5 gene

The *Irf5* gene polymorphisms are implicated with various autoimmune diseases such as SLE, RA, IBD, MS, systemic sclerosis (SSc) and Sjogren's syndrome (SS) [11,158–160]. The association of IRF5 polymorphism with autoimmune disease was first identified in a joint linkage association studies conducted in Swedish, Finnish and Icelandic populations which reported single nucleotide polymorphism (SNP) rs2004640 is strongly associated with SLE (unadjusted p-value $< 10^7$) [161]. Graham et al. reported that this SNP is located at 2b downstream of Ex1B promoter which causes an increase of Ex1B-driven IRF5 transcripts due to the T risk allele that creates a 5'donor splicing resulting in Ex1B to spliced into exon 2 and the IRF5 isoforms from Ex1B are associated with an elevated level of IRF5 and risk to SLE [162]. Several other IRF5 polymorphisms associated with SLE have also been reported, and at least four functional polymorphisms have been documented [163]. These polymorphisms are associated with higher IRF5 expression [164–167] confer better RNA stability [26,168] and associated with an elevated level of IFNα, a cytokine contributing to SLE [169]. Some of these IRF5 polymorphisms have also given rise to novel IRF5 isoforms which showed differential responses between healthy and SLE individuals [155,166].

Interestingly, CGGGG indel polymorphism and rs2004640 haplotypes which have been implicated in SLE susceptibility have been found to be associated with several autoimmune diseases such as RA, SSc, MS, and IBD highlighting the involvement of IRF5 in overlapping pathways of autoimmune diseases [163,170]. The

pathological roles of IRF5 in developing autoimmune diseases are well elucidated in genetic modification experiments *in vitro* and *in vivo*. Mounting evidence has shown IRF5 polymorphisms are associated with increased susceptibility of autoimmune diseases whereas the loss of IRF5 ameliorates pathological manifestation of the disease [11,171].

1.2.4.4 Protein structure of IRF5

Structure analysis of IRF5 has revealed multiple regulatory domains located within its polypeptide. To a large extent, these domains dictate the biological function of this protein (Figure 1.5). The IRF5 polypeptide contains a putative nuclear localisation signal (NLS) sequence in the N-terminal and the C-terminal, which ensure nuclear retention of IRF5 in infected cells [31,32]. In addition to the NLS, IRF5 also possess nuclear export signal (NES) sequence which is dependent on the nuclear export protein, chromosomal maintenance 1(CRM1) and is responsible for the retention of IRF5 in the cytoplasm [30]. Hence, both NLS and NES play an essential role in shuffling IRF5 between the cytoplasm and nucleus. Studies also showed IRF5 translocation to the nucleus is dependent on NLS and not due to homodimerisation of IRF5 or heterodimerisation with other interacting partners [30].

Furthermore, the serine rich region (SRR) located within the transactivation domain of the C-terminal is responsible for the phosphorylation and dimerization of IRF5, whilst the presence of an autoinhibitory domain influences the transcriptional activity. This was illustrated by a mutant IRF5 (missing of 50aa) which showed was a

better inducer of IFNα1 and IFNβ compared to the full-length IRF5 [32]. The presence of the PEST region in IRF5 is thought to control the protein stability of this transcription factor. However, COP9 signalosome (CSN) has recently been shown to interact with the N- and C- termini of IRF5 thereby controlling the protein stability through ubiquitin-proteasome pathway [172]. This was linked with the dissociation of the IRF5-CSN complex upon phosphorylation which resulted in rapid ubiquitination and proteasome degradation of IRF5 while some of the IRF5 may get translocated and performs its transcriptional activity. Therefore, CSN acts as an interacting partner that provides stability to IRF5 and regulates its degradation.

Figure 1.5 Schematic illustration of human IRF5 protein
DNA binding domain (DBD) resides within the N-terminal region, whereas the IRF association domain (IAD) where the protein interaction takes place resides in C-terminal. Two functional nuclear localization signals (NLS) are present, one residing in N-terminal and other is in C-terminal (black box). Nuclear export signal (NES) is located within the proline (P), glutamic acid (E), serine (S) and threonine (T) (PEST) domain represented in green box. The PEST domain is where the internal deletion occurs. The transactivation domain (grey box) is in the IAD domain which contains the serine rich region (SRR) represented in purple box. Autoinhibitory region of the polypeptide reside at the end of C-terminal (red box). This figure is adapted from our published review [13].

1.2.4.5 IRF5 activation and signalling

In unstimulated cells, IRF5 is found to reside in the cytoplasm, whereas upon stimulation it undergoes post-translational modification, dimerization and translocate in the nucleus which then binds to coactivator such as CREB-binding protein (CBP)/p300 to initiate the transcriptional activity of the targeted gene [148,173,174]. IRF5 exhibit diverse mode of transcriptional action by interacting with either activator or repressor via its N-terminal region by forming complexes at selected genes [175,176], therefore, resulting in the induction or suppression of the targeted genes. Activation of IRF5 is dependent on the post-translational modification such as phosphorylation and polyubiquitination. Several studies have revealed distinct phosphorylation sites with differential functions and mutation of amino residues could lead to alteration of IRF5 activity [148,173,177]. The IRF5 phosphorylation and translocation into nucleus in Newcastle disease virus (NDV) infected cells were affected when serine residue S477 and S480 (numbered as in IRF5V3) were replaced with alanine residues [32]. Phosphorylation of S425, S427, and S430 (numbered as in IRF5V4) triggers conformational rearrangement of the auto-inhibitory region of C-terminus allowing homo-dimerization whereas S436 stabilises the dimer conformation [173]. The phosphorylation of the serine residues is essential for the activation of IRF5 by triggering conformational changes that stimulate dimerization leading to translocation to nucleus and assembly with co-activator CBP/p300 for binding to targeted gene.

Furthermore, phosphorylation of IRF5 at serine residue is dependent on several kinases, as phosphorylation of S445 in mice was mediated by IκB kinase beta (IKKβ) kinase (S446 in human isoform1 and S462 in isoform 2) which was essential to produce inflammatory cytokines [178]. Mutation of this serine residue abolished IRF5 activation and inflammatory cytokine production. Similarly, Lopez et al. demonstrated that IKKβ kinase phosphorylates IRF5 at S462 in the human isoform2 resulting in its dimerization and nuclear translocation in human plasmacytoid dendritic cells (pDCs) cell line Gen2.2 [179]. Hence, structural phosphorylation-mediated signalling of IRF5 on serine sites is dependent on the isoforms, therefore, exhibiting differential roles.

The IRF5 can participate in downstream signalling stimulated by various TLRs. Signalling through TLRs are generally categorised into two pathways; the MyD88 pathway and TIR-domain containing TRIF pathways [3]. Interestingly, IRF5 was shown involved in the synergism of TLRs via both pathways to regulate inflammatory cytokines gene expression [180]. Activation of IRF5 by TLR7, TLR8, and TLR9 via the MyD88 signalling pathway is associated with interleukin-1 receptor-associated kinase 1 (IRAK1) and TNF receptor-associated factor (TRAF6) [34,149,181]. Subsequently, IRF5 undergoes phosphorylation mediated by TANK-binding kinase 1 (TBK1) and IKKβ [34,181] followed by dimerization and translocation into the nucleus for the activation of targeted genes. Interestingly, IRF5 can also be activated by receptor-interacting protein 2 (RIP-2) kinase in cooperation with TBK1 via NOD-2 signalling [182]. Lately, a novel role of IRAK4 activity in the

transforming growth factor-beta activated kinase (TAK1)- IKKβ-IRF5 axis was revealed whereby IRAK4 was shown to act through TAK1 and IKKβ, upon TLR8 stimulation [183]. In addition, Fu et al. showed NXF1, a mRNA export receptor selectively regulated TLR7-driven IRF5 transcriptional activity, indicating a novel function of NXF1 in IRF5 signalling [29]. In RLR- mitochondrial antiviral signalling (MAVS) pathways, IRF5 cooperated with IRF3 and IRF7 in myeloid dendritic cells (mDCs) to induce IFNβ during West Nile virus (WNV) [184]. Notably, IRF5 also participate in the Dectin-1-Syk signalling pathway in murine renal dendritic cells, leading to the production of IFNβ to protect infected *Candida albicans (C.albicans)* mice [185]. Collectively, IRF5 can be activated in response to various environmental stimuli via PRRs on the cells' surface and intracellular compartments by participating in downstream signalling of the PRRs.

1.2.4.6 Roles of IRF5 in T cells

The development of T cells is regulated by mainly IRF1, IRF2, IRF4, and IRF8 [6,7]. Meanwhile, IRF5 has been implicated in the activation and effector functions of T cells as described below.

1.2.4.6.1 Expression of IRF5 in T cells

Constitutive expression of IRF5 is barely detected in resting T cells, but upon stimulation with Herpes simplex virus (HSV)-1 and IFNα, IRF5 expression was greatly enhanced in periphery T cells [16]. IRF5 expression was also upregulated in T cells during parasitic infection, which corresponds to an increased expression of IRF5

mRNA level in CD5$^+$ T population in both spleen and liver especially in an early onset of the disease [17]. As a co-receptor, CD5 plays an important role in regulating thymocyte development and periphery T cells and at higher expression, CD5 is known to respond better to antigen than those with lower CD5 expression [186]. Moreover, mutant IRF5 transcripts with a missense mutation in the DNA binding domain of IRF5 were detected in the number of malignant T cells such as CEM and ATL [187]. It was been described as a dominant-negative mutant by interacting with wildtype IRF5 leading to the inhibition of IRF5 DNA binding and transactivation activity [187]. Recently, Ishikawa et al. reported that IRF5 was constitutively expressed in three distinct spliced isoforms: V1, V3, and V4 in all Human T cell leukaemia virus type 1 (HTLV-1) -infected T cell lines [18]. The IRF5 expression in these infected T cells was induced by a viral oncoprotein Tax which plays an important role in HTLV-1 replication. This protein could directly bind to IRF5V3 promoter, indicating that IRF5 is a Tax-regulated gene. However, high expression of IRF5 was also detected in ATL-derived T cells that do not express Tax protein, indicating that IRF5 could act independently of the Tax protein. Hence, it will be interesting to see how IRF5 expression is associated with the pathogenesis of HTLV-1 related diseases such as ATL.

1.2.4.6.2 Roles of IRF5 in T cells activation

Following antigen stimulation, T cells are activated and undergo changes in their surface markers as described earlier. These expressed molecules dictate the functional responses, including proliferation and differentiation of T cells to effector and

memory cells. Multiple studies have shown poor T cell activation in several murine SLE models with IRF5 deficiency. In particular, $Irf5^{-/-}$ RII Yaa lupus mice had significantly reduced activation markers such as CD69 and CD44 on splenic T cells due to a lower number of T cells expressing these markers [188]. Likewise, Yasuda et al. reported that $Irf5^{-/-}$ MRL/lpr mice had considerably lower splenic CD4$^+$ T cell numbers, suggesting that IRF5 may regulate T cell activation by controlling the T cell numbers [189]. However, the mechanisms on how IRF5 regulates the T cell numbers remain unknown. In another study, Xu et al. reported that the CD69$^+$ T cell subsets were largely abolished in $Irf5^{-/-}$ pristane-treated mice [15]. However, it is important to note, that the observed effect in this study was a consequent from impaired production of type 1 IFN in $Irf5^{-/-}$ mice rather than an IRF5 intrinsic effect on T cells, therefore suggesting IRF5 induced- type 1 IFN promotes T cell activation in pristane-treated mice. Together, these data indicate that IRF5 plays an important in T cell activation in lupus-induced mice.

1.2.4.6.3 Roles of IRF5 in T helper responses

In view of Th response driven by IgG subclasses, $Irf5^{-/-}$ showed impaired IgG1 and IgG2a/c production which are known to be associated with developing Th2 and Th1 responses, respectively [190]. Thereby, suggesting that IRF5 may play a crucial role in Th1/Th2 polarisation and it was confirmed later by numerous findings highlighting how IRF5 alters Th responses. For instance, Paun et al. showed $Irf5^{-/-}$ mice infected with *L. donovani*, had impaired Th1 response corresponding to defect in generating IFNγ CD4$^+$ T cells which are essential for Th1 differentiation [17]. Notably, liver of

Irf5^{-/-} mice infected with *L. donovani* had a significant reduction of IFNγ but higher expression of IL-4 and IL-10 mRNA compared to wildtype (WT) mice indicating a shift to Th2 cytokine expression due to lack of Th1 polarisation [17]. Also, IRF5 was shown to be involved in Th1/Th17 responses. Overexpression of IRF5 in macrophages co-cultured with human T cells were able to induce Th1 and Th17 responses by providing the necessary cytokine environment and upregulation of the T-bet and RORγt transcription factors for expansion and activation of Th1 and Th17 lineage respectively [191]. Moreover, the lack of IRF5 has been implicated with reduced Th1/Th17 responses during chronic inflammation in antigen-induced arthritis mice [192]. In a separate report, IRF5 was shown to have direct involvement in IFNγ and IL-17 CD4^{+} T generation when lymph node migratory DCs of *Irf5*^{-/-} mice sensitised with HDM and c-di GMP induce severe asthmatic (SA) phenotypes [193]. Furthermore, whole lung tissues of *Irf5*^{-/-} mice subjected to SA model, displayed higher mRNA expression for IL-4, IL-5, and IL-13 consistent with the observation seen in the lymph node cultures, hence supporting the idea that lack of IRF5 could promote Th2 responses and even in immunised mice that display Th1 and Th17 responses [193]. Similarly, a separate report by Bryne et al. showed that adoptive transfer of alveolar macrophages from *Irf5*^{-/-} mice into WT mice resulted in heightened airway hyper-reactivity and Th2 cytokines, particularly increased of IL-13^{+} CD4^{+} T lymphocytes as well as IL-13 secretion in the pulmonary environment after the exposure to house dust mite [20]. Moreover, in diabetic model rat lacking IRF5 specifically in the macrophages displayed increase of CD3^{+} T cells and upregulation of Th2 markers (GATA3 and IL-4) and IL-10 expression and

downregulation of Th1 markers (T-bet) in pancreatic islets [194]. Similar findings were observed in *Irf5*^{-/-} obese mice, as CD3^{+} T and GATA3^{+}IL-13^{+} Th2 cells were increased as well as the level of IL-5 and IL-13 [195]. Furthermore, in the hepatic stress-induced model, lacking IRF5 specifically in hepatic macrophages showed polarization to type 2 immuno-regulatory responses due to significant increased IL-10 associated with the expansion of FoxP3^{+} CD4^{+} T regulatory cells and as expected both IFNγ and IL-17 levels were reduced [196].

In *Irf5*^{-/-} pristane-treated mice, Feng et al. observed no changes of serum level Th1 cytokine, IL-12p40 but increased serum level of Th2 cytokines; IL-4, IL-5, and IL-10, which provided disease protection by driving IgG1 production (least pathogenic antibody), suggesting negative regulation of IRF5 in Th2 responses [197]. On the contrary, Xu et al. reported that IFNγ, IL-12p40/70 and IL-23 were downregulated while IL-4 cytokine was upregulated in pristane-treated *Irf5*^{-/-} mice [15]. Further investigation in the same study, revealed that the Th1/Th2 cell ratio was decreased in *Irf5*^{-/-} due to increase of IL-4 producing cells and similar findings were seen in type 1 IFN receptor-deficient mice (*IFNAR*^{-/-}), indicating that skewing to Th2 was due to diminished production of type 1 IFN and altered cytokine production in pristane-treated *Irf5*^{-/-} mice rather than the intrinsic role of IRF5 expression in T cell.

In stark contrast to previous findings that showed lack of IRF5 mounted lower Th1 and Th17 responses and shifted to Th2 responses, a Th1 type polarisation was observed as represented by the high IFNγ mRNA level but lower IL-4 and IL-6

58

mRNA level in the lungs and skin when $Irf5^{-/-}$ mice of bleomycin (BLM) -treated SSc were used [14]. Interestingly, IRF5 was found to bind to the T-bet promoter in CD4^{+} T cells suggesting that in the absence of IRF5, T-bet transcription factor may promote Th1 polarisation; therefore, IRF5 may serve as a repressor for the T-bet gene [14]. In view of this finding, the binding of IRF5 to the T-bet promoter was repressed in TLR4^{-/-} CD4^{+} T cells, thus indicating TLR4-activated IRF5 is directly involved in the suppression of Th1 cell differentiation [14]. This is in contrast with another study whereby IRF5 was shown to upregulate T-bet for expansion and activation of Th1 cells since the expression of mRNA for T-bet was significantly induced in human T cells co-cultured in IRF5 expressing macrophages [191]. Additional work is required to elucidate the underlying mechanism of transcriptional regulation of IRF5 on T-bet promoter in human T cells. In addition, the discrepancy of IRF5 in regulating Th1 response may differ due to animal models with different disease settings and differences in vitro and in vivo settings. Another possibility could be due to the effect of different TLR-mediated signalling in the activation of IRF5. TLR-7 mediated IRF5 activation has been reported to be necessary for the development of Th1 response in parasitic infection [17] on the other hand, TLR4-mediated IRF5 activation was shown to contribute Th2/Th17 inflammatory responses associated with SSc [14]. Collectively, IRF5 plays a pivotal role in modulating T helper responses by altering the functions of APCs such as macrophages and dendritic cells and influencing the cytokine production that drives the Th differentiation as well as participates in activation downstream of TLR-mediated signalling.

1.2.5 Gene transfer

1.2.5.1 Principles of gene transfer

Gene transfer is the process of delivering exogenous genetic materials into host cells. The use of mammalian cells as expression systems has been widely established to study the function of genes and production of recombinant protein [198]. Over the years, numerous developments in gene delivery methodologies have helped researchers to understand diverse biological processes through the manipulation and analysis of gene expression and its mechanism of regulation. Moreover, gene delivery is an indispensable genetic tool for various applications such as i) gene therapy, ii) production of recombinant proteins and vaccines, and iii) generation of transgenic cell lines and animals for research studies [199]. Delivery of exogenous genetic materials (e.g., DNA, siRNA) can be accomplished by using vectors that act as a vehicle to carry genes of interest into host cells. In general, vectors can be categorized into viral and non-viral vectors [199,200]. Viral vectors consist of viruses such as adenoviruses, retroviruses, and lentiviruses which deliver nucleic acids efficiently into target cells through infection [199–202]. Whereas the non-viral vectors (plasmids and DNA transposons) use either physical method (microinjection, electroporation, gene gun, and hydrodynamics application) or chemical method (polymers, liposomes, dendrimers, cationic lipid systems, and nanoparticles) [199–202] as the mode of delivery.

Regardless of the mode of delivery, gene transfer principles are categorized into three stages. First, the exogenous materials must be able to pass through the cell

membrane, then released into their targeted site and finally, the exogenous materials must be competent enough to be activated and interact with the host genome if necessary [199]. The process of understanding the function of a gene involves the manipulation of gene expression which can be achieved by overexpression (gain-of-function), reduction or inactivation of expression (loss-of function) of the targeted gene in a chosen model [203]. Gene transfer into host cells can result in short-term gene expression (transient) or long- term expression (stable). The transient expression refers to transfected DNA that is transferred temporarily and is not integrated into the host chromosome [198,199]. While stable expression is when transfected DNA is integrated into the chromosome and the recipient cells exhibit permanent changes in the expression [198,199].

1.2.5.2 Plasmids as vector

Plasmids are naturally occurring extrachromosomal DNA that can replicate independently and can be found in microorganisms such as bacteria, archaea, and yeast [204]. Most plasmids are circular and vary in sizes. They confer antibiotic resistance and virulence genes that are essential for the survival of their host cells under adverse conditions [204,205]. Plasmids are valuable tools in molecular biology as their easier to manipulate *in vitro*. To date, there are varieties of commercially available plasmids that are derived from natural plasmids or artificially construct as vectors for carrying gene of interest for various research application. Examples of the types of plasmids routinely used in molecular biology research are cloning plasmids, expression plasmids, reporter plasmids, viral plasmids, gene-knock plasmids and

genome engineering plasmids. The basic components of these constructed plasmids comprise of i) origin of replication (ori) which allows independent replication within the host cells, ii) multiple cloning sites (also known as polylinker) cleaved by restriction enzymes for insertion of the gene of interest and iii) selection markers such as gene encoding antibiotic resistance or metabolic enzymes that help with the identification of cells that uptake the plasmid [204–206]. In addition to these basic elements, other elements are combined for constructing plasmids to meet the objective of research study.

1.2.5.2.1 Cloning vector

The cloning vector provides backbone for the insertion of DNA interest and produces numerous copies of the DNA, through their replication and propagation in host organisms such as *E.coli* [207,208]. The number of plasmids (copy number) that can be propagated in host cells depends on factors such as the size of plasmid and the type of origin of replication [204]. Cloning of plasmids in *E.coli* is fast compared to other organisms and there are many diverse types of *E.coli* strains that can be used to propagate plasmids depending on the characteristics of the plasmids and their application [209]. The basic concept of cloning involves the process of cleaving vector with restriction enzymes to insert DNA fragment that is flanked with the same restriction enzyme sequences and recombined through an enzyme (ligase or topoisomerase) [206]. Over the past decade, with technological advancement cloning process has been tailored to be quick, easy, and efficient. One such example is the

application of TOPO cloning technology which is specially designed for the cloning of PCR products.

In this study, the cloning vector pCR-Blunt II-TOPO designed from TOPO cloning technology is used. This cloning vector contains the origin of replication sequences derived from the pUC plasmid family. Furthermore, it confers kanamycin resistance and allows propagation in *E.coli* strain such as Top 10 and DH5α competent cells in high copy number. The principle of TOPO cloning involves cloning of blunt-end PCR product (amplified DNA fragment) without the use of traditional restriction enzyme and ligase reagents separately. The blunt end PCR product is usually generated with the use of high fidelity Phusion DNA polymerase that exhibits 5' to 3' polymerase activity and 3' to 5' exonuclease activity [210].

1.2.5.2.2 Mammalian expression vector

Expression vectors allow transcription of the gene of interest and translation of its protein product [207]. Like cloning plasmid, expression plasmid has the basic components consisting of origin of replication, multiple cloning sites and selectable markers. In addition to these features, elements such as the promoter and regulatory sequence which are required for gene expression and protein synthesis are included [211]. The additional elements of the plasmids depend on compatibility of expression systems of the host cells. In the case of mammalian cells, the extra essential components of the expression vector include target promoter that drive gene expression and mRNA processing signals (e.g., mRNA intervening sequences, mRNA

cleavage, polyadenylation at the end of transcribed pre-mRNA) [198]. Most of the time, constitutive promoter derived from viruses such as the adenovirus major late promoter, human cytomegalovirus (CMV) immediate early promoter, Rous sarcoma virus (RSV) promoter, or Simian virus 40 (Sv40) early promoter are used as the specific promoter for mammalian cells [198]. Alternatively, for some application that requires induction of gene expression that could potentially be cytotoxic, inducible based promoter derived from bacterial repressor-operator sequences such as lactose (Lac) or tetracycline resistance (Tet) operon are utilized [198,212]. Moreover, other elements such as enhancers, introns, internal ribosome entry site, and chromatin remodelling factors may be included to increase the expression levels [212]. Unlike in bacteria cells, plasmids in mammalian cells do not replicate independently under the function of origin of replication [213]. Instead, viral-based for the origin of replication such as SV40 in the plasmids' sequence allows episomal-viral based replication cell lines that are infected with SV40 or express SV40 large T antigen [198,213].

In this study, pcDNA 3.1 (+) expression vector (Invitrogen, USA) that is designed for mammalian cells were used. The promoter of this vector is derived from immediate early promoter CMV, which is active in various cell types and can result in high level expression [198,214]. The multiple cloning sites of this vector are in the forward direction facilitating insertion of the gene of interest that is restricted by many different enzymes. In addition, this plasmid vector contains antibiotic resistance genes as selectable markers; geneticin for mammalian cells and ampicillin for bacterial cells.

1.2.5.2.3 Lentiviral vector

Gene transfer mediated by viruses is highly efficient due to their natural ability to infect cells. However, concern over safety and toxicity issues due to the possibility of producing WT infectious viruses has led researchers to explore various strategies to improvise the use of viruses as vectors through generation of recombinant viral vectors. One such approach is to design recombinant viral vectors with some of their virulence elements removed or replaced [199]. The recombinant viral vector can be generated by splitting the necessary components of the viral genomes into several plasmids. The process of plasmids-based systems for the generation of recombinant viral particle involves co-transfection of the plasmids into a producer cell line of which the viral particles are assembled and released into the culture media.

Lentiviruses are enveloped RNA viruses that belong to the retroviruses (*retroviridae*) family which convert their RNA into cDNA by reverse transcriptase to integrate into the host genome for replication [215]. Lentivirus that infects humans is known as the human immunodeficiency virus (HIV). Lentiviral vector derived from HIV has been widely used as a gene delivery tool as it provides stable and long-term gene expression in a wide variety of mammalian cells including non-dividing primary cells like neurons [216]. Besides that, it serves several benefits such as the ability to carry large inserts and exhibit low immunogenicity after some modification in the vector design.

The viral genome of lentivirus consists of env, gag, and pol which encodes for the viral glycoprotein, structural proteins, and reverse transcription and integration respectively and are framed by elements called long terminal repeats (LTRs) that are required for integration into the host genome and controlling gene expression [217–219]. In addition to these genes, HIV contains the accessory genes (*vif*, *vpr*, *vpu*, and *nef*) which encode for virulence factor and regulatory genes (*tat*, *rev*) that encodes for its replication [217–219]. Generation of viral vector particles depends on multiple plasmid proteins of which the genes are genetically separated, for instance, a) packaging plasmids that consists of *gag*, *pol*, *tat*, and *rev* genes that are required viral particle formation, b) transfer vector bearing the expression cassette for transgene insert, c) envelope glycoprotein for infectivity [220–222]. The production of recombinant lentivirus involves co-transfection of the plasmids into a producer cell line.

To date three-generation systems of HIV type 1 based lentiviral vector have been generated. The first-generation system closely resembles the WT HIV genome except that the packaging systems are modified whereby the helper plasmid that encode *gal-pol* and the envelope plasmid are driven by heterologous promoter rather than the viral LTR and the envelope HIV glycoprotein (gp120) is usually replaced with Vesicular stomatitis virus glycoprotein (VSV-G) to target for broader host cells [219,220]. The second and third generation vectors are designed such that the necessary components for virus production are split for increased biosafety of the use of lentiviral in the laboratory. In the second-generation system, the accessory genes

are removed from the packaging systems whereas in the third generation the packaging system is separated into two plasmids and *tat* gene is removed; (*gal* and *pol*) and (*rev*) [215,219–221]. In addition, the transfer vector in the third generation is modified such that a chimeric 5'LTR is fused to a heterologous promoter such as CMV or RSV and the U3 3'LTR is deleted from the viral genome to create self-inactivating vector which is replication- incompetent [202,215,219,222]. Of note, replacement of strong viral promoter or enhancer with a hybrid heterologous constitutive promoter reduces insertional mutagenesis and immune genotoxicity because of the absence of virulence factors, the third-generation lentiviral system is considered safe even to be used in clinical studies [215].

In this study, pLenti CMV GFP Puro, a third-generation lentiviral eGFP expression vector was used to carry the IRF5 cDNA construct. This lentiviral vector is a *tat* independent and self-inactivating lentiviral vector with puromycin drug selection and green fluorescence protein, (GFP) a reporter gene expression under CMV promoter (11). The GFP expression was used as an internal control to evaluate the transfection efficiency for the generation of recombinant lentivirus particles. In a second-generation lentiviral vector system, three plasmids are involved to produce virus. The second-generation system's transfer vector can only be packaged with second generation packaging system which encode *gag*, *pol*, *rev*, and *tat* because of the use of viral 5'LTR encoding the gene of interest is *tat* dependent (Figure 1.6). Whereas in third-generation system, the sequence is flanked with chimeric 5' LTR with a heterologous constitutive active promoter, hence *tat* is not necessary. The third-

generation system involves the co-transfection of four plasmids to produce virus (Figure 1.7). However, a third-generation system's transfer vector can be co-transfected together with either second (two plasmids) or third generation (three plasmids) packaging systems (12). Given that the use of four plasmids in third-generation lentiviral vector system can be cumbersome due to the addition of a plasmid in co-transfection in the packaging system, the second-generation packaging system (two plasmids, psPAX2 and PMD2G) was chosen to be transfected with third generation transfer vector (pLenti CMV GFP Puro) to produce recombinant lentivirus in this study.
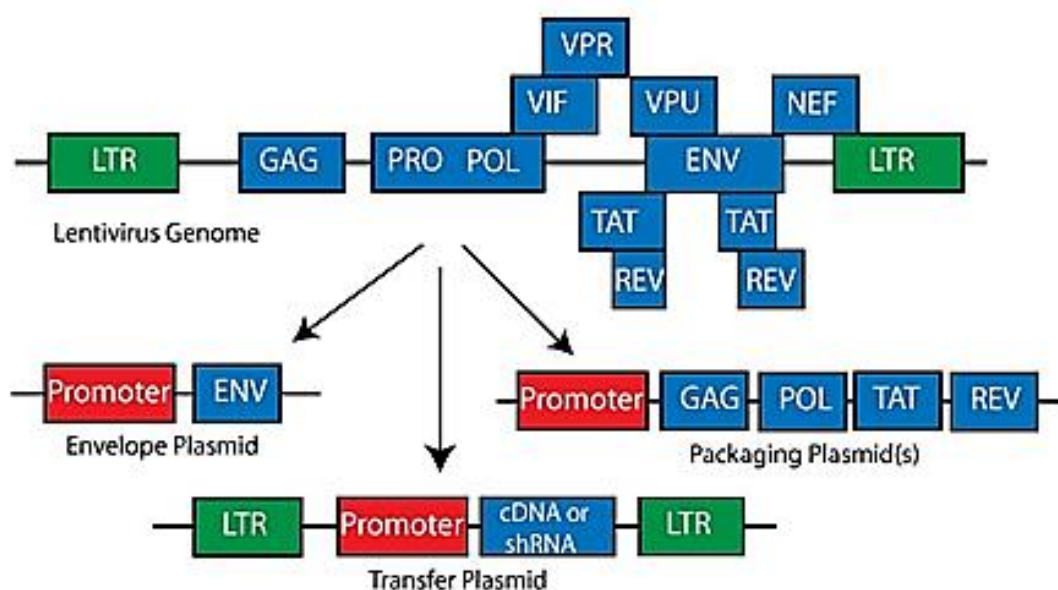
Figure 1.6 Schematic illustrations of the 2nd generation lentiviral plasmid. Image obtained from Addgene website.
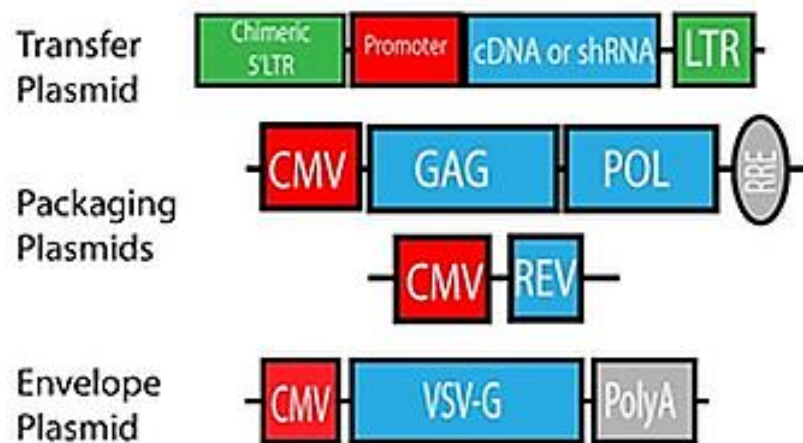
Figure 1.7 Schematic illustrations of the 3rd generation lentiviral plasmid. Image obtained from Addgene website.

1.2.5.3 Cell lines

1.2.5.3.1 Human embryonic kidney cells (HEK) 293T cells

These cells are derived from HEK cells that were transformed by adenovirus type 5 fragments [223]. Generation of HEK 293T cells involve the insertion of a temperature-sensitive version of simian virus 40 (SV-40) large T tumour antigen plasmid into HEK 293 cells [224,225]. The permissibility of transfection of 293 cells along with SV40T aids in the extra-chromosomal amplification of HIV-1 plasmid containing SV40 origin of replication makes it suitable for the production of HIV-1 based lentiviral vector particles [225]. The HEK 293 cells and its derivatives cells are widely used in cell biology and biotechnology for the various application including, small scale protein production, studying protein interaction and signal transduction, viral packaging, and biopharmaceutical [226]. Moreover, they are easy to manipulate to rapidly produce recombinant proteins via transient and stable gene expression [214,227]. In addition, these cells are also known to have high transfection efficiency and effectively generate functional proteins through proper translation machinery [227,228]. In this study, HEK 293T cells were used for transient transfection for the production of recombinant IRF5 proteins to examine DNA-protein interaction through pull-down assay and transcriptional activity on *Il13* promoter luciferase reporter assay. The cells were also used for the production of lentiviral particles obtained by transient transfection of lentiviral transfer, packaging, and envelope plasmids. Transfection of DNA into cells can be achieved through physical or chemical methods and each method has its own advantages and limitation [200,202,212]. Herein, the transfers of plasmids into HEK 293T cells were mediated by non-liposomal polymeric

Mirus Trans-IT X2 transfection reagent. The advanced formula of the transfection reagent is made of a combination of polymers and lipids which form a complex with negatively charged DNA, resulting in a positive net charge. The complex is now able to pass through the negatively charged cell membrane, facilitating the delivery of DNA into the cytoplasm compartment through endocytosis.

1.2.5.3.2 Jurkat cells

Using primary CD4$^+$ T cells allows researchers to have the opportunities to mimic *in vivo* environments as they exhibit normal physiology. For this reason, it makes primary cells as the ideal model to study immune responses. However, there are several disadvantages working with primary cells. One of the most challenging issues working with primary cells is that they have a short lifespan and difficult to cultivate continuously because they stop dividing after several passages (senescence). Hence, it is difficult to conduct overexpression or knockdown studies in primary cells. In addition, researchers often have to deal with issues with donors' variabilities in genotypes and phenotypes when working with primary cells. In accordance with these challenges, working with immortal cell lines often preferable as some of the difficulties aforementioned earlier can be overcome. Cell lines are convenient to cultivate, reproducible as they are derived from a homogenous population and they are easier to manipulate; to overexpress or knockdown particular gene of interest.

One of the most used cell lines in immunological studies are Jurkat cells. Jurkat cell lines are T cell leukemic cells established from the peripheral blood of 14-year-old with acute lymphoblastic T leukaemia that is originally known as the JM cell line [229]. Initial studies using this cell line found that the cells were heavily contaminated with mycoplasma and the process of eliminating the infection yielded healthy Jurkat cells named as the E6.1 clone [230]. A search through the cell library (American Type Culture Collection) revealed that there are many subclones of Jurkat cells that are modified from the WT E6.1 clone to lack certain genes. These mutants Jurkat subclones have been used as a model in numerous studies including TCR signaling, HIV infection, apoptosis, and necrosis pathway [230–233]. The E6.1 clone (refer to Jurkat cells in this thesis) expresses TCR and invariant signalling CD3 subunit and the standard cell line used by researchers [230]. Within the literature, Jurkat cells have been the popular human T cell line modelling primary CD4 T cells in the study for cytokine production [230,234–237]. Although Jurkat cells as immortalized T cells are not exact representatives of CD4 T cells, the signalling process for cytokine production appears to be similar [238]. As described in section 1.2.2.3.2, CD4$^+$ T cells are activated in response to cross-link of TCR/CD3 with MHC II complex followed by co-stimulatory CD28 molecule which triggers a cascade of signalling pathways that lead to activation of transcription factors which in turn activate various cytokines gene programmes, involved in T cells proliferation, survival, and effector functions. In an equivalent manner, Jurkat cells can be activated in response to co-stimulation of anti-CD3/CD28, and mitogens such as Concanavalin

A (ConA), combination of PMA and Ionomycin that mimic the physiological responses for T cells activation [230,237–239].

Available literature showed that cytokines profiles are restricted depending on the mitogens and physiological stimuli. For example, stimulation of Jurkat cells with conA is mainly restricted to IFNγ, IL-2, and IL-10 secretion [237,240]. On the other hand, stimulation with the physiological anti-CD3/CD28 was limited to IL-2 and IL-8 [234]. Previously a study done by Hu et.al used co-stimulation of PMA and Ionomycin to study Th1 and Th2 associated cytokine profiles (IFNγ, IL-2, IL-4, IL-5, IL-10, and IL-13) in Jurkat cells transfected with IRF4 [145]. The exact reason these mitogens produce different cytokine profiles are not clearly understood, although the mechanism of T cell activation is well established. For example, ConA is a plant lectin that works via TCR-CD3 complex (TCR dependent) which leads to activation of calcineurin and PKC signaling pathway in Jurkat to activate cytokine production [237]. Whereas, PMA and Ionomycin activate T cell activation bypassing the proximal signalling of TCR pathway (TCR-independent) [237,241]. Precisely, PMA mimics DAG which activates T cells via PKC pathway, whereas Ionomycin, activates Ca^{2+} calcineurin pathway leading to stimulation of transcription factors involved in modulating cytokines gene expression [237,242]. In this study, we adopted a similar approach to investigate the modulation of IRF5 in the Th1/Th2 cytokine profiles as upper mentioned in response to co-stimulation of PMA and Ionomycin. However, instead of using transfection by electroporation conducted by Hu and colleagues in the

aforementioned study, we used lentivirus to carry IRF5 into the genome of Jurkat cells. Jurkat cells are susceptible to viral entry as studies have demonstrated that HIV-based vector could efficiently deliver genes of interest into Jurkat cells [243–245]. In this notion, we used a lentiviral vector to deliver IRF5v4 and IRF5v5 cDNA into Jurkat cells to generate stably expressing IRF5 in Jurkat cells to study its ability to modulate the expression of Th1 and Th2 cytokine.

Chapter 2

2 Methodology

2.1 General Methods

2.1.1 Primers Preparation

All primers used were purchased from Integrated DNA Technologies (First Base Sdn. Bhd). Upon receiving, the lyophilized primers were briefly spun and dissolved with nuclease-free water (Amresco, LLC) to a final concentration of 100 μM. The working concentration for the primers was prepared by diluting the stock 1:10 with nuclease-free water, to a final concentration of 10 μM.

2.1.2 Polymerase Chain Reaction (PCR)

All reagents were thawed on ice and prepared according to the manufacturer's instructions. In general, 25 μl of PCR reaction per tube was prepared. A negative control without DNA template was included. Several types of DNA polymerases were used depending on the experiments. The PCR conditions and cycling of each experiment is described specifically in respecting sections. The PCR products were stored at -20^0C.

2.1.3 Agarose Gel Electrophoresis

2.1.3.1 Preparation of agarose gel

Ultrapure agarose powder (Vivantis Technologies Sdn Bhd) was weighed and added in 1x Tris-Borate- Ethylenediaminetetraacetic acid (EDTA), (TBE) (detail recipe of 1 x TBE is attached in Appendix-1.1) to a final concentration of 1.0% or 1.5% (w/v) in a conical flask depending on the experiment. The solution was dissolved by heating using the microwave. The gels were either stained before casting or after running. For pre-cast staining, 1 µl of GelRed nucleic acid stain (Biotium, Inc) was added and swirled gently to mix the solution. The gel was poured into a gel-casting tray with an appropriate comb and was allowed to solidify at room temperature for 20 to 40 minutes before use. For the post-staining method, the procedure is described in section 2.1.3.3.

2.1.3.2 Loading of samples in agarose gel

Solidified agarose gel was placed into Bio-Rad horizontal gel tank (Biorad, US) and covered with 1x TBE buffer up to the mark indicated in the tank. The comb was then gently removed. DNA samples were mixed with 6x loading dye (Vivantis Technologies Sdn Bhd) and 5 to 10 µl of the mixtures were loaded into each well. Gene Ruler 1kb Plus DNA ladder (Thermo Fisher Scientific, US) was also loaded along with the samples.

2.1.3.3 Gel running and DNA visualization

The Biorad electrophoresis unit was connected to the power supply and run at 80 Voltage (V), until the bromophenol dye line was a three-quarter down way of the gel. If DNA staining was added during the gel preparation (pre-cast gel), after the run, the gel image was directly captured on a UV transilluminator or image analyzer Biorad Gel Doc or Syngene (Synoptics,Ltd). While for the post-staining procedure, after the run, the agarose gel was placed in a container containing enough 3x gel staining solution to cover the gel. The immersed gel was incubated with rocking on a shaker for 15 minutes if it was freshly prepared and rinsed with water. For subsequent use, the gel was stained for 30 minutes and rinsed with water prior to viewing the gel. The prepared staining solution was reused up to five times within a week by placing the solution in a container protected from light.

2.1.4 DNA Extraction and purification from agarose gel

Desired fragment DNA was extracted from the gel using PureLink Quick Gel Extraction (Invitrogen, Thermo Fisher Scientific, US) according to the manufacturer's instructions. Briefly, the desired DNA band was excised using a clean scalpel. The extra gel that surrounded the desired band was trimmed to minimise the amount of gel. The gel was placed into a 1.5ml microcentrifuge tube (Bio plas, Inc) and weighed using weighing scale. It was made sure that the amount of gel did not exceed 400 mg. Next, gel solubilisation buffer was added into the tube containing excised gel at the ratio of 3:1. The tube was then placed in a water bath set at 50^0C for 10 minutes. Every three minutes, the tube was inverted to mix and ensured that the gel was

dissolved. The dissolved gel was incubated for an additional five minutes. Once the gel was completely dissolved, one gel volume of isopropanol was added to the dissolved gel and mixed well to increase DNA yields. The following steps involved binding of DNA into the extraction column and washing using the provided washing buffer and purified using centrifugation method as described in the manufacturer's manual. The purified DNA in the recovery tube was stored at -20^0C.

2.1.5 Measurement of nucleic acids concentration and purity

Microplate reader (EPOCH BioTek, BioTek Instruments Inc) or Nanodrop Spectrophotometer (Biodrop, UK) was used to measure DNA and RNA concentration. Each time before and after use, 10 µl of distilled water was added on the microspots and wiped with kimwhite tissue. Blank consisting of 2 µl nuclease-free water or RNase-free water (Qiagen, Germany) was first loaded and the instrument was set for reading samples. The same amount of sample was loaded and the absorbance was read.

2.1.6 Cultivation and Storage of Bacteria

Competent cells of *Escherichia coli (E.coli)* strains; Top10 (Invitrogen, Thermo Fisher Scientific, US), Max Efficiency DH5 alpha (DH5α) (Invitrogen, Thermo Fisher Scientific, US) and STBL3 (generously provided by Prof. Madya Dr. Syahrilnizam Abdullah, University Putra Malaysia) were cultured in Luria-Bertani (LB) medium or agar (detail recipe of LB medium and LB agar is attached in Appendix-1.1) supplemented with either 100 µg/ml ampicillin (Amresco, LLC) or 50 µg/ml kanamycin (Amresco, LLC) and incubated at 37^0C for either 8 hours or 16 hours

depending on the experiment. For long term storage of transformed bacteria containing recombinant plasmid, a single colony was picked and cultivated with LB medium containing its resistant antibiotic at 37^0C for overnight. The culture was then mixed with glycerol (Amresco, LLC) stock at a final concentration of 25% v/v (0.8ml of the cultured medium added into 0.8ml of 50% glycerol stock) in multiple vials and froze at -80^OC.

2.1.7 Preparation of competent cells by CaCl2 method

In this study, DH5α and STBL3 competent cells used were prepared in our laboratory. Competent cells were prepared according to Sambrook et.al. [246]. A starter culture was prepared by inoculating a single colony of *E.coli* strain STBL3 in 5 ml of LB medium and allowed to grow at 37^0C overnight with shaking at 200 rpm. The starter culture of 100 µl was diluted into 50 ml of fresh LB medium and was allowed to grow at 37^0C with shaking at 200 rpm. The following day, the growth of bacteria culture was monitored by measuring absorbance at 600 nm using a spectrophotometer at the interval of 30 minutes till optical density reached a mid-log phase 0.4-0.5 (~2-4 hours). From this stage onwards, the cells must remain cold thereby culture was chilled immediately on ice for 10 minutes and swirled occasionally. The bacteria culture was then pelleted by centrifugation at 3000 x g for 10 minutes at 4^0C. The supernatant was decanted and 6 ml of pre-chilled 10 mM MgCl$_2$ was added to the pellet and mixed gently. Next, the cells were incubated on ice for 45 minutes, and centrifuged at 3000 x g for 10 minutes at 4^0C. The supernatant was discarded and 400 µl of pre-chilled 10mM calcium chloride (CaCl$_2$) was added to

re-suspend the pellet, followed by the addition of 60 µl of 80% glycerol. The cell suspension was mixed gently and aliquot 50 µl into pre-chilled a microcentrifuge tubes on ice. The aliquots were immediately frozen and stored at -80^{0}C.

2.1.8 Transformation of competent cells

A tube of 50 µl of competent cells Top10, DH5α, or STBL3 were removed from the freezer and thawed on ice for 2 to 3 minutes. After thawing, 2 µl of plasmid DNA (300 ng-1 µg) was added into the competent cells. The mixture was gently swirled using a pipette tip and incubated on ice for 30 minutes, followed by heat-shocked for 30 seconds in 42^{0}C water bath. The tubes were immediately placed on ice for two minutes and 950 µl of LB media was added to the tube. The tubes were placed on shaking incubator horizontally and shaken at 200 rpm, 37^{0}C for one hour. Following this, 200 µl of the transformed cells were added on pre-warmed ampicillin (100 µg/ml) plates and the cells were spread evenly using a sterile L-shaped "hockey-stick" spreader. The remaining cells on the spreader were spread on another plate. The plates were incubated at 37^{0}C overnight. This step was done to obtain well-separated colonies. The same procedure was done for positive control by using 1 µl of 10 pg of pUC 19 that was provided in the commercialized kit. As for negative control, the same amounts of untransformed cells were plated on the agar plate without selective antibiotic.

2.1.9 Colony PCR

This procedure was performed to detect the presence or absence of recombinant plasmid following transformation. Few transformants were selected using sterile

toothpick by touching on the transformant and immediately transferred on a fresh agar plate containing 50 μg /ml kanamycin or 100 μg/ml ampicillin, depending on the antibiotic resistance gene encoded in the plasmid and incubated overnight at 37^0C. The same toothpick was dipped into a PCR reaction mixture and mixed for few seconds. The PCR conditions and cycling of each experiment are described specifically in respective sections. The PCR products were stored at -20^0C.

2.1.10 Plasmid Isolation

2.1.10.1 Small-scale

For a small scale of plasmid isolation, PureLink Quick Plasmid Miniprep Kit (Invitrogen, Thermo Fisher Scientific, US) was used. Bacteria containing the plasmid to be isolated were amplified in 10ml of LB media with selective antibiotic and grew at shaking incubator at 37^0C, 200 rpm for 16 hours. The plasmid was then isolated according to the manufacturer's instruction. Briefly, the steps involved harvesting the LB cultured by pelleting down the bacterial cells through centrifugation. The supernatant was discarded and the cell pellet was resuspended with resuspension buffer containing RNase A until it was homogenous and then lysed using lysis buffer. The mixture was gently mixed by inverting the capped tube until it was homogenous and incubated for five minutes. Next, the mixture was precipitated using precipitation buffer and centrifuged to isolate the supernatant which was then used to bind to silica membrane columns. The silica membrane column was then spun and washed with washing buffer twice. The purified plasmid DNA was eluted with nuclease-free water and stored at -20^0C.

2.1.10.2 Large -scale

For a large scale of plasmid isolation, Plasmid Maxi Kit (Qiagen, Germany) was used. Bacteria containing the plasmids to be extracted were amplified in a starter culture, consisting of 10 ml of LB media with selective antibiotic and grew at shaking incubator at 37^0C, 200 rpm for 8 hours. Following this, 200 µl of starter culture was diluted in 200 ml of LB medium with selective antibiotic and grew at shaking incubator at 37^0C, 200 rpm for 16 hours. The rest of the steps were done according to the manufacturer's instructions. Briefly, the steps include harvesting the LB culture, resuspending the cell pellet, followed by lysis and precipitation. The isolated supernatant was bound to a Qiagen-tip made of resin and impurities were washed several times with wash buffer. The plasmid DNA was eluted with high-salt buffer and later concentrated and desalted by isopropanol precipitation.

2.1.11 Restriction Enzyme Digestion

All restriction enzymes used were purchased from (New England Biolab, US). The reagents were thawed on ice and prepared as shown in Table 2.1 and performed according to the manufacturer's instruction. Depending on the experiment, either single or double digestion was carried out. If single digestion, only one restriction enzyme was added, while for double digestion, two enzymes were added. Upon adding all the reagents, the mixture was spun briefly by centrifugation. The mixture was then incubated for three hours at 37^0C.

Table 2.1 Reaction mixture for restriction digestion.

Reagents	Working concentration/ Volume
Restriction enzymes *	10U, 0.5 µl
Cut Smart Buffer	10x, 5 µl
DNA	1 µg
Nuclease Free Water	Up to 50 µl

*BamHI, SalI, XbaI, EcoRI or HindIII.

2.1.12 Ligation

Linearized fragments of the vector backbone and insert were excised and purified with a gel extraction kit as described in section 2.1.4. DNA concentration and purity were measured as described in section 2.1.5. Prior to ligation, the mass of insert required for ligation reaction was calculated using New England Biolab ligation online calculator. For the calculation, the length of insert and vector were inserted according to experiments. The vector mass was kept at 50 ng and the molar ratio of vector to insert, 1:3 was used as recommended for cohesive ends. The mass of insert was calculated following the formula as below.

Required mass (g) = desired insert/vector molar ratio x mass of vector (g) x ratio of insert to vector lengths

The linearized fragments of vector and insert were ligated using 0.1 µl, 1U T4 DNA ligase (Thermo Fisher Scientific, US), 4 µl of 5X DNA Ligase reaction buffer (Thermo Fisher Scientific, US) and total reaction volume was brought up to 20 µl with addition of nuclease-free water. The mixture was centrifuged briefly and

incubated at 16^0C for overnight, and later stored in -20^0C prior to transformation as described in Section 2.1.8.

2.1.13 DNA sequencing

DNA sequencing for confirmation of positive constructed plasmids was performed by First Base Sdn. Bhd.

2.1.14 Cell culture

2.1.14.1 Cell lines and culture conditions

The HEK 293T cells (generously provided by Dr. Leong Chee Onn, International Medical University) were maintained in DMEM (Cellgro Mediatech, US) supplemented with 4.5g/L glucose, L-glutamine, sodium pyruvate, 10% heat-inactivated fetal bovine serum, FBS (Sigma Aldrich), and 1% penicillin/streptomycin (Gibco, Thermo Fisher Scientific, US). Jurkat cells (obtained from cell culture bank of University of Nottingham Malaysia Campus) were cultured in, RPMI medium (Cellgro Mediatech, US) supplemented as above, with additional component of 25mM HEPES.

2.1.14.1.1 Thawing of HEK 293T cells

Prior to the thawing of cells, pre-warm complete DMEM media was added into the T-75 flask (Orange Scientific, Belgium). Cryopreserved cells were thawed by immediately immersing the cryovial (SPL Life Sciences, Korea) in a 37ºC water bath. The cells were transferred into the flask containing the culture media and swirled

gently to mix the cells. The flask then transferred into a 5% CO_2 incubator and incubated till late afternoon or evening to allow the cells to attach to the flask. The flask was observed using the light microscope to check whether the cells were attached. Media was then replenished by removing all the media gently and replaced with complete DMEM to the flask. The flask was placed back into the incubator and allowed to grow. The cells were regularly inspected till they reach confluency.

2.1.14.1.2 Thawing of Jurkat cells

Prior to the thawing of cells, pre-warm complete RPMI media was added into the T-25 flask (Orange Scientific, Belgium). Cryopreserved cells were thawed by immediately immersing the cryovial in a 37ºC water bath. The cells were transferred into the flask containing the culture media and swirled gently to mix the cells. The flask then transferred into a 5% CO_2 incubator and incubated till late afternoon or evening to allow the cells to settle at bottom. Once the cells have settled at the bottom of the flask was carefully removed from the incubator without shaking the flask. With gentle aspiration, the supernatant above the settled cells was aspirated out without disturbing the cells and fresh complete media were added into the flask. This was done to ensure that dimethyl sulfoxide (DMSO) in the frozen cells was sufficiently removed, as it can be toxic to cultured cells. The DMSO was not removed by centrifugation to limit stress to the cells. The flask was placed back into the incubator and the cells were inspected the next day for viability of the cells. If the viability was low, the dead cells were removed using lymphoprep (STEMCELL Technologies Inc) as described in the following section.

2.1.14.1.3 Lymphoprep to separate viable and dead Jurkat cells

Lymphoprep is a density gradient medium widely used for the isolation of mononuclear cells by applying the principle of cell density. It can also be used for the isolation of viable cells from a pool of cells containing dead cells especially, for suspension cells. The process of centrifugation allows dead cells and debris to sediment at the bottom, whereas the viable cells form an interphase layer between lymphoprep and culture media. An equal volume of pre-warmed lymphoprep was first added into the conical tube (Orange Scientific, Belgium) was added, followed by cell suspension. The mixture was centrifuged at 600xg for 20 mins without break (acceleration 1 and deceleration 0). Following centrifugation, the topmost layer of the mixture, which appeared distinct due to colour of the culture media, was gently aspirated, leaving about 1 to 2 ml of the media. It was ensured not to touch the interface layer during the removal of the media. Then, the interface layer which was seen as a light band (contain viable cells) in between the media and lymphoprep was gently aspirated into a new tube. The cells were washed with complete media about 10 ml by centrifugation at 1000 rpm for 10 minutes. The supernatant was discarded and the pellet was resuspended with 5- 10 ml of complete media according to the cell pellet. The cells were observed under the light microscope and media was top up if necessary.

2.1.14.1.4 Cells maintenance of HEK 293T cells

As adherent cells, once cells reached about 70-80% confluency, the culture medium was removed by aspiration. The cells were then washed briefly with phosphate buffer

saline (PBS) without Ca^{2+} and Mg^{2+} (Cellgro Mediatech, US). The cells were detached using 0.25% of Trypsin-EDTA (Gibco, Thermo Fisher Scientific, US). To stop the reaction, complete DMEM was added and the mixture was transferred into the centrifuge tube. The cells were spun at 1500 rpm for 5 minutes and the supernatant was discarded to remove trypsin and get rid of dead cells. Complete media was added into the pellet, resuspended, and split at the desired ratio. The cells were observed under the light microscope and placed the flask into 37^0C, 5% CO_2 incubator. The cells were monitored regularly and media was changed after two or three days depending on the confluency.

2.1.14.1.5 Maintenance of Jurkat cells

As for suspension cells, the cells were maintained by the addition of fresh media or replacement of media, without the need of trypsin to detach the cells from flask. The cells were maintained at a cell concentration between 1×10^5 and 1×10^6 viable cells/mL and subcultured every two to three days depending on cell density.

2.1.14.1.6 Counting cells using haemocytometer

For cell counting of HEK 293T cells, the cells were first detached using trypsin followed by inactivation, centrifugation, and re-suspend with complete media as described earlier in the method for cell maintenance. A small aliquot of cells (~0.5 ml) of cells was transferred into a 1.5 ml microcentrifuge tube. Cells were diluted if too dense. Following a proper mix of the cells suspensions, 10 μl of the cells were mixed with 10 μl of trypan blue and loaded into haemocytometer for counting. The total numbers of viable cells were counted following the formula as shown below.

Following counting, appropriate concentrations of cells were seed into flasks or plates according to certain concentrations depending on the experiment. For seeding of 96 wells plate, the desired volume of cells and media were transferred into the reservoir and were aliquoted into the wells using a multi-channel pipettor. For 6 wells plate and culture flasks, the cells were directly seeded containing the appropriate amount of media. In addition to cell seeding, the total number of viable cells was also counted prior to freezing cells.

Formula: $\dfrac{\text{Total number of viable of cells x dilution factor x } 10^4}{\text{Number of squares of counted}}$

2.1.14.1.7 Freezing of cells

The cells were expanded at adequate cell density for the desired number of vials to be freeze. The cells were counted as described above. The number of vials and freezing media were prepared based on the concentrations of cells. After counting, the cells were centrifuged at 1000 rpm for 10 minutes and supernatant was discarded. The freezing media containing 90% FBS + 10% DMSO (Nacalai Tesque, Inc) that has been pre-chilled to cell pellet to achieve a final concentration of 7×10^6 to 10×10^6 cells/ml. The cells suspensions were gently mixed by repeated pipetting up and down. About 1 ml of the cells suspension was aliquoted into each cryovial tubes and stored at -80°C for short-term. For long-term storage, the vials were transferred into a liquid nitrogen freezer after they have been in the -80°C freezer at least overnight.

2.1.15 Gene expression by Reverse transcription PCR (RT-PCR)

2.1.15.1 RNA isolation

Isolation RNA was done using RNeasy mini kit (Qiagen, Germany), through the mini spin column technology according to the protocol provided by the manufacturer. Briefly, the cell pellet was lysed with 350 µl of RLT buffer using pipette by pipetting up and down several times. One volume of 70% ethanol was added to the homogenised lysate and mixed well by pipetting. The lysate was transferred to a RNeasy spin column placed in a 2 ml collection tube and centrifuged for 15 seconds at 8000 x g. The flow-through was discarded and 500 µl of buffer RPE was added to the spin column and centrifuged at the same condition. The flow-through was discarded. This procedure was repeated twice. To eliminate any carryover of buffer RPE, the spin column was placed in a new 2 ml collection tube and centrifuged at full speed for 1 minute. To elute RNA 30 µl of RNase-free water was added. The concentration and purity of RNA was determined as described in 2.1.5. For long-term storage, RNA was aliquoted into few tubes and stored at -80^0C freezer.

2.1.15.2 Genomic DNA elimination

Prior to first-strand cDNA synthesis, RNA was first treated with RQ1 RNase-Free DNase (Promega, US) according to the manufacturer's instruction. Briefly, for every 1µg of RNA sample, 1µl of RQ1 10x Buffer was added, followed by 1 µl of RQ1 RNase- DNase solution. RNase free water was added to final volume of 10 µl. The mixture was mixed gently through pipetting and quickly spun. The mixture was then

incubated at room temperature for 30 minutes. To stop the reaction, 1 µl of RQ1 DNase stop solution was added into the sample and incubated at 65^0C for 10 minutes.

2.1.15.3 RT-PCR

The following reagents; 1 µl of 100 µM Oligo (dT) 18 primer (Thermo Fisher Scientific, US), 1 µl of 10mM dNTP mix (Bioline, US), 4 µl of 5X ProtoScript II RT Reaction Buffer (New England Lab, US), 2 µl of 0.1M DTT (New England Lab, US) and 1 µl of ProtoScript II Reverse Transcriptase (New England Lab, US) were added into the tube containing 10 µl of RNA sample mixture that was treated for genomic DNA elimination as described in above section 2.1.15.2. The samples were incubated at 42^0C for 50 minutes, followed by inactivation of the enzyme at 85°C for 5 minutes. The reaction product of the first-strand cDNA synthesis was used diluted with nuclease-free water at 1:20 ratio and used as template for PCR. The PCR reagents comprising of reaction buffer, $MgCl_2$, dNTPs and Biotaq polymerase used were purchased from Bioline, US. The PCR reaction was prepared as in Table 2.2 and carried out using Biorad Thermocycler (Biorad) as in Table 2.3.

Table 2.2 Reaction mixture for RT-PCR.

Reagents	Volume (µl)
Nuclease free water	9.25
10 x NH_4 reaction buffer	2.5
50 µM $MgCl_2$	0.5
10 mM dNTP	0.5
10 µM Primer F	1.0
10 µM Primer R	1.0
BioTaq Polymerase	0.25
cDNA (template)	10.0
Total volume	25

Table 2.3 Condition for RT-PCR cycling.

Steps	Temperature	Time	Cycling
Initial denaturation	94^0C	2 minutes	1x
Denaturation	94^0C	30 seconds	
Annealing	*58-60^{0}C	20 seconds	*20-35x
Extension	72^0C	20 seconds	
Final extension	72^0C	10 minutes	1x
Cooling	4^0C	indefinite	1x

*Annealing temperature and cycling number differs between target genes

2.1.16 Western blot analysis

2.1.16.1 Whole cell protein extraction

For sample preparation, $2x10^6$ cells were harvested and pelleted by centrifugation at 1000 rpm for 10 minutes at room temperature. The cells were washed with ice-cold PBS twice to remove any remaining media. To dissolve the cell pellet, 1 ml of PBS. The cells were then transferred into a 1.5 ml tube and centrifuged. The supernatant was removed by careful pipetting. To lyse the cell pellet, 40 μl of radioimmunoprecipitation assay (RIPA) lysis buffer (detail recipe of RIPA buffer is attached in Appendix-1.1) containing halt protease inhibitor cocktail (Thermo Fisher Scientific, US) was added to the cell pellet and vortexed briefly to ensure proper mix. The sample was incubated for 30 minutes on ice. For complete lysis, the tube was immersed into liquid nitrogen to freeze and later thawed on ice and vortex briefly. The freeze-thaw procedure was done five times. The lysate was then centrifuged at 10,000 x g for 10 minutes at 4^0C to pellet any cell debris. The supernatant containing soluble protein was carefully transferred into a new tube kept on ice.

2.1.16.2 Bicinchoninic acid (BCA) protein assay

Concentrations of protein were quantified using Pierce BCA Protein Assay kit (Thermo Fisher Scientific, US) in 96-well plate (Orange Scientific, Belgium) according to the manufacturer's instructions. To prepare the working reagent, Reagent A was mixed at a 50:1 ratio to Reagent B and 200 μl of the mixture was added to each well. Samples were aliquoted at 25 μl/well in duplicate. The bovine serum albumin (BSA) standard that was provided in the kit was diluted to 20 – 2000 μg/ml and used to generate the standard curve. Once completed, the plate was covered and incubated at 37^0C for 30 minutes. Absorbance was read at 562nm using a microplate reader.

2.1.16.3 Sodium dodecyl sulphate-polyacrylamide gel electrophoresis (SDS-PAGE)

A SDS-PAGE gel consists of resolving and stacking gels. The resolving gel also known as the separating gel forms the lower section of the SDS-PAGE and the stacking gel forms the upper section of the SDS-PAGE gel. The final concentration of bis-acrylamide used for the resolving gel was 10% and for the stacking gel, was 4%. The gel mixtures of resolving and stacking gels were prepared following the order as written in Table 2.4 below. The resolving gel mixture was pipetted quickly into the assembled BioRad Mini-PROTEAN Gel System (Biorad, US) and overlaid with isopropanol (Fisher Scientific, UK). Isopropanol was added to remove any bubbles and to ensure even gel formation. Once the resolving gel was polymerized, overlaid isopropanol was discarded. The stacking gel mixture was pipetted over the top of the resolving gel and gel comb was placed immediately. Equal volume of 40 μg samples

and 2X Laemmli sample buffer (Biorad, US) containing 5% β-mercaptoethanol were mixed (Sigma Aldrich) and denatured by incubating in a thermocycler at 95^0C for 5 minutes. The samples were then kept on ice for cooling. Once the stacking gel polymerized, the gel cassette was placed into the inner chamber of the gel tank and 1x running buffer (detail recipe is attached in Appendix-1.1) was filled till full and the comb was removed gently. Equal amounts of samples, 5 µl were loaded into wells of the gel along with 5 µl of Spectra broad range multicolour protein ladder (Thermo Fisher Scientific, US). About 200 ml of 1x running buffer was filled outside the inner chamber of the gel and the lid of tank was covered. The gel was run at 120V, 400mA for 1 hour 20 minutes until the line of dye reached the bottom of the gel.

Table 2.4 Solutions for preparing resolving and stacking gels.

Resolving (10%)		Stacking (4%)	
ddH$_2$O	4.0 ml	ddH$_2$O	3.0 ml
1.5M Tris-Cl (pH 8.8) (Biorad, US)	2.5 ml	0.5M Tris-Cl (pH 6.8) (Biorad, US)	1.26 ml
30% Bis-Acrylamide (Sigma Aldrich)	3.3 ml	30% Bis-Acrylamide	0.66 ml
10% SDS (Biorad, US)	100 µl	10% SDS	50 µl
10% Ammonium persulfate (APS) (Fisher Scientific, UK)	100 µl	10% APS	25 µl
TEMED (Biorad, US)	5 µl	TEMED	5µl
Total	10 ml	Total	5ml

2.1.16.4 Immunoblotting

Once the protein was separated in SDS-PAGE gel, gel was removed from the gel cassette and trimmed to remove the stacking gel section. Nitrocellulose membrane (Biorad, US) and filter papers (Thermo Fisher Scientific, US) were cut to fit the

dimension of gel and were pre-wetted along with filter pads (Biorad, US) with ice-cold transfer buffer (detail recipe is attached in Appendix-1.1). The blot components were assembled as shown in Figure 2.1 and a blotting roller was used to get rid of bubbles. The assembled gel sandwich was placed in the electrode module. The electrode module was placed inside the buffer tank together with a frozen cooling unit which functions to prevent overheating of blot during electrophoresis. Transfer buffer was filled sufficiently and the lid of transfer tank was covered. The blot was run at 100v, 400mA for 1 hour. After the transfer, the membrane was removed gently from the sandwich and blocked with blocking solution made of 3% BSA (Sigma Aldrich) with 0.1% of Tween-20 (Vivantis Technologies Sdn Bhd) in PBS for 1hr at room temperature on a rocker platform (40 rpm). The membrane was then washed with 0.1% Tween-20 in PBS (PBST) for 5 minutes with vigorous shaking (60 rpm) repeated three times. The membrane was incubated with primary antibody for 1 hour on a rocker platform (40 rpm). Mouse monoclonal IgG1 antibody against IRF5 (Santa Cruz, USA, Ref.No. SC-56714) diluted 1:1000 with 3% BSA in PBST were used as the primary antibody for the detection of IRF5v4 or IRF5v5 protein. The same IRF5 antibody was used for detection of IRF5v4 or IRF5v5 because no specific antibodies to each IRF5 isoform are available, to date. Meanwhile, goat polyclonal antibody IgG (Santa Cruz, USA, Ref.No. SC-1616) diluted with 1:1000 with 3% BSA in PBST was used as the primary antibody for the detection Actin (housekeeping protein). After the incubation, excess unbound primary antibody was washed for three times as described earlier. Following the washing step, the membrane was incubated with secondary antibody for 1 hour on a rocker platform (40 rpm). Horseradish Peroxidase (HRP)-

conjugated goat anti-mouse IgG (Thermo Fisher Scientific, USA, Ref.No.31430), diluted at 1:10 000 with 3% BSA in PBST was used as secondary antibody for detection of IRF5v4 or IRF5v5. For Actin, HRP-conjugated donkey anti-goat polyclonal IgG (Thermo Fisher Scientific, USA, Ref.No.PA1-28664) diluted at 1:5000 with 3% BSA in PBST was used as the secondary antibody. The excess unbound secondary antibody was removed through washing three times as described earlier. Following the washing step, protein band was detected on the membrane, as described below.
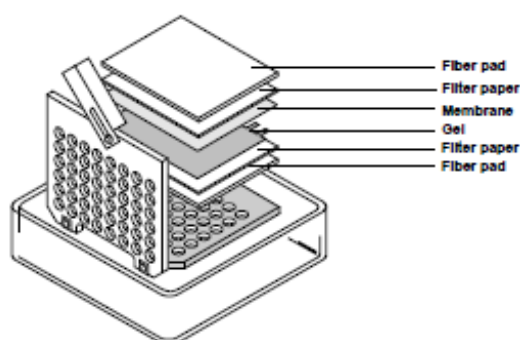
Figure 2.1 Assembly of gel and membrane sandwich.
Image obtained from Biorad website.

2.1.16.5 Enhanced chemiluminescense (ECL) detection

The membrane was kept in PBST to prevent drying out. Any excess PBST was gently removed by gentle tapping on a paper towel. The ECL signal was generated by Pierce ECL Western Blotting Substrate (Thermo Fisher Scientific, US). To prepare the working reagent, Reagent A was mixed at a 1:1 ratio to Reagent B in dark. The processed membrane was placed on a rigid plastic cover with the membrane carrying the protein of interest facing up. Following this 1 ml of the ECL substrate reagent, was added to the membrane and overlaid with a rigid plastic cover to ensure the membrane is fully covered with the western blotting substrate. The membrane was incubated for 5 minutes in dark and the chemiluminescense signal was captured either by Gel Doc System or CL-exposure film (Thermo Fisher Scientific, US) as described in the following section.

2.1.16.6 Film development

The procedure was performed in a dark room. Both the Kodak developer and fixer solutions (Sigma Aldrich) were diluted 1:4 in water. The membrane was taped inside of an aluminium film cassette (Cole Parmer, US) and 5 x 7 inches CL-Xposure film (Thermo Fisher Scientific, US) was exposed to the surface of the blot. The film was incubated with gentle rinsing in developer solution for 30 seconds, water for 30 seconds, fixer solution for 30 seconds, and final rinse in water for 30 to 60 seconds.

2.1.16.7 Stripping for reprobing

The mild stripping protocol was adapted from the Abcam protocol. Enough mild stripping buffer (detail recipe attached in Appendix-1.1) was added to cover the

membrane and incubated for 5 minutes. Following the incubation, the buffer was discarded and the membrane was incubated with PBS for 10 minutes. After 10 minutes, the PBS was discarded and fresh PBS was added to the membrane for another 10 minutes. The membrane was washed with PBST twice and ready for blocking stage. The blocking and probing steps were done as described earlier.

2.1.17 Nuclear protein extraction using NEPER protein extraction kit

Cells were harvested and gently washed twice with PBS, trypsinised for 10 minutes at 37^OC, and pelleted at 500 x g for 5 minutes. The pellets were washed with PBS again to remove any residual reagent and the supernatant was discarded. Nuclear protein was extracted using the NEPER nuclear and cytoplasmic protein extraction kit (Thermo Fisher Scientific, US). The cell samples and the extraction reagents were kept on ice throughout the experiment to prevent proteolysis. The three main reagents of the kit, CER I, CER II, and NER were prepared at 200:11:100 ratio as per manufacturer's guidelines. The volumes of CER I (and thus CER II and NER) required would then depend on the packed cell volume at 1:10 ratio. For example, 10 μl of pelleted cell would require 100 μl of CER I. Halt protease inhibitor cocktail was added to CER I and NER at 1:100 ratio. For example, 200 μl of CER I and 100μl of NER were added with 2 μl and 1 μl of the protease inhibitors, respectively. Next, ice-cold CER I was added to the pellets and subsequently vortexed at the highest speed for 15 seconds to fully resuspend the cell pellets. After incubation on ice for 10 minutes, CER II was added to the cells, vortexed at the highest speed for 5 seconds, incubated for 1 minute on ice, and vortexed for another round. The mixture was

centrifuged at maximum speed (16,000 rpm) at 4^0C for 5 minutes. The supernatant (cytoplasmic fractions) was immediately transferred to pre-chilled tubes on ice and stored at -80^0 C for troubleshooting if required. To obtain the nuclei protein fraction, the remaining pellets were suspended in NER reagent followed by four cycles of vortexing for 15 seconds at the highest speed and incubation on ice for 10 minutes during each interval. Following centrifugation, the supernatant (nuclei fraction) was immediately transferred to pre-chilled tubes on ice and stored at -80^0C.

2.1.18 Enzyme- linked immunosorbent assay (ELISA)

2.1.18.1 Measurement of cytokine secretions IFNγ, IL-2, IL-4, IL-5, and IL-10

Cytokine secretions by stimulated and non-stimulated cells were assayed by using human OptiEIA ELISA kits (BD Pharmigen, Biosciences US) according to the manufacturer's instruction. Briefly, the Immuno ELISA plates (SPL Life Sciences, Korea) were prepared one day prior to the experiment. This was done by coating the plate with 100 µl diluted capture antibody to the working concentration in coating buffer (0.1 M sodium carbonate). The plate was sealed and incubated at 4^0C overnight. The following day, the capture antibody was removed by decanting it into the sink and blotting it against a paper towel. Each coated well was washed with wash buffer (PBS with 0.05 % Tween-20, PBST) using a squirt bottle. The washing was done by filling the wells fully with the wash buffer and decant, followed by blotting against a paper towel at the final wash. This was done to ensure for complete removal of wash buffer which is critical for superior performance. The coated wells were blocked using assay diluent (PBS with 10% FBS) for 1 hour and washed three times.

While waiting, the standards were diluted with assay diluent to the highest concentration and the samples were thawed on ice. Following the washing step, 100 µl of each sample and control were added into appropriate wells. The serial dilutions of standards were done within the plate by pipetting 100 µl of assay diluent into each standard well except for the highest concentration standard well. The highest concentration of standard, 200 µl was into the appropriate wells and mixed well. From these wells, 100 µl was aspirated and pipetted into the second-highest concentration of standards to create two–fold dilution. These dilutions were continued to the lowest concentration and the extra 100 µl of the final well was discarded. The plate was sealed and incubated for 2 hours. The solutions in the wells were aspirated and washed five times. After that, 100 µl of the working detector (detection antibody+ Streptavidin- HRP reagent diluted in assay diluent) was added into each well and incubated for 1 hour. The solution was removed by aspiration and washing steps was repeated seven times, with an interval of 30 seconds to 1 minute waiting time. For each well, 100 µl of tetramethylbenzidine (TMB) substrate reagent (BD Pharmigen, Biosciences USA) was added and incubated for 30 minutes at room temperature in dark. To stop the reaction, 50 µl of stop solution (1M phosphoric acid) was added into each well and the absorbance was read at 450 nm and 570 nm within 30 minutes using EPOCH Biotek plate reader (BioTek Technologies, Inc). The wavelength correction was done by subtraction of absorbance at 570 nm from the absorbance at 450 nm. The detection limits for IL-2, IL-4, IL-5, and IL-10 are 7.8 pg/ml, while for IFNγ is 4.7 pg/ml. Each sample was performed in duplicate to ensure for reproducibility. The

mean of samples was calculated from duplicate and subtracted the mean zero of standard absorbance. The concentration values for samples were obtained from interpolation of standards curve using the Graphpad Prism 8.

2.1.18.2 Measurement of cytokine secretion IL-13

Cytokine secretions by stimulated and non-stimulated cells were assayed by using the human DuoSet ELISA kit (R&D Systems, US) according to the manufacturer's instruction. The reason for using a kit purchased from R&D Systems was because BD Pharmigen, Biosciences did not supply human IL-13 kit at the moment. As for the steps, the Immuno ELISA plates were prepared one day prior to the experiment. This was done by coating the plate with 100 µl diluted capture antibody to the working concentration in PBS. The plate was sealed and incubated at room temperature overnight. The following day, the capture antibody was removed by decanting it into the sink and blotting it against a paper towel. Each coated well was washed with wash buffer (PBST) using a squirt bottle. The washing was done by filling the wells fully with the wash buffer and decant, followed by blotting against a paper towel at the final wash. This was done to ensure for complete removal of wash buffer which is critical for superior performance. The coated wells were blocked using reagent diluent (1% BSA in PBS) for 1 hour and washed for three times. While waiting, the standards were diluted with reagent diluent to the highest concentration and the samples were thawed on ice. Following the washing step, 100 µl of each sample and control were added into appropriate wells. The serial dilutions of standards were done within the plate by pipetting 100 µl of assay diluent into each standard well except for the

highest. The highest concentration of standard, 200 µl was into the appropriate wells and mixed well. From these wells, 100 µl was aspirated and pipetted into the second highest concentration of standards to create two–fold dilution. These dilutions were continued to the lowest concentration and the extra 100 µl of the final well was discarded. The plate was sealed and incubated for 2 hours. The solutions in the wells were aspirated and washed for three times. After that, 100 µl of the detection antibody that was diluted in reagent diluent at working concentration was added into each well and incubated for 2 hours. The solution was removed by aspiration and washing steps was repeated three times. Following the washing step, 100 µl of working dilution of Streptavidin-HRP was added into each well and incubated for 20 minutes at room temperature in dark. The solution was aspirated and washing step was repeated three times. Next, 100 µl of TMB substrate reagent was added into each well and incubated for 30 minutes at room temperature in dark. For each well, 50 µl of stop solution (1M H_3PO_3) was added and the absorbance was read at 450 nm and 570 nm within 30 minutes using EPOCH Biotek plate reader reader. The wavelength correction was done by subtraction of absorbance at 570 nm from the absorbance at 450 nm. The detection limit for IL-13 is 93.8 pg/ml. Each sample was performed in duplicate to ensure for reproducibility. The mean of samples was calculated from duplicate and subtracted the mean zero of standard absorbance. The concentration values for samples were obtained from interpolation of standards curve using the Graphpad Prism 8.

2.2 Experimental design

The investigations in this study were divided into two phases. The study was first started with isolation of IRF5v4 and IRF5v5 cDNA from human B cells, followed by phases 1 and 2. In phase 1, the transcriptional regulations of IL-13 by IRF5v4/IRF5v5 were conducted. While in phase 2, the modulations of IRF5v4/v5 on the expression of cytokines were assessed. The steps involved in each phase are summarized as in Figure 2.2.
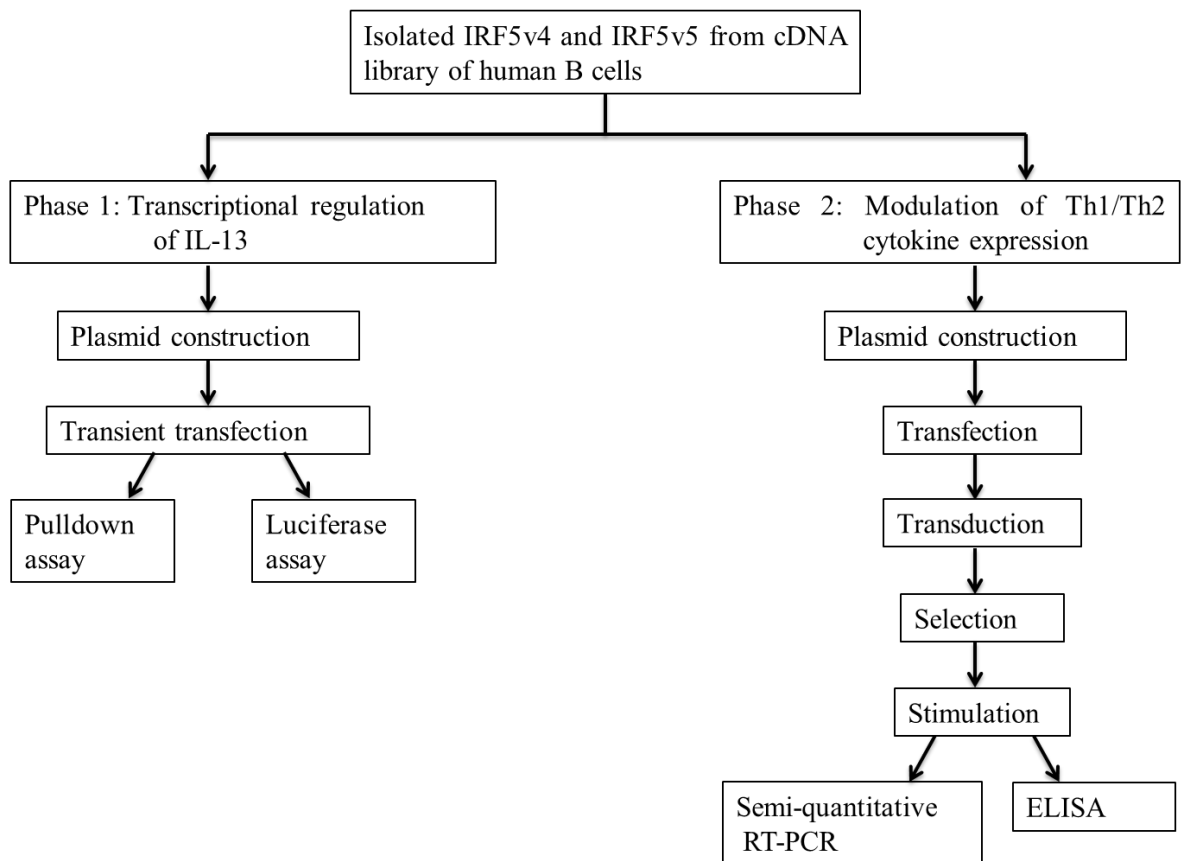
Figure 2.2 Flow chart of experimental design

2.2.1 Amplification of human IRF5 from B cells cDNA library

Full length of human IRF5 was obtained from cDNA of B cells, kindly provided by Prof. Dr. Chow Sek Chuen, Monash University Malaysia. Sequences of the primers for amplification IRF5 were adapted from Barnes et.al [31] and modified with the addition of restriction enzymes *Bam*HI and *Sal*I sequences, incorporated at the 5' and 3' ends of the primers as follow:

Forward:5'GGATCCTCTGCCATGAACCAGTCCATC3'

Reverse: 5'GTCGACAGCCTTGTTATTGCATGCCAGC3'

The expected product size is approximately 1500 bp. The PCR reaction mixture and conditions were prepared as in Table 2.5 and 2.6, respectively. The PCR amplicon was then loaded into 1% agarose gel and the fragment of the expected size, 1500 bp was excised and purified as described in section 2.1.4.

Table 2.5 Reaction mixture of PCR for amplification of human IRF5 from B cells cDNA library.

Reagents	Volume (µl)
Nuclease free water	14.875
GoTaq Flexi reaction buffer	5.0
25 µM MgCl$_2$	1.5
10 mM dNTP	0.5
10 µM Primer F	1.0
10 µM Primer R	1.0
GoTaq Polymerase	0.125
DNA (template)	1.0
Total volume	25

Table 2.6 Condition of PCR cycling for amplification of human IRF5 from B cells cDNA library.

Steps	Temperature	Time	Cycling
Initial denaturation	94^0C	2 min	1x
Denaturation	94^0C	45 s	
Annealing	*55-62^{0}C	45s	30x
Extension	72^0	2 min	
Final extension	72^0C	10 min	1x
Cooling	4^0C	indefinite	1x

* Several optimisations of the PCR condition involving different annealing temperature was tested.

2.2.2 Cloning of IRF5 in TOPO cloning vector

Following successful amplification of IRF5, the purified PCR gel product was cloned into a pCR-Blunt II-TOPO cloning vector (Figure 2.3) (Invitrogen, Thermo Fisher Scientific, US). The reaction mixture was prepared as in Table 2.7 and mixed gently. The mixture was incubated for 5 minutes at room temperature and then kept on ice for transformation with Top10 competent cells (provided by the commercial kit) as described in section 2.1.8 and plated on LB agar with 50 µg/ml of kanamycin. Five colonies were selected and cultured in 10 ml of LB medium containing 50 µg/ml of kanamycin. The plasmids were extracted using a miniprep kit and digested with *Bam*HI and *Sal*I to screen for the positive clones containing IRF5 cDNA inserts. The positive clones were sent for DNA sequencing to verify and confirm the presence of IRF5 spliced variants (IRF5v4 and IRF5v5), the two variants that were chosen to be studied in this project. The positive clones encoding IRF5v4 and IRF5v5 were selected and propagated in LB medium containing 50 µg/ml of kanamycin and glycerol stock (25% v/v) was prepared for long-term storage.
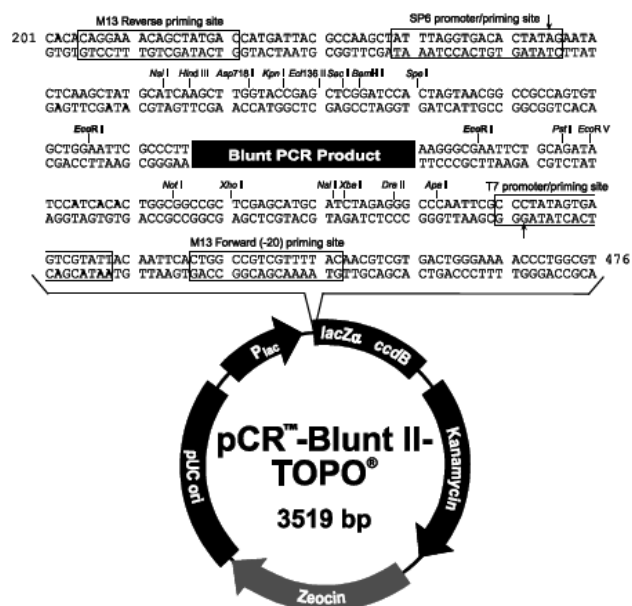
Figure 2.3 The map of pCR-Blunt II-TOPO.
Image obtained from Thermofisher website.

Table 2.7 Reaction mixture for TOPO-cloning.

Reagent	Volume
PCR product	4µl
Salt solution	1µl
pCR II- Blunt-TOPO	1µl
Final volume	6ul

2.2.3 Plasmid constructions

2.2.3.1 Construction of pLenti-IRF5v4 and pLenti-IRF5v5

Following confirmation of DNA sequencing, the clones of TOPO vector harbouring IRF5v4 and IRF5v5 with restriction enzyme sequences of *Bam*HI and *Sal*I were propagated in 10 ml LB medium containing 50µg/ml kanamycin. Similarly, pLenti CMV GFP Puro (Addgene 17448) (Figure 2.4) a third-generation lentiviral vector, was amplified in 10 ml LB medium with 100 µg/ml of ampicillin medium. The isolated plasmids were then linearized with the same restriction enzymes, *Bam*HI and *Sal*I and visualized in 1% agarose gel. Fragments of lentiviral transfer vector (pLenti) backbone without GFP and the inserts, IRF5v4 and IRF5v5 were excised from the gel and purified. Subsequently, both IRF5 variants fragments were cloned into pLenti vector (Figure 2.5) by ligation using T4 DNA ligase as described in section 2.1.12. The ligated plasmids were transformed into STBL3 strain of *E. coli* competent cells using the heat-shock method as described in section 2.1.8 and selected on 100 µg/ml ampicillin in LB agar. Colony PCR and restriction digest were performed to confirm the presence of IRF5 variants in the constructed recombinant pLenti vector. The colony PCR reaction and cycling condition are as in Table 2.8 and 2.9, respectively. The PCR amplicon was assessed with 1% agarose gel electrophoresis.

Figure 2.4 The map of pLenti CMV GFP Puro.
Image obtained from Addgene website.
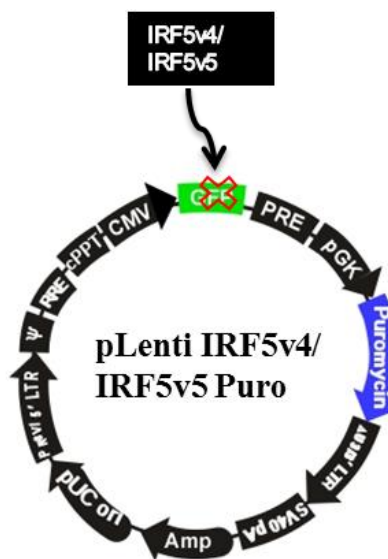
Figure 2.5 The map of constructed pLenti carrying IRF5v4 or IRF5v5.
The GFP fragment was replaced by IRF5v4 or IRF5v5 insert. The plasmid backbone
is adapted from Addgene website and modified to illustrate the construction plasmids
in this project.

Table 2.8 Colony PCR reaction mixtures for amplification of IRF5v4 and IRF5v5.

Reagents	Volume (µl)
Nuclease free water	15.875
GoTaq Flexi reaction buffer	5.0
25 µM MgCl$_2$	1.5
10 mM dNTP	0.5
10 µM Primer F	1.0
10 µM Primer R	1.0
GoTaq Polymerase	0.125
Total volume	25

Table 2.9 Condition of PCR cycling for verification of IRF5v4 and IRF5v5 with *Bam*HI and *Sal*I sequences.

Steps	Temperature	Time	Cycling
Initial denaturation	94^{0}C	2 min	1x
Denaturation	94^{0}C	45s	
Annealing	62^{0}C	45s	30x
Extension	72^0	2 min	
Final extension	72^{0}C	10 min	1x
Cooling	4^{0}C	indefinite	1x

2.2.3.2 Construction of pcDNA-IRF5v4 and pcDNA-IRF5v5

Sequences of the primers for amplification IRF5v4 and IRF5v5 were designed based on IRF5 variant 4 (IRF5v4) (NCBI accession: AY504947.1) and variant 5 (IRF5v5) (NCBI accession: AY693665.1) and modified with the addition of restriction enzymes *Bam*HI and *Xba*I sequences, incorporated at the 5' and 3' ends of the primers as shown below.

Forward:5'-TCGGATCCATGAACCAGTCCATCCCA-3',

Reverse:5'TCTAGAAGCCTTGTTATTGCATGCCAGC-3.

The PCR condition and cycling condition is shown in Table 2.10 and 2.11, respectively. Amplified fragments of IRF5v4 (1492bp) and IRF5v5 (1540bp) inserts were cloned into pCR Blunt II TOPO vector following the reaction set up as in Table 2.7. The mixture was mixed well, incubated for 5 minutes at room temperature, and then kept on ice for transformation with Top10 competent cells as described in section 2.1.8 and plated on LB agar with 50 µg/ml of kanamycin. Five colonies were selected and cultured in 10 ml of LB medium containing 50 µg/ml of kanamycin. The plasmids were extracted using the miniprep kit as described in section 2.1.10.1 and digested with *Bam*HI and *Xba*I following the steps described in section 2.1.11 to screen for the positive clones containing IRF5v4 and IRF5v5 inserts. The positive clones were sent for DNA sequencing to confirm the presence of both IRF5 spliced variants. Following confirmation of DNA sequencing, the clones of TOPO vector harbouring IRF5 variants were propagated in 10ml LB medium containing 50µg/ml kanamycin. Similarly, pCDNA3.1 (+) mammalian expression vector (Invitrogen, USA) (Figure 2.6) was amplified in 10ml LB medium with 100µg/ml of ampicillin medium. The isolated plasmids were then linearized with the same restriction enzymes, *Bam*HI and *Xba*I and visualized in 1% agarose gel. The linearized backbone was gel purified as described in section 2.1.4. Both inserts were then cloned into the linearized pCDNA3.1 (+) backbone separately and ligated using T4 DNA ligase as described in section 2.1.12. The ligated plasmids were transformed into the DH5α competent cells using heat-shock method as described in section 2.1.8 and selected on 100 µg/ml ampicillin in LB agar. The positive clones were confirmed by colony PCR following the PCR reaction in Table 2.8 and cycling condition as in Table 2.11. The

PCR product was visualized in 1% agarose gel. Restriction digestion analysis was

also performed for further verification.

Table 2.10 Reaction mixture of PCR for amplification of IRF5v4 and IRF5v5 for blunt end cloning.

Reagents	Volume (µl)
Nuclease free water	16.25
Phusion High Fidelity reaction buffer	5.0
10 mM dNTP	0.5
10 µM Primer F	1.25
10 µM Primer R	1.25
Phusion High Fidelity polymerase	0.25
DNA (template)	1.0
Total volume	25

Table 2.11 Condition of PCR cycling for amplification of IRF5v4 and IRF5v5 with *Bam*HI and *Xba*I sequences.

Steps	Temperature	Time	Cycling
Initial denaturation	98^0C	30 seconds	1x
Denaturation	98^0C	10 seconds	
Annealing	60^0C	30 seconds	30x
Extension	72^0C	30 seconds	
Final extension	72^0C	5 minutes	1x
Cooling	4^0C	indefinite	1x
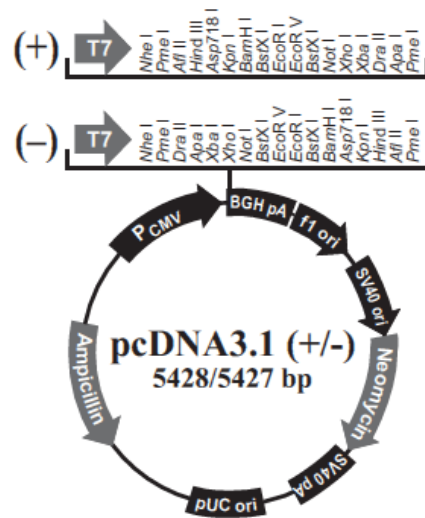
Figure 2.6 The map of pcDNA3.1 (+).
Image obtained from Thermofisher website.

2.2.4 Transient transfection for pull down assay

Plasmids DNA for transfection experiments were purified by miniprep as described in section 2.1.10.1. For this experiment, the cells were transiently co-transfected with constructed pcDNA 3.1 (+) expression vector consisting IRF5v4 or IRF5v5 and human MyD88-YFP expression plasmid (kindly provided by Prof. Dr. Kate Fitzgerald, University Massachusetts Medical School, US) at the ratio of 1:1 (6.3μg of total plasmid/reaction). Individual plasmids were included as controls. Empty pcDNA3.1 (+) was used to make up the total amount of DNA. One day before transfection, $1x10^6$ HEK 293T cells were seeded in T-25 flask containing 6.5mL of complete DMEM without antibiotic, penicillin/streptomycin to achieve about 70-80% confluency. The following day, the plasmids were added to 630 μl of OptiMEM (Gibco, Thermo Fisher Scientific, US) according to the desired combinations and amounts in 1.5 ml microcentrifuge tubes and gently mixed by pipetting. Next, 19 μl of TransIT-X2 Dynamic Delivery System transfection reagent (Mirus Bio LLC,) was added to the mixture and gently mixed by pipetting. After incubation at room temperature for 30 minutes, the mixture was added dropwise to different areas of the flask and incubated at 37^0C overnight. Fresh complete medium was replaced and a further incubation of 24 hours was allowed before harvest for the protein extraction step.

2.2.5 Biotinylated oligonucleotide DNA pull down assays and western blot analysis

Samples were extracted using the NEPER protein extraction kit as described in section 2.1.17. Concentrations of protein were quantified using the BCA protein assay kit in a 96-well plate as described in section 2.1.16.2. The DNA pull-down assay was performed using Dynabeads M280 Streptavidin (Invitrogen, Thermo Fisher Scientific, US). The sequence of *Il13/ISRE* was obtained from the Genomatix database and the oliogonucleotides were synthesised by Integrated DNA Technologies (First Base Sdn. Bhd). Additional sequences were obtained from the human *IL-13* chromosome sequence (NCBI accession no: NC_012090.1) and added at both 5' and 3' end to facilitate better binding. Biotinylated antisense oligonucleotides were annealed with corresponding sense oligonucleotides as in Table 2.12. Scrambled oligonucleotide generated using http://mkwak.org/oligorand/ was included as control. Biotinylated *Il13/ISRE* or scrambled oligonucleotide at 15 µg was coupled with Dynabeads at room temperature for 2 hours. Beads were washed and incubated with 150 µg of protein lysates for 2 hours at 4°C. Following extensive washing, the specifically bound proteins were separated using 10% SDS-PAGE and detected by western blot analysis as described in section 2.1.16. The blots were incubated with ECL substrate reagent and the chemiluminescence signal was captured using x-ray film as described in section 2.1.16.5 and 2.1.16.6, respectively.

Table 2.12 Sequences of oligonucleotides used for pull down assay.

Oligonucleotides	Sequence (5' → 3')
IL13-ISRE-S (51 nts)	5'- TAAGAGACTGGTTCATCGAAAAAATAAAACTCCCCAAATTC CCATAGCTGG-3'
IL13-ISRE-ASB (51 nts)	5'-biotin- CCAGCTATGGGAATTTGGGGAGTTTTATTTTTTCGATGAACC AGTCTCTTA-3'
Scrambled-S (51 nts)	5'- CATACATCAACAAGAGCCACCCGCAAAGCTAAGCCTTAGG ATGATCGCATA-3'
Scrambled-ASB (51 nts)	5'-biotin- TATGCGATCATCCTAAGGCTTAGCTTTGCGGGTGGCTCTTGT TGATGTATG-3'
S: sense ASB: antisense biotinylated	

2.2.6 Transient transfection and dual luciferase reporter assay

The HEK293T cells were seeded at 5 x 10^4 cells/well at 100 µl in a 96-well flat bottom plate. The cells were transfected with 25, 50, 75, or 100 ng of IRF5v4, IRF5v5 or MyD88 expression plasmids at varying combinations. In co-transfection of MyD88 together with IRF5v4 or IRF5v5, different amounts of expression plasmids were added. When increasing the concentration of MyD88 (25-100 ng), the concentration of IRF5v4 or IRF5v5 was kept constant at 100 ng, whereas when the concentration of IRF5v4 or IRFv5 (25-75 ng) was increased, the concentration of MyD88 was kept constant at 100 ng. The reporter human *IL13* promoter luciferase plasmid (Addgene 11784) was added at 40 ng and internal control Renilila luciferase control plasmid was included at 10 ng (both of the plasmids were kindly provided by Prof. Dr. Kate Fitzgerald, University Massachusetts Medical School, US). Empty vector pCDNA 3.1 (+) was added to make up the total amount of DNA to 250 ng/well. TransIT-X2

Dynamic Delivery System was used as the transfection reagent diluted in Opti-MEM. Luciferase signals were measured in cell lysates 24 hours post-transfection using the Dual Luciferase assay kit (Promega, US). Briefly, the cells were washed with PBS and 50 μl/well of 1X PLB lysis buffer was added into each well. The plate was incubated for 15min at room temperature with intermittent rocking to improve cell lysis. A total of 20 μl of cell lysate was aliquoted to a 96-well flat bottom white plate pre-filled with 40ul of LARII solution and luminescence signal was read using the VarioSkan Flash multiwell plate reader (Thermo Scientific) at 10s exposure time. After that, 40 μl of Stop & Glo reagent was added and vortexed briefly before reading at the same setting. Values were expressed as ratios of the luminescence from the firefly (experimental plasmid: IL-13) to renilla (control plasmid) for normalisation. Experiments were repeated three times in triplicate.

2.2.7 Transient transfection for recombinant lentivirus production

Plasmids DNA for transfection experiments were purified by maxiprep as described in section 2.1.10.2. The production of recombinant lentivirus in this project involves co-transfection of transfer vector, packaging, and envelope plasmids in HEK 293T cells (Figure 2.7). Seeding of 5×10^6 HEK 293T cells, were done in T- 75 cell culture flask containing 15mL of complete DMEM without antibiotic, penicillin/streptomycin the day before transfection to achieve about 70-80% confluency. The ratio 1: 2.4 of DNA to transfection reagent was utilized in this experiment. The amount of three plasmids, transfer (pLenti, pLenti_IRF5v4 or pLenti_IRF5v5), psPAX2 (Addgene 12260, Figure 2.8) and envelope plasmid, pmD2G (Addgene 12259, Figure 2.9) at the

ratio of 4:3:1 respectively was used [247,248]. Transfection was carried out in separate T-75 flasks, whereby one of the flasks were used to transfect control vector (pLenti-GFP) together with the helper plasmids (psPAX2 and pmD2G) and another flask was used for constructed pLenti-IRF5v4 or IRF5v5 together with the helper plasmids. All three plasmids were mixed in a sterile conical tube containing 1857 µl of Opti-MEM. 45 µl of TransIT-X2 transfection reagent was added dropwise into the conical tube containing the plasmids and OptiMEM and incubated undisturbed for 30 minutes for complex formation. The mixture was swirled using a pipette tip and was slowly added onto the cells dropwise. The flask was rocked in circular and sideways to distribute the complex evenly over the cells. The cells were incubated at 37^0C and 5% CO_2 for 16 hours. On the next day, transfection media was removed and replaced with 15 ml of complete DMEM and incubated for 24 hours. After 24-hour incubation, the first harvest of viral supernatant was collected and stored in 4^0C. Another 15ml of fresh complete DMEM was added and cells were further incubated for 24 hours prior to the second harvest of viral supernatant. The 24-48 hours post-transfection viral harvests were pooled and centrifuged at 1500 rpm for 5 minutes at 4^0C and filtered using 0.45µm polyethersulfone (PES) filter (Sartorius,Germany). The cell-free supernatant was stored at 4^0C for not more than 24 hours, and used for transduction. This is because repeated freeze-thaw has reported to reduce transduction efficiency [249]. The efficiency of transfection was accessed by GFP expression by lentivirus produced by the control pLenti vector using a fluorescence microscope. The percentage for transfection efficiency was roughly estimated through visual inspection of GFP expression seen under the fluorescence microscope.
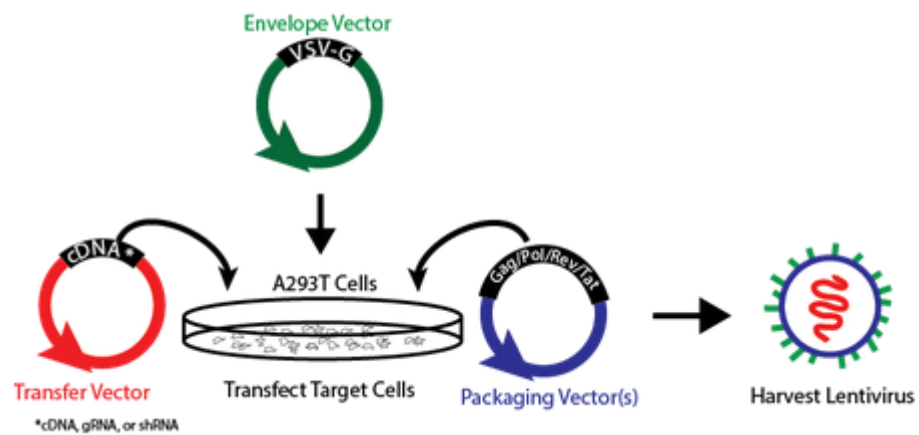
Figure 2.7 Schematic illustrations of recombinant lentivirus production.
Image obtained from Addgene website.
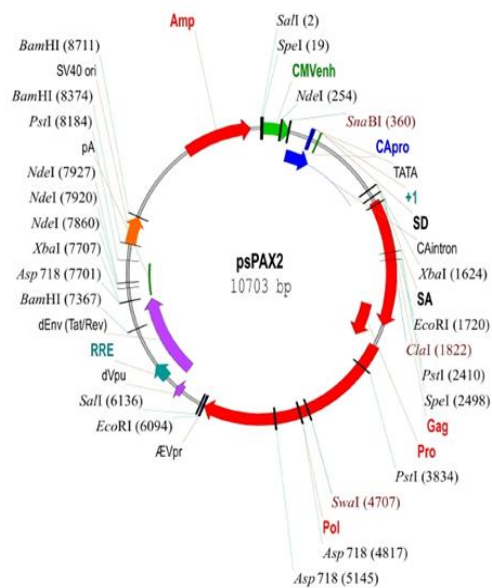
Figure 2.8 The map of psPAX2.
Image obtained from Addgene website.
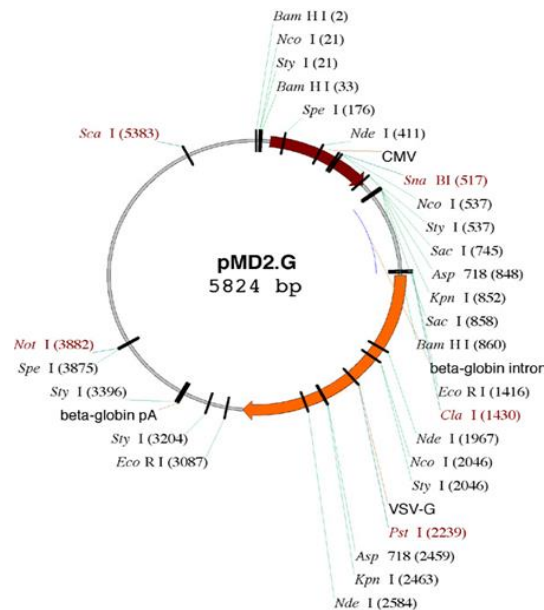
Figure 2.9 The map of pMD2.G
Image obtained from Addgene website.

2.2.8 Transduction of Jurkat cells

The protocol was adapted from Darse et al. with slight modification [250]. Briefly, 2 x 10^5 cells were seeded in six separate centrifuge tubes with 2 ml of complete RPMI containing 8 µg/ml of the final concentration of hexadimethrine bromide (Sigma-Aldrich). For each tube, 2ml of fresh virus supernatant was added except into one tube, which was set as negative control (without virus). The cells were spinoculated at 1,200 x g for 90 minutes at 25^0C. After spinoculation, cells were resuspended and added into each well. After 24 hours infection, the medium was replaced with 2 ml of fresh complete media by centrifugation. The cells were further incubated for another 48 hours. The efficiency of transduction was accessed by GFP expression by lentivirus produced by the control pLenti vector using a fluorescence microscope. The

percentage for transfection efficiency was roughly estimated through visual inspection of GFP expression seen under the fluorescence microscope.

2.2.9 Stable clone selection

2.2.9.1 Puromycin titration

For each well, 2×10^5 of Jurkat cells in 2ml of complete media were seeded in each well at 6 well-plates. Puromycin (Gibco, Thermo Fisher Scientific, US) was added at concentrations of 0.5, 1, 2, 5, and 10 µg/ml separately into the respective well. The first well was set as negative control (without puromycin). The cells were incubated at 37^0C, 5% CO_2 for 72 hours. The viability of cells was assessed by trypan blue and counted as described in section 2.1.14.1.6.

2.2.9.2 Polyclonal selection

Transduced cells were subcultured for two weeks with complete RPMI media containing a final volume of 5 µg/ml puromycin. Untransduced cells were used as the negative control.

2.2.9.3 Monoclonal selection

The protocol was adopted from Lieber et.al with some modifications [251]. Briefly, 1×10^4 cells were prepared in 20 ml media. From the tube, 5 µl of cells were aspirated into tube containing 5 ml of RPMI complete media, 5 µg/ml puromycin and 5 ml of self-conditioned media. Self-conditioned media was collected from healthy growing Jurkat cells culture (untransduced cells), whereby the cells were spun down and the supernatant was collected into a sterile tube and filtered using a 0.22 µm

119

polyvinylidenefluoride (PVDF) filter (Merckmillipore, Merck&CO). After that, 100 µl of the diluted cell suspension were pipetted in each well. The cells were incubated undisturbed at 37^0C in 5% CO_2 for 2 hours. Later the wells were inspected and the wells with only a single colony were marked. The plate was incubated undisturbed at 37^0C in 5% CO_2 for three weeks with regular inspection for confluency. Once the monoclonal cells were established, the selected monoclonal cells were used within 15 passage numbers.

2.2.10 Confirmation of IRF5v4 and IRF5v5 stably expressed Jurkat cells by RT-PCR

The cells were counted and 2 x10^6 of untransduced Jurkat cells, IRF5v4 and IRF5v5 stably expressed Jurkat culture cells were harvested by centrifugation at 1000 rpm for 10 minutes at 25^0C. The supernatant was discarded by aspiration and the cells pellet was saved for RNA isolation. The cells pellet was lysed with 350 µl of RLT lysis buffer that was provided in the RNA isolation kit and kept at -20^0C for overnight. The following day, samples were prepared for gene expression by RT-PCR as described in section 2.1.15. The target gene, primers sequence, annealing temperature, and amplicon size are shown in Table 2.13. The cDNA of IRF5 and β-actin expression was generated by 30 cycles of PCR amplification following the PCR reaction and cycling condition in Table 2.2 and Table 2.3, respectively. The PCR products were visualized in 1.5% agarose gel electrophoresis.

Table 2.13 Primers and PCR product for determination of IRF5 and β-actin expression.

Target gene	Primer sequence (5' → 3') Forward (F), Reverse (R)	Annealing temperature (^{0}C)	Amplicon size (bp)	References
IRF5	F:5'-CCTTAACAAGAGCCGGGACT-3' R:5'-GCTCCAGGACCTCAGAGAGA-3'	58	398	Constructed using Bioedit software (detail steps is attached in Appendix-1.2)
β-actin	F:5'-AGAGCTACGAGCTGCCTGAC-3' R:5'-AGCACTGTGTTGGCGTACAG-3'	58	182	[252]

2.2.11 Confirmation of IRF5v4 and IRF5v5 stably expressed Jurkat cells by western blot analysis

The cells were counted and 2 x10^6 of untransduced Jurkat, IRF5v4, and IRF5v5 stably expressed Jurkat cells were harvested by centrifugation at 1000 rpm for 10 minutes at 25^{0}C. The supernatant was discarded by aspiration and the cells pellet for whole protein extraction and quantification as described in sections 2.1.16.1 and 2.1.16.2, respectively. Each sample, 40 μg of proteins, was separated by 10% SDS-PAGE at a constant voltage of 120 V for 1 hour 20 mins and then transferred onto nitrocellulose membrane for immunoblotting as described in section 2.1.16.3 and 2.1.16.4, respectively. Chemiluminescence signal was generated using ECL substrate and captured using GelDoc System as described in section 2.1.16.5. The detected membrane blot was strip using mild-stripping buffer as described in section 2.1.16.7. The detection of housekeeping gene was then performed with incubation with primary and secondary antibody as mentioned in section 2.1.16.3. Chemiluminescence signal was generated using ECL substrate and captured using GelDoc System as described in section 2.1.16.5.

2.2.12 Titration of mitogens concentration for optimal stimulation

For cell activation, the combination of two mitogens; PMA, (Nacalai Tesque, Inc) and Ionomycin (Calbiochem Merck, Merck & Co) were used. To determine the optimal concentration for cell activation, 2x10^6 cells of Jurkat cells (untransduced cells) were cultured in the combination of concentration of PMA (5, 10, 25, 50 ng/ml) and Ionomycin (0.5 or 1 μM) or left untreated for 24 hours. After 24 hours, the viability of

cells was assessed by trypan blue as described in section 2.1.14.1.6 and the supernatant of the cell culture was processed as in section 2.2.14 that was used for IL-2 ELISA assay as described in section 2.1.18.1.

2.2.13 Mitogen stimulation for cytokine production by mRNA analysis

The cells were counted and 2 x10^6 of untransduced Jurkat, IRF5v4, and IRF5v5 stably expressed Jurkat cells were cultured in presence or absence of 25 ng/ml of PMA and 1μM of Ionomycin for 6 hours. After 6 hours the cultured cells were spun down by centrifugation at 1000 rpm for 10 minutes at room temperature. The supernatant was discarded by aspiration and the cells pellet was saved for RNA isolation. The cells pellet was lysed with 350 μl of RLT lysis buffer (Qiagen) and kept in -20^{0}C for overnight. The following day, samples were prepared for gene expression by RT-PCR as described in section 2.1.15. The target gene, primers sequence, annealing temperature, and amplicon size is shown in Table 2.14. The PCR amplicon was then loaded into 1.5% agarose gel and the band of the expected size was quantified using Image J software. The quantified values obtained from each cDNA band's intensity were divided with the intensity of the DNA ladder marker (500 bp).The relative expression values were calculated from ratios of cytokines to the housekeeping gene, β-actin. The experiments were conducted three times.

2.2.14 Mitogen stimulation for cytokine production by protein analysis

The cells were counted and 2 x10^6 of untransduced Jurkat, IRF5v4, and IRF5v5 stably expressed Jurkat cells were cultured in the presence or absence of 25 ng/ml of PMA and 1μM of Ionomycin for 24 hours. After 24 hours the cultured cells were spun

down by centrifugation at 1000 rpm for 10 minutes at 4^0C. The supernatant was transferred into a sterile tube and kept on ice. The collected supernatant was mixed well by pipetting up and down several times. The supernatant was aliquoted into several 1.5 ml microcentrifuge tubes with 250 µl each and immediately kept on ice. The tubes were later transferred to -80^0C till use. The tubes were thawed on ice prior to use and the samples were assayed by ELISA as described in section 2.1.18. Experiments were performed three times in duplicates.

2.2.15 Statistical analysis

The statistical analysis was performed using GraphPad Prism 8 software. A two-way ANOVA with Tukey multiple comparison tests was used. Values are expressed as mean ± standard error of mean.

Table 2.14 Primers and PCR product size for Th1 and Th2 cytokines gene expression.

Target gene	Primer sequence (5' → 3') Forward (F), Reverse (R)	Annealing temperature (^{0}C)	Amplicon size (bp)	References
IFNγ	F:5'-TGGGTTCTCTTGGCTGTTACTGCC-3' R:5'-TACTGGGATGCTCTTCGACCTCGA-3'	60	453	[253]
IL-2	F:5'-CAAGAATCCCAAACTCACCAGG-3' R:5'-CAATGGTTGCTGTCTCATCAGC-3'	60	250	[254]
IL-4	F:5'-CGGACACAAGTGCGATATCACC-3' R:5'-CCAACGTACTCTGGTTGGCTTCC-3'	60	331	[254]
IL-13	F:5'-TGCAATGGCAGCATGGTATG-3' R:5'-GCAGGTCCTTTACAAACTGG-3'	60	213	[255]

Chapter 3

3 Results

3.1 Isolation of human IRF5 spliced variants from B cells cDNA library

As mentioned earlier, the human *Irf5* gene exists as multiple spliced variants that give rise to distinct isoforms (Figure 1.4). In the present study, we used human IRF5 spliced isoforms encoding variant 4 and variant 5 sequences. Both IRF5 variants are derived from exon 1A that have higher translational efficiency compared to the other exons (1B, 1C and 1D) [28]. Of note, these variants differ in their exon 6; as IRF5v5 contains full genomic sequence while IRF5v4 confers deletion within the region. As mentioned earlier, constitutive expression of IRF5 has been detected in B cells, monocytes, macrophages, dendritic cells, and NK cells but barely in T cells. In terms of transcripts derived from exon1A, the constitutive expression of the variants is predominantly found in B cells and plasmacytoid dendritic cells [27,162]. For this study, IRF5 cDNA was obtained from the cDNA library of human B cells by PCR amplification using primers that were designed with restriction enzymes *Bam*HI and *Sal*I as described in section 2.2.1. Higher annealing temperatures of 60^0C and 62^0C were used, since no clear amplification of IRF5 band was seen at lower annealing temperatures (Appendix 2.1.) Both the annealing temperature of 60^0C and 62^0C gave the correct fragment of the expected band of approximately 1500 bp as seen in Figure 3.1. However, more non-specific bands were seen at an annealing temperature of 62^0C compared to 60^0C. Hence, an annealing temperature of 60^0C was chosen as the optimal annealing temperature for subsequent PCR cycling.
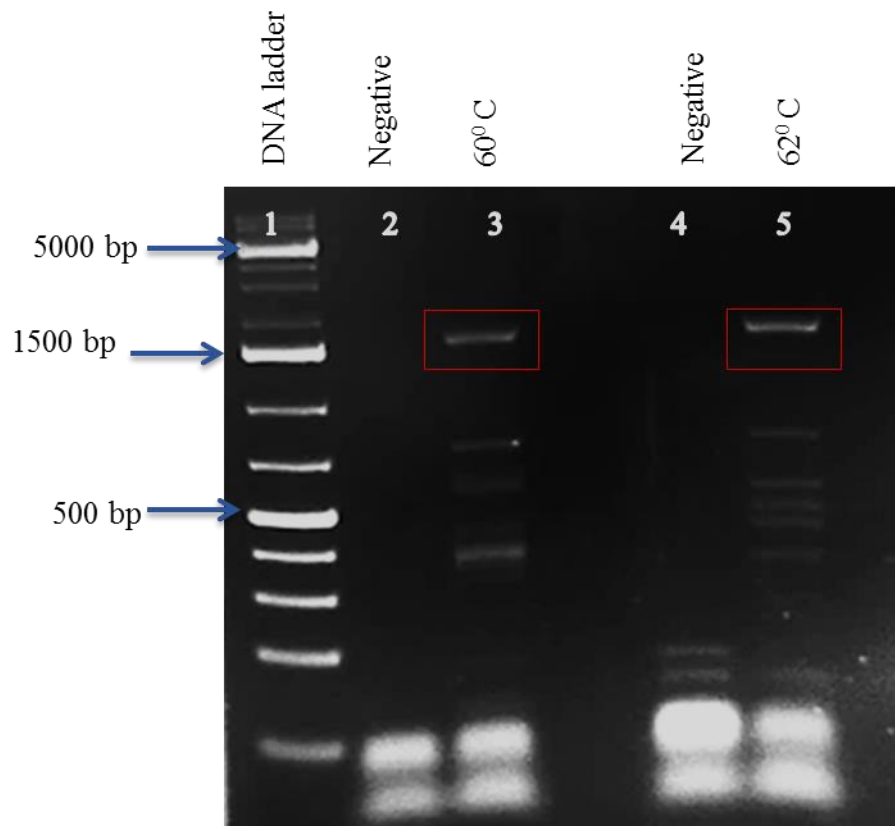
Figure 3.1 Amplification of IRF5 from cDNA of B cells.
The amplification of IRF5 coding sequences with expected band of approximately 1500 bp was seen at 60^0C (Lane 3) and a sharp distinct band was seen at 62^0C (Lane 5) as indicated by the red box. Negative control (no template) was included in Lane 2 and Lane 4. 1kb Plus DNA ladder was loaded in Lane 1 and the major marker band size has been labelled as shown in blue arrow.

Following successful amplification of IRF5, the PCR product was gel-purified and inserted into the TOPO cloning vector with 50 µg/ml kanamycin selections. A total of five colonies of transformants were selected and colony PCR was done to verify the presence of IRF5 cDNA in the selected transformants. As seen in Figure 3.2, all the transformants showed a clear band with the expected size of approximately 1500 bp. For further verification, plasmids from the transformants were isolated and were digested with restriction enzymes, *Bam*HI and *Sal*I as shown in Figure 3.3. As seen from the gel image, all the transformants gave correct fragments after digestion, indicating that cloning of IRF5 cDNA was successful. To determine which of the positive clones encoded for IRF5v4 and IRF5v5 cDNA sequences, all the five positive clones were sent for DNA sequencing. The sequencing results revealed that transformant 1 encoded IRF5v5 and transformant 3 encoded IRF5v4 (Sequencing results are presented in Appendix- 2.2(a)). Sequence alignment of these two IRF5 spliced variants showed that IRF5v4 confer deletion of 48 nucleotides, while IRF5v5 showed no deletion as they expected to be. The differences in sequences between these two spliced variants are illustrated in Figure 3.4.
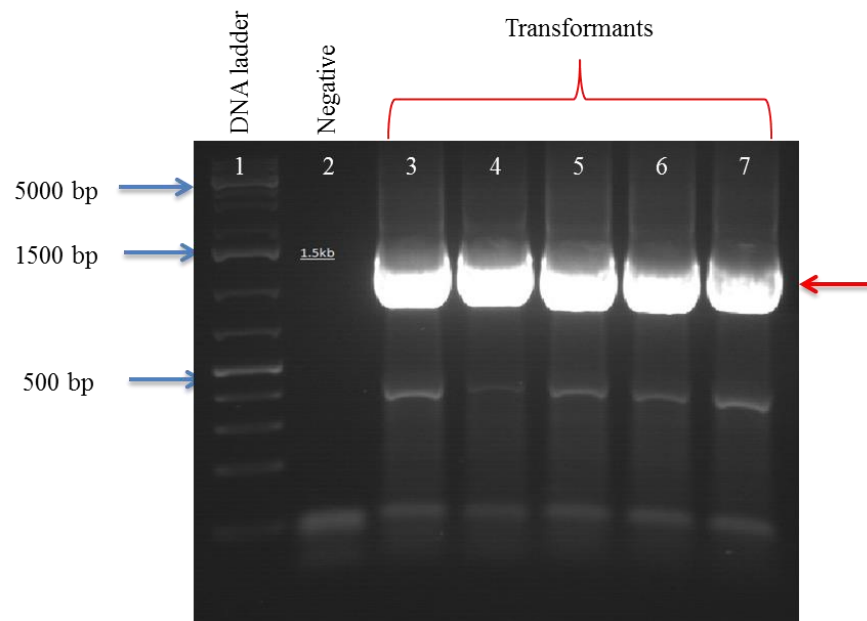
Figure 3.2 Colony PCR of Top-10-IRF5 harbouring *Bam*HI and *Sal*I.
PCR product of the five transformants was loaded in Lane 3 to Lane 7. All the transformants showed bands of the expected band size of approximately 1500 bp as indicated by the red arrow. 1kb Plus DNA ladder was loaded in Lane 1 and the major marker band size has been labelled as shown in blue arrow. Negative control (no template) was included in Lane 2.

Figure 3.3 Restriction digestions of TOP10- TOPO-IRF5 transformants with *Bam*HI and *Sal*I.

Transformants from the PCR screening were digested with *Bam*HI and *Sal*I restriction enzymes. All digested transformants loaded in Lane 2 to 6 gave bands at the expected band size (1500 bp) as indicated in by the red box. 1kb Plus DNA ladder was loaded in Lane 1 and the major marker band size has been labelled as shown in blue arrow.

Figure 3.4 Pairwise sequence alignments of human IRF5v4 and IRF5v5 coding sequences.

The dashed lines highlighted by the red box indicate deletion (48 nucleotides) within IRF5v4 in comparison to IRF5v5 sequences, which showed no deletion as expected.

3.2 DNA binding activity and transcriptional activation of IL-13 by IRF5

3.2.1 Construction of pcDNA-IRF5v4 and pcDNA-IRF5v5 expression vector

To examine the effect of transcriptional activity of IL-13 by IRF5, pcDNA 3.1+ mammalian expression vector harbouring IRF5v4 or IRF5v5 (represented as pcDNA-IRF5v4 and pcDNA-IRF5v5) was first established. Plasmids of IRF5v4 and IRF5v5 derived from TOPO cloning as described in section 3.1 were used as template to generate PCR fragments of IRF5 spliced variants with ends of *Bam*HI and *Xba*I to accommodate for ligation into pcDNA3.1+ expression vector. The PCR products were gel purified and cloned into pCR-Blunt II-TOPO as described in section 2.2.3.2. The cloning strategy for construction of TOPO-IRF5v4 and TOPO-IRF5v5 containing *Bam*HI and *Xba*I sequences is illustrated as in Figure 3.5. The cloning was verified with colony PCR, whereby a total of ten colonies; five colonies for each IRF5v5 and IRF5v4 were selected (v5c1 – v5c5 and v4c1 – v4c5) for screening.
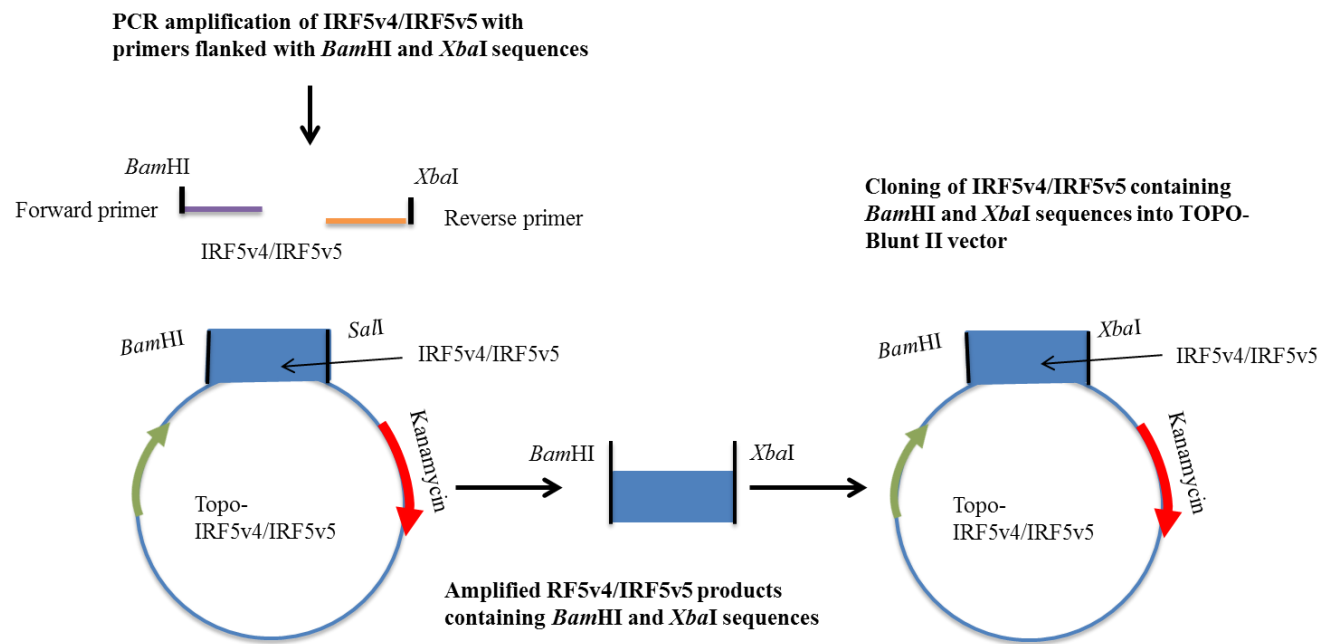
Figure 3.5 The cloning strategy for construction of TOPO-IRF5v4 and TOPO-IRF5v5 harbouring *Bam*HI and *Xba*I sequences.

As observed from the gel image (Figure 3.6), all the IRF5v5 colonies (v5c1 –

v5c5) showed bands of the expected size (1540 bp), whereas for IRF5v4 colonies,

only three colonies showed bands of the expected size (1492 bp). The other two

colonies (v4c4 and v4c5) have no inserts; thus, these two colonies were omitted in

further verification. Following colony PCR, the presence of IRF5v4 and IRF5v5

cDNA inserts were verified through restriction enzyme digestion of *Bam*HI and *Xba*I.

As expected, the gel electrophoresis of the digested products resulted in estimated

bands of approximately 1500 bp for IRF5v4 and IRFv5 inserts as seen in Figure 3.7.

DNA sequencing of the positive transformants confirmed the presence of IRF5v4 and

IRF5v5 cDNA in respective clones sent for verification (results are presented in

Appendix-2.2(b)).
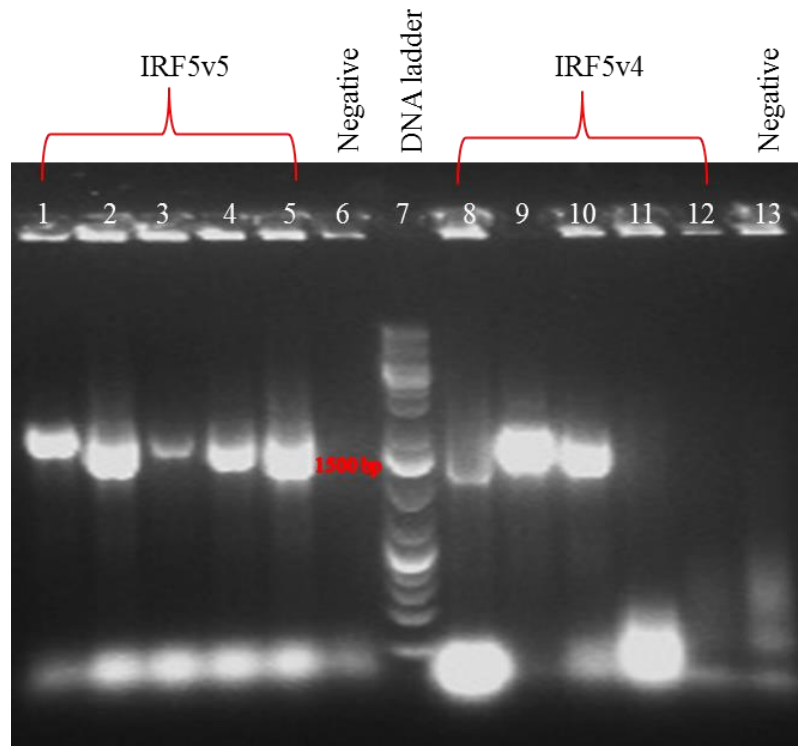
Figure 3.6 Colony PCR screening of transformants TOP10-TOPO-IRF5v5 and TOP10-TOPO-IRF5v4.

It was done to verify the presence of recombinant plasmids carrying the IRF5v5 and IRF5v4 fragments harboured *Bam*HI and *Xba*I sequences. All the transformants of IRF5v5 (v5c1-v5c5; from lane 1 to 5) showed expected band size (1540 bp). On the other hand, only three transformants of IRF5v4 (v4c1-v4c3; from lane 8-10) showed expected band size (1492 bp). 1kb Plus DNA ladder was loaded in Lane 7 and one of the major marker band size; 1500 bp was labelled red. Negative control (no template) was included in Lane 6 and Lane 13.
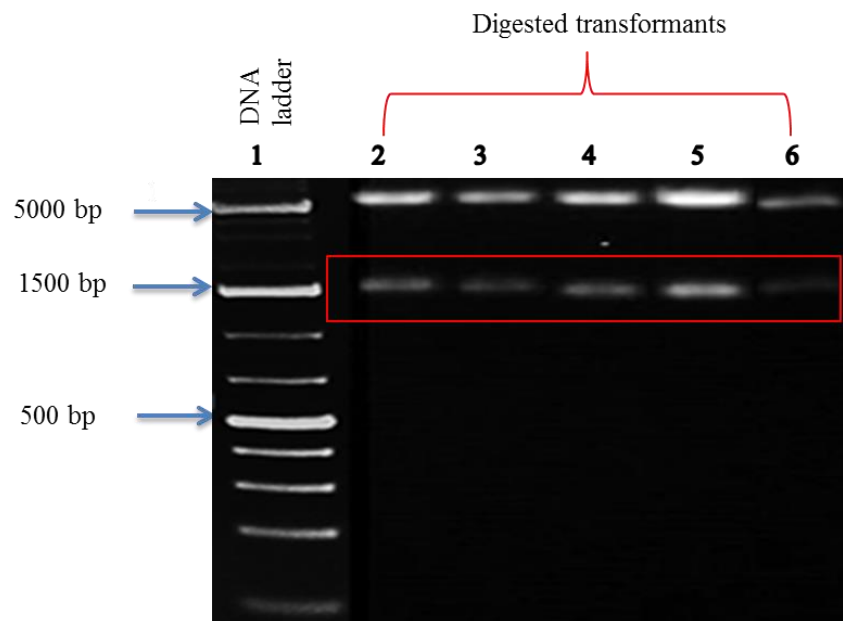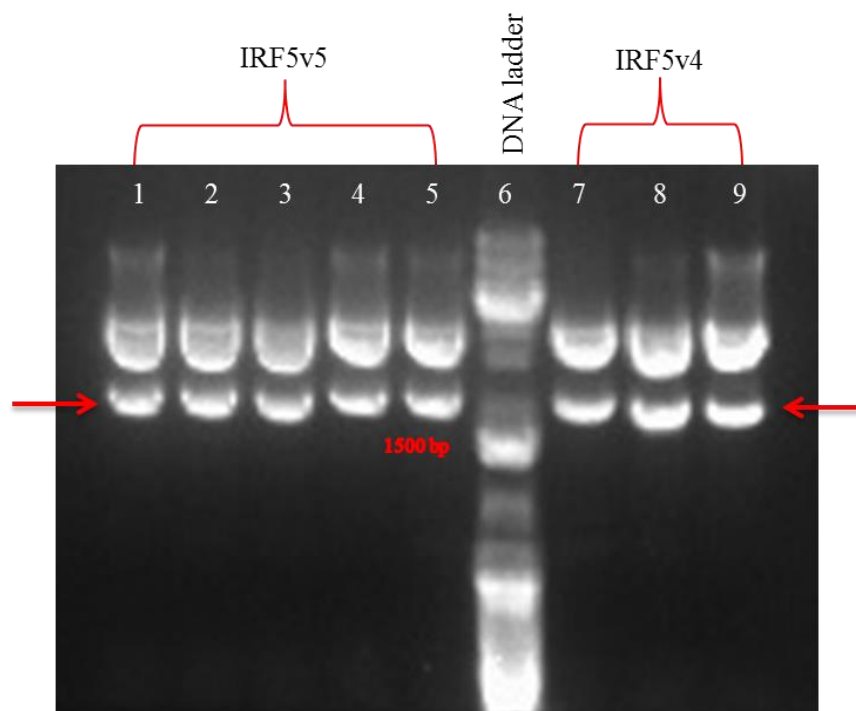
Figure 3.7 Restriction digestions of TOP10- TOPO-IRF5v4/v5 transformants with *Bam*HI and *Xba*I.
Transformants from the PCR screening were digested with *Bam*HI and *Xba*I restriction enzymes. The digested fragments of IRF5v5 (v5c1-v5c5; from lane 1 to 5) and IRF5v4 (v4c1-v4c3; from lane 7-9) showed expected band size of approximately 1500 bp as indicated by the red arrow. 1kb Plus DNA ladder was loaded in Lane 6 and one of the major marker band size; 1500 bp was labelled red.

The expression vector, pcDNA 3.1 (+) was engineered to carry DNA fragments of IRF5v4 or IRF5v5. To do so plasmids from TOPO cloning vector harbouring IRF5v4 or IRF5v5 and pcDNA 3.1 were extracted and linearized with the same restriction enzymes, *Bam*HI and *Xba*I. Gel electrophoresis of the digested product resulted in estimated bands consisting approximately of 5300 bp for pcDNA vector backbone and approximately 1500 bp for IRF5 inserts respectively (Figure 3.8). The fragment of the expected bands of pcDNA and IRF5 variants were excised

136

and purified, followed by ligation and transformation into DH5α competent cells. The cloning strategy for the construction of pcDNA-IRF5v4 and pcDNA-IRF5v5 are illustrated in Figure 3.9. The positive clones for each spliced variant constructed into pcDNA were selected with 100 µg/ml ampicillin. Colony PCR was performed to verify the presence of inserts and the integrity of DNA was analysed with 1% agarose gel as shown in Figure 3.10. Results from the colony PCR confirmed that IRF5 inserts have been successfully incorporated into pcDNA 3.1+.
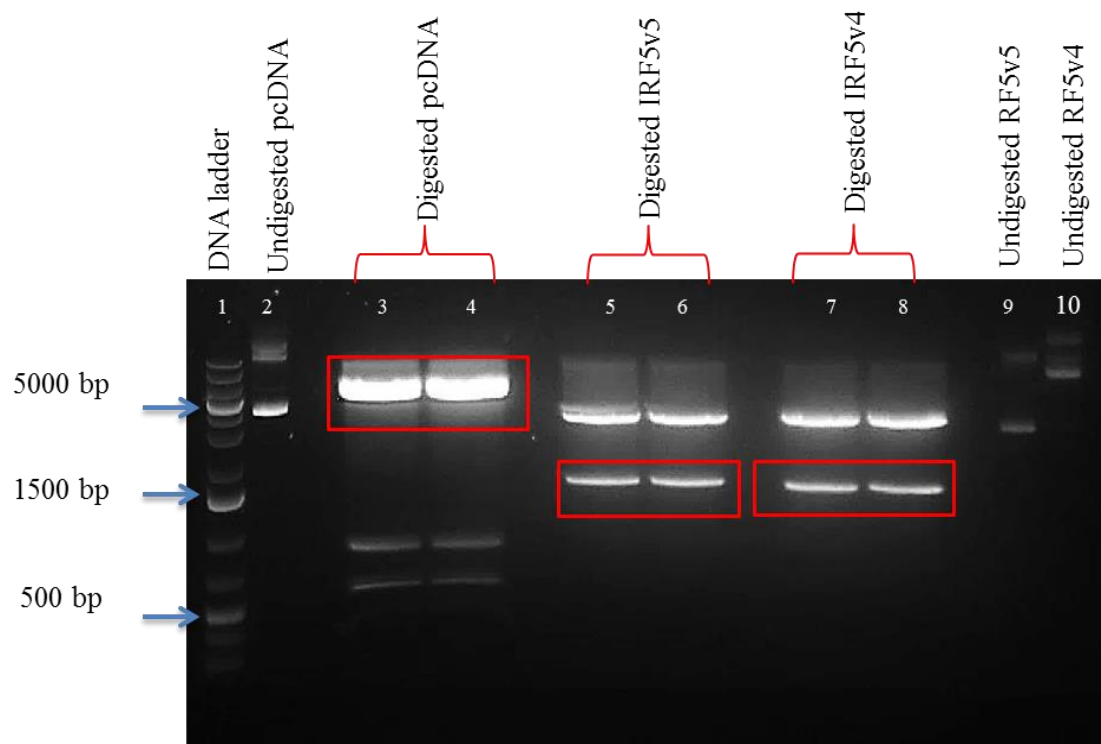
Figure 3.8 Restriction digestions of extracted plasmids using *Bam*HI and *Xba*I of pcDNA 3.1, TOPO-IRF5v5 and TOPO-IRF5v4.

The pcDNA vector, TOPO-IRF5v4 and TOPO-IRF5v4 were either digested with *Bam*HI and *Xba*I or left undigested. The digested fragments were loaded into two combined wells in respective lanes as indicated by the red box. As seen in Lane 3-4, the pcDNA vector backbone without GFP sequences gave fragment of 5300 bp. While digested TOPO-IRF5v5 and TOPO-IRF5v4 gave fragments of approximately 1500 bp as seen in Lane 5-6 and Lane 7-8 respectively. 1kb Plus DNA ladder was loaded in Lane 1 and the major markers band sizes has been labelled as shown in blue arrow. The undigested pcDNA vector, TOPO-IRF5v5 and TOPO-IRF5v4 plasmid were loaded into Lane 2, 9 and 10 respectively.

138
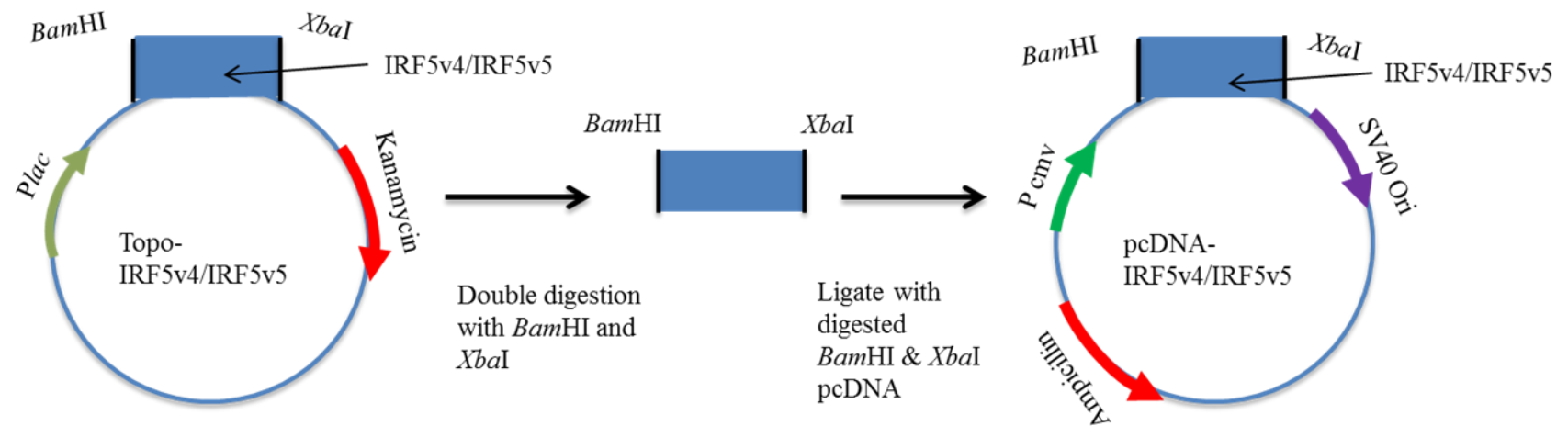
Figure 3.9 The cloning strategy for construction of pcDNA-IRF5v4 or pcDNA-IRF5v5.
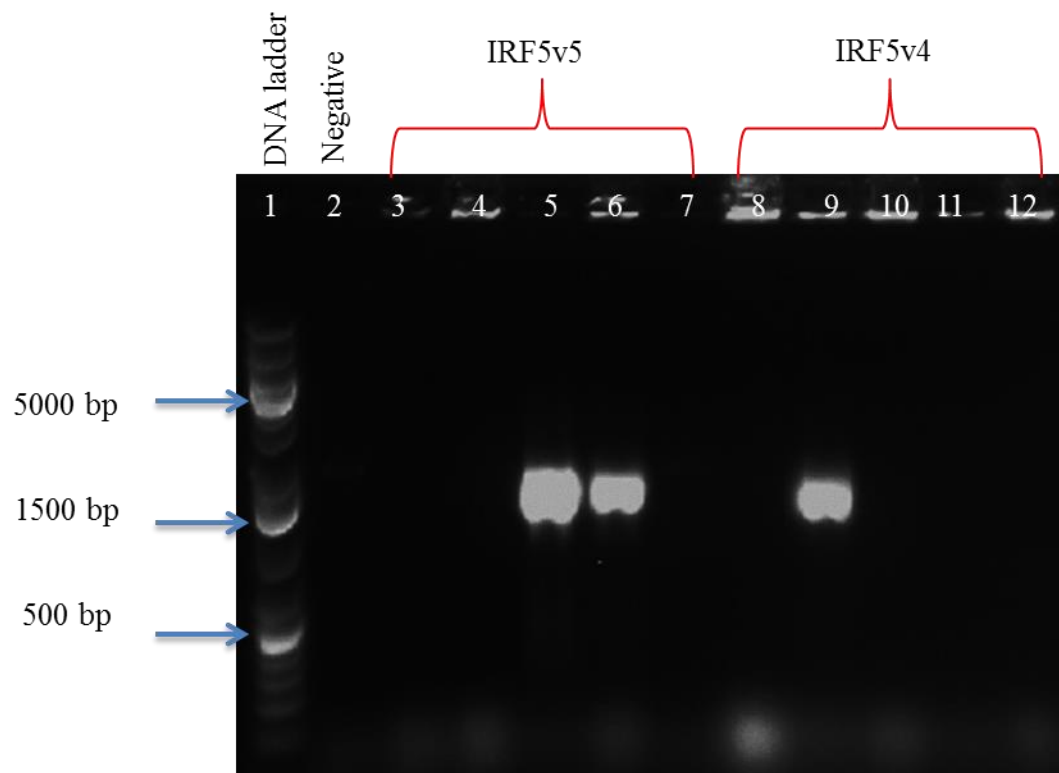
Figure 3.10 Colony PCR screening of transformants DH5α-pcDNA3.1- IRF5v5 and transformants DH5α-pcDNA3.1- IRF5v4.

PCR screening of transformants for identification of IRF5v5 were loaded into Lane 3-7, while for transformants IRF5v4 were loaded into Lane 8-12. Out of five selected transformants, two positive transformants showed the presence of IRF5v5 (Lane 5 and 6), while only one transformant showed the presence of IRF5v4 (Lane 9). 1kb Plus DNA ladder was loaded in Lane 1 and the major markers band sizes has been labelled as shown in blue arrow. Negative control (no template) was included in Lane 2.

3.2.2 Establishment of transient transfection protocol for pull down assay

To examine whether IRF5 can bind to the ISRE region of the *IL13* promoter, a DNA pull-down assay was conducted. The DNA pull-down assay is a fast, reliable, and useful method to determine whether proteins, in this case, transcription factor binds to DNA within the target region [256]. To do so, a transient transfection experiment was performed followed by isolation of nuclear protein from lysates of transfected cells which were used in a pull-down assay. The protocol for transient transfection was adapted from the previous study conducted by our group [190]. The ratio of plasmid DNA to transfection reagent used was 1:3 following the manufacturer's recommendation. MyD88 expression plasmid used in this project was conjugated with a reporter gene; yellow fluorescent protein (YFP) which was helpful in evaluating whether the experiments carried out following the protocol designed were ideal and successful.

In the initial phase of the investigation, a trial was conducted. For this trial experiment, pcDNA-IRF5v5 and MyD88 were used. Equal amounts of pcDNA-IRF5v5 and MyD88 expression plasmids were co-transfected into HEK 293T cells. Individual plasmids were included as control and empty pcDNA was added to bring the same total amount of DNA in each well. Based on the results, no YFP expression was detected in untransfected cells (Figure 3.11(a)) and transfected cells with IRF5v5 (Figure 3.11(b)). On the other hand, cells transfected with MyD88 showed about 60-70% of YFP expression when visually inspected as shown in Figure 3.11(c). A similar

result was observed when cells were co-transfected with IRF5v5 and MyD88 as shown in Figure 3.11 (d).
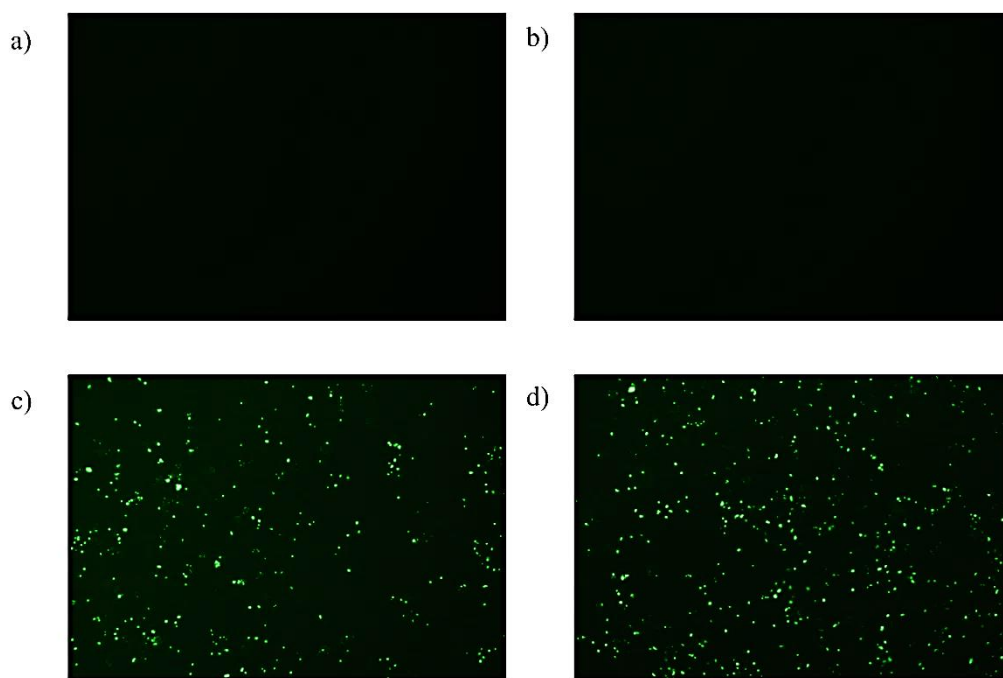
Figure 3.11 Visualisation of YFP expressions in HEK 293T cells at day 2 post-transfection.
(a) untransfected cell, (b) transfected with IRF5v5 plasmid, (c) transfected with MyD88 and (d) co-transfected IRF5v5 and MyD88 plasmids. Photos were taken under Nikon Inverted Microscope Eclipse TS2R under fluorescent light (x100 magnification). The exposure time of fluorescent photos were 600 milliseconds.

Following the assessment through a fluorescence microscope, we checked whether the transfected cells expressed the targeted protein of interest. Cells were lysed and the whole protein was subjected to western blot and detected using an anti-IRF5 antibody. As seen in Figure 3.12, a sharp band was clearly seen from cell lysate

containing transfected IRF5v5 as well as in the co-transfected cells of IRF5v5 and MyD88. In addition, as expected no band was detected in untransfected cells or with cells transfected with MyD88 plasmid in absence of IRF5v5. From these results, we confirmed that our protocol used as described in section 2.2.4 was optimal for successful transient transfection.
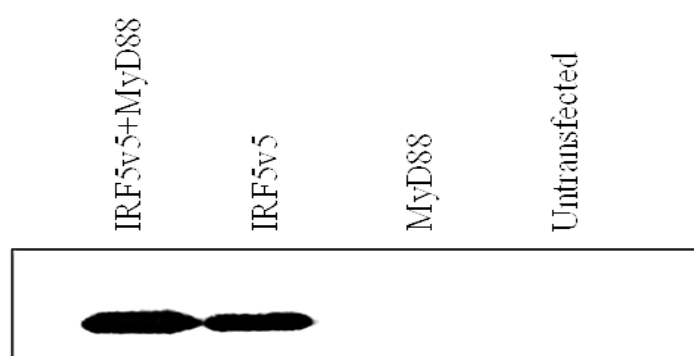
Figure 3.12 Confirmation of IRF5v5 protein by western blot analysis during trial. The presence of ~60kDa representing IRF5v5 protein was detected in whole cell lysates from cells co-transfected with MyD88 and IRF5v5 plasmids and cells with transfected IRF5v5 plasmid alone without MyD88. As expected, no band was detected from protein extracted from cells transfected with MyD88 plasmid alone as well as in untransfected cells. The chemiluminescense signal was captured by CL-exposure film.

3.2.3 Binding of IRF5v4 and IRF5v5 to ISRE region of *IL13* promoter

The HEK 293T cells were transiently transfected either with pcDNA-IRF5v4 or pcDNA-IRF5v5 in the presence and absence of human MyD88 expression plasmid at 1:1 ratio to 6.3µg of the total plasmid. Individual plasmids were included as control and empty pcDNA was added to bring the same total amount of DNA in each well (6.3 µg plasmid per reaction). Double-stranded oligodeoxynucleotides (51 nucleotides) corresponding the ISRE region or its mutant (scrambled

oligodeoxynucleotides) were synthesized and biotin-labelled at the 5'end of the negative strand, as described in section 2.2.5. The nuclear protein of transfected cells lysates were incubated with biotinylated oligonucleotides corresponding to the ISRE site immobilized on magnetic streptavidin beads and the specifically bound proteins were eluted and identified by western blot with incubation of IRF5 antibodies. The input lanes (Input) contained 30% of the proteins that were used for pull-down and subjected to western blot with incubation of IRF5 antibodies. The Input is important control to validate whether extracted nuclear protein from the transfected cells, indeed contained the expressed proteins of the individual plasmids as indicated. The results confirmed the presence of IRF5v4 (Figure 3.13(a)) and IRF5v5 (Figure 3.13(b)) protein from the nuclear lysates of transfected cells with IRF5v4 and IRF5v5 expression plasmid represented by the ~ 60 kDa protein band. As expected, no band was detected from the lysates of transfected either with MyD88 or empty vector, pcDNA 3.1.

It is known that ectopic MyD88 activates IRF5 [190]. When IRF5v4 or IRF5v5 were co-transfected with MyD88, the nuclear lysates were shown to be pulled down by *IL13/ISRE* specific DNA fragment as depicted in Figure 3.13(c) and 3.13(d) respectively. This is represented by the presence of the expected band size of ~60 kDa protein corresponding to IRF5v4 and IRF5v5 protein. Notably, the band was only detected when nuclear lysates containing both the MyD88 and IRF5v4 expressing plasmids were pulled down by *IL13/ISRE* specific DNA fragment (Figure 3.13(c)). Whereas in the absence of MyD88 expression plasmid, there was no band detected

144

from nuclear lysate containing IRF5v4 expression plasmid alone. On the contrary, IRF5v5 band was detected when nuclear lysates containing IRF5v5 expression plasmid alone was pulled down by *IL13/ISRE* specific DNA fragment (Figure 3.13(d)). Remarkably, co-transfection of MyD88 and IRF5v5 resulted in much enhanced band size corresponding to IRF5v5 protein. None of these IRF5 isoforms bound to the scrambled oligonucleotide internal control under the same condition, implying the specificity of the pull-down assay for the association of IRF5/*Il13-ISRE* rather than the presence of any non-specific binding. Taken together, these data demonstrated that both IRF5v4 and IRF5v5 can bind to the ISRE region of *Il13* promoter, thereby suggesting binding of these IRF5 variants could serve as significant role in regulating the expression of IL-13.
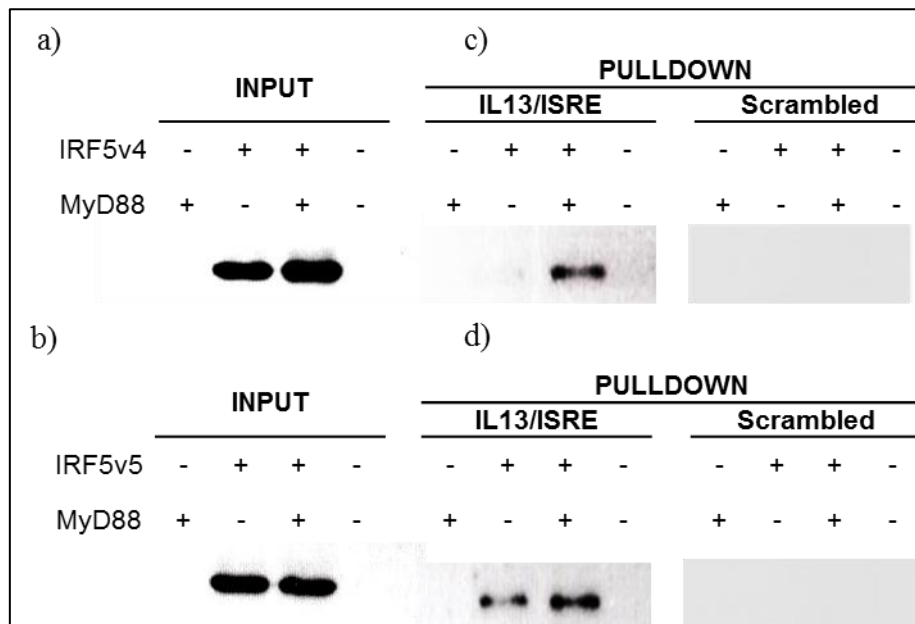
Figure 3.13 DNA pull down assay of IRF5v4 and IRF5v5 using *IL13/ISRE* specific fragment.

Input represents verification of western blot performed using 30% of nuclear lysates prior to pulldown assay to confirm the presence of expressed protein as indicated by the detected band. Band was seen from nuclear protein lysates from HEK 293T cells transfected with IRF5v4 with or without the presence of MyD88 (a), IRF5v5 with or without the presence of MyD88 (b). No band was detected from the lysates of transfected either with MyD88 or empty vector, pcDNA 3.1. For the pulldown, nuclear protein lysates were incubated with biotinylated oligodeoxynucleotides corresponding to ISRE site and detected by western blot. Band was seen from nuclear protein lysates from HEK 293T cells transfected with IRF5v4 in presence of MyD88 (c) and IRF5v5 with or without presence of MyD88 (d). No band was detected from nuclear lysates of cells transfected with MyD88 alone and empty vector, pcDNA 3.1 as well as when the nuclear protein lysates from each transfected cells incubated with scrambled oligodeoxynucleotides.

3.2.4 Transcriptional activity of *IL13* promoter by IRF5v4 and IRF5v5

To examine whether the binding of IRF5 variants to the ISRE region on the *Il13* promoter has a functional role, transient transfection was performed to evaluate the activity of luciferase reporter construct driven by *Il13* promoter. The experiment was conducted following optimized protocol performed by our group in previous study [10,190]. In this project, the transient transfection involved the co-transfection of the individual IRF5 variants together with *Il13* promoter luciferase reporter and with the presence or absence of MyD88 in HEK 293T cells. A constant amount of both the reporter *Il13* promoter luciferase plasmid and internal control T4 Renilla were included as described in methodology section 2.2.6. In order to check for any background signal interference between the two reporter plasmids used in this reporter assay, important controls (transfection of *Il13* promoter and T4 renilla plasmids alone) were included in the experiments (see Appendix 2.3). Based on the results, there was no signal interference between the two reporters since no high background signal was observed. To be precise, in the absence of renilla signal reporter, the luminescence recorded from firefly luciferase reporter containing *Il13* promoter (IL-13-firefly luciferase) was 0.067. While, in absence of IL-13-firefly luciferase reporter, the luminescence signal recorder from renilla reporter was 0.012. Co-transfection of the two reporter plasmids gave luminescence signal of 0.043.

As part of our investigation of studying the effect of IRF5v4 and IRF5v5 on IL-13 transcriptional activation, we wanted to evaluate whether the amount of

IRF5v4, IRF5v5 and MyD88 had any influence on the *Il13* promoter activity. Therefore, HEK 293T cells were co-transfected with IL-13-firely luciferase together with various amounts of IRF5v4 or IRF5v5 and MyD88 expressing plasmids in presence of renilla reporter. For better visualization, the observed effect, and values of relative luciferase units from the luminescence signals recorded are presented as in Figure 3.14. Based on the results, the presence of MyD88 alone without IRF5v4 or IRF5v5 led to some enhancement of *Il13* promoter activity. In terms of relative luciferase of *Il13* promoter activity, when the concentration of MyD88 was increased from 25 ng to 75ng, the values were found to increase from 0.22 to 0.47. However, the level dropped to 0.32 when the highest 100 ng concentration of MyD88 was tested.

Unlike MyD88, increasing concentration of IRF5v4 or IRF5v5 alone had a negligible effect on *Il13* promoter activity, as there was only a slight increase of signal levels observed above the basal level. In the situation when the varying amount of MyD88 was tested in the presence of 100 ng of IRF5v4, there was no gradual increment of *Il13* promoter activity seen. In fact, *Il13* promoter activity seemed reduced when the concentration of MyD88 was increased in presence of IRF5v4. Nonetheless, it was worth mentioning that a combination of 100 ng of IRF5v4 and 25 ng of MyD88 showed the highest *Il13* promoter activity with an increase of 27-fold compared with the control (basal activity from well transfected with empty vector in presence of IL-13 firefly and renilla luciferase plasmids). However, the *Il13* promoter activity seemed reduced when the concentration of MyD88 was increased in the

presence of 100 ng IRF5v4. The fold of change decreased from 27-fold (25 ng of MyD88) to 18-fold (100ng) compared to control. Meanwhile, in the presence of a constant amount of MyD88 (100 ng), increasing the amounts of IRF5v4 did not show much variation in the luminescence reading between the different amounts of IRF5v4 tested (ranged from 21 to 22- fold).

On other hand, co-transfection of varying amounts of MyD88 together with a constant amount of IRF5v5 (100ng) demonstrated enhanced *Il13* promoter activity proportionately to the increasing concentration of MyD88 ranged 25 to 100 ng (from 10 to 12- fold of change relative to control). A greater augmentation effect of *Il13* promoter activity was observed when MyD88 was kept constant at 100 ng and the amount of IRF5v5 was increased from 25 ng to 50 ng; the fold of change relative to control noticed was 21 and 24- fold, respectively. However, at higher concentrations; 75 ng and 100 ng of IRF5v5, the signal levels decreased to 23- fold and 18- fold relative to control, respectively. Taken together, increasing the concentration of MyD88 in the presence of IRF5v4 (constant 100 ng) did not enhance *Il13* promoter activity proportionally. Rather, *Il13* promoter activity was reduced with increasing MyD88 level in the presence of IRF5v4. Whereas co-transfection of IRF5v5 and MyD88, demonstrated enhanced *Il13* promoter activity proportionally in a dose-dependent manner.
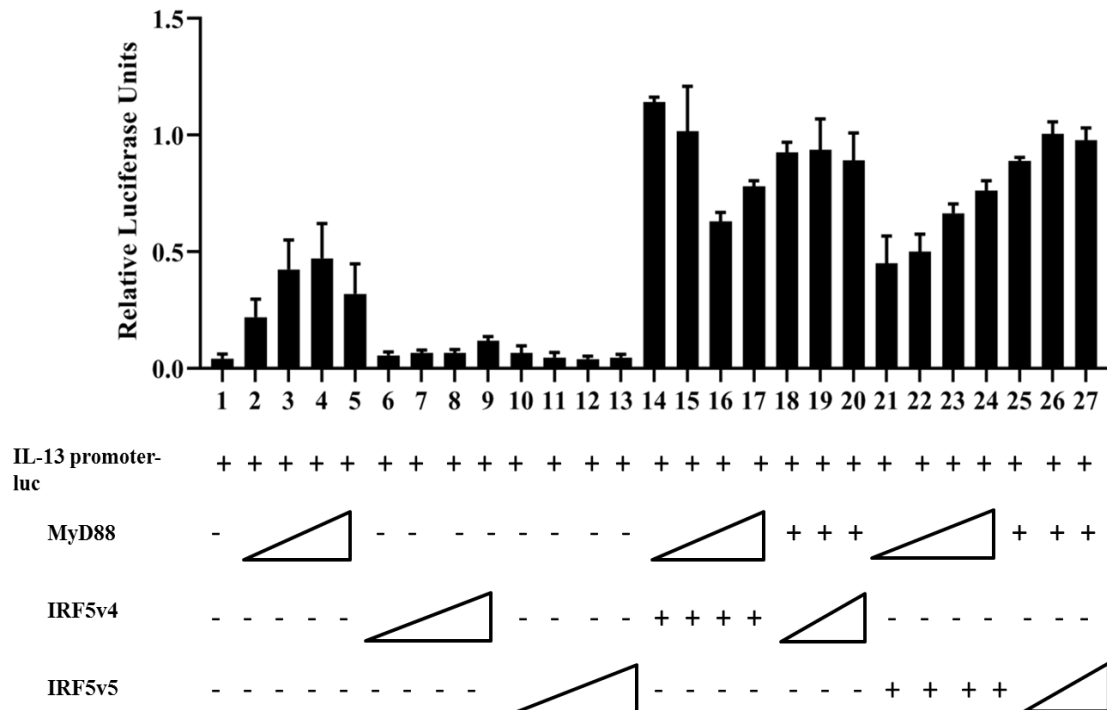
Figure 3.14 Activation of *IL13* promoter activities.
The HEK 293T cells were co-transfected with IL-13 luciferase reported plasmid, Renilla luciferase plasmid and empty plasmid (Lane 1), or with varying concentrations of specific expression plasmid increased from 25, 50, 75, and 100 ng as represented by the triangle slope (MyD88; Lane 2-5), (IRF5v4;Lane 6-9) and (IRF5v5; Lane 10-13). For co-transfection of MyD88 with IRF5 spliced isoforms expression plasmids, a varying combination was tested. MyD88 was added at increasing concentration 25-100ng, while keeping the concentration of IRF5v4 (Lane 14-17) or IRF5v5 (Lane 21-24) constant at 100ng. On the other hand, when concentration of MyD88 was kept constant at 100ng, the concentration of IRF5v4 (Lane 18-20) and IRF5v5 (Lane 25-27) were increased from 25-75ng. Luciferase activities were measured 24 hour post-transfection. The (+) and (-) signs represent the present or absence of specific expression plasmid. Results were expressed as Relative Expression (RE) from the values obtained from IL-13 firefly luciferase activity normalised to renilla luciferase activity in each transfected well.The values presented as mean ± standard error of mean from three independent experiments, each performed in triplicates wells.

3.3 Establishment of stable overexpressing IRF5v4 and IRF5v5 cells

3.3.1 Construction of lentiviral vector carrying IRF5v4 and IRF5v5 inserts

To examine the potential role of IRF5 in regulating Th1 and Th2 associated cytokines expression, stably expressing IRF5v4 and IRF5v5 clones in Jurkat cells was established. This was done first by the construction of a lentiviral vector harbouring IRF5v5 and IRF5v5 separately. The cloning strategy is summarized in Figure 3.15. The pLenti-GFP, was manipulated to carry DNA of IRF5 spliced variants. To do so, DNA fragment encoding GFP was removed and replaced with IRF5v4 or IRF5v5 DNA fragments. The process involved extracting plasmids from TOPO vector harbouring IRF5v4 or IRF5v5 and pLenti transfer vector and linearized with the same restriction enzymes, *Bam*HI and *Sal*I. Gel electrophoresis of the digested product resulted in estimated bands consisting 7900 bp and 1500 bp for vector backbone and IRF5 spliced variants respectively (Figure 3.16). The desired digested fragments of pLenti and IRF5v4 and IRF5v5 as in Figure 3.16, were excised and purified. DNA concentration of the extracted fragments was measured. Ligations were performed with a molar ratio of 1:3, vector to insert incubated overnight at 16^0C and the reaction mixture was transformed into STBL3 cells. A total of five colonies of the transformants for IRF5v4 and IRF5v5 each were picked and the presence of inserts from the transformants was investigated by colony PCR. Isolated plasmids from TOPO-IRF5v4 or TOPO-IRF5v5 were included as a positive control. As seen in Figure 3.17, only one positive transformant (transformant 3) was positive for IRF5v4 inserts. While for IRF5v5, four out of five transformants (transformant 1, 2, 3 and 5) were positive carrying IRF5v5 insert (Figure 3.18). To further verify whether these

positive clones harbour the IRF5 variants, two of the positive clones, transformant3 of IRF5v4 and transformant 1 of IRF5v5 were selected and verified with restriction digest with *Bam*HI and *Sal*I (Figure 3.19). From these results, it was confirmed that cloning of IRF5v4 and IRF5v5 into pLenti were successful as represented by their expected band sizes, 1500 bp.
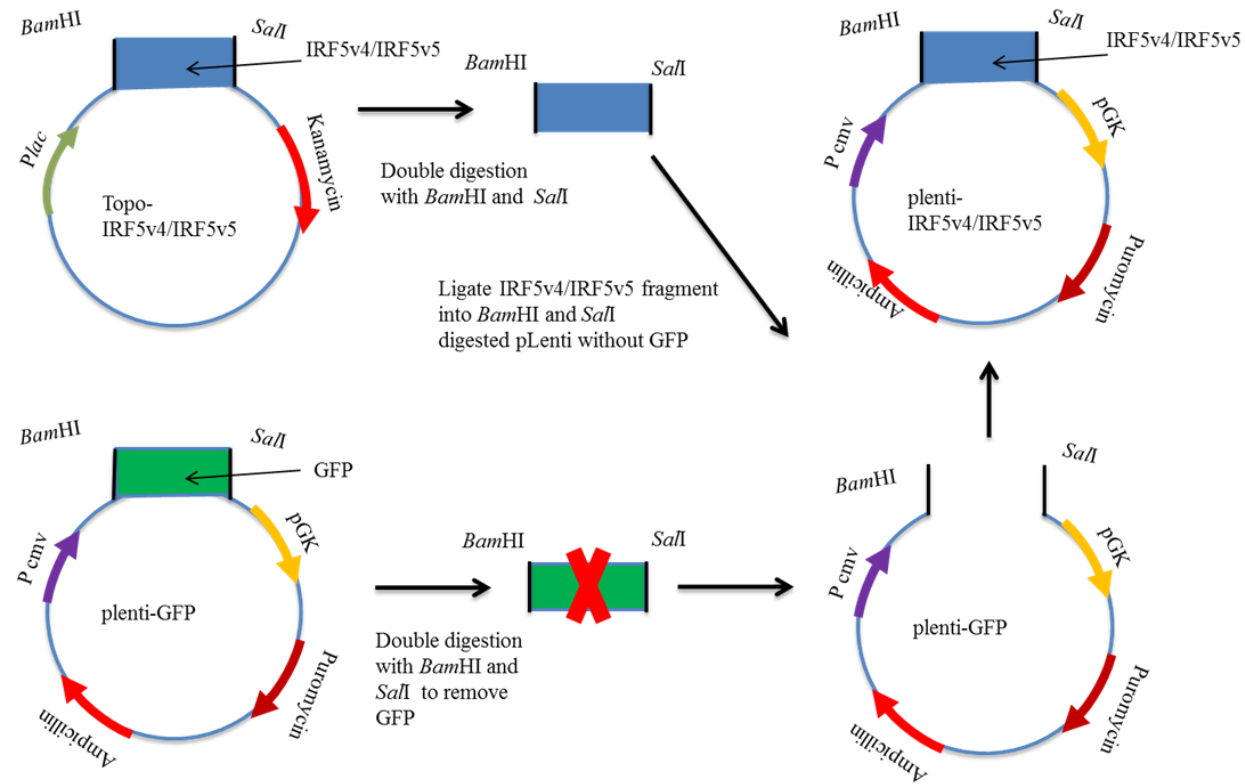
Figure 3.15 Cloning strategy of pLenti-IRF5v4 and IRF5v5 construction.
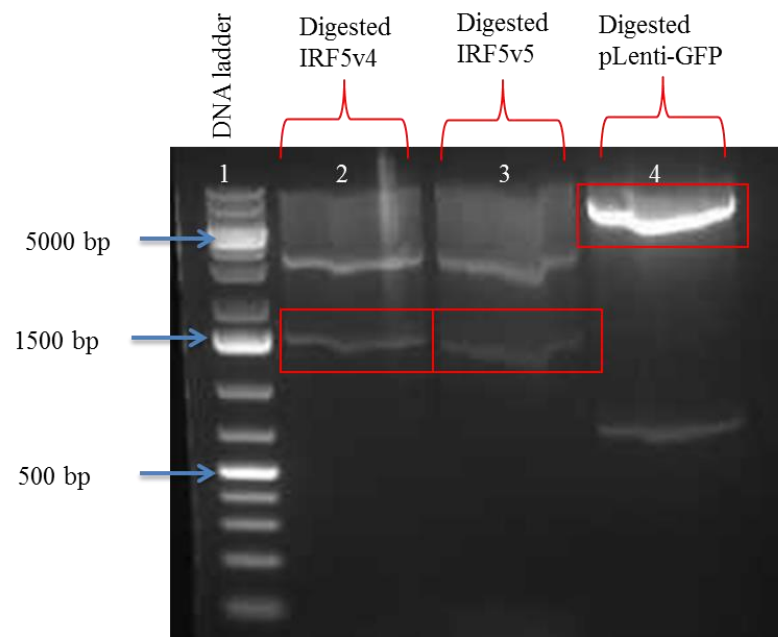
Figure 3.16 Restriction digestions of extracted plasmids of pLenti, TOPO-IRF5v4 and TOPO-IRF5v5 using *Bam*HI and *Sal*I.

The digested IRF5v4 (combined wells Lane 2) and IRF5v5 (combined wells Lane 3) from TOPO plasmids gave fragments of approximately 1500 bp. Meanwhile, digested pLenti containing the vector backbone gave fragment of approximately 7900 bp. The digested fragments used for ligations are highlighted in red box. 1kb Plus DNA ladder was loaded in Lane 1 and the major markers band sizes has been labelled as shown in blue arrow.
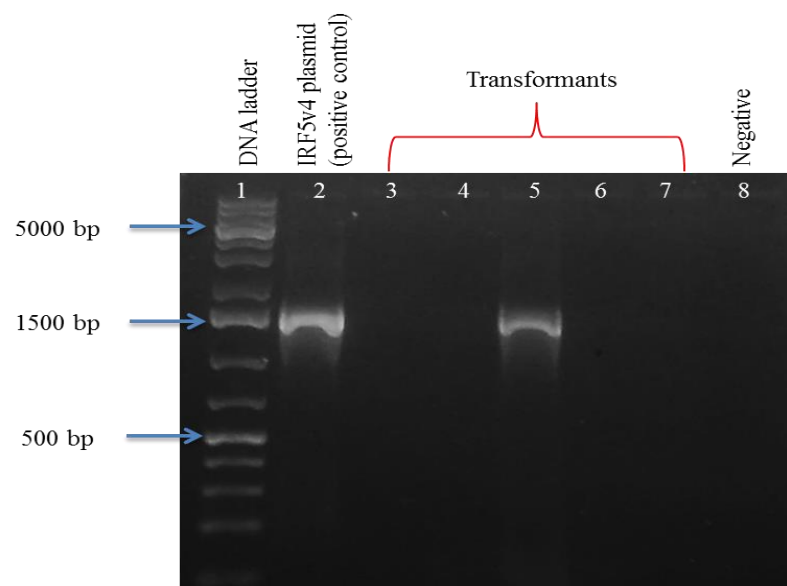
Figure 3.17 Colony PCR screening of transformants STBL3-pLenti-IRF5v4.
PCR screening of transformants for identification of IRF5v4 were loaded into Lane 3-7. Out of five selected transformants, only one positive transformant showed the presence of IRF5v4 (Lane 5). 1kb Plus DNA ladder was loaded in Lane 1 and the major markers band sizes has been labelled as shown in blue arrow. Isolated plasmid of IRF5v4 was included as positive control (Lane 2). Negative control was loaded in lane 8.
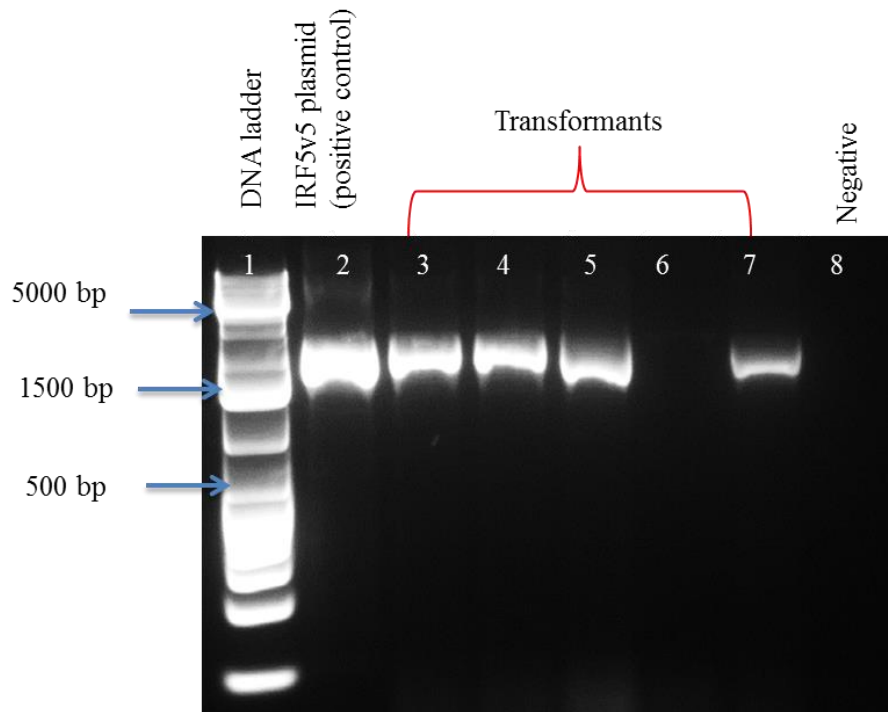
Figure 3.18 Colony PCR screening of transformants STBL3-pLenti-IRF5v5.
PCR screening of transformants for identification of IRF5v5 were loaded into Lane 3-7. All showed the presence of IRF5v5, except one (Lane 6). 1kb Plus DNA ladder was loaded in Lane 1 and the major markers band sizes has been labelled as shown in blue arrow. Isolated plasmid of IRF5v5 was included as positive control (Lane 2). Negative control was loaded in lane 8.
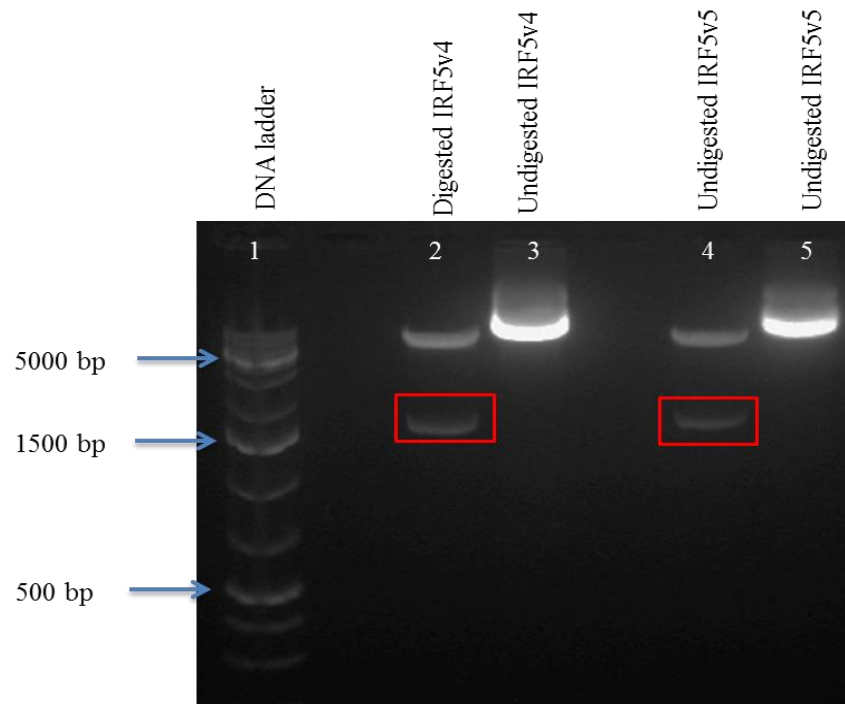
Figure 3.19 Restriction digestions of extracted plasmids of STBL3-IRF5v4 andSTBL3-IRF5v5 using *Bam*HI and *Sal*I.

STBL3-IRF5v4 and STBL3-IRF5v5 were digested with *Bam*HI and *Sal*I and loaded into lane 2 and 4, respectively. The digested fragments of approximately 1500bp are highlighted in the red box. Undigested STBL3-IRF5v4 and STBL3-IRF5v5 were loaded into lane 3 and lane 5. 1kb Plus DNA ladder was loaded in Lane 1 and the major markers band sizes has been labelled as shown in blue arrow.

3.3.2 Production of recombinant lentiviral virus harbouring IRF5v4 and IRF5v5 sequences

3.3.2.1 Optimisation of transient transfection for lentivirus production

Production of recombinant lentivirus was carried out by transient co-transfection of three plasmids, transfer vectors (either pLenti-GFP or pLenti-IRF5v4 or pLenti-IRF5v5), packaging plasmid (psPAX2) and envelope plasmid (pmD2G) into HEK 293T cells mediated by Mirus Trans-IT X2 transfection reagent. In this view, by

157

chance all the three plasmids get contained within a single cell and recombination of the plasmids genes take place, resulting in the production of lentiviral particles that would be released into the culture media. The efficiency of transfection for lentiviral production depends on three main factors; (a) ratio of DNA plasmids to transfection reagent, (b) ratio of the three plasmids and (c) the total amount of plasmid DNA in the culture flask [257]. Due to the numerous protocols available for lentivirus production, it was pertinent to adapt and modify the available protocols for the production of lentivirus in our lab. The ratio of DNA to Mirus transfection reagent (1:2.4) and the ratio of the three plasmids; transfer, packaging, envelope at 4:3:1 respectively were tested for lentiviral production.

The transfer vector pLenti-GFP which expresses GFP was utilized as a positive control to monitor the efficiency and success of transfection through visibility of green fluorescence evaluated by fluorescence microscope during the establishment of lentivirus production protocol. As seen in Figure 3.20 (a), untransfected HEK 293T cells never show any GFP expression. On other hand, GFP expression was observed from cells transfected with pLenti-GFP together with the helper plasmids. Figure 3.20 (b) shows that GFP expression was visible on day 2 post-transfection, with about 60-70% of the cells showed green fluorescence. Meanwhile, on day 3 post-transfection the transfected cells demonstrated about 80-90% of green fluorescence and the intensity of GFP expression was brighter and clearly visible, indicating efficient transfection and viral protein translation (Figure 3.20 (c)).
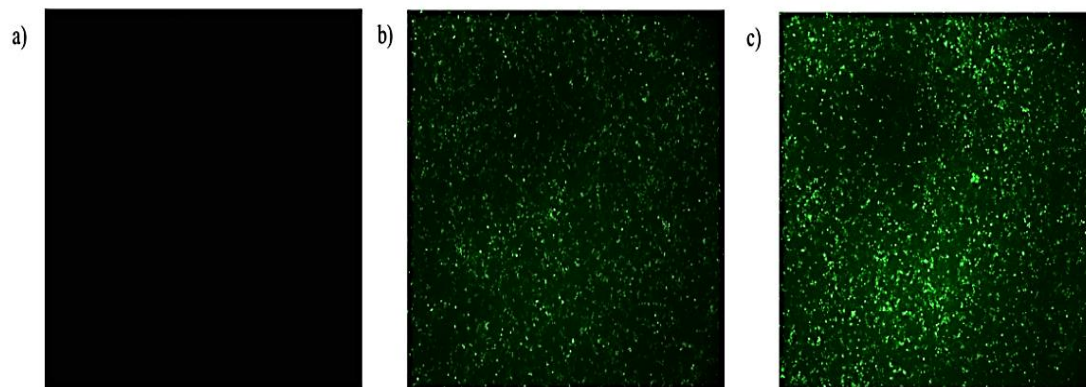
Figure 3.20 Visualisation of GFP expressions during trial experiment in HEK 293T cells.
(a) untransfected (b) transfected with recombinant lentivirus expressing GFP at day 2 post-transfection and (c) transfected with recombinant lentivirus expressing GFP HEK 293 T cells at day 3 post-transfection. Photos were taken under Nikon Upright Microscope Eclipse Ei under fluorescent light (x100 magnification). The exposure time of fluorescent photos were 600 milliseconds.

Another crucial factor that was taken into consideration was the confluency of cells for transfection. From literature, it was found out that 50-80% confluency of cells is recommended for optimal lentiviral production [225,258]. This is because the insufficient number of cells results in low virus output, while excess cell density can handicap the cell growing condition. During the establishment of protocol, a phenomenon was observed whereby over confluent cells tend to get detached easily from the flask and resulted in poor transfection as well transduction efficiency (see Appendix-2.5). We found that 5×10^6 HEK 293T cells cultured in T-75 flask in 15 ml of media were the ideal seeding number that allowed cells to be at 70-80% of confluency.

3.3.2.2 Lentivirus production for experimental lentiviral constructs

Following the establishment of transfection protocol for lentivirus production, the production of lentivirus expressing IRF5v4 or IRF5v5 were carried out. Since GFP fragments were removed to construct experimental transfer vectors (pLenti-IRF5v4 or pLenti-IRF5v5), by inserting IRF5v4 or IRF5v5 fragment in replacement of GFP fragment, there was no reporter marker to track these constructed experimental vectors during transient transfection for recombinant lentivirus production. Therefore, the production of recombinant lentivirus harbouring IRF5v4 or IRF5v5 was conducted in parallel with pLenti-GFP in separate T-75 flasks to ensure the setting for successful transfection for virus production.

As seen in Figure 3.21(a), co-transfection of pLenti-GFP along with the two helper plasmids (psPAX2 and pmD2G) in HEK 293T cells exhibited about 60-70% of green fluorescence at day 2 of post-transfection similar to the results obtained in the preliminary experiment conducted as described above. In addition, the morphology of the transfected cells was examined under the bright-field view. The photo bright-field of transfected cells shows the presence of syncytia represented by the multi-nucleated cells (in black arrow) that was caused by the translation of glycoprotein of VSV-G (envelope protein), indicating successful transfection and sign for lentivirus production [251,259]. On the third day of post-transfection, fluorescent microscopy showed GFP was expressed about 80-90% as seen in Figure 3.21 (b). From these data, it was deduced that the production of lentivirus was successful and ready to be used for transduction experiments.

160
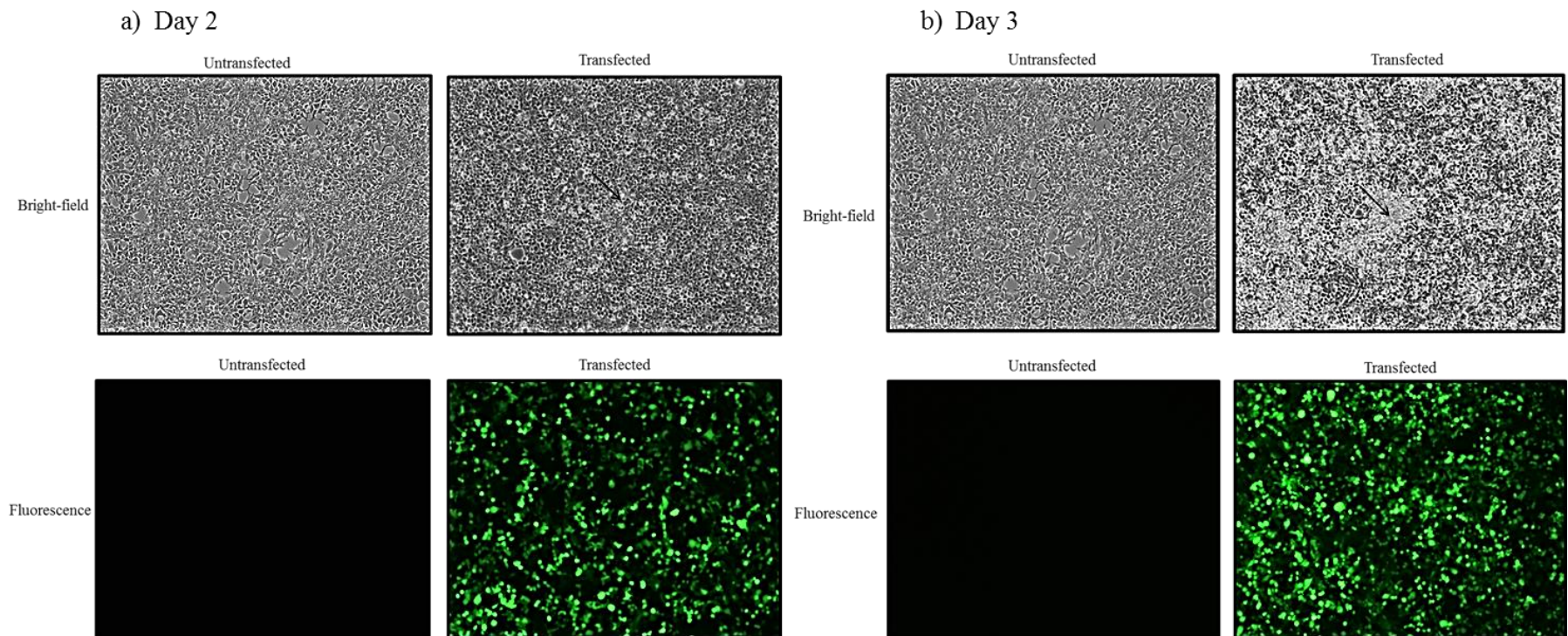
Figure 3.21 Production of recombinant lentivirus expressing GFP in HEK 293T cells visualized on post-transfection days.

a) On day 2 post-transfection. (b) On day 3 post-transfection. The formation of syncytia is indicated by black arrow. Photos were taken under Nikon Inverted Microscope Eclipse TS2R underbright field or fluorescent light (x200 magnification). The exposure time of fluorescent photos were 600 milliseconds. The black arrow-head shows the presence of syncytia in transfected cells.

3.3.3 Transduction of lentivirus harbouring IRF5v4 and IRF5v5 in Jurkat cells

3.3.3.1 Optimisation of transduction

The presence of GFP expression visualized by fluorescence microscope after transfection reveals the efficiency of transfection but it does not display the infectivity of the lentivirus. It was necessary to ensure the recombinant lentivirus harvested was infectious for proper gene delivery to target cells [260]. Also, it was important to make sure that there was no cell toxicity from viral infections that could cause large cell death, resulting in a lower transduction rate. Crude viral supernatant is usually sufficient for in vitro transduction [261]. Most of the existing protocols used 6 well-plates with seeding of cells at $2x10^5$ cells/well and 8μg/ml of polybrene with various amounts of lentivirus supernatant used [250,262,263]. The function of polybrene is to enhance transduction efficiency. As a cationic polymer, polybrene counteracts the repulsive electrostatic effect exerted by the negatively charge virus lipid and cell membrane [264]. This, in turn, mediates virus adsorption into the cell membrane, thereby increasing the efficiency of the transduction rate. A titration on HEK293T cells, the cell density and amount of polybrene used was applied according to the protocols with little modifications on the amount of lentivirus supernatant tested. Based on the results, the minimal volume of lentiviral supernatant inoculum that showed some GFP expression was 0.6ml (Figure 3.22(b)) and the highest volume, 2 ml tested showed greater transduction efficiency of more than 90% GFP expression seen (Figure 3.22(f)). Moreover, about 95% of viable cells were observed through the evaluation of trypan blue, indicating no cell toxicity from viral infections with the

amount of virus supernatant used for transduction. This data provided evidence that

the recombinant lentivirus produced was infectious and good transduction efficiency

was achieved with crude viral supernatant.
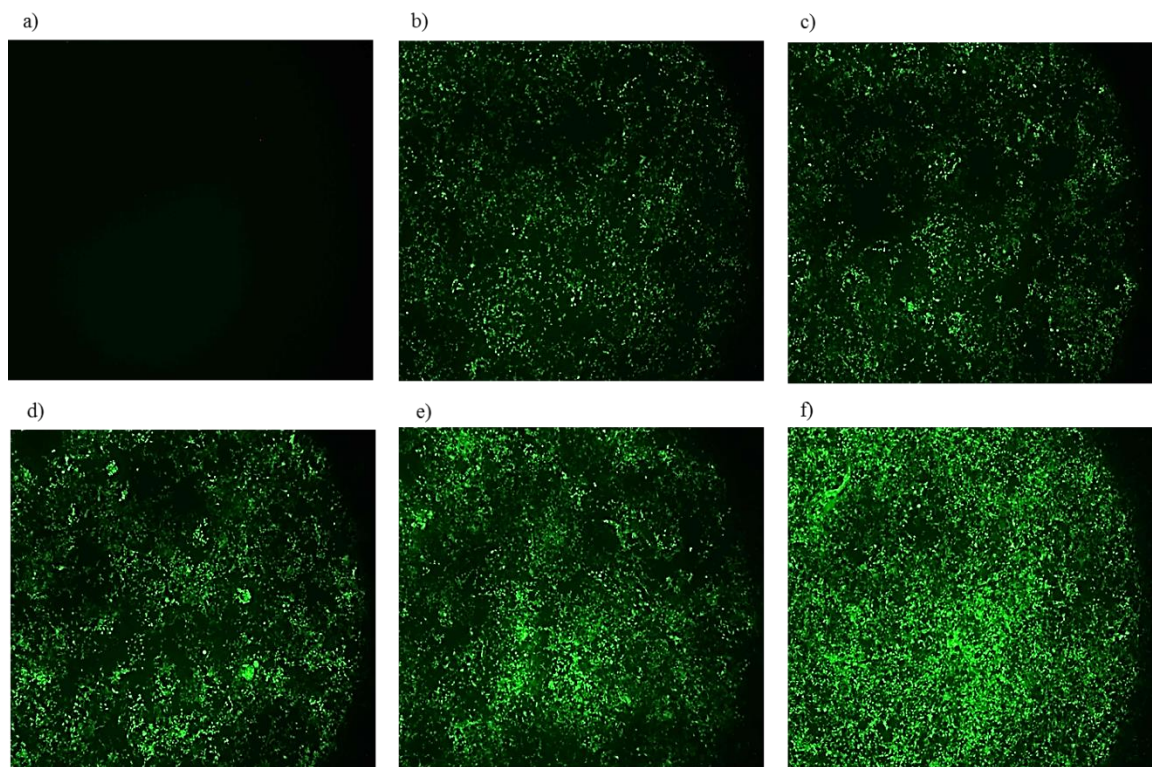
Figure 3.22 Titers of lentivirus expressing GFP in transduced HEK 293T cells.
 (a) untransduced, (b) 0.6 ml of lentivirus, (c) 0.8ml of lentivirus, (d) 1ml of lentivirus, (e) 1.5ml and (f) 2ml of lentivirus. Photos were taken under Nikon Upright Microscope Eclipse Ei under fluorescent light (x100 magnification). The exposure time of fluorescent photos were 600 milliseconds.

Transduction is more permissible in the adherent cell lines, thus spinoculation is not required transduction in HEK 293T cells. But this is not the same for suspension cells like Jurkat cells. Numerous researchers have conducted transduction of Jurkat cells by spinoculation along with the presence of polybrene, which has shown to enhance transduction of lentiviral vector by virus binding to the cells [245,265–267]. Hence, taking this into consideration we conducted a trial to establish a transduction protocol for Jurkat cells. As described in the methodology section 2.2.8, $2x10^5$ cells/well of Jurkat cells were transduced with 2 ml of virus supernatant in presence of 8ug/ml of polybrene by spinoculation. After 72 hours of transduction, GFP expression was accessed by fluorescence microscope. As expected, no GFP expression was observed in untransduced cells (Figure 3.23(a)). Meanwhile, the transduced cells showed a great transduction efficiency of more than 70% of GFP expression accessed by fluorescence microscope as displayed in Figure 3.23(b). The results confirmed the efficient transduction by the infectious virus that was produced. Furthermore, no cell toxicity from viral infection was noticed as about 95% of viable cells were observed by the evaluation of trypan blue.
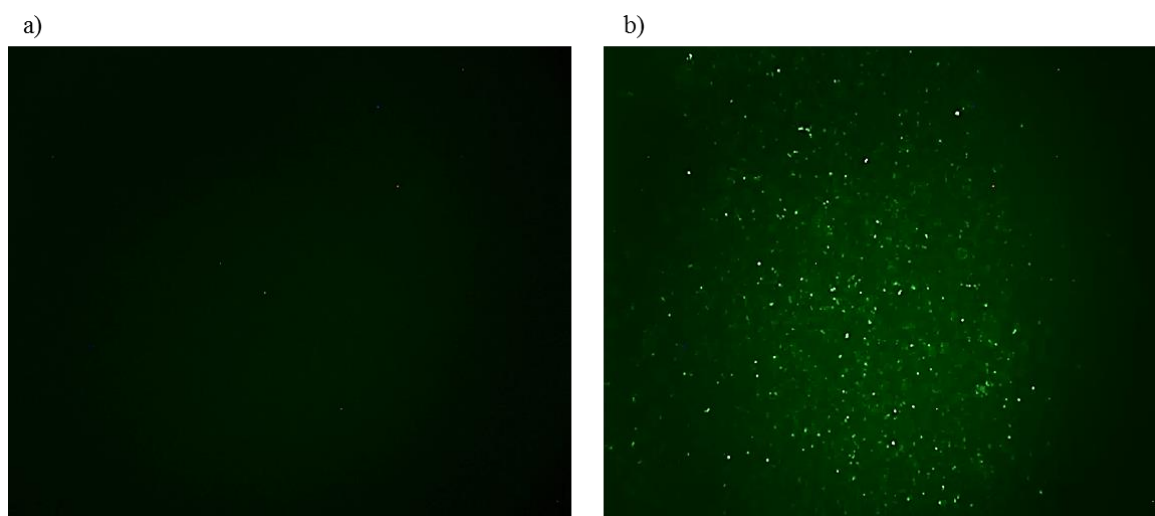
Figure 3.23 Visualisation of GFP expression during trial experiment for transduction of Jurkat cells with lentivirus harbouring GFP.
(a) untransduced (b) day 2 post-transductions. Photos were taken under Nikon Upright Microscope Eclipse Ei under fluorescent light (x100 magnification). The exposure time of fluorescent photos were 600 milliseconds.

3.3.3.2 Transduction of lentiviral constructs

Following the establishment of transduction protocol, transduction of Jurkat cells with recombinant lentivirus harbouring IRF5v4 or IRF5v5 was carried out. The experiment was conducted in parallel with a control transfer vector, pLenti-GFP in a separate culture flask to track a successful transduction experiment. As seen in Figure 3.24, the bright field photo of transduced cells revealed that infection with lentivirus did not alter the morphology of Jurkat cells, implying no cell toxicity from the lentiviral transduction. Moreover, the transduction of Jurkat cells with virus supernatant obtained from transfection of the pLenti vector expressing GFP displayed about 70-80% of green fluorescence, similar to the results obtained from the trial experiment. From these data, it was deduced that Jurkat cells were efficiently transduced by the infectious lentiviral constructs.

165
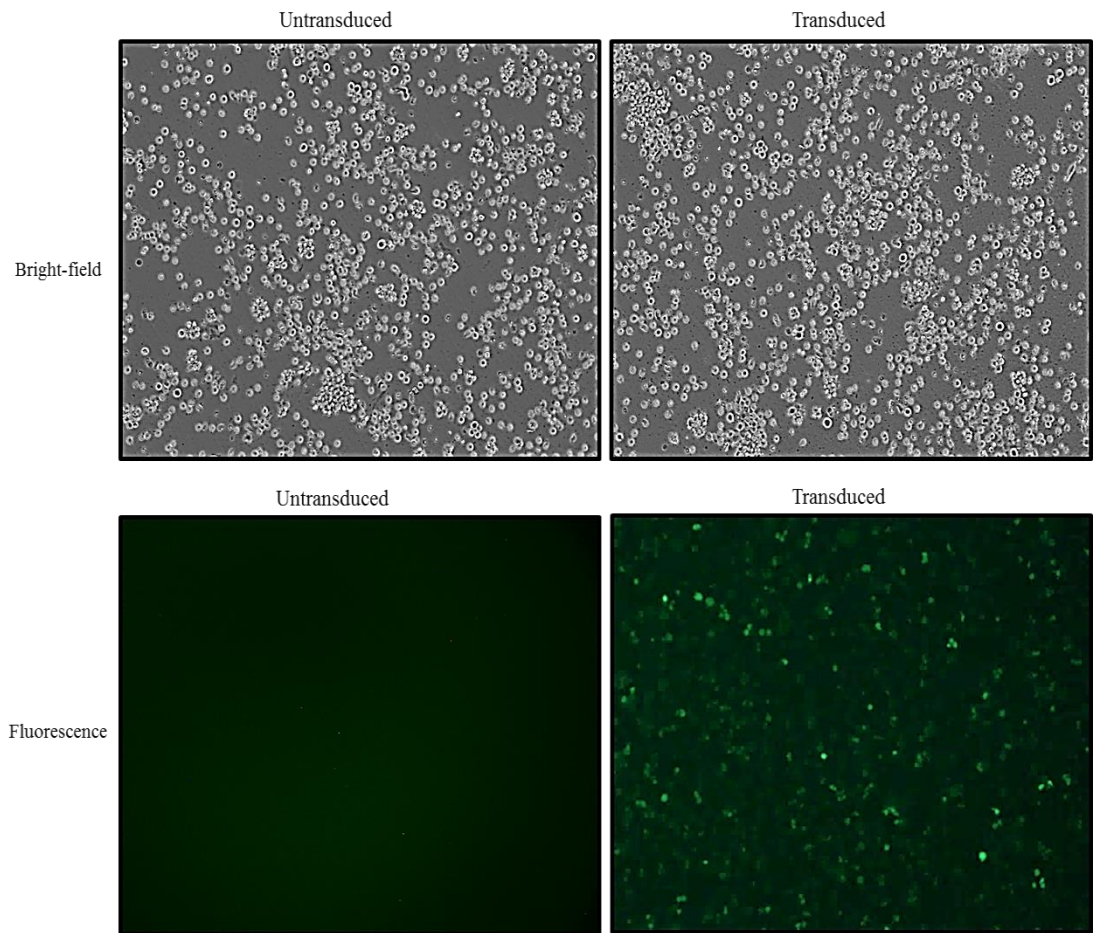
Figure 3.24 Detection of GFP expressions from transduced Jurkat cells with lentivirus harbouring GFP at day 3 post-transduction.
Photos were taken under Nikon Inverted Microscope Eclipse TS2R under bright field or fluorescent light (x200 magnification). The exposure time of fluorescent photos were 600 milliseconds.

3.3.4 Puromycin selection for stably expressing IRF5v4 and IRF5v5 in Jurkat cells

3.3.4.1 Polyclonal cells selection

Control transfer vector pLenti-GFP and the experimental constructed pLenti-IRF5v4 and pLenti-IRF5v5 encode the puromycin-N-acetyl transferase (*Puro*) in their plasmid backbone and constitutively express it. For cells to survive and proliferate when grown in complete media supplemented with puromycin, the cells must express *Puro*, the puromycin resistance gene. Thus, only transduced cells with recombinant lentivirus which constitutively expresses the *Puro* gene, will survive when grown in complete media containing puromycin, whereas those cells without the *Puro* gene will die because puromycin is toxic to cells. Prior to the puromycin selection of the transduced cells, puromycin titration was carried out to obtain the minimal dose that can kill untransduced Jurkat cells. This killing dose is dependent on the increasing concentration of puromycin from the range of 0-10 µg/ml that is capable to kill 100% untransduced cells in 72 hours. The cell viability was accessed with trypan blue and it was observed that at the concentration of 5µg/ml and 10µg/ml all the untransduced cells were dead. The minimum dose of 5µg/ml of puromycin that kills all untransduced cells was chosen as the optimal antibiotic concentration for selection process.

Selection of transduced Jurkat cells in puromycin containing media typically takes two weeks to achieve the population of cells that contain only integrated transgene as any unintegrated cells would have died [251,268,269]. These bulk cells

that survived from the antibiotic selection are referred to as polyclonal cells. The success of the puromycin selection process was initially checked with polyclonal cells generated from lentiviral harbouring GFP gene. Figure 3.25 shows the photo of the polyclonal cells visualized under a fluorescence microscope, which revealed the presence of GFP expression. Hence, confirming that the surviving cells were comprised of stably expressed population. As mentioned earlier, there was no reporter protein that may act as an indicator for experimental constructed lentiviral IRF5v4 or IRFv5. The presence of IRF5v4 or IRF5v5 in the polyclonal cells generated from the experimental lentiviral constructs were checked through detection of the transcript and protein level through reverse transcription PCR (RT-PCR) and western blot analysis respectively.
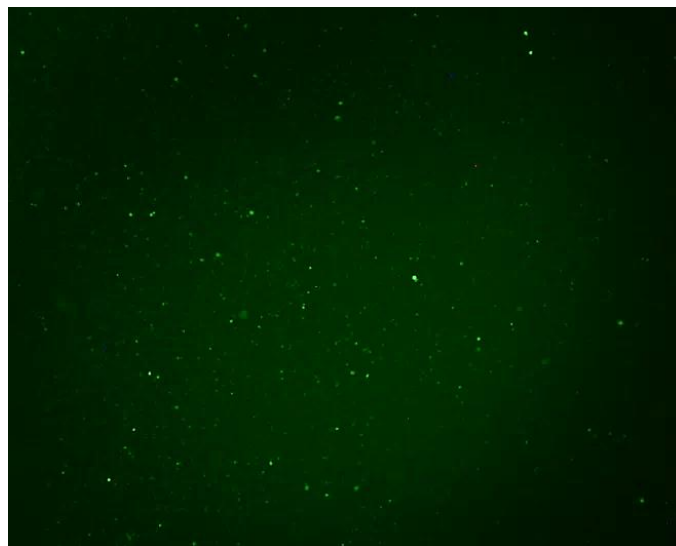
Figure 3.25 Visualisation of GFP expressions in polyclonal cells generated from Jurkat cells transduced with lentiviral harbouring GFP.
Photos were taken under Nikon Upright Microscope Eclipse Ei under fluorescent light (x100 magnification). The exposure time of fluorescent photos were 600 milliseconds.

The RT-PCR method involves the reverse transcription of mRNA to complementary cDNA (cDNA) and detectable levels of the cDNA by PCR amplification [270]. Amplified PCR products are visualized in agarose gel electrophoresis mediated by DNA staining solution. In the initial stage of the experiment, several important experimental conditions were optimized to ensure reproducibility and effective results. Total RNA was isolated from unstimulated and stimulated cells and the RNA integrity was determined as described in section 2.1.5. The purity of the total RNA samples (ratio of 260/280 nm) ranged from 1.8 to 2 while the concentration ranged from 300-500 ng/μl. The isolated RNA samples were treated with DNAse to remove any genomic DNA contamination. Next, to verify whether primers designed specifically amplified the IRF5 spliced isoforms at optimal annealing temperature, gradient PCR was conducted using IRF5v5 plasmid as template. The results showed bands of expected sizes corresponding to the IRF5v5 (presented in Appendix-2.6), and annealing temperature of $58^{0}C$ was chosen for the amplification of IRF5 spliced variants. Subsequently, the mRNA level of IRF5v4 and IRF5v5 from respective polyclonal cells were evaluated. As seen in Figure (3.26 (a)), untransduced cells did not show either IRF5v4 or IRF5v5 expression as expected because Jurkat cells lack endogenous IRF5 expression [18,150,154]. Meanwhile, it was observed that the transcript of mRNA level of IRF5v5 was higher than IRF5v4 as represented by the intensity of bands. This variation of different level of transcript between IRF5v4 and IRF5v5 is to be expected because the copy number of lentivirus integrating into the genome of the cells were not controlled.

To further confirm the results above, protein level was evaluated through western blot following the protocol that has been established by our group which was performed during routine experiments. To ensure the specificity of IRF5 antibody used in this study, untransduced Jurkat cells and cells transfected with pLenti-GFP were included as negative control. As seen in Figure 3.26 (b), no IRF5 was detected in cell lysates isolated from untransduced Jurkat and pLenti-GFP. On the other hand, approximately 60 kDa bands corresponding to the IRF5v4 and IRF5v5 protein were detected from respective polyclonal cells as shown in Figure 3.26 (b). Hence, the western blot results correlate with RT-PCR findings. From these results, it was deduced that experimental lentiviral constructs had successfully integrated the transgene of IRF5v4 or IRF5v5 in Jurkat cells.
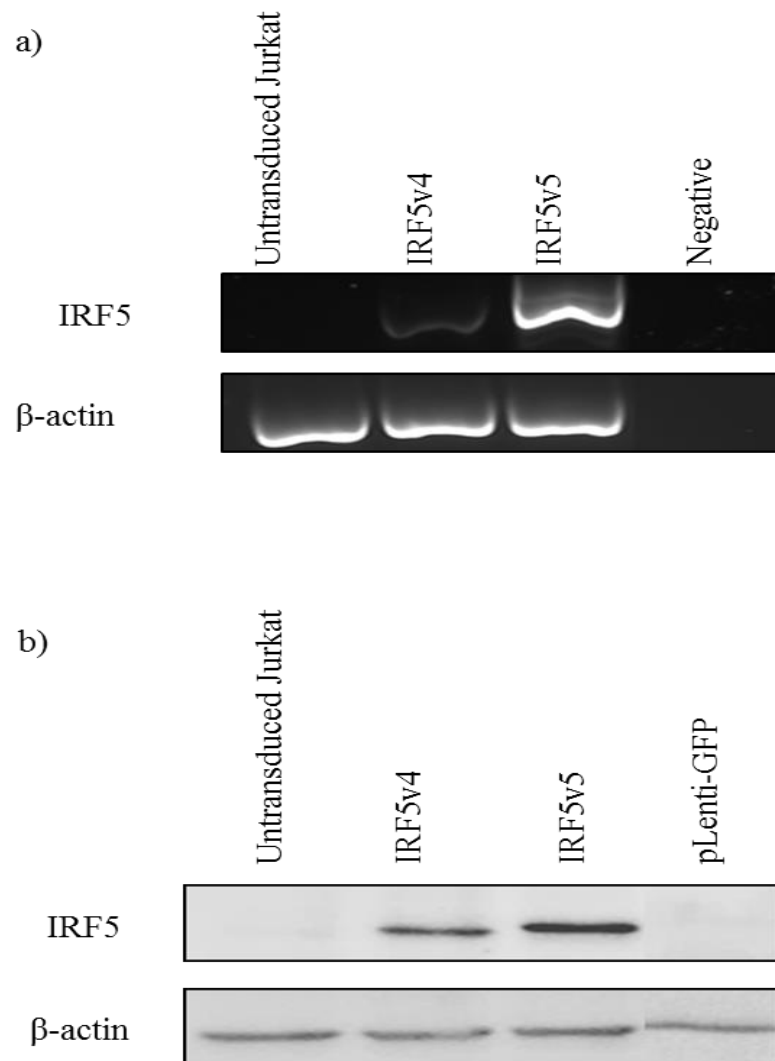
Figure 3.26 Confirmation of overexpression of IRF5v4 and IRF5v5 in polyclonal cells.
a) mRNA of IRF5v4 (314 bp) and IRF5v5 (382 bp) in polyclonal cells determined by reverse transcription PCR, as shown in lane 2 and 3 respectively. Housekeeping gene, β-actin as the loading control (182bp) was included in the analysis. Untransduced Jurkat cells (lane 1) and non-template control (lane 4) was included as negative control. b) Western blot analysis for detection of IRF5v4 (lane 2) and IRF5v5 (lane 3) (approximately 60kDa). Housekeeping protein actin act as the loading control (43kDa) was included as part of the analysis. Untransduced Jurkat (lane 1) and cells transfected with pLenti-GFP (lane 4) were included as negative control. The chemiluminescense signal was captured by Gel Doc imager.

3.3.4.2 Monoclonal cells selection

Polyclonal cells constitute heterogeneous transgene expression levels [251]. The limitation of using polyclonal cells in overexpression experiment is that over time transgene population of polyclonal cells may drop because cells with high levels of the transgene may have a slower growth rate, therefore the rapidly growing low-level transgene expressors may take over the culture. Hence, we decided to proceed with monoclonal selection for the generation of a stable population of cells that express either IRF5v4 or IRF5v5 homogenously. Following confirmation of IRF5v4 and IRF5v5 expression in the polyclonal cells, these cells were used for the generation of monoclonal cells through limiting dilution. Limiting dilution is a traditional method for obtaining clonally identical cells (monoclonal) of stable expressing transgene derived from isolated single cells cultured in multi-well plates [212]. Several monoclonal cells were isolated and expanded in culture with complete media containing 5 µg/ml of puromycin. The clones were screened for the presence of overexpression of IRF5v4 and IRF5v5 using western blot analysis. From the result seen in Figure 3.27, three clones expressing IRF5v4 (referred as to B8, F9, and G3) and one clone expressing IRF5v5 (referred to as H3) were found to have stable high IRF5 expression as depicted as in Figure 3.27. Alas, during the cell growth maintenance only two clones; G3 and H3 were identified as the best performing clones in terms of possessing healthy cell behaviour. Taken together, stably overexpressing IRF5v4 and IRF5v5 were successful achieved through lentiviral transduction. Two monoclonal cells representing IRF5v4 (G3) and IRF5v5 (H3)

expressing Jurkat cells were selected as a model to study the effect of these IRF5

spliced variants in modulating Th1 and Th2 cytokines.
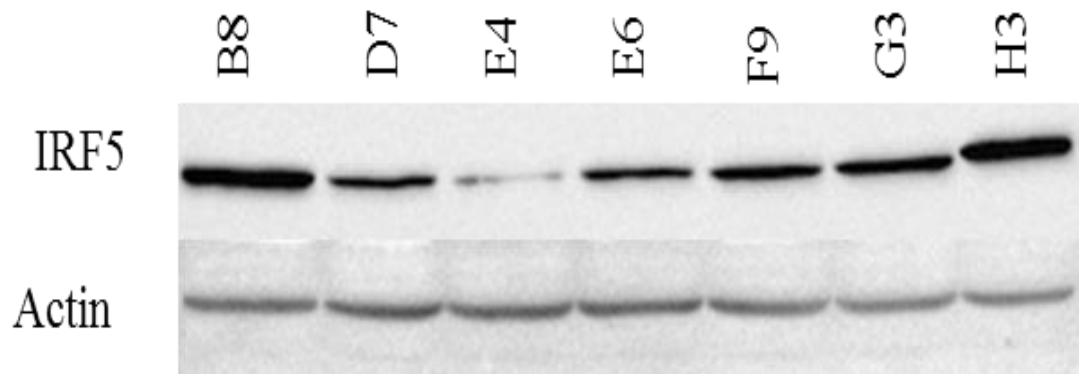
Figure 3.27 Confirmation of overexpression of IRF5v4 and IRF5v5 in monoclonal cells.
Different expression levels of IRF5v4 in monoclonal cells (B8, D7, E4, E6, F9 and G3) and one monoclonal showed the presence of IRF5v5 (H3). The bands were detected at approximately of 60kDa.Housekeeping protein actin act as the loading control (43kDa) was included as part of the analysis. The chemiluminescense signal was captured by Gel Doc imager.

3.4 Modulations of IRF5v4 and IRF5v5 in Th1 and Th2 cytokine expression

Since IRF5v4 and IRF5v5 was able to bind to the ISRE region of *Il13* promoter and transactivate its promoter activity. Next, we examined whether these IRF5 isoforms is capable of inducing IL-13 expression. At the same time, we evaluated the potential role of IRF5v4 and IRF5v5 in modulating Th1 and Th2 cytokines in Jurkat cells. To do so, Jurkat stably expressing IRF5 (G3 clone; IRF5v4 and H3 clone; IRF5v5) were stimulated with PMA and Ionomycin. The cytokines mRNA expression levels were measured through semi-quantitative RT-PCR and the secretion was assayed using ELISA. Parental (untransduced) Jurkat cells were included as control cells.

3.4.1 Analysis of Th1 and Th2 cytokines mRNA by semi-quantitative RT-PCR

3.4.1.1 Determination of PCR conditions

Although real-time PCR is often the preferable method due to its advanced technology and rapid quantification, semi-quantitative RT-PCR is still useful and reliable method when small number of cytokines panel are studied. In addition, it is cost-effective compared to real-time PCR, as it does not require sophisticated machine and reagents. Also, it can be easily done in different laboratory settings. The experimental conditions were first tested to achieve effective semi-quantitative measurement of the targeted PCR amplicons. The sequences of primers for amplification of IFNγ, IL-2, IL-4, IL-5, IL-10, and IL-13 were obtained from previous published articles [253–255]. To verify that the primers specifically amplified the desired cytokine at optimal annealing temperature, gradient PCR was conducted using

cDNA samples from PMA-Ionomycin stimulated Jurkat cells which served as positive control. Jurkat cells were stimulated with 25 ng/ml of PMA and 1uM of Ionomycin for 6 hours. Annealing temperature for gradient PCR amplification tested was ranged from 50-68^{0}C. The results are as presented in Appendix- 2.9. Annealing temperature of 60^{0}C which showed distinct band was chosen for the amplification of IFNγ, IL-2, IL-4, and IL-13. With regards to IL-5 and IL-10, no band was detected from the PCR products. Hence, these two cytokines were not included in the following experiments.

When performing semi-quantitative RT-PCR it is important to determine the optimal number of cycles. This is to ensure that the PCR was done at the exponential phase and for a clear visible band on agarose gel for quantification [271]. To determine the optimal number of PCR amplification for desired cytokine genes, PCR at different number of cycles using cDNA samples from stimulated cells was conducted. The number of PCR cycles selected was 20, 25, and 30, for β-actin, IFNγ, and IL-2. While for IL-4 and IL-13, 20, 25, 30 and 35 cycles were tested. The results are depicted in Figure 3.28. From the results, PCR amplification done for 20 and 25 cycles showed unclear bands for all the cytokines as well as for β-actin, the housekeeping gene. However, at 30th cycle, clear bands were seen for β-actin, IFNγ, and IL-2 transcripts. With regards to IL-4 and IL-13 transcripts, sharper and clearer bands were visualized at the 35th cycle. Therefore, for subsequent experiments, 30 cycles of PCR were selected for amplification of β-actin, IFNγ, and IL-2. Whereas for amplification of IL-4 and IL-13; 35 cycles were chosen.
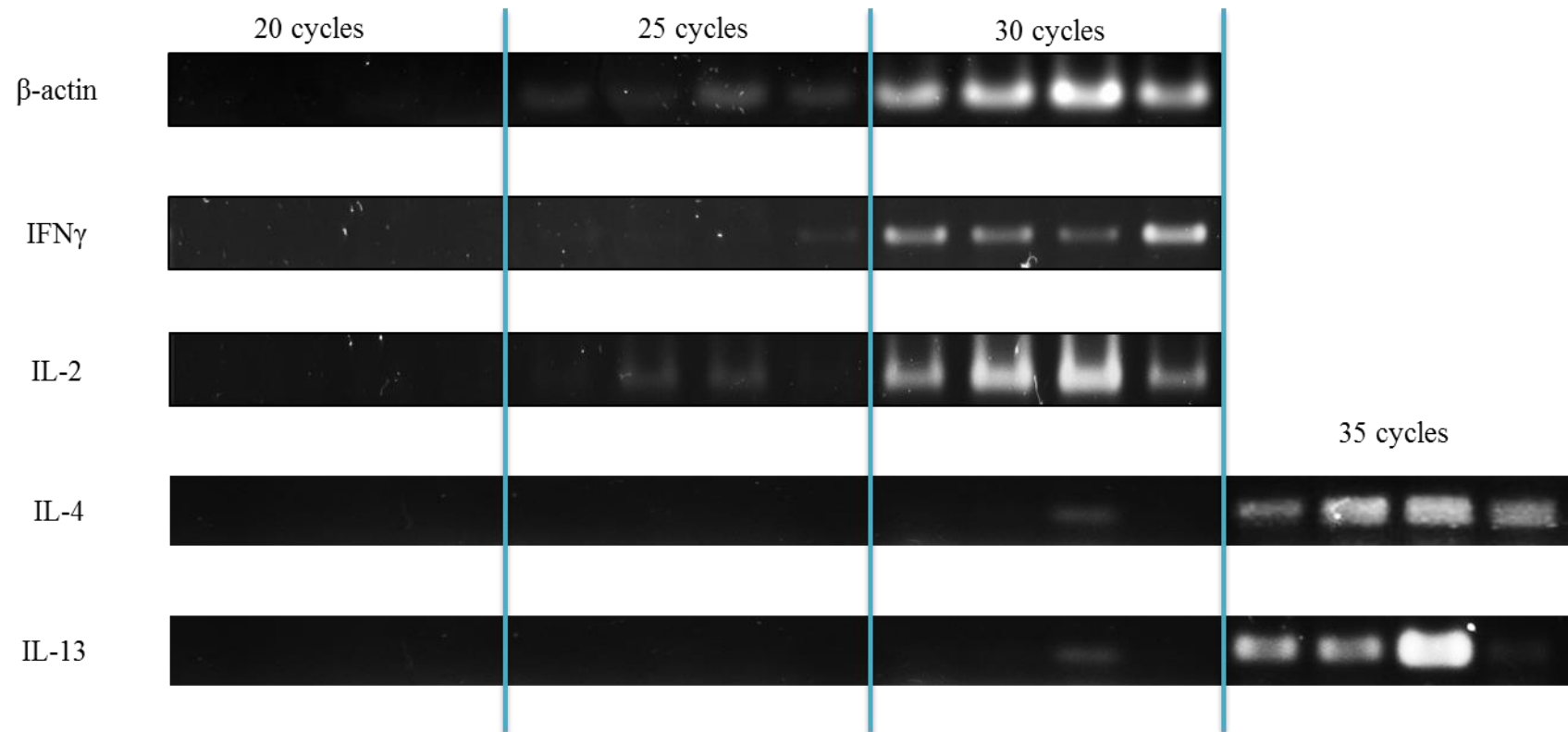
Figure 3.28 Determination of exponential range for amplification of cytokines gene and housekeeping gene by RT-PCR analysis. Parental Jurkat cells were stimulated with PMA and Ionomycin for 6 hours, and used for cDNA preparation. The amplification of PCR was done at 20th, 25th and 30th cycles to amplify β-actin, IFNγ and IL-2. Additional amplification of 35th cycle was included for IL-4 and IL-13. The PCR products were visualized using gel electrophoresis.

3.4.1.2 Semi-quantitative RT-PCR

Cells were cultured in the presence or absence of 25 ng/ml of PMA and 1 μM Ionomycin for 6 hours. The RT-PCR was performed using cDNA samples prepared as described in section 2.1.15.3. The PCR amplicons were visualized in gel electrophoresis as presented in Appendix- 2.10. The intensity of bands of agarose gels was converted using the ImageJ analyser. The relative expression values obtained for each cytokine specific PCR reactions were normalized against respective β-actin bands to compensate for the variation among cDNA samples. The relative expression levels of IFNγ, IL-2, IL-4, and IL-13 in unstimulated and stimulated cells from three individual experiments are presented in Figure 3.29. According to the results, IRF5v5 cells expressed the highest IFNγ mRNA level represented by the relative value of 1.78 compared to IRF5v4 and control cells with relative values of 0.73 and 0.75, respectively. In terms of IL-2, both IRF5v4 and IRF5v5 cells induced higher IL-2 expression than control cells upon stimulation. In particular, the relative expression values of IL-2 was about 2-fold higher in stimulated IRF5v4 cells (2.55) and IRF5v5 cells (2.18) compared to stimulated control cells (1.13) but these differences were not statistically significant.

With regards to IL-4, a Th-2 related cytokine, both IRF5v4, and IRF5v5 cells displayed lower transcript levels of IL-4 in comparison to stimulated control cells upon stimulation. Particularly IRF5v4 cells had a relative expression value of 0.96 and IRF5v5 had 0.43, whereas control cells had a remarkably higher relative value of 1.79. In terms of fold change relative to control cells, IRF5v4 cells demonstrated a reduction of about 2-fold while

IRF5v5 cells had a reduction of about 4-fold. Interestingly, stimulated IRF5v4 cells exhibited a significantly high expression of IL-13, another member of Th2 cytokine when compared to stimulated IRF5v5 cells and stimulated control cells. Stimulated IRF5v4 cells had an increment of 2-fold meanwhile stimulated IRF5v5 cells displayed the opposite; a reduction of 2-fold change relative to control cells. The relative expression value of IL-13 was 1.68, 0.3, and 0.71 for stimulated IRF5v4, IRF5v5, and control cells, respectively. In all, IRF5v4 and IRFv5 showed the differential effect in regulating Th1 and Th2 associated cytokines upon stimulation. While IRF5v4 had no effect on IFNγ mRNA expression, IRF5v5 was able to induce IFNγ mRNA expression. In terms of IL-2 expression, IRF5v4 was able to induce IL-2 better than IRF5v5. Moreover, IRF5v5 showed reduced expressions of Th2 cytokines; IL-4 and IL-13. On the other hand, IRF5v4 demonstrated higher expression of IL-13 but lower of IL-4 expression.
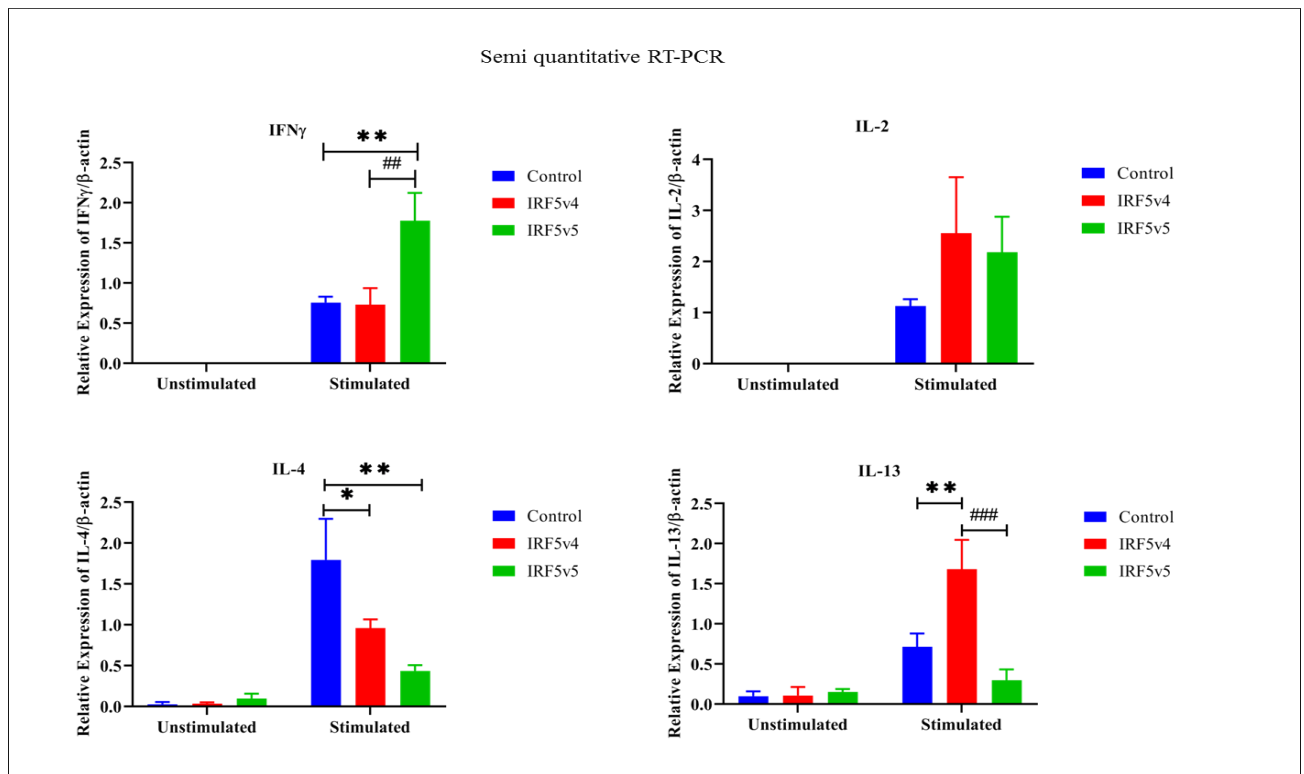
Figure 3.29 Semiquantitative RT-PCR of IFNγ, IL-2, IL-4, IL-5, IL-10 and IL-13 mRNA levels.

The cDNA samples were prepared from unstimulated cells or cells stimulated with PMA-Ionomycin for 6 hours and used for PCR as described in the methodology section. The PCR amplicon was visualized through gel electrophoresis and the intensity of the band was quantified using Image J software. The relative expression was calculated as the expression ratio of each gene against β-actin. Values are expressed as mean ± standard error of mean from three independent experiments performed in duplicates (n=3). Statistical analysis was done using two-way ANOVA with Tukey multiple comparison tests. The asterisk represents **$p < 0.001$, p* < 0.01 when cells were compared to control cells and ###$p < 0.0005$, ##$p < 0.001$ when cells were compared to IRF5v4 cells.

3.**4.2 Analysis of Th1 and Th2 cytokine production by ELISA**

Although PMA and Ionomycin are regarded as potent pharmacological agents for inducing cytokine production, at the same time these agents are also known to cause cell death when cultured in extended time (16-24 hours) [231,272]. In this regard, it was necessary to evaluate whether the cell death after stimulation was associated with secreted cytokines rather than toxicity induced by the mitogen. Therefore, to know which combination of concentration of PMA and Ionomycin will provide the best cell stimulation for cytokine production, a concentration profile of different concentrations of PMA (5 ng/ml, 10 ng/ml, 25 ng/ml, and 50 ng/ml) and (0.5 µM and 1 µM) Ionomycin were tested using control cells. Analysis of ELISA of IL-2 supernatant from stimulated control cells was employed as a strategy to evaluate the dose- response of PMA-Ionomycin. Cell viability was assessed through trypan blue. From the results Figure 3.30, we observed that 1 µM of Ionomycin produced 2-fold of higher IL-2 secretion, in comparison to 0.5 µm of Ionomycin used to stimulate parental Jurkat cells. At the concentration of 25 ng/ml PMA and 1 µM Ionomycin, stimulated Jurkat cells produced the highest amount of IL-2 (489.29 pg/ml) compared to the rest of the concentrations. Although there were a lot of cells dead after stimulation, a relatively high amount of cytokines were secreted when the cells were stimulated 25 ng/ml of PMA and 1 µM Ionomycin. Hence, this concentration was used throughout the stimulation experiment.

IL-2
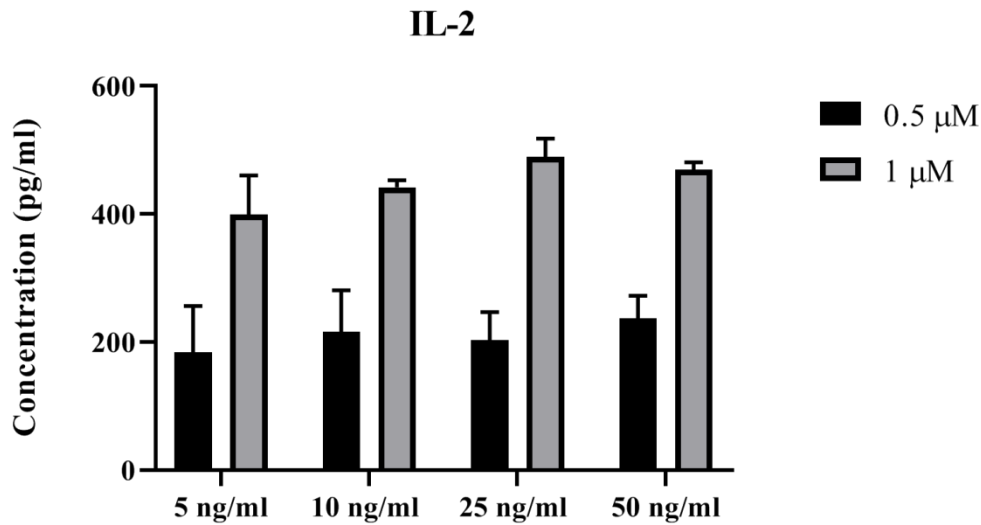
Figure 3.30 Optimisation for IL-2 production by PMA-Ionomycin stimulated Jurkat cells. Jurkat cells were stimulated with range of PMA concentration 5 ng-50 ng/ml in presence of 0.5 μM ionomycin represented by black bar or PMA concentration 5ng-50ng/ml in presence of 0.5μM ionomycin represented by grey bar for 24 hours. Supernatants were then collected and analysed for IL-2 cytokine content by ELISA. The results are presented as mean ± standard error of mean from two independent experiments (n=2) performed in duplicate wells.

Next, Th1 and Th2 cytokines profile in IRF5v4 or IRF5v5 expressing Jurkat cells were evaluated in response to with or without stimulation of 25 μg/ml PMA and 1 μM Ionomycin, in parallel with control Jurkat cells. After 24 hours, culture supernatant was collected and assayed for cytokine production by ELISA as described in methodology section 2.2.14. As seen in Figure 3.31, stimulated IRF5v4 and IRF5v5 cells displayed two-fold higher levels of IL-2 secretion in comparison to stimulated control cells. The highest level of IL-2 was secreted by IRF5v5 cells (859.15 pg/ml, $p < 0.001$) followed by IRF5v4 cells (805.97 pg/ml, $p < 0.001$) compared to control cells (407.68 pg/ml, $p < 0.001$). Unstimulated cells did not show any detectable amount of IL-2 above the detection limit of 7.8 pg/ml. With

regards to the Th-1 related cytokine, IFNγ levels was found lower in the stimulated IRF5v5 compared to stimulated control cells. Nonetheless, no significant difference was observed in the IFNγ secretion between stimulated control (52.94 pg/ml) and IRF5v5 cells (48.11 pg/ml). However, IFNγ secretion was significantly diminished in stimulated IRF5v4 cells, suggesting inhibitory effect of IRF5v4 in IFNγ production. Like IL-2, unstimulated cells did not show any detectable amount of IFNγ above the detection limit of 7.8 pg/ml. Remarkably, both cells of IRF5v4 and IRF5v5 cells were found to produce a significantly moderate amount of IL-10, a Th2-related cytokine compared to control cells upon stimulation. The levels of IL-10 secretion in the stimulated IRF5v4 and IRF5v5 cells were 8.80 pg/ml and 8.86 pg/ml, respectively. As for other Th2 cytokines that were assayed by ELISA, we found that none of the cells tested had detectable levels of IL-4 and IL-5 upon stimulation. Surprisingly, stimulated control cells that were known to secrete IL-13 higher than unstimulated cells as reported in previous studies was found to have a lower detectable amount of IL-13 in our study [145,273,274]. A similar trend of lower IL-13 levels was observed among the stimulated IRF5v4 and IRF5v5 cells in comparison to the unstimulated group. Altogether, in response to stimulation, both IRF5v4 and IRF5v5 cells were able to secrete higher levels of IL-2 and IL-10 compared to control cells. On the other hand, IRF5v4 had a diminished level of Th1-IFNγ cytokine.
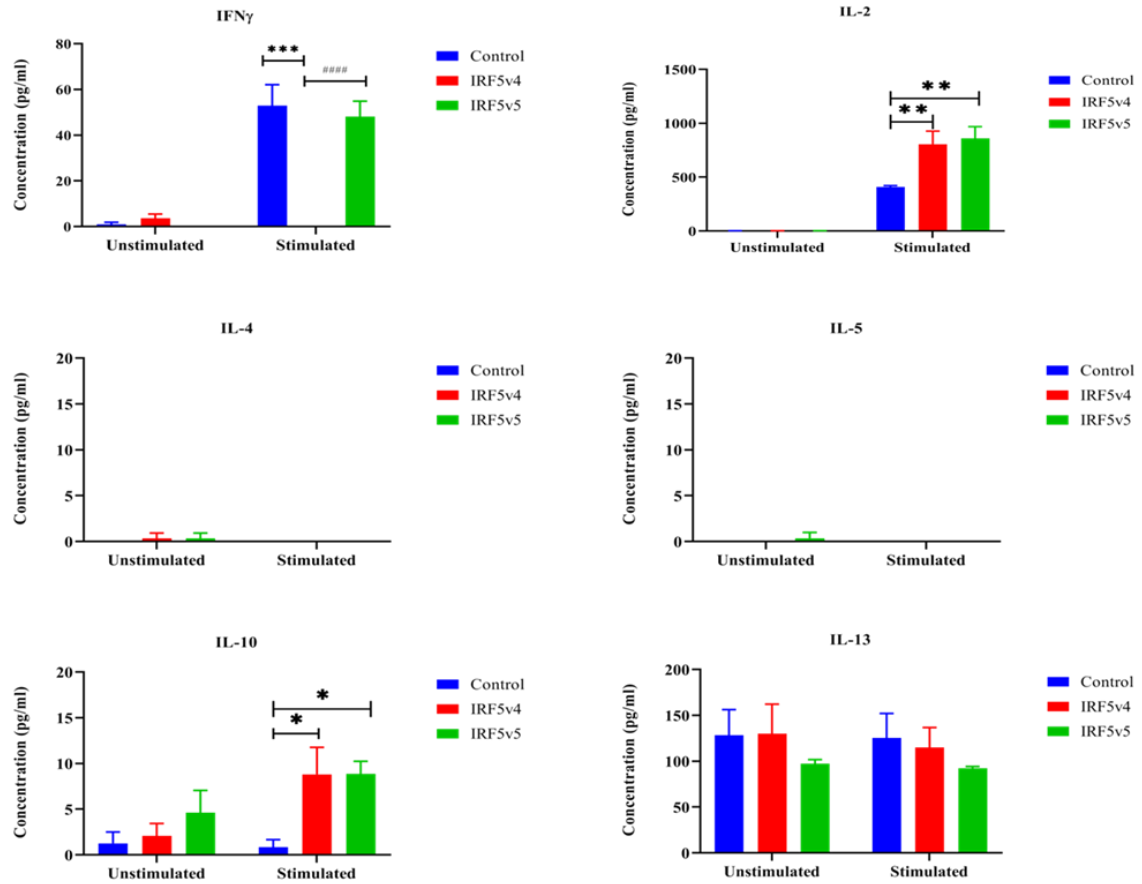
ELISA

Figure 3.31 Measurement of IFNγ, IL-2, IL-4, IL-5, IL-10 and IL-13 secretion by ELISA. Supernatants from unstimulated cells or cells stimulated with PMA-Ionomycin for 24 hours were harvested and assayed using ELISA. The results are presented as mean ± standard error of mean from three independent experiments performed in duplicates wells (n=3). Statistical analysis was by a two-way ANOVA with Tukey multiple comparison tests. Values are expressed as mean ± standard error of mean from three independent experiments performed in duplicates (n=3). The asterisk represents ***p < 0.0005, **p < 0.001, p* < 0.01 when cells were compared to control cells and ####p < 0.0001 when cells were compared to IRF5v4 cells.

Chapter 4

4 Discussion

IRF5, a member of IRFs has recently gained much attention for its role in regulating inflammatory responses and autoimmune diseases. Over the years, mounting evidence has shown the importance of IRF5 role in the regulation of cytokine and chemokine expressions [11,13,171]. As a transcription factor, IRF5 has been shown to recognise and bind to the ISRE motif on the promoter of its target genes and modulated their responses [27,275,276]. In the present study, the binding of IRF5 to the ISRE motifs on human *Il13* promoter was assessed through a pulldown assay. As a part of the pull-down assay, it was pertinent to produce IRF5v4 and IRF5v5 expressed protein. The proteins (IRF5v4 and IRF5v5) were required to evaluate the binding to the cognate sequence, in this case, ISRE motifs of the *Il13* promoter. The study started with the isolation of IRF5 encoding variant 4 and variant 5 from cDNA library of B cells and cloned into TOPO cloning vector. The positive transformants containing IRF5v4 and IRF5v5 coding sequences were identified through DNA sequencing. Upon the successful cloning and identification of IRF5v4 and IRF5v5 coding sequences, the pcDNA 3.1(+) vector was used to carry IRF5v4 or IRF5v5 individually. Constructions of the pcDNA harbouring IRF5v4 or IRF5v5 were confirmed through colony PCR which showed the estimated band sizes visualized through gel electrophoresis (Figure 3.10).

As part of the protocol establishment for transient transfection, a trial experiment was conducted by using MyD88 expression vector expressing YFP as positive control to evaluate whether the designed transfection experimental procedure conducted was successful. The transient transfection protocol was adapted from the previous study conducted by our group [10,190]. For this trial experiment, pcDNA-IRF5v5 and MyD88 expression plasmids were used. The ratio of plasmid DNA to transfection reagent used was 1:3 following the manufacturer's recommendation. Meanwhile, ratio of 1:1 of pcDNA-IRF5v5 and MyD88 was used for co-transfection. The reason this ratio was chosen was to avoid any potential bias that may arise from the different levels of protein expressed by the plasmids. For example, if more of IRF5v5 expressing plasmid were transfected than MyD88, then more IRF5v5 protein will be expressed compared to MyD88. Consequently, the observed results would then reflect the effect contributed by the high-abundant IRF5v5 expressed protein and low- abundant MyD88 expressed protein. Therefore, equal amount of pcDNA-IRF5v5 and MyD88 expression plasmids (1:1 ratio) were co-transfected into HEK 293T cells. After 48 hours, the cells were visualised through fluorescence microscope. The results demonstrated the presence of about 70% of YFP expression visualized from cells transfected with MyD88, Figure 3.11 (c) and in the cells that were co-transfected with IRF5v5 and MyD88, Figure 3.11 (d). This data suggested that the transfection protocol used was optimal, since MyD88 was successfully expressed in the transfected cells as represented by the presence of YFP expression visualised through fluorescence microscope. Since no reporter protein was conjugated to IRF5v5 plasmid, therefore no fluorescence was observed in these transfected cells, Figure

185

3.11 (b). Similarly, untransfected cells did not show any fluorescence (Figure 3.11 (a)). To further confirm that the transfected cells indeed expressed the recombinant protein, the cells lysate were analysed by immunoblotting and detected with IRF5 antibody. The results showed a clearly visible band of ~60kDa protein corresponding to IRF5 expected size from the cell lysates of transfected cells with IRF5v5, and from the cells co-transfected with IRF5v5 and MyD88 (Figure 3.12). Both results obtained from the fluorescence microscope and western blot that showed the expressed protein of MyD88 and IRF5 respectively. These results specified that expression from the respective recombinant plasmids had successfully translated into proteins.

Production of proteins to be used for DNA pulldown assay was carried out by transient transfection following the established protocol. The HEK 293T cells were transiently transfected either with pcDNA-IRF5v4 or pcDNA-IRF5v5 in the presence and absence of MyD88 expression plasmid. After 48 hours of transfection, nuclear proteins were extracted from the cell lysates. Extracts of nuclear proteins, free from cytosolic proteins were used because our aim was to determine the interactions of nuclear transactivators, in this case, IRF5 (DNA binding protein) to bind on its cognate regulatory sequences (ISRE) [277]. From the total amount of nuclear proteins extracted, 30% of the proteins were subjected to western blot with incubation of IRF5 antibodies to validate the presence of expressed proteins in transfected cells prior to the pulldown assay. As seen in Figure 3.13 (a) and Figure 3.13 (b), the presence of ~60 kDa protein corresponding to IRF5v4 and IRF5v5 proteins respectively; were

detected in nuclear lysates extracted from cells transfected with IRF5v4 or IRF5v5 either in the presence or absence of MyD88 expression plasmid. It is known that both IRF5v4 and IRF5v5 cDNA encode similar protein size as previously reported [16]. Hence, the detected band with an expected protein size corresponding to the IRF5 spliced isoforms proved the presence of expressed proteins in the nuclear lysates. Moreover, the levels of IRF5v4 and IRF5v5 proteins in the nuclear lysates were comparable. Presences of IRF5v4 and IRF5v5 in their respective nuclear lysates in absence of MyD88 is consistent with previous studies which showed that cells expressing ectopic IRF5 were detected in the nuclear lysates [31,32,190]. It is widely understood that, in unstimulated cells, IRF5 predominantly present in the cytoplasm and upon activation mostly translocated into the nucleus. Nonetheless, some amount of IRF5 can be found in the nucleus. This is attributed to structural properties of IRF5 polypeptides of possessing two NLS and 1 NES, which are important for its shuffle into nucleus and cytoplasm respectively, as described in detail in section 1.2.4.4. Therefore, this explains why expressions of ectopic IRF5 isoforms without MyD88 were detected in the nuclear lysates.

To mimic TLR mediated activation of IRF5, we used overexpression of MyD88 in HEK 293 T cells. From the pulldown assay results, we observed only the MyD88-activated IRF5v4 bound to the ISRE region of *Il13*, indicating that the binding was completely dependent on the expression of MyD88 (Figure 3.13(c)). On contrary, IRF5v5 was able to bind to the ISRE region of *Il13* in the absence of MyD88 whereas in the presence of MyD88, the binding of IRF5v5 to the ISRE region

of *Il13* was much enhanced (Figure 3.13 (d)). The binding of ectopic IRF5v5 without activation of MyD88 indicates that some low level of IRF5v5 present in the nuclear lysates was able to bind to the *Il13/ISRE* region in uninduced state (unstimulated cells). Previous findings on low level nuclear IRF5 from unstimulated cells binding to target gene sequences have been contradictory [31–33,149]. This could be attributed to different activity of IRF5 depending on cell-type, assays used (pulldown or ChiP assay) and origin of IRF5 (human IRF5v4 or murine IRF5). To the best of our knowledge, this is the first study that showed nuclear IRF5v5 and not IRF5v4 from unstimulated HEK 293T cells (without ectopic MyD88) were able to bind *Il13/ISRE* oligonucleotide. The exact mechanism however is not clearly understood. In a crystallography study, Chen and co-workers revealed that IRF5v4's autoinhibitory domain (reside within carboxyl-terminal) masked DNA binding domain (within amino-terminal) suggesting a closed state monomer in the unstimulated cells [173]. In a separate study by Korczeniewska et.al, cytoplasmic IRF5v4 was found bound to CSN complex protein in uninduced cells, resulting masking of DNA binding domain [172]. Consequently, this prevents the binding of IRF5v4 to the target gene sequence in unstimulated cells. On contrary, little is known about nuclear IRF5 (both IRF5v4 and IRFv5) activity in unstimulated cells. Perhaps, IRF5 is well known as latent transcriptional factor that gets activated in response to stimuli, thus it is more relevant to understand the mechanism of IRF5 activity in stimulated condition. Nonetheless, we speculate that there may be some yet to discover endogenous kinase that could have selectively interacted with nuclear IRF5v5, allowing conformational changes for binding to *Il13/ISRE*. The speculation is made based on previous studies which

demonstrated phosphorylation by kinases on distinct serine residues of different IRF5 isoforms led to altered activities as elaborated in section 1.2.4.5. In accordance to that, some unknown endogenous kinase in HEK293 T cells may have phosphorylated specific serine residue of IRF5v5 which facilitated its binding to *IL13/ISRE* in absence of MyD88. It is important to point out that the observed results were not likely due to elevated level of IRF5v5 than IRF5v4 because from the immunoblot we can observe that overexpressing IRF5v5 and IRF5v4 (without MyD88 activation) had comparable levels (Figure 3.13 (a) and (b)). Further studies are warranted to confirm our hypothesis. One way this can be done is by screening IRF5v5 interacting partner present in the nuclear lysate using affinity purification coupled with mass spectrometry (AP-MS) analysis in HEK 293T cells [29]. Taken together, our results showed IRF5v/v5 exhibited differential response in binding *IL13/ISRE* in absence of MyD88. Importantly, both MyD88 activated spliced isoforms of IRF5 can bind to ISRE region of *Il13* promoter, hence suggesting that the binding of IRF5 spliced isoforms could serve an important role in the expression of IL-13.

Using a luciferase reporter construct driven by *Il13* promoter, we demonstrated that the binding of IRF5 isoforms; IRF5v4 and IRF5v5 to the ISRE region on *Il13* promoter were functional (Figure 3.14). Both MyD88-activated IRF5 isoforms were demonstrated to enhance the *Il13* promoter activity, supporting the notion that MyD88 is required for the transcriptional activation of IRF5 as reported previously [190]. In absence of MyD88, increasing the concentration of IRF5v4 or IRF5v5 alone did not show enhancement of *Il13* promoter activity above the basal

levels. The lack effect of IRF5 in activating its target gene promoter without MyD88 is consistent with previous studies, thus supporting our findings that ectopic IRF5 alone does not stimulate *IL13* promoter activity [10,33,190]. On the other hand, MyD88 alone showed some stimulatory activity of *Il13* promoter at the different concentrations used, suggesting that there could be some endogenous transcription factors that got activated downstream of MyDD88 and contributed to the *Il13* promoter activity. For instance, IRF3; another member of the IRF family and the ubiquitiously present transcription factor, nuclear factor kappa B (NF-κB). Both transcription factors are known to participate downstream of the MyD88 signalling pathway [33,278]. Interestingly, previous studies have detected endogenous IRF3 in HEK 293T cells [33]. Moreover, a prior study by Pahl and collegues have linked NF-κB with IL-13 [279]. In the study, the authors showed that synthesis of IL-13 in activated purified human T cells was inhibited when the cells were treated with a NF-κB inhibitor, thus suggesting the importance of the NF-κB pathway in regulating IL-13 expression.

Regarding co-expression of IRF5 and MyD88, we tested the activity of IRF5 isoforms in two conditions; a) keeping the concentration of IRF5 isoforms at 100 ng while varied MyD88 concentration gradually (25,50,75 and 100 ng) and b) keeping the concentration of MyD88 constant (100 ng) while increasing the concentration of IRF5 isoforms (25,50 and 75 ng). The results showed that increasing concentration of MyD88 gradually when IRF5v5 was kept at the highest concentration (100 ng) led to enhancement of *Il13* promoter activity proportionally in a dose-dependent manner.

Likewise at the lower expression of IRF5v5 (25 and 50 ng concentration) and highest MyD88 expression (100 ng) showed a similar increment of *Il13* promoter activity but the stimulatory activity of IRF5v5 were reduced when IRF5v5 was at higher levels (75 and 100 ng concentration). This data indicates while the stimulatory activity of IRF5v5 was dependent on MyD88 expression, at higher levels of IRF5v5 and MyD88 expression resulted in reduced activation of the *IL13* promoter. On the other hand, the co-expression of IRF5v4 and MyD88 did not show gradual enhancement in a dose-dependent manner. In fact, *Il13* promoter activity was reduced with increasing MyD88 level in the presence of IRF5v4. Strikingly, at the lowest level of MyD88 (25ng) expression and the highest level of IRF5v4 (100ng), led to the highest stimulatory activity of *Il13* promoter, suggesting high expression of MyD88 negatively interfere with the transcriptional activity of IRF5v4.

In prior published murine study, Paun et al. have reported that levels of endogenous IRF3 and exogenous IRF3 and IRF5 in co-transfected MyD88 were low when the expression levels were checked through western blot [33]. Therefore, suggesting the possibility of degradation of IRF3 and IRF5 induced by overexpression of MyD88. Indeed, a subsequent study has demonstrated that human IRF5 was degraded by TRIM21 in response to TLR7 activation in isoform-specific manner [156]. The TRIM21 known to regulate the stability of IRFs was shown to selectively destabilize IRF5v1 and IRF5v5 (that contain insertion in the PEST domain) and not IRF5v2 and IRF5v3 (confer deletion in the PEST domain), indicating isoform that is missing of the PEST domain are resistant to TRIM21 degradation [156]. The authors

showed that TRIM21 interacted with IRF5v5 and inhibited the transactivation of its target gene *IFNA* promoter. With this regard, we hypothesise in effect of high expression level of MyD88; IRF5v5 could have interacted with TRIM21, which subsequently inhibited its ability to transactivate *Il13* promoter activity. While IRF5v4 confers the deletion in PEST domain, it may have not subjected to TRIM21 degradation but its reduced activity could have been caused by another reason. In line with this, Eames et.al identified that IRF5v3/v4 interacted with co-factor KAP1(also known as TRIM28) a well-known transcriptional repressor; in HEK293 cells stably expressing TLR4 (HEK293-TLR4 cell line) through proteomic screening approach [176]. The KAP1 was found to form complex with IRF5, which led to inhibition of IRF5 regulated target cytokine gene, TNF in both human and mouse macrophages stimulated with TLR4 ligand, lipopolysaccharide (LPS). The authors suggested that the mode of the inhibitory mechanism employed by KAP1 was presumably by forming a complex with IRF5 which led to the recruitment of methyltransferase SETDB1; whose responsibility is to modify the chromatin into a closed state on the TNF locus, thereby preventing its transcription. By taking account of findings reported by Eames et al., we postulate that IRF5v4 may have interacted with KAP1. The actions of KAP1 could have begun supposedly when the MyD88 expression levels were high, thereby interacting with IRF5v4 and caused inhibition of its activity.

Another recent study showed that Lyn, a non-receptor tyrosine kinase interacted with IRF5 independent of its kinase activity but inhibited the post-transcriptional modifications of IRF5, causing inactivation of IRF5 via the TLR-

192

MyD88 pathway [280]. Human protein atlas web domain search showed that Lyn is expressed in HEK cells. In addition, a study done by Gray and colleagues has described that they used HEK 293 cells a model for endogenous Lyn kinase to examine its interaction with myeloid differentiation factor-2 (MD-2), a critical component of the signaling receptor complex involved in TLR4 signaling in response to LPS stimulation [281]. Taking this into consideration, there is a strong possibility of IRF5v4 or IRF5v5 to have interacted with Lyn in our study in relation to aforementioned study. Collectively, we speculate high level of MyD88 expression could have increased the endogenous TRIM21, KAP1 and Lyn expression, thus interacted with IRF5v4 or IRF5v5 in relation to aforementioned studies. This hypothesis should be validated in future studies.

Previous studies have shown that IRF4 regulated IL-13 expression along with other Th2 cytokines [145]. Like IRF5, IRF4 has also been reported to bind to the same region of MyD88 and induce various cytokines and chemokine production through a common molecular pathway, that is anchored by MyD88 [8]. In line with this, we investigated whether IRF5 could possibly function as another modulator like IRF4. We employed the approach of gene overexpression to study the effect of IRF5 in cytokine production in Jurkat cells by lentiviral transduction. Lentiviral vectors are useful tools for gene delivery because of their ability to achieve stable and long-term transgene expression. Numerous studies have reported the use of lentiviral vectors for carrying cDNA in overexpression studies [282–284]. In this project, the third generation of lentiviral vector, pLenti-GFP-CMV-Puro was utilized as a transfer

vector to carry the transgene sequences of IRF5v4 or IRF5v5. The GFP sequence was removed to accommodate the cloning of the IRF5v4 or IRF5v5 sequence into the transfer vector. The cloning of IRF5v4 and IRF5v5 into the transfer vector was confirmed as represented by their expected band sizes approximately 1500 bp as shown in Figure 3.19.

In terms of lentivirus production, a three plasmid expression system was used to produce lentivirus particles by transient transfection mediated by Mirus transfection reagent. The process involves co-transfection of transfer vector consisting of pLenti expressing GFP, pLenti harbouring either IRF5v4 or IRF5v5 together with the helper plasmids; psPAX2 and pmD2G. The production of the lentivirus is accomplished through trans-complementation, whereby by change all three plasmids get contained into a single cell and together express all the viral proteins that assemble into infectious lentiviral particles [249]. Since the transfection efficiency is important in a multi-plasmid transfection system for generating productive lentiviral particles [257], a trial experiment was tested to the experimental conditions using lentivirus expressing GFP as a positive control to evaluate the transfection efficiency. The reporter gene, GFP here acts as an indicator of the translated protein that has been expressed by transfected plasmid, thus implying the transfection was successful. From the preliminary experiment, we found that the ratio of DNA to transfection reagent (1:2.4), the ratio of the three plasmids; transfer, packaging, and envelope at 4:3:1 respectively was optimal for production of lentiviral particle. This was supported by

the results that showed 80-90% of GFP expression at day 3 of post-transfection, firmly demonstrating efficient transfection and viral protein translation (Figure 3.20).

The titre of crude viral supernatants usually ranged from 1 to 5×10^7 infectious particles[285]. Although several studies have employed the technique of concentrating lentivirus and titre, this is particularly important for some difficult to transfect cells such as primary cells and for the use *in vivo* experiment that requires a control of transduction rate [245,247,251,258,286]. Nonetheless, many studies have reported the use of fresh viral supernatant to transduced cells [245,247,251,258]. Moreover, the use of virus supernatant is a faster and simpler approach to transduce cells. A trial experiment was conducted to investigate whether the virus packaging was indeed, successful, and infectious virus was released into the culture medium. For this trial experiment, the easy-to transduce cells, HEK 293T cells were used for transduction with lentivirus expressing GFP. Aside from checking the infectious virus produced, we also tittered on different volumes of the viral supernatant to test an adequate amount for transduction without causing any toxicity. From the results, we found that transduction with 2 ml of virus supernatant showed greater transduction efficiency with more than 90% GFP expression seen (Figure 3.22(f)). Hence, we deduced that lentiviral produced by the transient transfection was transduction-competent lentiviral particles. Following this, we checked the transduction protocol with Jurkat cells. In terms of enhancement of transduction, spinoculation (refers to centrifugation without break) of suspension cells has shown to enhance transduction of lentiviral vector by virus binding to the cells [287]. The same transduction protocol

195

used for HEK 293T cells were performed for transduction of Jurkat cells, with the additional step of spinoculation. After 72 hours, the transduced Jurkat cells were assessed by fluorescence microscope and the results showed a great transduction efficiency of 70-80% of GFP expression consistent with the findings we found when HEK 293T cells were transduced with 2ml of viral supernantant (Figure 3.23).

Upon the establishment of protocols for lentivirus production by transfection and transduction of the lentiviral supernatant into Jurkat cells, we conducted the experiments using lentiviral constructs of IRF5v4 and IRF5v5. To produce experimental lentiviral constructs of IRF5v4 or IRF5v5, it was done in parallel with lentiviral containing GFP in separate flasks. Unlike the transfer vector that carry GFP in its backbone, no reporter gene was conjugated in these experimental lentiviral constructs of IRF5v4 and IRF5. To ensure that the experimental conditions during this transient transfection experiment were conducive, the expression of GFP was evaluated in the cells transfected with pLenti-GFP. The results correlated with the findings obtained in the trial experiment, as more than 90% of transfection efficiency was achieved as represented by the green fluorescence visualised through fluorescence microscope (Figure 3.21). Hence, from this result, we anticipated that the transfection experiment could work effectively for the lentiviral constructs too. In the same way, for the transduction experiment, we included lentiviral expressing GFP as a positive control to evaluate transduction efficiency in Jurkat cells. The transduced cells showed a great transduction efficiency of more than 70% of GFP expression depicted in Figure 3.24.

It is crucial to ensure the transduced cells were indeed carrying the transgene that was successfully integrated within the genome of Jurkat cells. This is because there are chances of pseudotransduction happening, a phenomenon whereby target proteins were produced in packaging cells or by transiently transferred plasmids instead of *de novo* synthesis of protein from integrated transgene as reported in previous studies [288]. Consequently, this can lead to loss expression of transgene after cell division, interrupting downstream experiments. In addition, stable cells are known to produce consistent functional proteins [212]. Therefore, following transduction, the stably expressing transgene cells were selected under puromycin antibiotic, the selectable marker. Puromycin is an aminonucleoside antibiotic produced by *Streptomyces alboniger*. It inhibits peptidyl transfer on both prokaryotic and eukaryotic ribosomes which cause premature chain termination during translation [289,290]. As mentioned in section 3.3.4.1, the pLenti-GFP and the engineered pLenti-IRF-v4 and pLenti-IRF-5v5 encode *Puro* gene in their plasmid backbone and constitutively express it. Therefore, during the antibiotic selection, those cells with stably integrated transgene and constitutively expressed the resistant gene, *Puro*, will survive when grown in a medium containing puromycin, whereas those untransduced cells and cells that uptake plasmid transiently will not survive the antibiotic selection. The selection process for stably expressing cells typically takes about two weeks [251,268,269]. By this time, any unintegrated DNA would be eventually diluted to extinction during the expansion, allowing only the cells with integrated constructed DNA to grow. This is because *Puro* gene is passed onto the daughter cells during cell division for them to survive and proliferate, resulting in a pool of cells with integrated

197

gene over time [291]. The entire cell population that survived the puromycin selection is referred to as polyclonal cells. Out of curiosity, we first checked the presence of the transgene in the polyclonal Jurkat cells expressing GFP that were generated from transduction of pLenti-GFP lentiviral. The cells exhibit green fluorescence under the fluorescence microscope indicating that the population of cells comprise of stably generated cells expressing GFP (Figure 3.25).

To confirm the presence of IRF5v4 and IRF5v5 in the polyclonal cells generated from the experimental lentiviral constructs, both mRNA and protein expressions were assessed by reverse transcription PCR and western blot analysis, respectively. The results demonstrated that the fragments corresponding to IRF5v4 and IRF5v5 cDNA was presented only in polyclonal cells generated from transduction of Jurkat cells with pLenti-IRF5v4 or pLenti-IRF5v5 respectively (Figure 3.26 (a)). Moreover, both untransduced cells and the cells transduced with pLenti-GFP did not show detection of IRF5 protein (Figure 3.26 (b)). This is to be expected because Jurkat cells lack endogenous IRF5 expression and its expression is barely detected in this cell line [18,150,154]. Previously, IRF5 expression has been detected upon HTLV-1 viral infection, although constitutive expression of IRF5 is barely detected in resting T cells [18]. In the same study, Ishikiwa et.al demonstrated that IRF5 expression in HTLV-1 infected T cell lines were upregulated by the Tax protein (viral oncoprotein important for viral replication), that was because the Tax protein could bind to IRF5v3 promoter and induce its expression [18]. It is important to note that, in the present study we used the third-generation lentiviral particles that

do not encode Tax protein as a tool to deliver IRF5 cDNA in Jurkat cells and no upregulation of IRF5 was detected in the transduced Jurkat using pLenti-GFP virus (Figure 3.26(b)). Therefore, the IRF5 expression detected in lentiviral construct pLenti-IRF5v4 or pLenti-IRF5v5 were due to *de novo* synthesis of IRF5 from the coding sequence delivered into Jurkat cells. Congruent to RT-PCR (Figure 3.26 (a)), western blot analysis confirmed the presence of IRF5v4 and IRF5v5 proteins in the stably expressing cells. The detection of ~60kDa protein bands correspond to the expected protein size of IRF5v4 and IRF5v5 (Figure 3.26 (b)). Collectively, these observations confirmed that IRF5v4 or IRF5v5 transgene was successfully integrated into the genome of infected Jurkat cells and expressed by the cells' machinery through proper transcription and translation processes.

Polyclonal cells constitute of heterogeneous transgene expression level, which means the population of cells containing both high and low expression levels of the transgene [251]. Over the time, transgene population of polyclonal cells may drop because cells with high levels of the transgene may have a slower growth rate, therefore the rapidly growing low-level transgene expressors may take over the culture. To avoid the drift effect towards low transgene expression and obtain a homogenously higher level of expression of the IRF5 isoforms, the early passage of polyclonal cells was used to isolate a single cell (monoclonal) through the limiting dilution method. It is worth mentioning that during the limiting dilution process, cells were supplemented with self-conditioned media. The self- conditioned media consist

of culture-free media collected from the healthy growing parental Jurkat cells (untransduced cells) which are rich in secreted growth factors. These growth factors enhance the growth of the single-cell isolated [286]. From the limiting dilution, several monoclonal were identified and allowed to grow to reach confluency at least 30 to 50%. After clonal expansion, cells were randomly chosen and further expanded in separate flasks with complete media supplemented with 5 µg/ml of puromycin. From the screening process, three clones expressing IRF5v4 (Figure 3.27), B8, F9, and G3 and the one clone expressing IRF5v5 H3 were found to express high levels of IRF5. While two clones; D7 and E6 showed a substantial level of IRF5v4. Another clone E4 had a low expression of IRF5v4. It was first planned to study the effects of clones with differential overexpression of IRF5v4, since we had five clonal cells, excluding E4 that showed reasonably high levels of IRF5v4. However, during the cell growth maintenance, we noticed that some clones displayed poor health and behaviour. During routine cell maintenance, morphological of the cells examined through an inverted microscope, showed that B8, D7, E6, and F9 clones exhibited the characteristics of excessive clumping of cells; as multiple cells tend to aggregate and formed big clumps of cells. These cells also had an extended lag phase and lower density compared to parental Jurkat cells (untransduced) and cells of G3 and H3 clones, although it is important to mention that cells of G3 and H3 clones grew slower than control cells. After several passages, the cell growth of the clones; B8, D7, E6 and F9 stagnated.

One of the reasonable explanations for the poor cell behaviour exhibited by some of the high expressing IRF5v4 clones (B8, D7, E6, and F9) could be due to the metabolic burden experienced by high expressed proteins. Stress exerts by high production of proteins due to overexpression of gene product can lead to genomic stability and trigger apoptosis pathway [212,292]. In addition, it could also be due to positional effects brought lentiviral vector through random integration of the gene of interest into the genome of the cells, although it is important to note that chances of insertional mutagenesis and genotoxicity are low when a third generation of the lentiviral vector is used [292]. Moreover, most retroviral are known to target the transcriptional active site [212,293]. As such, we speculate that there is possibility of insertion of IRF5v4 gene to the transcriptional active site that involved in cell division, causing poor cell growth behaviour. In regards to reduced cell growth by some of the IRF5v4 clones, a similar finding was reported by Barnes et al., whereby overexpression of IRF5v3/v4 in BJAB B cell lymphoma led to a 10 to 30% of reduction in cell growth compared to control cells. Detailed analysis by the same group, described that overexpression of IRF5 in BJAB cell line, induced G2-M cell cycle arrest and apoptosis as well as inhibited colony formation in soft agar and tumour formation in nude mice independent of tumour suppressor, p53 which is known to exhibit similar activities of arresting cycle arrest and promoting apoptosis [151]. Although, in an earlier study IRF5 was shown to act downstream of p53 as described by Mori et al. [294], Barnes et al. demonstrated that IRF5 directly target and upregulated cell cycle and apoptosis genes, independent of p53, thus indicating IRF5 is a crucial mediator of cell cycle arrest and cell death [151]. In another study,

Yanai and colleagues showed murine IRF5 was able to induce apoptosis but not cell cycle arrest in mouse fibroblast in response to DNA damage in genotoxic stress [295]. Also, in the same study, the authors showed that IRF5 induced apoptosis in mouse fibroblast in response to DNA damage caused by oncogenesis and viral infection. A recent study reported TLR-7 mediated activation of IRF5 was shown to promote IFNγ$^+$ CD4 T cell death because of its ability to enhance death receptor 5 (DR5)-induction cell apoptosis in CD4 T during chronic parasitic infection, *L.donovani* [19]. As several lines of investigation supported the role of IRF5 in mediating cell growth arrest and cell death, we infer that the poor cell health and behaviours exhibited by some of the high expressing of IRF5v4 could due to the ability of IRF5 inducing cell cycle arrest and apoptosis in Jurkat cells. Nevertheless, we cannot exclude the fact that lentiviral random integration and the metabolic burden could also contribute to the effect seen in some of the IRF5v4 clones. It is worth extending these findings in future studies to elucidate the function of IRF5 in regulating cell growth and apoptosis in Jurkat cells, to understand its intrinsic properties in T cells.

The screening of stably overexpressing IRF5 isoforms in Jurkat cells yield two healthy and best performing stable clones; G3 (IRF5v4) and H3 (IRFv5). Due to time constraint, it was decided to progress work with these two clones as the priority was to evaluate the modulation of IRF5 on Th1 and Th2 cytokines, rather than an attempt to produce multiple clones with differential expression. To ensure that the expression of IRF5 was not lost over the time, cells were continuously grown in selective media containing puromycin and used within 15 passage numbers. Of note, we noticed

intensity of IRF5 expression decreased gradually with cultivation for the clonal cells due to gene silencing, a common phenomenon seen with the use of CMV promoters [212]. The gene silencing with associated to methylation of chromatin rather than an effect caused by the positional effect of integrated DNA, because as mentioned earlier lentiviral vectors are known to target the transcriptionally active site of the genome integrate their DNA [212,293]. Nevertheless, reactivation of the silenced gene under the control of CMV promoter has been reported [296,297]. For instance, Gerolami et al. showed that silenced GFP transgene in transduced cells by the lentiviral vector with CMV promoter was restored upon treatment with PMA and Ionomycin [296]. Consistent with this finding, we found the altered reduction of IRF5 expression in stable cells was recovered to its original high level upon PMA and Ionomycin stimulation (Appendix 2.8). Of note, we noticed Jurkat cells stimulated with PMA and Ionomycin did not show any expression of IRF5, implying that PMA and Ionomycin did not upregulate IRF5 rather it restored the silenced gene expression in the cells (Appendix 2.8). In this view, the clones were maintained detectable and comparable levels of IRF5 at each time-point analysed.

To examine the possibility of IRF5 in regulating IL-13 expression as well as to evaluate the intrinsic role of IRF5 in modulating Th1 and Th2 responses, we assessed Th1 and Th2 cytokines in overexpressed IRF5v4 and IRF5v5 in Jurkat cells in response to co-stimulation of PMA and Ionomycin. As mentioned in section 3.4.2, PMA and Ionomycin stimulation is known to mediate cell death when cells were stimulated over a longer time, beyond 16-24 hours. The reason for this is that as part

of its stimulatory role of activating T cells, PMA and Ionomycin are known to cause activated induced cell death (AICD) [231,272]. Under normal physiology, T cell activation is regulated by AICD which leads to upregulation of death receptor and ligands (Fas/FasL and TNFα/TNF) [96,97]. This AICD phenomenon is necessary to efficiently remove activated lymphocytes, in response to a feedback mechanism to maintain ongoing immune response and maintain peripheral T cell tolerance. As a member of the death receptor family of the tumour necrosis factor (TNF) receptor superfamily, Fas is localised on surface of many cells, whose engagement with its ligand (FasL) causes a cascade of caspase signalling leading to apoptosis [298]. Activation of PMA and Ionomycin leads to upregulation of FasL which then bound to expressed Fas antigen on the cell surface inducing cell death either through autocrine or paracrine manner [272]. During the optimization step, a concentration profile of several concentrations of PMA and Ionomycin were tested to evaluate the cytokine production and cell death after 24hr stimulation. Secretion of IL-2 from activated Jurkat cells were chosen as strategy to optimize the concentration of PMA/Ionomycin, because as a growth factor, IL-2 cytokine is a crucial indicator of successful T cell activation. Based on the results obtained as shown in Figure 3.30, a combination of 25 μg/ml PMA and 1μM Ionomycin yielded the highest concentration of IL-2 secretion. When the cell viability was evaluated through trypan blue exclusion, we found the combination of 25 μg/ml PMA and 1μM Ionomycin had a lower number of dead cells compared to all the other concentration tested. Hence, this concentration of mitogen combination was chosen for the T cell activation experiment. While the effort was

taken to ensure that we limit cell death during PMA and Ionomycin to produce optimal induction of IL-2 production using control cells, we were surprised to notice that IRF5v4 and IRF5v5 cells had less than 1% of the viable cell compared to control cells which had about ~10% of viable cells when evaluated through trypan blue exclusion throughout 24-hours T cell activation. This observation suggests that IRF5v4 and IRF5v5 cells are more susceptible to PMA and Ionomycin stimulation than control cells. Interestingly, IRF5 has been associated with Fas-mediated apoptosis in several different murine cells including hepatocytes and dendritic cells, presumably by acting upstream of caspase 8 activation, leading to apoptosis [196,299,300]. This could explain why IRF5v4 and IRF5v5 expressing Jurkat cells had more dead cells than control cells upon PMA and Ionomycin stimulation. Further studies are required to confirm these findings to dissect the IRF5 role in Fas-mediated apoptosis specific to human T cells upon mitogen stimulation.

Prior to semi-quantitative RT-PCR analysis, the amplification of PCR products was optimised using parental Jurkat cells that served as control cells. As seen in Figure 3.28, the results illustrate that transcripts bands were clearly seen when 30 cycles for IFNγ, IL-2 and β-actin and 35x cycles for IL-4 and IL-13 were done. This data implies that IL-4 and IL-13 have a low copy number of mRNA in activated Jurkat cells compared to β-actin, IFNγ, and IL-2. Thus, both IL-4 and IL-13 detection requires a higher PCR amplification cycling number for visualization and quantification. In light of the analysis of cytokine mRNA expression by RT-PCR analysis, we found overexpressed IRF5v4 and IRF5v5 in Jurkat cells had detectable

mRNA levels of the four cytokines IFNγ, IL-2, IL-4, and IL-13 similar to control cells (Figure 3.30). In terms of cytokine secretion assayed by ELISA, our results showed that control cells were able to induce IFNγ and IL-2 production and not IL-4, IL-5, IL-10, and IL-13 upon stimulation (Figure 3.31). Likewise, both IRF5v4 and IRF5v5 cells had a similar cytokines induction profile, exclusive of IL-10 secretion which was unique to IRF5 isoform cells (Figure 3.31). Although, stimulated IRF5v4 and IRF5v5 cells induced IL-10 production, we did not detect IL-10 mRNA transcripts during the PCR amplification optimization process (Appendix 2.9, Figure 13). Comparably, we did not detect IL-10 mRNA in stimulated control cells (Appendix 2.9, Figure 12). Available literature has shown that stimulation of Jurkat cells in response to PHA and PMA were able to induce endogenous IL-10 mRNA and protein after 24 hours stimulation [301,302]. In our study, endogenous IL-10 protein was not significantly induced in control cells stimulated with PMA and Ionomycin for 24 hours, because the measured IL-10 level was lower than the detection limit (7.8pg/ml). Whereas in the mRNA analysis, the time point we used for cell stimulation was 6 hours, therefore no IL-10 expression was detected in both control and IRF5 expressing cells. The reason we did not analyse IL-10 mRNA after 24 hours of stimulation was due to insufficient viable cells for RNA isolation. This was ascribed to the higher number of cell death induced by co-stimulation of PMA and Ionomycin for extended period described earlier. Therefore, the contrasting observation in our study in reference to IL-10 mRNA and IL-10 secretion as well as other studies could be attributed to distinct types of mitogens used and the time point of mRNA analysis done. In addition to failure in detecting IL-10 mRNA, we also did not detect IL-5 mRNA in

both control and IRF5v5 cells during the PCR optimization step (Appendix 2.9, Figure 12, and Figure 13 respectively). While we know from the literature that Jurkat cells do not produce significant endogenous IL-5 expression upon activation [303], we could not exclude the potential role of IRF5 in inducing IL-5 expression in Jurkat cells. Therefore, we checked IL-5 mRNA expression in stimulated IRF5 cells but found no detection of IL-5 transcripts. Nonetheless, the failure in detecting IL-5 and IL-10 mRNA after 6 hours PMA and Ionomycin stimulation does not conclusively rule out the potential role of IRF5 isoforms in regulating IL-5 and IL-10 expression, as no positive control cells were included during the optimization steps, which is the limitation of this study.

In regards to IL-13, it was unexpected to observe that stimulated control Jurkat cells had almost similar level of IL-13 secretion with unstimulated cells (slightly above the detection limit 93.8 pg/ml). Hence, indicating that the induction of IL-13 in stimulated control cells was not successful. However, previous findings have reported that Jurkat cells stimulated with PMA and Ionomycin were able to secrete about 200-300 pg/ml, higher than unstimulated cells [145,273,274]. The discrepancy for low detection of the IL-13 protein level in stimulated Jurkat cells in our studies compared to previous studies which demonstrated a profound detectable amount of IL-13 protein can be explained based on a numerous variables involved in experimental design. Some of the variables noted from these studies were different concentration of PMA and Ionomycin, used different ELISA kits, different cell numbers, and time point analyzed. For instance, by using $1x\ 10^6$ of Jurkat cells stimulated with 50 ng/ml

of PMA and 1μM for 24 hours, Hu et al. showed that the stimulated cells were able to secrete IL-13 of about 200 pg/ml measured by using ELISA kit from R& D Systems [145]. In another study conducted by Doyle et al., showed that $1\text{x }10^6$ Jurkat cell stimulated with 20 ng/ml of PMA and 1μM for 24 hours were able to secrete about 300 pg/ml of IL-13 detected by using eBioscience ELISA kit [273]. A separate study by Rubenfeld and colleagues were able to detect about 350 pg/ml of IL-13 from the supernatant of stimulated $0.5\text{-}1\text{x}10^6$ of Jurkat cells with 50 ng/ml and 0.5μM for 18 hours, assayed using Beckman-Coulter ELISA kit [274]. However, in our hands' cell supernatant harvested from $1\text{x }10^6$ Jurkat cells stimulated with 25 ng/ml of PMA and 1μM for 24 hours did not induce IL-13 secretion above the levels of unstimulated cells, when assayed using R&D Systems ELISA kit. Given that, there are different subclones of Jurkat cells available with distinctive features as discussed in section 1.2.5.3.2, the use of different subclones would result in different outcomes. From these three studies, only one study conducted by Doyle et al. provided the information of types of Jurkat cells used; E6.1 clone of Jurkat cells, which was the same model we used [273]. Unfortunately, we were unsuccessful to reproduce similar findings in detecting IL-13 upon PMA and Ionomycin stimulation. Upon seeking technical specialty help, we confirmed no chance of interference in the media could mask the ELISA readings, as we checked through the troubleshooting procedure that involved serial dilution of the media from cultured cells in the presence or absence of PMA and Ionomycin and examined the differences in the absorbance readings (data not shown). Due to time constraints, it was not possible to extend the experiment using different commercially available kits or assays (intracellular cytokine staining, dot plot, or

ELISPOT) or use positive control cells (e.g peripheral blood mononuclear cells, PBMCs) to check the sensitivity of the kit. It remains unclear why IL-13 was detected low in control cells upon PMA and Ionomycin stimulation. Although, it will be essential to exert the highest degree of scrutiny to verify the low detection of IL-13 in activated Jurkat cells in future studies, our mRNA analyses of IL-13 transcripts levels are extremely encouraging which will be discussed in detail below.

Data gathered from mRNA (Figure 3.29) and ELISA (Figure 3.31) analysis in the present study, showed that both overexpressed IRF5v4 and IRF5v5 Jurkat cells augmented IL-2 gene and protein expression upon activation in comparison to control cells. Although known as a Th1 type cytokine, IL-2 is a growth factor that is required for both Th1 and Th2 differentiation [121]. The elevated induction of IL-2 production by IRF5 isoform cells, strongly suggests that IRF5 play role in T cell activation. One such way to confirm the enhancement of T cell activation by IRF5 is to assess the early T cell activation marker, CD25 (also known as IL-2 receptor α chain) whose expression is upregulated upon IL-2 production [93]. However, due to the high number of cell death after 24 hours of stimulation resulted in insufficient number of viable cells. Hence, we could not assess CD25 expression by flow cytometry to confirm the influence of IRF5v4 and IRF5v5 in T cell proliferation. Interestingly, a previously published work has reported that glutamine, the most abundant amino acid was able to protect Jurkat cells from cell damage & apoptosis in response to PMA/ionomycin stimulation [304]. The authors also reported that glutamine at

various concentrations ranged (0.01-2 mM) was able to increase IL-2 production, cell proliferation, and as well as cell viability in Jurkat cells treated with PMA/Ionomycin. In the future, it would be interesting to explore the use of glutamine as a strategy to limit cell death upon PMA and Ionomycin stimulation to examine CD25 activation marker in IRF5- T cell-intrinsic manner. In addition to IL-2, both IRF5v4 and IRF5v5 cells displayed a similar trend of inducing IL-10 production compared to control cells upon stimulation. Based on ELISA analysis, stimulated IRF5 isoforms showed significantly moderate secretion of IL-10 compared to stimulated control cells. Although there was only moderate production of IL-10, it still demonstrates the involvement of IRF5 isoforms in regulating IL-10 production. From previously published studies, the role of IRF5 in regulating IL-10 production has been contradictory. In murine macrophages, IRF5 was shown to induce IL-10 production downstream of TLR signaling [305], however, in human inflammatory macrophages, IRF5v3/v4 directly targeted IL-10 promoter and suppressed its activity [191]. Herein, our results showed that both IRF5v4 and IRF5v5 were able to induce IL-10 production in Jurkat cells (T cell line) upon activation. Hence, these findings highlight the multi-faceted role of IRF5 in regulating IL-10 in cell-type specific manner.

In relation to the differential response of IRF5v4 and IRF5v5 towards regulating the expression of Th1/Th2 cytokines upon stimulation, we observed that IRF5v5 favoured Th1 polarization characterized by upregulation of IFNγ mRNA level and concurrently downregulated IL-4, IL-13 mRNA levels, the Th2 cytokines. In

protein levels, IRF5v5 had a higher level of IFNγ compared to IRF5v4, however, its level is slightly lower when compared to the control cells. Noteworthy, our findings on IRF5v5 displaying Th1 skewed characteristic correlates with previous studies which demonstrated lack of IRF5 led to skewed Th2 phenotypes in different experimental murine disease model, highlighting the role of IRF5 in regulating Th1 responses [17,193,195,196]. Since human IRF5v5 and murine IRF5 are closely related as described earlier in section 1.1, there is a strong possibility that they may share similar functions. In line with this, our findings on overexpression of IRF5v5 in Jurkat cells in downregulating the expression of IL-13 are in favour of previous published data that reported lack of IRF5 in murine models displayed higher IL-13 secretion, implying that in presence of murine IRF5 it may repress IL-13 expression [20,195]. Besides that, in midst of drafting this thesis, a latest study by Yan et al. documented that IRF5 modulated Th1 and Th2 associated cytokines in T cell-intrinsic manner [306]. Similar to our findings on IRF5v5, the authors showed that IRF5 enhanced Th1 associated cytokines (IFNγ) but reduced Th2 associated cytokines (IL-4 and IL-13) in murine CD4$^+$ T cells. The same study also reported similar results obtained from human CD4$^+$ T from the individuals with high IRF5 disease risk genetic carriers in response to CD3/CD28 activation (physiological stimulation of T cells). The authors described the use of IRF5 genetic variants (rs2004640/rs2280714 TT/TT), which are the two functional single nucleotide polymorphisms (SNPs) within the IRF5 gene which contribute to risk haplotypes associated with IRF5 mediated diseases such as SLE [28]. However, these disease haplotypes do not define the

predominant isoforms of IRF5 (v1,v4-6) [28]. Nonetheless, the similarities between our studies on IRF5v5 and the aforementioned studies provided hint that full length of IRF5 without deletion (variant 5) may have similar biological activities with the high expressing IRF5 disease risk haplotype (rs2004640/rs2280714 TT/TT), thereby contributing to novel information of the function of IRF5 in modulating human Th-associated cytokines.

One of the possible reasons for IRF5v5 to favour Th1 skewed condition could be explained based on cross-regulatory mechanism possessed by Th cells (described in section 1.2.2.4) [99,106]. We infer that stimulated IRF5v5 expressing Jurkat cells were polarized towards the Th1 phenotypes driven by IFNγ and its master regulator (T-bet) thus subsequently inhibited those Th2 related cytokines expression. This is further supported by previous studies that demonstrated T-bet inhibited IL-4 and IL-13 genes directly by binding to their promoters and suppressing the transcriptional activity of IL-4 and IL-13 [307,308]. Interestingly, our luciferase assay result demonstrated the ability of IRF5v5 in inducing *IL13* promoter activity, however, an opposing effect was observed in stimulated IRF5v5 expressing Jurkat cells which showed reduced IL-13 mRNA level. One plausible explanation for this contrasting observation could be attributed to the potential of IRF5v5 involvement with T-bet in Jurkat cells, in relation to previously published findings in murine studies. For instance, Jourdan et.al reported IRF5 deficiency in a diabetic rat model, showed downregulation of Th1 markers (T-bet) in pancreatic islets, indicating a potential role of IRF5 directly regulating T-bet [194]. Strikingly, in a separate report, IRF5 was

shown to bound on the T-bet promoter in CD4$^+$ T and suppressed its activity, implying that IRF5 does not involve in positive regulation of T-bet transcriptional activity [14]. Although IRF5 does not play a role in transcriptional activation of T-bet, this does not impede the likelihood of IRF5 interaction with T-bet on a protein level as proposed by Brune et al. [120]. In this hypothetical review article, the authors proposed a novel signaling pathway for the involvement of IRF5 downstream of DE6, an adaptor protein of the SWEF family which is expressed in T and age-associated B cells (ABCs) [120]. The ABCs are unique B cells associated with autoimmunity that can express high levels of T-bet [321]. A recent publication showed that in a situation when IRF5 level was high, IRF5 was found to escape DE6 negative regulation in ABCs, and upon translocation into the nucleus, IRF5 recruited T-bet to its binding site in ABCs cells [309]. In accordance with that, Brune et al. proposed that under the similar situation in T cells, IRF5 may function as an interacting protein partner of T-bet by recruiting T-bet to its DNA binding sequences. As such this is another exciting research area to be explored in the future to elucidate IRF5v5-T-bet regulatory mechanism in T cells.

In regards to IRF5v4, our results showed that stimulated IRF5v4 expressing Jurkat cells showed depleted IFNγ protein level, suggesting its indirect role in inhibiting IFNγ production. While at the transcription level, IRF5v4 did not alter IFNγ mRNA level because it had a similar level with control cells. Thus, we speculate that IRF5v4 may participate in the later phase of IFNγ regulation. Of note, we observed

that stimulated IRF5v4 expressing cells produced IL-10 production as described earlier. It is widely established that IL-10 as Th2 cytokine can cross regulate Th1 responses [310,311]. In accordance to that, the depleted level of IFNγ could have contributed by IL-10. Puzzlingly, stimulated IRF5v5 expressing cells also secreted IL-10 but did not exhibit the diminished level of IFNγ. This could ascribe to our hypothesis that IRF5v5 may interact with T-bet as discussed earlier, which consequently allows continuous production of IFNγ while in presence of IL-10. On that note, there is the possibility that IRF5v4 may not interact with T-bet, the key transcription factor required for IFNγ production, unlike IRF5v5. Previous studies have reported that IRF5 spliced isoforms function differently in regulating target genes [13,16,29]. However, the effects of isoforms on IRF5 activity in regulating target genes are not widely understood. Whether the structure of IRF5v4 which confers deletion within the exon 6 and PEST domain could contribute to altered binding ability of IRF5v4 to T-bet but not IRF5v5 (encodes full-length without deletion) requires further investigation. One way this can done is by employing the approach of crystallography to study the structure interaction of IRF5v4 and IRF5v5 with T-bet.

Besides that, we observed that IRF5v4 showed a differential response towards regulating the expression of Th2 associated cytokines upon stimulation. Based on the RT-PCR (Figure 3.29) analysis, IRF5v4 selectively upregulated IL-13 but at the same time downregulated IL-4 mRNA level. The increase in IL-13 expression correlates

with the luciferase assay which showed that MyD88 activated IRF5v4 was capable of inducing IL-13 transcriptional activity, thereby indicating IRF5v4 regulates IL-13 expression. Remarkably, IRF5v4 was able to induce IL-13 mRNA despite a substantial high IFNγ mRNA levles, which is contrary to IRF5v5 and control cells that displayed reduced expression of IL-13 when IFNγ mRNA level was elevated. The exact reason of why IRF5v4 cells had increased IL-13 but reduced IL-4 expression is not clearly understood. Both IL-4 and IL-13 are closely related in many ways. For instance, they are homologous to each other, located on the same chromosome 5 in humans and 11 in mice and shares similar biological activities in the aspect of allergies mediated diseases [125,312]. Moreover, IL-4 and IL-13 shares similar receptor and signaling pathway at least in T cells, hence it is expected that IL-4 and IL-13 are co-expressed in T cells [125]. Interestingly, literature has supported that the expression of IL-4 and IL-13 can be differently expressed in T cells. One study reported that lactacystin, a proteasome inhibitor selectively induced IL-4 mRNA level but reduced IL-3 mRNA levels in PMA and Ionomycin activated Jurkat cells [313]. Thus, suggesting that proteasome may play differential role in regulating IL-4 and IL-13 transcription. As such, regarding our study, whether IRF5v4 could have interacted with proteasome that led to reduced IL-4 mRNA level remains as an intriguing question to be explored in the future.

Chapter 5

5 Conclusion and future directions

5.1 Conclusion

This thesis describes the study done to examine the transcriptional role of IRF5 in regulating IL-13 expression as well as assessed the ability of IRF5 in modulating Th1 and Th2 associated cytokines *in vitro*. Humans *Irf5* gene is differently spliced giving rise to at least nine isoforms. Two of IRF5 isoforms which are predominately present and transcriptional active; IRF5v4 and IRF5v5 were studied. We successfully isolated these IRF5 spliced isoforms from cDNA library of B cells. Following the amplification of IRF5v4 and IRF5v5 encoding sequences, construction of expression vectors encoding either IRF5v4 or IRFv5 were done using pcDNA mammalian expression vector. Transient transfection using HEK 293T cells were done to produce proteins for pull down assay. We used MyD88 expressing plasmid to mediate activation of IRF5 spliced isoforms. Using pull down assay we showed that the IRF5 spliced isoforms had slight difference in their DNA binding activity to the ISRE bound oligonucleotide corresponding to ISRE region. We found that ectopic IRF5v4 binding to oligonucleotide ISRE was completely dependent on MyD88. On the other hand, ectopic IRF5v5 alone was able to bind oligonucleotide corresponding to ISRE region, although its interaction was greatly enhanced when activated by MyD88. Our

results confirmed that IRF5v4 and IRF5v5 can bind to the functional element of ISRE element on human *IL13* promoter.

Since both IRF5v4 and IRF5v5 were able to bind ISRE region of *IL13* promoter, the transcriptional role of IRF5 on *IL13* promoter activation was examined using a heterologous luciferase reporter construct driven by *IL13* promoter. Expression vectors encoding IRF5v4 and IRF5v5 were constructed for transient transfection. In the transient transfection, HEK 293T cells were transfected with IRF5v4 or IRF5v5 in the presence and absence of MyD88 expression plasmid at various concentrations (25-100ng). From the results, we found that in presence of MyD88 both the IRF5 spliced isoforms were able to stimulate the activation of *IL13* promoter, whereas in absence of MyD88 neither of these spliced isoforms could induce significant activity. In addition, the stimulatory activity of *IL13* promoter was proportionate to increasing concentration of MyD88 and IRF5v5, although at higher concentration of MyD88 led to reduced activity. Conversely, for IRF5v4, increasing the concentration of MyD88 did not enhance activation of IL-13 proportionally. In fact, increasing MyD88 led to lower transcriptional activation of IL-13 by IRF5v4. The reduced transcriptional activity of IRF5 spliced isoform by higher level of MyD88, suggest degradation or negative regulation of IRF5 spliced isoforms through their interaction with some endogenous proteins.

To assess the potential role of IRF5 in modulating Th1 and Th2 associated cytokines, we evaluated the effect of IRF5v4 and IRF5v5 in Jurkat cells in response to co-stimulation of PMA and Ionomycin. We constructed lentiviral vectors encoding for IRF5v4 or IRF5v5 and genetically modified Jurkat cells with our lentiviral constructs to ectopically express IRF5v4 or IRF5v5. The stably overexpressing IRF5v4 or IRF5v5 were achieved through limiting dilution method and cells with comparable transgene levels were used. In regards to IRF5 role in modulating Th cytokine expression, our results showed that both IRF5v4 and IRF5v5 exhibited differential response towards regulating the cytokines associated with Th1 and Th2. The semi-quantitative RT-PCR results showed that upon PMA and Ionomycin stimulation, stably expressing IRF5v5 increased IFNγ gene expression whilst led to inhibition of IL-4 and IL-13 gene expression. In protein level, IRF5v4 led to diminished level of IFNγ secretion, suggesting its contribution to inhibition of IFNγ production. Meanwhile, IRF5v5 showed no effect in IFNγ secretion. These results suggest potential role of IRF5v5 in regulating IFNγ transcription, through its interaction with T-bet, leading to Th1 polarisation. Conversely, IRF5v4 showed induction of IL-13 expression and inhibition of IFNγ and IL-4 gene expression, suggesting its potential role in differently promoting Th2 associated cytokine expression. Of note, both IRF5v4 and IRF5v5 were shown to upregulate IL-2 gene expression and IL-2 secretion, suggesting it potential role in augmenting T cell activation responses. With regards to IL-10, both IRF5v4 and IRF5v5 were able to secrete moderate amount of IL-10. Taken together, although the mechanism of underlying IRF5 differential response exerted by its spliced isoforms remains to be

elucidate in detail, the data presented by this study provides an insight into involvement of IRF5v4 and IRF5v5 in inducing human *IL13* promoter activity as well as their modulation in the expression of cytokines in human T cells line. The summary of findings obtained from this study is illustrated in Figure 5.1.
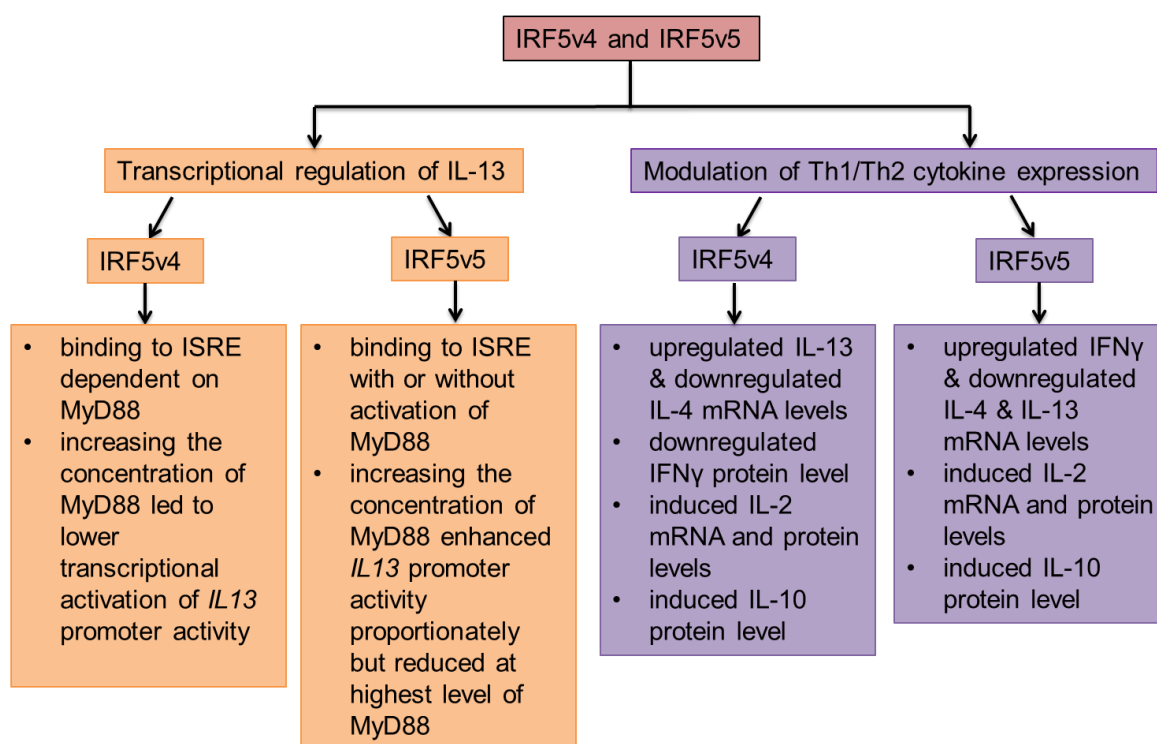
Figure 5.1 Key summary of findings obained from this study.

5.2 Limitations and Future considerations

The following are limitations in this study and suggestions for the future research

1. In the pull-down assay we found that IRF5v5 were able to bound to oligonucleotide corresponding to *IL13/ISRE* element in absence of MyD88, indicating that IRF5v5 may have interacted with some endogenous adaptor proteins that could have activated it and subsequently facilitated its binding to *IL13/ISRE*. Future work can focus on revealing IRF5v5 interacting proteins present in nuclear lysates (without ectopic MyD88). This can be done by screening IRF5v5 interacting partner through proteomic studies, using affinity purification coupled with mass spectrometry (AP-MS) analysis in HEK 293T cells.

2. In luciferase reporter assay, we showed that transcriptional activation of IRF5v5 was dependent on MyD88. However, increasing concentration of MyD88 to higher level led to reduced activity of IRF5v5. On the other hand, IRF5v4 at the lowest concentration of MyD88 showed enhanced luciferase activity. Higher expression level of MyD88 led to suppression of transcriptional activity of IRF5v4. Therefore, our results indicate that while MyD88 activation is required for IRF5 transcriptional activity, higher level of MyD88 had negative effect on the IRF5 induction of *IL13* promoter activity. In future, it would be worth extending these findings to study the negative regulation of TRIM21, KAP1, and Lyn on IRF5 transactivation and

transcription of IL-13 to elucidate the detailed mechanism involved in TLR-mediating signaling in affecting IRF5 activity for regulation of IL-13 cytokine.

3. During routine examination of the expression level of IRF5v4 and IRF5v5 prior to PMA and Ionomycin stimulation experiment, we observed intensity of IRF5v4 or IRF5v5 expression in stably expressing cells decreased gradually upon cultivation of the cells as the cells take time to reach confluency. This was due to gene silencing, a common phenomenon seen with use of CMV promoters [212]. The gene silencing was restored upon stimulation of PMA and Ionomycin. In future, lentiviral vector under inducible promoter can be used to overcome this gene silencing problem when PMA and Ionomycin are not required in the studies [198,212].

4. During the establishment of stably expressing IRF5v4 and IRF5v5 cells in Jurkat cells, we observed slower and stagnated growth rate in some of IRF5v4 expressing cells. Since, IRF5 have been implicated in regulating cell cycle and cell death, further studies in this area can provide additional insight whether IRF5 has similar effect in T cells.

5. In semi-quantitative RT-PCR analysis, we showed that IRF5v5 was able to induce IFNγ expression in Jurkat cells upon PMA and Ionomycin stimulation. In line, with several investigations by previous studies supporting its potential

involvement with T-bet, our findings can be extended in further studies to confirm the potential role of IRF5v5 in interacting with T-bet.

6. During our RT-PCR optimisation step, we were not able to detect IL-5 and IL-10 mRNA from stimulated IRF5 expressing cells. The failure in not detecting IL-5 and IL-10 mRNA does not conclude that IRF5v4/IRF5v5 did not involve in regulation of the two cytokines mentioned. Importantly, in our ELISA we showed that IRF5 able to induce IL-10, thus suggesting its role in regulating the expression of IL-10. In future, including positive control cells (peripheral blood mononuclear cells or HuT 78 cells- T cell lymphoma cells, another $CD4^+$ T cell line model)) would be helpful to evaluate the effectiveness of RT-PCR parameter as well as to be used in comparison for presence or absence of mRNA interest.

7. Our findings showed IRF5v4 differential regulated the expression IL-4 and IL-13 expression in Jurkat cells in response to PMA and Ionomycin. Since previous studies have implicated the potential role of proteasome in differently regulating IL-4 and IL-13 expression, further studies can explore the association of IRF5v4 with proteasome in regulating these Th2 cytokines differently.

8. While IL-13 mRNA was detected in stimulated Jurkat cells as expected, but the protein secretion of IL-13 quantitated was lower than unstimulated cells.

Thus, highlighting that induction of IL-13 in stimulated control cells was not successful. The production of IL-13 in Jurkat cells are not widely reported, although there were at least three studies that have shown Jurkat cells can secrete profound amount of IL-13 upon PMA and Ionomycin stimulation as previously discussed. Interestingly, our findings correlate with a recent finding that showed that activation of Jurkat with PMA and Ionomycin induced Th1 phenotype as characterised by the profound secretion of IFNγ and IL-2 but not IL-13 [238]. The aforementioned study also revealed that IL-13 can be induced in Jurkat cells by stimulating the cells into Th2 type skewed condition through PMA/CD28. Hence, it is important to address this issue in the future. In addition, a comparative study can be done using positive control cells such as purified CD4$^+$ T cells and HuT78 cells that are known to produce IL-13 [234]. Although Jurkat cells have been extensively used for cytokine studies, a recent report revealed that Jurkat cells harbour several genomic abnormalities associated with key molecules in TCR signalling, genomic stability and *o*-linked glycosylation (a post-translation modification) [314]. Therefore, caution should be taken in future investigation when using Jurkat cells by taking note the defects of Jurkat cells. Despite the reported defects in Jurkat cells reported, there are still ongoing work published using Jurkat to evaluate cytokine as revealed through Pubmed search. In future work, it is highly recommended that a comprehensive study to be conducted to assess the cytokines profile in Jurkat cells in response to different strength of stimuli and

mitogens in comparison with positive controls [234,315]. This would be inevitable helpful to find optimal activation for cytokines in interest.

6 References

1. Singh H, Khan AA, Dinner AR, Yamane H, Paul WE, Spits H, et al. Gene regulatory networks in the immune system. Trends Immunol [Internet]. 2014 May [cited 2016 Aug 30];35(5):211–8. Available from: http://linkinghub.elsevier.com/retrieve/pii/S147149061400057X

2. Tamura T, Yanai H, Savitsky D, Taniguchi T. The IRF family transcription factors in immunity and oncogenesis. Annu Rev Immunol [Internet]. 2008 Jan 27 [cited 2015 Feb 24];26:535–84. Available from: http://www.annualreviews.org/doi/abs/10.1146/annurev.immunol.26.021607.0 90400

3. Honda K, Taniguchi T. IRFs: master regulators of signalling by Toll-like receptors and cytosolic pattern-recognition receptors. Nat Rev Immunol [Internet]. 2006 Sep [cited 2014 Oct 14];6(9):644–58. Available from: http://dx.doi.org/10.1038/nri1900

4. Martino M, Rocchi G, Escelsior A, Fornaro M. Immunomodulation Mechanism of Antidepressants: Interactions between Serotonin/Norepinephrine Balance and Th1/Th2 Balance. Curr Neuropharmacol [Internet]. 2012 Jun [cited 2015 May 4];10(2):97–123. Available from: http://www.pubmedcentral.nih.gov/articlerender.fcgi?artid=3386509&tool=pm centrez&rendertype=abstract

5. Kidd P. Th1/Th2 balance: the hypothesis, its limitations, and implications for health and disease. Altern Med Rev [Internet]. 2003 Aug [cited 2015 Mar 30];8(3):223–46. Available from: http://www.ncbi.nlm.nih.gov/pubmed/12946237

6. Zhao G-N, Jiang D-S, Li H. Interferon regulatory factors: at the crossroads of immunity, metabolism, and disease. Biochim Biophys Acta - Mol Basis Dis. 2015;1852(2):365–78.

7. Lohoff M, Mak TW. Roles of interferon-regulatory factors in T-helper-cell differentiation. Nat Rev Immunol [Internet]. 2005 Feb [cited 2015 Feb 24];5(2):125–35. Available from: http://dx.doi.org/10.1038/nri1552

8. Negishi H, Ohba Y, Yanai H, Takaoka A, Honma K, Yui K, et al. Negative regulation of Toll-like-receptor signaling by IRF-4. Proc Natl Acad Sci U S A [Internet]. 2005 Nov 1 [cited 2015 Feb 24];102(44):15989–94. Available from: http://www.pnas.org/content/102/44/15989.full

9. Cretney E, Xin A, Shi W, Minnich M, Masson F, Miasari M, et al. The transcription factors Blimp-1 and IRF4 jointly control the differentiation and function of effector regulatory T cells. Nat Immunol [Internet]. 2011 Apr [cited 2015 Feb 24];12(4):304–11. Available from: http://dx.doi.org/10.1038/ni.2006

10. Lien C, Fang C-M, Huso D, Livak F, Lu R, Pitha PM. Critical role of IRF-5 in regulation of B-cell differentiation. Proc Natl Acad Sci U S A [Internet]. 2010 Mar 9 [cited 2015 Feb 24];107(10):4664–8. Available from:

http://www.pnas.org/content/107/10/4664.abstract

11. Eames HL, Corbin AL, Udalova IA. Interferon regulatory factor 5 in human autoimmunity and murine models of autoimmune disease. Transl Res [Internet]. 2016 Jan [cited 2016 Jun 10];167(1):167–82. Available from: http://www.ncbi.nlm.nih.gov/pubmed/26207886

12. Almuttaqi H, Udalova IA. Advances and challenges in targeting IRF5, a key regulator of inflammation. FEBS J [Internet]. 2019 May 21 [cited 2019 Jun 4];286(9):1624–37. Available from: http://www.ncbi.nlm.nih.gov/pubmed/30199605

13. Kaur A, Lee L-HL-H, Chow S-CS-C, Fang C-MC-M. IRF5-mediated immune responses and its implications in immunological disorders. Int Rev Immunol [Internet]. 2018 Jul 9 [cited 2018 Nov 19];37(5):1–20. Available from: https://www.tandfonline.com/doi/full/10.1080/08830185.2018.1469629

14. Saigusa R, Asano Y, Taniguchi T, Yamashita T, Ichimura Y, Takahashi T, et al. Multifaceted contribution of the TLR4-activated IRF5 transcription factor in systemic sclerosis. Proc Natl Acad Sci U S A [Internet]. 2015 Dec 8 [cited 2016 Oct 2];112(49):15136–41. Available from: http://www.ncbi.nlm.nih.gov/pubmed/26598674

15. Xu Y, Lee PY, Li Y, Liu C, Zhuang H, Han S, et al. Pleiotropic IFN-Dependent and -Independent Effects of IRF5 on the Pathogenesis of Experimental Lupus. J Immunol [Internet]. 2012 Apr 15 [cited 2016 Jul 17];188(8):4113–21. Available from: http://www.jimmunol.org/cgi/doi/10.4049/jimmunol.1103113

16. Mancl ME, Hu G, Sangster-Guity N, Olshalsky SL, Hoops K, Fitzgerald-Bocarsly P, et al. Two discrete promoters regulate the alternatively spliced human interferon regulatory factor-5 isoforms. Multiple isoforms with distinct cell type-specific expression, localization, regulation, and function. J Biol Chem [Internet]. 2005 Jun 3 [cited 2015 Jul 1];280(22):21078–90. Available from: http://www.ncbi.nlm.nih.gov/pubmed/15805103

17. Paun A, Bankoti R, Joshi T, Pitha PM, Stäger S. Critical role of IRF-5 in the development of T helper 1 responses to Leishmania donovani infection. PLoS Pathog [Internet]. 2011 Jan 6 [cited 2015 Feb 24];7(1):e1001246. Available from: http://journals.plos.org/plospathogens/article?id=10.1371/journal.ppat.1001246

18. Ishikawa C, Senba M, Barnes BJ, Mori N. Constitutive expression of IRF-5 in HTLV-1-infected T cells. Int J Oncol [Internet]. 2015 Jul [cited 2016 Jun 10];47(1):361–9. Available from: http://www.ncbi.nlm.nih.gov/pubmed/26004104

19. Fabié A, Mai LT, Dagenais-Lussier X, Hammami A, van Grevenynghe J, Stäger S. IRF-5 Promotes Cell Death in CD4 T Cells during Chronic Infection. Cell Rep [Internet]. 2018 Jul 31 [cited 2019 Jun 1];24(5):1163–75. Available from: http://www.ncbi.nlm.nih.gov/pubmed/30067973

20. Byrne AJ, Weiss M, Mathie SA, Walker SA, Eames HL, Saliba D, et al. A critical role for IRF5 in regulating allergic airway inflammation. Mucosal Immunol [Internet]. 2017 May 19 [cited 2018 Mar 21];10(3):716–26. Available

from: http://www.ncbi.nlm.nih.gov/pubmed/27759022

21. Rael EL, Lockey RF. Interleukin-13 signaling and its role in asthma [Internet]. Vol. 4, World Allergy Organization Journal. BioMed Central Ltd.; 2011 [cited 2020 Oct 21]. p. 54–64. Available from: /pmc/articles/PMC3651056/?report=abstract

22. Browne EP. Regulation of B-cell responses by Toll-like receptors. Immunology [Internet]. 2012 Aug [cited 2020 Jan 22];136(4):370–9. Available from: http://www.ncbi.nlm.nih.gov/pubmed/22444240

23. Seyfizadeh N, Seyfizadeh N, Gharibi T, Babaloo Z. Interleukin-13 as an important cytokine: A review on its roles in some human diseases. Acta Microbiol Immunol Hung [Internet]. 2015 Dec [cited 2019 Apr 21];62(4):341–78. Available from: http://www.ncbi.nlm.nih.gov/pubmed/26689873

24. Wills-Karp M. Interleukin-13 in asthma pathogenesis. Immunol Rev [Internet]. 2004 Dec [cited 2015 Apr 7];202:175–90. Available from: http://www.ncbi.nlm.nih.gov/pubmed/15546393

25. Phipps S, Hansbro N, Lam CE, Foo SY, Matthaei KI, Foster PS. Allergic sensitization is enhanced in early life through toll-like receptor 7 activation. Clin Exp Allergy [Internet]. 2009 Dec [cited 2015 Feb 24];39(12):1920–8. Available from: http://www.ncbi.nlm.nih.gov/pubmed/19735273

26. Kozyrev S V, Lewén S, Reddy PMVL, Pons-Estel B, Argentine Collaborative Group, Witte T, et al. Structural insertion/deletion variation in IRF5 is associated with a risk haplotype and defines the precise IRF5 isoforms expressed in systemic lupus erythematosus. Arthritis Rheum [Internet]. 2007 Apr [cited 2016 Oct 25];56(4):1234–41. Available from: http://www.ncbi.nlm.nih.gov/pubmed/17393452

27. Cheng T-F, Brzostek S, Ando O, Van Scoy S, Kumar KP, Reich NC. Differential activation of IFN regulatory factor (IRF)-3 and IRF-5 transcription factors during viral infection. J Immunol [Internet]. 2006 Jun 15 [cited 2016 Oct 25];176(12):7462–70. Available from: http://www.ncbi.nlm.nih.gov/pubmed/16751392

28. Kozyrev S V, Alarcon-Riquelme ME. The genetics and biology of Irf5-mediated signaling in lupus. Autoimmunity [Internet]. 2007 Dec [cited 2016 Jun 10];40(8):591–601. Available from: http://www.ncbi.nlm.nih.gov/pubmed/18075793

29. Fu B, Zhao M, Wang L, Patil G, Smith JA, Juncadella IJ, et al. RNAi Screen and Proteomics Reveal NXF1 as a Novel Regulator of IRF5 Signaling. Sci Rep [Internet]. 2017 Dec 2 [cited 2018 Mar 21];7(1):2683. Available from: http://www.nature.com/articles/s41598-017-02857-z

30. Lin R, Yang L, Arguello M, Penafuerte C, Hiscott J. A CRM1-dependent nuclear export pathway is involved in the regulation of IRF-5 subcellular localization. J Biol Chem [Internet]. 2005 Jan 28 [cited 2016 Jun 10];280(4):3088–95. Available from: http://www.ncbi.nlm.nih.gov/pubmed/15556946

31. Barnes BJ, Moore PA, Pitha PM. Virus-specific activation of a novel interferon regulatory factor, IRF-5, results in the induction of distinct interferon alpha

genes. J Biol Chem [Internet]. 2001 Jun 29 [cited 2015 Jun 29];276(26):23382–90. Available from: http://www.ncbi.nlm.nih.gov/pubmed/11303025

32. Barnes BJ, Kellum MJ, Field AE, Pitha PM. Multiple regulatory domains of IRF-5 control activation, cellular localization, and induction of chemokines that mediate recruitment of T lymphocytes. Mol Cell Biol [Internet]. 2002 Aug [cited 2016 Jun 10];22(16):5721–40. Available from: http://www.ncbi.nlm.nih.gov/pubmed/12138184

33. Paun A, Reinert JT, Jiang Z, Medin C, Balkhi MY, Fitzgerald KA, et al. Functional characterization of murine interferon regulatory factor 5 (IRF-5) and its role in the innate antiviral response. J Biol Chem [Internet]. 2008 May 23 [cited 2015 Feb 5];283(21):14295–308. Available from: http://www.jbc.org/cgi/doi/10.1074/jbc.M800501200

34. Balkhi MY, Fitzgerald KA, Pitha PM. Functional regulation of MyD88-activated interferon regulatory factor 5 by K63-linked polyubiquitination. Mol Cell Biol [Internet]. 2008 Dec [cited 2015 Jun 29];28(24):7296–308. Available from: http://www.pubmedcentral.nih.gov/articlerender.fcgi?artid=2593423&tool=pmcentrez&rendertype=abstract

35. Wu J, Brown M. Epigenetics and Epigenomics. In: Hematology [Internet]. Elsevier; 2018 [cited 2019 Dec 21]. p. 17–24. Available from: https://www.sciencedirect.com/science/article/pii/B9780323357623000020

36. Crick F. Central dogma of molecular biology. Nature [Internet]. 1970 Aug 8 [cited 2019 Dec 21];227(5258):561–3. Available from: http://www.ncbi.nlm.nih.gov/pubmed/4913914

37. Li J, Liu C. Coding or Noncoding, the Converging Concepts of RNAs. Front Genet [Internet]. 2019 May 22 [cited 2019 Dec 5];10:496. Available from: https://www.frontiersin.org/article/10.3389/fgene.2019.00496/full

38. Lee TI, Young RA. Transcriptional regulation and its misregulation in disease. Cell [Internet]. 2013 Mar 14 [cited 2019 Dec 14];152(6):1237–51. Available from: http://www.ncbi.nlm.nih.gov/pubmed/23498934

39. Moraes F, Góes A. A decade of human genome project conclusion: Scientific diffusion about our genome knowledge. Biochem Mol Biol Educ [Internet]. 2016 [cited 2019 Dec 14];44(3):215–23. Available from: http://www.ncbi.nlm.nih.gov/pubmed/26952518

40. Rosenberg LE, Rosenberg DD, Rosenberg LE, Rosenberg DD. Structure of Genes, Chromosomes, and Genomes. In: Human Genes and Genomes [Internet]. Academic Press; 2012 [cited 2019 Dec 14]. p. 75–96. Available from: https://www.sciencedirect.com/science/article/pii/B9780123852120000068

41. Barrett LW, Fletcher S, Wilton SD. Regulation of eukaryotic gene expression by the untranslated gene regions and other non-coding elements. Cell Mol Life Sci [Internet]. 2012 Nov 27 [cited 2019 Dec 4];69(21):3613–34. Available from: http://link.springer.com/10.1007/s00018-012-0990-9

42. Lelli KM, Slattery M, Mann RS. Disentangling the Many Layers of Eukaryotic Transcriptional Regulation. Annu Rev Genet [Internet]. 2012 Dec 15 [cited

2019 Dec 4];46(1):43–68. Available from:
http://www.annualreviews.org/doi/10.1146/annurev-genet-110711-155437

43.   Rosenberg LE, Rosenberg DD, Rosenberg LE, Rosenberg DD. Expression of
Genes and Genomes. In: Human Genes and Genomes [Internet]. Academic
Press; 2012 [cited 2019 Dec 14]. p. 97–116. Available from:
https://www.sciencedirect.com/science/article/pii/B978012385212000007X

44.   Griesenbeck J, Tschochner H, Grohmann D. Structure and Function of RNA
Polymerases and the Transcription Machineries. Subcell Biochem [Internet].
2017 [cited 2019 Dec 10];83:225–70. Available from:
http://www.ncbi.nlm.nih.gov/pubmed/28271479

45.   Watson JD. Molecular Biology of the Gene [Internet]. Pearson; 2014. (Always
learning). Available from:
https://books.google.com.my/books?id=BjuXMgEACAAJ

46.   Talbert PB, Meers MP, Henikoff S. Old cogs, new tricks: the evolution of gene
expression in a chromatin context. Nat Rev Genet [Internet]. 2019 Mar 18
[cited 2019 Dec 14];20(5):283–97. Available from:
http://www.nature.com/articles/s41576-019-0105-7

47.   Maston GA, Evans SK, Green MR. Transcriptional regulatory elements in the
human genome. Annu Rev Genomics Hum Genet [Internet]. 2006 [cited 2019
Dec 14];7:29–59. Available from:
http://www.ncbi.nlm.nih.gov/pubmed/16719718

48.   Danino YM, Even D, Ideses D, Juven-Gershon T. The core promoter: At the
heart of gene expression. Biochim Biophys Acta - Gene Regul Mech [Internet].
2015 Aug [cited 2019 Dec 10];1849(8):1116–31. Available from:
http://www.ncbi.nlm.nih.gov/pubmed/25934543

49.   Haberle V, Stark A. Eukaryotic core promoters and the functional basis of
transcription initiation. Nat Rev Mol Cell Biol [Internet]. 2018 [cited 2019 Dec
10];19(10):621–37. Available from:
http://www.ncbi.nlm.nih.gov/pubmed/29946135

50.   Venkatesh S, Workman JL. Histone exchange, chromatin structure and the
regulation of transcription. Nat Rev Mol Cell Biol [Internet]. 2015 Mar [cited
2019 Dec 14];16(3):178–89. Available from:
http://www.ncbi.nlm.nih.gov/pubmed/25650798

51.   Bhagavan NV, Ha C-E, Bhagavan NV, Ha C-E. Regulation of Gene
Expression. Essentials Med Biochem [Internet]. 2015 Jan 1 [cited 2019 Dec
14];447–64. Available from:
https://www.sciencedirect.com/science/article/pii/B9780124166875000245

52.   Gibcus JH, Dekker J. The context of gene expression regulation. F1000 Biol
Rep [Internet]. 2012 [cited 2019 Dec 21];4. Available from:
https://www.ncbi.nlm.nih.gov/pmc/articles/PMC3318259/

53.   Allen BL, Taatjes DJ. The Mediator complex: a central integrator of
transcription. Nat Rev Mol Cell Biol [Internet]. 2015 Mar 18 [cited 2019 Dec
12];16(3):155–66. Available from: http://www.nature.com/articles/nrm3951

54.   Soutourina J. Transcription regulation by the Mediator complex. Nat Rev Mol
Cell Biol [Internet]. 2018 Apr 6 [cited 2019 Dec 12];19(4):262–74. Available

from: http://www.nature.com/articles/nrm.2017.115

55. Verger A, Monté D, Villeret V. Twenty years of Mediator complex structural studies. Biochem Soc Trans [Internet]. 2019 [cited 2019 Dec 21];47(1):399–410. Available from: http://www.ncbi.nlm.nih.gov/pubmed/30733343

56. de Klerk E, 't Hoen PAC. Alternative mRNA transcription, processing, and translation: insights from RNA sequencing. Trends Genet [Internet]. 2015 Mar [cited 2019 Dec 14];31(3):128–39. Available from: http://www.ncbi.nlm.nih.gov/pubmed/25648499

57. Hershey JWB, Sonenberg N, Mathews MB. Principles of translational control: an overview. Cold Spring Harb Perspect Biol [Internet]. 2012 Dec 1 [cited 2019 Dec 21];4(12). Available from: http://www.ncbi.nlm.nih.gov/pubmed/23209153

58. Liu Y, Beyer A, Aebersold R. On the Dependency of Cellular Protein Levels on mRNA Abundance. Cell [Internet]. 2016 Apr 21 [cited 2019 Dec 14];165(3):535–50. Available from: http://www.ncbi.nlm.nih.gov/pubmed/27104977

59. Saraswathy N, Ramalingam P, Saraswathy N, Ramalingam P. Phosphoproteomics. Concepts Tech Genomics Proteomics [Internet]. 2011 Jan 1 [cited 2019 Dec 14];203–11. Available from: https://www.sciencedirect.com/science/article/pii/B9781907568107500158

60. Knorre DG, Kudryashova N V, Godovikova TS. Chemical and functional aspects of posttranslational modification of proteins. Acta Naturae [Internet]. 2009 Oct [cited 2019 Dec 14];1(3):29–51. Available from: http://www.ncbi.nlm.nih.gov/pubmed/22649613

61. Kellie S, Al-Mansour Z. Overview of the Immune System. In: Micro and Nanotechnology in Vaccine Development [Internet]. William Andrew Publishing; 2017 [cited 2020 Jan 20]. p. 63–81. Available from: https://www.sciencedirect.com/science/article/pii/B978032339981400004X

62. Chen L, Deng H, Cui H, Fang J, Zuo Z, Deng J, et al. Oncotarget 7204 www.impactjournals.com/oncotarget Inflammatory responses and inflammation-associated diseases in organs [Internet]. Vol. 9, Oncotarget. 2018 [cited 2019 May 16]. Available from: www.impactjournals.com/oncotarget/

63. Bagatini MD, Cardoso AM, Reschke CR, Carvalho FB. Immune System and Chronic Diseases 2018. J Immunol Res [Internet]. 2018 [cited 2020 Jan 20];2018:8653572. Available from: http://www.ncbi.nlm.nih.gov/pubmed/30474045

64. Suresh R, Mosser DM, Ablasser A, Bauernfeind F, Hartmann G, Latz E, et al. Pattern recognition receptors in innate immunity, host defense, and immunopathology. Adv Physiol Educ [Internet]. 2013 Dec [cited 2016 Jul 17];37(4):284–91. Available from: http://www.ncbi.nlm.nih.gov/pubmed/24292903

65. Introduction to the Immune Response. In: Primer to the Immune Response [Internet]. Academic Cell; 2014 [cited 2020 Jan 20]. p. 3–20. Available from: https://www.sciencedirect.com/science/article/pii/B9780123852458000017

66. Patel P. Innate and Adaptive Immunity: Barriers and Receptor-Based

Recognition. In: Immunity and Inflammation in Health and Disease [Internet]. Academic Press; 2018 [cited 2020 Jan 20]. p. 3–13. Available from: https://www.sciencedirect.com/science/article/pii/B9780128054178000019

67. Carrillo JLM, García FPC, Coronado OG, García MAM, Cordero JFC. Physiology and Pathology of Innate Immune Response Against Pathogens. In: Rezaei N, editor. Physiology and Pathology of Immunology [Internet]. Rijeka: IntechOpen; 2017. Available from: https://doi.org/10.5772/intechopen.70556

68. McDonald DR, Levy O. Innate Immunity [Internet]. Clinical Immunology Content Repository Only!; Jan 1, 2019 p. 39-53.e1. Available from: https://www.sciencedirect.com/science/article/pii/B978070206896600003X

69. Smale ST. Transcriptional regulation in the innate immune system. Curr Opin Immunol [Internet]. 2012 Feb [cited 2019 Dec 28];24(1):51–7. Available from: http://www.ncbi.nlm.nih.gov/pubmed/22230561

70. Components of the Immune System [Internet]. Primer to the Immune Response Academic Cell; Jan 1, 2014 p. 21–54. Available from: https://www.sciencedirect.com/science/article/pii/B9780123852458000029

71. Carlson BM, Carlson BM. The Lymphoid System and Immunity. Hum Body [Internet]. 2019 Jan 1 [cited 2020 Jan 20];209–39. Available from: https://www.sciencedirect.com/science/article/pii/B9780128042540000089

72. Noakes PS, Michaelis LJ. Innate and adaptive immunity [Internet]. Diet, Immunity and Inflammation Woodhead Publishing; Jan 1, 2013 p. 3–33. Available from: https://www.sciencedirect.com/science/article/pii/B9780857090379500011

73. Chaplin DD. The Human Immune Response. In: Clinical Immunology [Internet]. Content Repository Only!; 2019 [cited 2019 Dec 19]. p. 3-17.e1. Available from: https://www.sciencedirect.com/science/article/pii/B9780702068966000016

74. Lewis DE, Blutt SE. Organization of the Immune System. Clin Immunol [Internet]. 2019 Jan 1 [cited 2019 Dec 16];19-38.e1. Available from: https://www.sciencedirect.com/science/article/pii/B9780702068966000028

75. Alikhan MA, Ricardo SD. Mononuclear phagocyte system in kidney disease and repair. Nephrology (Carlton) [Internet]. 2013 Feb [cited 2020 Jan 20];18(2):81–91. Available from: http://www.ncbi.nlm.nih.gov/pubmed/23194390

76. Antigen Processing and Presentation. In: Primer to the Immune Response [Internet]. Academic Cell; 2014 [cited 2020 Jan 20]. p. 161–79. Available from: https://www.sciencedirect.com/science/article/pii/B9780123852458000078

77. Carty SA, Riese MJ, Koretzky GA. T-Cell Immunity. In: Hematology [Internet]. Elsevier; 2018 [cited 2019 Dec 23]. p. 221–39. Available from: https://www.sciencedirect.com/science/article/pii/B9780323357623000214

78. Hoffman W, Lakkis FG, Chalasani G. B Cells, Antibodies, and More. Clin J Am Soc Nephrol [Internet]. 2016 Jan 7 [cited 2020 Jan 20];11(1):137–54. Available from: http://www.ncbi.nlm.nih.gov/pubmed/26700440

79. Yu Y-H, Lin K-I. Factors That Regulate the Generation of Antibody-Secreting

Plasma Cells. In: Advances in immunology [Internet]. Adv Immunol; 2016 [cited 2020 Jan 20]. p. 61–99. Available from: http://www.ncbi.nlm.nih.gov/pubmed/27235681

80. Goodnow CC, Vinuesa CG, Randall KL, Mackay F, Brink R. Control systems and decision making for antibody production. Nat Immunol [Internet]. 2010 Aug 20 [cited 2018 Mar 21];11(8):681–8. Available from: http://www.ncbi.nlm.nih.gov/pubmed/20644574

81. Koch U, Radtke F. Mechanisms of T Cell Development and Transformation. Annu Rev Cell Dev Biol [Internet]. 2011 Nov 10 [cited 2017 Mar 23];27(1):539–62. Available from: http://www.ncbi.nlm.nih.gov/pubmed/21740230

82. Harrington LE. T-Cell Development. In: Clinical Immunology [Internet]. Content Repository Only!; 2019 [cited 2019 Dec 19]. p. 119-125.e1. Available from: https://www.sciencedirect.com/science/article/pii/B9780702068966000089

83. Kumar B V, Connors TJ, Farber DL. Human T Cell Development, Localization, and Function throughout Life. Immunity [Internet]. 2018 [cited 2019 Dec 16];48(2):202–13. Available from: http://www.ncbi.nlm.nih.gov/pubmed/29466753

84. The T Cell Receptor: Proteins and Genes. In: Primer to the Immune Response [Internet]. Academic Cell; 2014 [cited 2020 Jan 20]. p. 181–96. Available from: https://www.sciencedirect.com/science/article/pii/B978012385245800008X

85. T Cell Development, Activation and Effector Functions. In: Primer to the Immune Response [Internet]. Academic Cell; 2014 [cited 2020 Jan 20]. p. 197–226. Available from: https://www.sciencedirect.com/science/article/pii/B9780123852458000091

86. van den Broek T, Borghans JAM, van Wijk F. The full spectrum of human naive T cells. Nat Rev Immunol [Internet]. 2018 [cited 2019 Dec 16];18(6):363–73. Available from: http://www.ncbi.nlm.nih.gov/pubmed/29520044

87. Smith-Garvin JE, Koretzky GA, Jordan MS. T cell activation. Annu Rev Immunol [Internet]. 2009 [cited 2019 Dec 17];27:591–619. Available from: http://www.ncbi.nlm.nih.gov/pubmed/19132916

88. Gorentla BK, Zhong X-P. T cell Receptor Signal Transduction in T lymphocytes. J Clin Cell Immunol [Internet]. 2012 Oct 27 [cited 2019 Dec 16];2012(Suppl 12):5. Available from: http://www.ncbi.nlm.nih.gov/pubmed/23946894

89. Huse M. The T-cell-receptor signaling network. J Cell Sci [Internet]. 2009 May 1 [cited 2019 Dec 16];122(Pt 9):1269–73. Available from: http://www.ncbi.nlm.nih.gov/pubmed/19386893

90. Peterson EJ, Maltzman JS. T-Cell Activation and Tolerance. Clin Immunol [Internet]. 2019 Jan 1 [cited 2019 Dec 16];183-196.e1. Available from: https://www.sciencedirect.com/science/article/pii/B9780702068966000120

91. Gaud G, Lesourne R, Love PE. Regulatory mechanisms in T cell receptor

signalling. Nat Rev Immunol [Internet]. 2018 [cited 2019 Dec 17];18(8):485–97. Available from: http://www.ncbi.nlm.nih.gov/pubmed/29789755

92. Esensten JH, Helou YA, Chopra G, Weiss A, Bluestone JA. CD28 Costimulation: From Mechanism to Therapy. Immunity [Internet]. 2016 [cited 2019 Dec 17];44(5):973–88. Available from: http://www.ncbi.nlm.nih.gov/pubmed/27192564

93. Shipkova M, Wieland E. Surface markers of lymphocyte activation and markers of cell proliferation. Clin Chim Acta [Internet]. 2012 Sep 8 [cited 2019 Dec 17];413(17–18):1338–49. Available from: http://www.ncbi.nlm.nih.gov/pubmed/22120733

94. Rudd CE, Taylor A, Schneider H. CD28 and CTLA-4 coreceptor expression and signal transduction. Immunol Rev [Internet]. 2009 May [cited 2019 Dec 17];229(1):12–26. Available from: http://www.ncbi.nlm.nih.gov/pubmed/19426212

95. Ville S, Poirier N, Blancho G, Vanhove B. Co-Stimulatory Blockade of the CD28/CD80-86/CTLA-4 Balance in Transplantation: Impact on Memory T Cells? Front Immunol [Internet]. 2015 Aug 10 [cited 2019 Dec 17];6:411. Available from: http://journal.frontiersin.org/Article/10.3389/fimmu.2015.00411/abstract

96. Häcker G, Bauer A, Villunger A. Apoptosis in activated T cells: what are the triggers, and what the signal transducers? Cell Cycle [Internet]. 2006 Nov 1 [cited 2019 Dec 17];5(21):2421–4. Available from: http://www.ncbi.nlm.nih.gov/pubmed/17102629

97. Zhan Y, Carrington EM, Zhang Y, Heinzel S, Lew AM. Life and Death of Activated T Cells: How Are They Different from Naïve T Cells? Front Immunol [Internet]. 2017 [cited 2019 Dec 17];8:1809. Available from: http://www.ncbi.nlm.nih.gov/pubmed/29326701

98. Luckheeram RV, Zhou R, Verma AD, Xia B, Luckheeram RV, Zhou R, et al. CD4+T Cells: Differentiation and Functions. Clin Dev Immunol [Internet]. 2012 [cited 2016 Jul 19];2012:1–12. Available from: http://www.hindawi.com/journals/cdi/2012/925135/

99. Zhu J. T Helper Cell Differentiation, Heterogeneity, and Plasticity. Cold Spring Harb Perspect Biol [Internet]. 2018 Aug 1 [cited 2019 Dec 17];10(10):a030338. Available from: http://www.ncbi.nlm.nih.gov/pubmed/28847903

100. Gagliani N, Huber S. Balancing pro- and anti-inflammatory CD4+ T helper cells in the intestine. In: Chan J, editor. Autoimmune Diseases [Internet]. Rijeka: IntechOpen; 2012. Available from: https://doi.org/10.5772/48183

101. Gagliani N, Huber S. Basic Aspects of T Helper Cell Differentiation. Methods Mol Biol [Internet]. 2017 [cited 2019 Dec 17];1514:19–30. Available from: http://www.ncbi.nlm.nih.gov/pubmed/27787789

102. Saravia J, Chapman NM, Chi H. Helper T cell differentiation. Cell Mol Immunol [Internet]. 2019 Jul 12 [cited 2019 Dec 17];16(7):634–43. Available from: http://www.nature.com/articles/s41423-019-0220-6

103. Magee CN, Boenisch O, Najafian N. The role of costimulatory molecules in

directing the functional differentiation of alloreactive T helper cells. Am J Transplant [Internet]. 2012 Oct [cited 2019 Dec 17];12(10):2588–600. Available from: http://www.ncbi.nlm.nih.gov/pubmed/22759274

104. Tao X, Constant S, Jorritsma P, Bottomly K. Strength of TCR signal determines the costimulatory requirements for Th1 and Th2 CD4+ T cell differentiation. J Immunol [Internet]. 1997 Dec 15 [cited 2019 Dec 17];159(12):5956–63. Available from: http://www.ncbi.nlm.nih.gov/pubmed/9550393

105. Rogers PR, Croft M, Jorritsma P, Bottomly K. CD28, Ox-40, LFA-1, and CD4 modulation of Th1/Th2 differentiation is directly dependent on the dose of antigen. J Immunol [Internet]. 2000 Mar 15 [cited 2019 Dec 17];164(6):2955–63. Available from: http://www.ncbi.nlm.nih.gov/pubmed/9550393

106. Zhu J, Paul WE. Peripheral CD4+ T-cell differentiation regulated by networks of cytokines and transcription factors. Immunol Rev [Internet]. 2010 Nov [cited 2019 Dec 22];238(1):247–62. Available from: http://www.ncbi.nlm.nih.gov/pubmed/20969597

107. Broere F, Apasov SG, Sitkovsky M V., van Eden W. A2 T cell subsets and T cell-mediated immunity. In: Principles of Immunopharmacology [Internet]. Basel: Birkhäuser Basel; 2011 [cited 2019 Dec 22]. p. 15–27. Available from: http://link.springer.com/10.1007/978-3-0346-0136-8_2

108. Eagar TN, Miller SD. Helper T-Cell Subsets and Control of the Inflammatory Response. In: Clinical Immunology [Internet]. Content Repository Only!; 2019 [cited 2019 Dec 22]. p. 235-245.e1. Available from: https://www.sciencedirect.com/science/article/pii/B9780702068966000168

109. Hirahara K, Nakayama T. CD4+ T-cell subsets in inflammatory diseases: beyond the Th1/Th2 paradigm. Int Immunol [Internet]. 2016 Apr [cited 2019 Dec 22];28(4):163–71. Available from: http://www.ncbi.nlm.nih.gov/pubmed/26874355

110. Moudgil KD, Choubey D. Cytokines in autoimmunity: Role in induction, regulation, and treatment [Internet]. Vol. 31, Journal of Interferon and Cytokine Research. Mary Ann Liebert Inc.; 2011 [cited 2020 Oct 8]. p. 695–703. Available from: www.liebertpub.com

111. Kamali AN, Noorbakhsh SM, Hamedifar H, Jadidi-Niaragh F, Yazdani R, Bautista JM, et al. A role for Th1-like Th17 cells in the pathogenesis of inflammatory and autoimmune disorders. Mol Immunol. 2019 Jan 1;105:107–15.

112. Munitz A, Foster PS. T H 9 cells: In front and beyond T H 2 [Internet]. Vol. 129, Journal of Allergy and Clinical Immunology. Mosby Inc.; 2012 [cited 2020 Oct 8]. p. 1011–3. Available from: www.jacionline.org:

113. Nakayamada S, Takahashi H, Kanno Y, O'Shea JJ. Helper T cell diversity and plasticity. Curr Opin Immunol [Internet]. 2012 Jun [cited 2019 Dec 17];24(3):297. Available from: http://www.ncbi.nlm.nih.gov/pubmed/22341735

114. Nakayama T, Hirahara K, Onodera A, Endo Y, Hosokawa H, Shinoda K, et al. Th2 Cells in Health and Disease. Annu Rev Immunol [Internet]. 2017 Apr 26

[cited 2020 Oct 8];35(1):53–84. Available from:
http://www.annualreviews.org/doi/10.1146/annurev-immunol-051116-052350

115. Raphael I, Nalawade S, Eagar TN, Forsthuber TG. T cell subsets and their signature cytokines in autoimmune and inflammatory diseases [Internet]. Vol. 74, Cytokine. Academic Press; 2015 [cited 2020 Oct 13]. p. 5–17. Available from: https://www.ncbi.nlm.nih.gov/pmc/articles/PMC4416069/

116. Annunziato F, Cosmi L, Liotta F, Maggi E, Romagnani S. Human Th1 dichotomy: origin, phenotype and biologic activities. Immunology [Internet]. 2014 Oct 5 [cited 2019 Dec 21];144(3):343. Available from: http://www.ncbi.nlm.nih.gov/pubmed/25284714

117. Burrell CJ, Howard CR, Murphy FA, Burrell CJ, Howard CR, Murphy FA. Adaptive Immune Responses to Infection. In: Fenner and White's Medical Virology [Internet]. Academic Press; 2017 [cited 2019 Dec 21]. p. 65–76. Available from: https://www.sciencedirect.com/science/article/pii/B9780123751560000060

118. Leung S, Liu X, Fang L, Chen X, Guo T, Zhang J. The cytokine milieu in the interplay of pathogenic Th1/Th17 cells and regulatory T cells in autoimmune disease [Internet]. Vol. 7, Cellular and Molecular Immunology. Nature Publishing Group; 2010 [cited 2020 Oct 13]. p. 182–9. Available from: www.nature.com/cmi

119. Zhu J, Yamane H, Paul WE. Differentiation of effector CD4 T cell populations (*). Annu Rev Immunol [Internet]. 2010 [cited 2019 Dec 23];28:445–89. Available from: http://www.ncbi.nlm.nih.gov/pubmed/20192806

120. Brune Z, Rice MR, Barnes BJ. Potential T Cell-Intrinsic Regulatory Roles for IRF5 via Cytokine Modulation in T Helper Subset Differentiation and Function. Front Immunol [Internet]. 2020 Jun 3 [cited 2020 Oct 6];11:1143. Available from: www.frontiersin.org

121. Liao W, Lin J-X, Leonard WJ. IL-2 family cytokines: new insights into the complex roles of IL-2 as a broad regulator of T helper cell differentiation. Curr Opin Immunol [Internet]. 2011 Oct [cited 2019 Dec 23];23(5):598–604. Available from: http://www.ncbi.nlm.nih.gov/pubmed/21889323

122. Zhu J. T helper 2 (Th2) cell differentiation, type 2 innate lymphoid cell (ILC2) development and regulation of interleukin-4 (IL-4) and IL-13 production [Internet]. Vol. 75, Cytokine. Academic Press; 2015 [cited 2020 Oct 16]. p. 14–24. Available from: /pmc/articles/PMC4532589/?report=abstract

123. Yagi R, Zhu J, Paul WE. An updated view on transcription factor GATA3-mediated regulation of Th1 and Th2 cell differentiation. Int Immunol [Internet]. 2011 Jul [cited 2019 Dec 23];23(7):415–20. Available from: http://www.ncbi.nlm.nih.gov/pubmed/21632975

124. Huber M, Lohoff M. IRF4 at the crossroads of effector T-cell fate decision. Eur J Immunol [Internet]. 2014 Jul 1 [cited 2020 Oct 15];44(7):1886–95. Available from: http://doi.wiley.com/10.1002/eji.201344279

125. Bao K, Reinhardt RL. The differential expression of IL-4 and IL-13 and its impact on type-2 immunity [Internet]. Vol. 75, Cytokine. Academic Press; 2015 [cited 2020 Oct 16]. p. 25–37. Available from:

/pmc/articles/PMC5118948/?report=abstract

126. Pope SD, Medzhitov R. Emerging Principles of Gene Expression Programs and Their Regulation. Mol Cell [Internet]. 2018 [cited 2019 Dec 10];71(3):389–97. Available from: http://www.ncbi.nlm.nih.gov/pubmed/30075140

127. Lambert SA, Jolma A, Campitelli LF, Das PK, Yin Y, Albu M, et al. The Human Transcription Factors. Cell [Internet]. 2018 [cited 2019 Dec 15];172(4):650–65. Available from: http://www.ncbi.nlm.nih.gov/pubmed/29425488

128. Transcription Factors. In: Reference Module in Biomedical Sciences [Internet]. Elsevier; 2014 [cited 2019 Dec 15]. Available from: https://www.sciencedirect.com/science/article/pii/B9780128012383054660

129. Wingender E, Schoeps T, Haubrock M, Dönitz J. TFClass: a classification of human transcription factors and their rodent orthologs. Nucleic Acids Res [Internet]. 2015 Jan [cited 2019 Dec 15];43(Database issue):D97-102. Available from: http://www.ncbi.nlm.nih.gov/pubmed/25361979

130. Taniguchi T, Ogasawara K, Takaoka A, Tanaka N. IRF family of transcription factors as regulators of host defense. Annu Rev Immunol [Internet]. 2001 Jan [cited 2015 Apr 14];19:623–55. Available from: http://www.ncbi.nlm.nih.gov/pubmed/11244049

131. Miyamoto M, Fujita T, Kimura Y, Maruyama M, Harada H, Sudo Y, et al. Regulated expression of a gene encoding a nuclear factor, IRF-1, that specifically binds to IFN-beta gene regulatory elements. Cell [Internet]. 1988 Sep 9 [cited 2015 Apr 16];54(6):903–13. Available from: http://www.ncbi.nlm.nih.gov/pubmed/3409321

132. Lee H-R, Kim MH, Lee J-S, Liang C, Jung JU. Viral interferon regulatory factors. J Interferon Cytokine Res [Internet]. 2009 Sep [cited 2015 May 4];29(9):621–7. Available from: http://www.pubmedcentral.nih.gov/articlerender.fcgi?artid=2956608&tool=pmcentrez&rendertype=abstract

133. Honda K, Takaoka A, Taniguchi T. Type I interferon [corrected] gene induction by the interferon regulatory factor family of transcription factors. Immunity [Internet]. 2006 Sep [cited 2015 Jan 5];25(3):349–60. Available from: http://www.sciencedirect.com/science/article/pii/S1074761306003943

134. Battistini A. Interferon Regulatory Factors in Hematopoietic Cell Differentiation and Immune Regulation. http://dx.doi.org/101089/jir20090030 [Internet]. 2009 Dec [cited 2016 Jul 18];29(12):765–80. Available from: http://www.ncbi.nlm.nih.gov/pubmed/19929577

135. Lohoff M, Ferrick D, Mittrucker HW, Duncan GS, Bischof S, Rollinghoff M, et al. Interferon regulatory factor-1 is required for a T helper 1 immune response in vivo. Immunity [Internet]. 1997 Jun [cited 2015 May 4];6(6):681–9. Available from: http://www.ncbi.nlm.nih.gov/pubmed/9208841

136. Taki S, Sato T, Ogasawara K, Fukuda T, Sato M, Hida S, et al. Multistage regulation of Th1-type immune responses by the transcription factor IRF-1. Immunity [Internet]. 1997 Jun [cited 2015 May 4];6(6):673–9. Available from: http://www.ncbi.nlm.nih.gov/pubmed/9208840

137. Coccia EM, Passini N, Battistini A, Pini C, Sinigaglia F, Rogge L. Interleukin-12 induces expression of interferon regulatory factor-1 via signal transducer and activator of transcription-4 in human T helper type 1 cells. J Biol Chem [Internet]. 1999 Mar 5 [cited 2015 May 4];274(10):6698–703. Available from: http://www.ncbi.nlm.nih.gov/pubmed/10037767

138. Galon J, Sudarshan C, Ito S, Finbloom D, O'Shea JJ. IL-12 induces IFN regulating factor-1 (IRF-1) gene expression in human NK and T cells. J Immunol [Internet]. 1999 Jun 15 [cited 2015 May 4];162(12):7256–62. Available from: http://www.ncbi.nlm.nih.gov/pubmed/10358173

139. Kano S, Sato K, Morishita Y, Vollstedt S, Kim S, Bishop K, et al. The contribution of transcription factor IRF1 to the interferon-gamma-interleukin 12 signaling axis and TH1 versus TH-17 differentiation of CD4+ T cells. Nat Immunol [Internet]. 2008 Jan [cited 2015 May 4];9(1):34–41. Available from: http://www.ncbi.nlm.nih.gov/pubmed/18059273

140. Lohoff M, Duncan GS, Ferrick D, Mittrücker HW, Bischof S, Prechtl S, et al. Deficiency in the transcription factor interferon regulatory factor (IRF)-2 leads to severely compromised development of natural killer and T helper type 1 cells. J Exp Med [Internet]. 2000 Aug 7 [cited 2015 May 4];192(3):325–36. Available from: http://www.pubmedcentral.nih.gov/articlerender.fcgi?artid=2193225&tool=pmcentrez&rendertype=abstract

141. Elser B, Lohoff M, Kock S, Giaisi M, Kirchhoff S, Krammer PH, et al. IFN-gamma represses IL-4 expression via IRF-1 and IRF-2. Immunity [Internet]. 2002 Dec [cited 2015 Feb 24];17(6):703–12. Available from: http://www.sciencedirect.com/science/article/pii/S1074761302004715

142. Scharton-Kersten T, Contursi C, Masumi A, Sher A, Ozato K. Interferon Consensus Sequence Binding Protein-deficient Mice Display Impaired Resistance to Intracellular Infection Due to a Primary Defect in Interleukin 12 p40 Induction. J Exp Med [Internet]. 1997 Nov 3 [cited 2015 May 4];186(9):1523–34. Available from: http://jem.rupress.org/content/186/9/1523.long

143. Tominaga N, Ohkusu-Tsukada K, Udono H, Abe R, Matsuyama T, Yui K. Development of Th1 and not Th2 immune responses in mice lacking IFN-regulatory factor-4. Int Immunol [Internet]. 2003 Jan [cited 2015 May 4];15(1):1–10. Available from: http://www.ncbi.nlm.nih.gov/pubmed/12502720

144. Rengarajan J. Interferon Regulatory Factor 4 (IRF4) Interacts with NFATc2 to Modulate Interleukin 4 Gene Expression. J Exp Med [Internet]. 2002 Apr 8 [cited 2014 Dec 29];195(8):1003–12. Available from: http://jem.rupress.org/content/195/8/1003.long

145. Hu C-M, Jang SY, Fanzo JC, Pernis AB. Modulation of T cell cytokine production by interferon regulatory factor-4. J Biol Chem [Internet]. 2002 Dec 20 [cited 2015 Feb 24];277(51):49238–46. Available from: http://www.ncbi.nlm.nih.gov/pubmed/12374808

146. Lohoff M, Mittrücker H-W, Prechtl S, Bischof S, Sommer F, Kock S, et al.

Dysregulated T helper cell differentiation in the absence of interferon regulatory factor 4. Proc Natl Acad Sci U S A [Internet]. 2002 Sep 3 [cited 2015 May 4];99(18):11808–12. Available from: http://www.pubmedcentral.nih.gov/articlerender.fcgi?artid=129350&tool=pmc entrez&rendertype=abstract

147. Honma K, Kimura D, Tominaga N, Miyakoda M, Matsuyama T, Yui K. Interferon regulatory factor 4 differentially regulates the production of Th2 cytokines in naive vs. effector/memory CD4+ T cells. Proc Natl Acad Sci U S A [Internet]. 2008 Oct 14 [cited 2015 Feb 24];105(41):15890–5. Available from: http://www.pnas.org/content/105/41/15890.full

148. Ryzhakov G, Eames HL, Udalova IA. Activation and function of interferon regulatory factor 5. J Interferon Cytokine Res [Internet]. 2015 Feb [cited 2016 Jun 10];35(2):71–8. Available from: http://www.ncbi.nlm.nih.gov/pubmed/25259415

149. Takaoka A, Yanai H, Kondo S, Duncan G, Negishi H, Mizutani T, et al. Integral role of IRF-5 in the gene induction programme activated by Toll-like receptors. Nature [Internet]. 2005 Mar 10 [cited 2015 Mar 30];434(7030):243–9. Available from: http://www.ncbi.nlm.nih.gov/pubmed/15665823

150. Li D, De S, Li D, Song S, Matta B, Barnes BJ. Specific detection of interferon regulatory factor 5 (IRF5): A case of antibody inequality. Sci Rep [Internet]. 2016 [cited 2016 Oct 2];6:31002. Available from: http://www.ncbi.nlm.nih.gov/pubmed/27481535

151. Barnes BJ, Kellum MJ, Pinder KE, Frisancho JA, Pitha PM. Interferon regulatory factor 5, a novel mediator of cell cycle arrest and cell death. Cancer Res [Internet]. 2003 Oct 1 [cited 2016 Jun 10];63(19):6424–31. Available from: http://www.ncbi.nlm.nih.gov/pubmed/14559832

152. Yamashita M, Toyota M, Suzuki H, Nojima M, Yamamoto E, Kamimae S, et al. DNA methylation of interferon regulatory factors in gastric cancer and noncancerous gastric mucosae. Cancer Sci [Internet]. 2010 Jul [cited 2016 Jun 10];101(7):1708–16. Available from: http://www.ncbi.nlm.nih.gov/pubmed/20507321

153. Li Q, Tainsky MA. Epigenetic Silencing of IRF7 and/or IRF5 in Lung Cancer Cells Leads to Increased Sensitivity to Oncolytic Viruses. Katoh M, editor. PLoS One [Internet]. 2011 Dec 14 [cited 2016 Jun 10];6(12):e28683. Available from: http://dx.plos.org/10.1371/journal.pone.0028683

154. Clark DN, Read RD, Mayhew V, Petersen SC, Argueta LB, Stutz LA, et al. Four Promoters of IRF5 Respond Distinctly to Stimuli and are Affected by Autoimmune-Risk Polymorphisms. Front Immunol [Internet]. 2013 [cited 2016 Jun 10];4:360. Available from: http://www.ncbi.nlm.nih.gov/pubmed/24223576

155. Wen F, Ellingson SM, Kyogoku C, Peterson EJ, Gaffney PM. Exon 6 variants carried on systemic lupus erythematosus (SLE) risk haplotypes modulate IRF5 function. Autoimmunity [Internet]. 2011 Mar [cited 2016 Oct 25];44(2):82–9. Available from: http://www.ncbi.nlm.nih.gov/pubmed/20695768

156. Lazzari E, Korczeniewska J, Ní Gabhann J, Smith S, Barnes BJ, Jefferies CA.

TRIpartite motif 21 (TRIM21) differentially regulates the stability of interferon regulatory factor 5 (IRF5) isoforms. PLoS One [Internet]. 2014 [cited 2016 Oct 2];9(8):e103609. Available from: http://www.ncbi.nlm.nih.gov/pubmed/25084355

157. Clark DN, Lambert JP, Till RE, Argueta LB, Greenhalgh KE, Henrie B, et al. Molecular Effects of Autoimmune-Risk Promoter Polymorphisms on Expression, Exon Choice, and Translational Efficiency of Interferon Regulatory Factor 5. J Interf Cytokine Res [Internet]. 2014 May [cited 2016 Oct 5];34(5):354–65. Available from: http://online.liebertpub.com/doi/abs/10.1089/jir.2012.0105

158. Kristjansdottir G, Sandling JK, Bonetti A, Roos IM, Milani L, Wang C, et al. Interferon regulatory factor 5 (IRF5) gene variants are associated with multiple sclerosis in three distinct populations. J Med Genet [Internet]. 2008 Jun [cited 2016 Oct 25];45(6):362–9. Available from: http://www.ncbi.nlm.nih.gov/pubmed/18285424

159. Carmona FD, Martin J-E, Beretta L, Simeón CP, Carreira PE, Callejas JL, et al. The Systemic Lupus Erythematosus IRF5 Risk Haplotype Is Associated with Systemic Sclerosis. Kuwana M, editor. PLoS One [Internet]. 2013 Jan 23 [cited 2016 Oct 25];8(1):e54419. Available from: http://dx.plos.org/10.1371/journal.pone.0054419

160. Miceli-Richard C, Gestermann N, Ittah M, Comets E, Loiseau P, Puechal X, et al. The CGGGG insertion/deletion polymorphism of the IRF5 promoter is a strong risk factor for primary Sjögren's syndrome. Arthritis Rheum [Internet]. 2009 Jul [cited 2016 Oct 25];60(7):1991–7. Available from: http://www.ncbi.nlm.nih.gov/pubmed/19565491

161. Sigurdsson S, Nordmark G, Göring HHH, Lindroos K, Wiman A-C, Sturfelt G, et al. Polymorphisms in the tyrosine kinase 2 and interferon regulatory factor 5 genes are associated with systemic lupus erythematosus. Am J Hum Genet [Internet]. 2005 Mar [cited 2016 Jul 18];76(3):528–37. Available from: http://www.ncbi.nlm.nih.gov/pubmed/15657875

162. Graham RR, Kozyrev S V, Baechler EC, Reddy MVPL, Plenge RM, Bauer JW, et al. A common haplotype of interferon regulatory factor 5 (IRF5) regulates splicing and expression and is associated with increased risk of systemic lupus erythematosus. Nat Genet [Internet]. 2006 May 16 [cited 2016 Oct 25];38(5):550–5. Available from: http://www.nature.com/doifinder/10.1038/ng1782

163. Alonso-Perez E, Suarez-Gestal M, Calaza M, Kwan T, Majewski J, Gomez-Reino JJ, et al. Cis-regulation of IRF5 expression is unable to fully account for systemic lupus erythematosus association: analysis of multiple experiments with lymphoblastoid cell lines. Arthritis Res Ther [Internet]. 2011 May 31 [cited 2016 Oct 25];13(3):R80. Available from: http://www.ncbi.nlm.nih.gov/pubmed/21627826

164. Sigurdsson S, Göring HHH, Kristjansdottir G, Milani L, Nordmark G, Sandling JK, et al. Comprehensive evaluation of the genetic variants of interferon regulatory factor 5 (IRF5) reveals a novel 5 bp length polymorphism as strong

risk factor for systemic lupus erythematosus. Hum Mol Genet [Internet]. 2008 Mar 15 [cited 2016 Oct 25];17(6):872–81. Available from: http://www.ncbi.nlm.nih.gov/pubmed/18063667

165. Rullo OJ, Woo JMP, Wu H, Hoftman ADC, Maranian P, Brahn BA, et al. Association of IRF5 polymorphisms with activation of the interferon alpha pathway. Ann Rheum Dis [Internet]. 2010 Mar [cited 2016 Oct 12];69(3):611–7. Available from: http://www.ncbi.nlm.nih.gov/pubmed/19854706

166. Stone RC, Du P, Feng D, Dhawan K, Rönnblom L, Eloranta M-L, et al. RNA-Seq for Enrichment and Analysis of IRF5 Transcript Expression in SLE. Tsokos GC, editor. PLoS One [Internet]. 2013 Jan 18 [cited 2016 Oct 25];8(1):e54487. Available from: http://dx.plos.org/10.1371/journal.pone.0054487

167. Feng D, Stone RC, Eloranta M-L, Sangster-Guity N, Nordmark G, Sigurdsson S, et al. Genetic variants and disease-associated factors contribute to enhanced interferon regulatory factor 5 expression in blood cells of patients with systemic lupus erythematosus. Arthritis Rheum [Internet]. 2010 Feb [cited 2016 Oct 25];62(2):562–73. Available from: http://www.ncbi.nlm.nih.gov/pubmed/20112383

168. Cunninghame Graham DS, Manku H, Wagner S, Reid J, Timms K, Gutin A, et al. Association of IRF5 in UK SLE families identifies a variant involved in polyadenylation. Hum Mol Genet [Internet]. 2007 Mar 15 [cited 2016 Oct 25];16(6):579–91. Available from: http://www.ncbi.nlm.nih.gov/pubmed/17189288

169. Niewold TB, Kelly JA, Flesch MH, Espinoza LR, Harley JB, Crow MK. Association of the IRF5 risk haplotype with high serum interferon-alpha activity in systemic lupus erythematosus patients. Arthritis Rheum [Internet]. 2008 Aug [cited 2017 Mar 23];58(8):2481–7. Available from: http://www.ncbi.nlm.nih.gov/pubmed/18668568

170. Lazzari E, Jefferies CA. IRF5-mediated signaling and implications for SLE. Clin Immunol [Internet]. 2014 Aug [cited 2015 Jun 17];153(2):343–52. Available from: http://www.sciencedirect.com/science/article/pii/S152166161400148X

171. Xu W-D, Pan H-F, Xu Y, Ye D-Q. Interferon regulatory factor 5 and autoimmune lupus. Expert Rev Mol Med [Internet]. 2013 Jan 24 [cited 2019 May 22];15:e6. Available from: http://www.journals.cambridge.org/abstract_S1462399413000070

172. Korczeniewska J, Barnes BJ. Corrected and Republished from: The COP9 Signalosome Interacts with and Regulates Interferon Regulatory Factor 5 Protein Stability. Mol Cell Biol [Internet]. 2018 Jan 16 [cited 2021 May 19];38(3). Available from: /pmc/articles/PMC5770539/

173. Chen W, Lam SS, Srinath H, Jiang Z, Correia JJ, Schiffer CA, et al. Insights into interferon regulatory factor activation from the crystal structure of dimeric IRF5. Nat Struct Mol Biol [Internet]. 2008 Nov [cited 2016 Oct 25];15(11):1213–20. Available from: http://www.ncbi.nlm.nih.gov/pubmed/18836453

174. Balkhi MY, Fitzgerald KA, Pitha PM. IKKα negatively regulates IRF-5 function in a MyD88–TRAF6 pathway. Cell Signal. 2010;22(1):117–27.

175. Feng D, Sangster-Guity N, Stone R, Korczeniewska J, Mancl ME, Fitzgerald-Bocarsly P, et al. Differential requirement of histone acetylase and deacetylase activities for IRF5-mediated proinflammatory cytokine expression. J Immunol [Internet]. 2010 Nov 15 [cited 2016 Oct 25];185(10):6003–12. Available from: http://www.ncbi.nlm.nih.gov/pubmed/20935208

176. Eames HL, Saliba DG, Krausgruber T, Lanfrancotti A, Ryzhakov G, Udalova IA. KAP1/TRIM28: an inhibitor of IRF5 function in inflammatory macrophages. Immunobiology [Internet]. 2012 Dec [cited 2016 Oct 25];217(12):1315–24. Available from: http://www.ncbi.nlm.nih.gov/pubmed/22995936

177. Chang Foreman H-C, Van Scoy S, Cheng TT-F, Reich NNC, Sigurdsson S, Nordmark G, et al. Activation of interferon regulatory factor 5 by site specific phosphorylation. Mossman KL, editor. PLoS One [Internet]. 2012 Jan 8 [cited 2015 May 12];7(3):e33098. Available from: http://journals.plos.org/plosone/article?id=10.1371/journal.pone.0033098

178. Ren J, Chen X, Chen ZJ. IKKβ is an IRF5 kinase that instigates inflammation. Proc Natl Acad Sci U S A [Internet]. 2014 Dec 9 [cited 2015 May 13];111(49):17438–43. Available from: http://www.ncbi.nlm.nih.gov/pubmed/25326420

179. Lopez-Pelaez M, Lamont DJ, Peggie M, Shpiro N, Gray NS, Cohen P. Protein kinase IKKβ-catalyzed phosphorylation of IRF5 at Ser462 induces its dimerization and nuclear translocation in myeloid cells. Proc Natl Acad Sci [Internet]. 2014 Dec 9 [cited 2016 Jul 17];111(49):17432–7. Available from: http://www.pnas.org/lookup/doi/10.1073/pnas.1418399111

180. Ouyang X, Negishi H, Takeda R, Fujita Y, Taniguchi T, Honda K. Cooperation between MyD88 and TRIF pathways in TLR synergy via IRF5 activation. Biochem Biophys Res Commun. 2007;354(4):1045–51.

181. Schoenemeyer A, Barnes BJ, Mancl ME, Latz E, Goutagny N, Pitha PM, et al. The Interferon Regulatory Factor, IRF5, Is a Central Mediator of Toll-like Receptor 7 Signaling. J Biol Chem [Internet]. 2005 Apr 29 [cited 2016 Jul 18];280(17):17005–12. Available from: http://www.jbc.org/cgi/doi/10.1074/jbc.M412584200

182. Pandey AK, Yang Y, Jiang Z, Fortune SM, Coulombe F, Behr MA, et al. NOD2, RIP2 and IRF5 Play a Critical Role in the Type I Interferon Response to Mycobacterium tuberculosis. Cossart P, editor. PLoS Pathog [Internet]. 2009 Jul 3 [cited 2016 Jul 17];5(7):e1000500. Available from: http://dx.plos.org/10.1371/journal.ppat.1000500

183. Cushing L, Winkler A, Jelinsky SA, Lee K, Korver W, Hawtin R, et al. IRAK4 kinase activity controls Toll-like receptor-induced inflammation through the transcription factor IRF5 in primary human monocytes. J Biol Chem [Internet]. 2017 Sep 10 [cited 2018 Mar 21];292(45):18689–98. Available from: http://www.ncbi.nlm.nih.gov/pubmed/28924041

184. Lazear HM, Lancaster A, Wilkins C, Suthar MS, Huang A, Vick SC, et al.

IRF-3, IRF-5, and IRF-7 Coordinately Regulate the Type I IFN Response in Myeloid Dendritic Cells Downstream of MAVS Signaling. Basler CF, editor. PLoS Pathog [Internet]. 2013 Jan 3 [cited 2016 Jun 10];9(1):e1003118. Available from: http://dx.plos.org/10.1371/journal.ppat.1003118

185. del Fresno C, Soulat D, Roth S, Blazek K, Udalova I, Sancho D, et al. Interferon-β Production via Dectin-1-Syk-IRF5 Signaling in Dendritic Cells Is Crucial for Immunity to C. albicans. Immunity. 2013;38(6):1176–86.

186. Freitas CMT, Hamblin GJ, Raymond CM, Weber KS. Naïve helper T cells with high CD5 expression have increased calcium signaling. Houtman JCD, editor. PLoS One [Internet]. 2017 May 31 [cited 2018 Mar 13];12(5):e0178799. Available from: http://dx.plos.org/10.1371/journal.pone.0178799

187. Yang L, Zhao T, Shi X, Nakhaei P, Wang Y, Sun Q, et al. Functional analysis of a dominant negative mutation of interferon regulatory factor 5. PLoS One [Internet]. 2009 [cited 2016 Oct 25];4(5):e5500. Available from: http://www.ncbi.nlm.nih.gov/pubmed/19430534

188. Richez C, Yasuda K, Bonegio RG, Watkins AA, Aprahamian T, Busto P, et al. IFN regulatory factor 5 is required for disease development in the FcgammaRIIB-/-Yaa and FcgammaRIIB-/- mouse models of systemic lupus erythematosus. J Immunol [Internet]. 2010 Jan 15 [cited 2016 Jul 18];184(2):796–806. Available from: http://www.ncbi.nlm.nih.gov/pubmed/20007534

189. Yasuda K, Watkins AA, Kochar GS, Wilson GE, Laskow B, Richez C, et al. Interferon regulatory factor-5 deficiency ameliorates disease severity in the MRL/lpr mouse model of lupus in the absence of a mutation in DOCK2. PLoS One [Internet]. 2014 Jan [cited 2015 Jun 17];9(7):e103478. Available from: http://www.pubmedcentral.nih.gov/articlerender.fcgi?artid=4116215&tool=pmcentrez&rendertype=abstract

190. Fang C-M, Roy S, Nielsen E, Paul M, Maul R, Paun A, et al. Unique contribution of IRF-5-Ikaros axis to the B-cell IgG2a response. Genes Immun [Internet]. 2012 Jul [cited 2015 Feb 24];13(5):421–30. Available from: http://dx.doi.org/10.1038/gene.2012.10

191. Krausgruber T, Blazek K, Smallie T, Alzabin S, Lockstone H, Sahgal N, et al. IRF5 promotes inflammatory macrophage polarization and TH1-TH17 responses. Nat Immunol [Internet]. 2011 Mar [cited 2016 Jun 10];12(3):231–8. Available from: http://www.ncbi.nlm.nih.gov/pubmed/21240265

192. Weiss M, Byrne AJ, Blazek K, Saliba DG, Pease JE, Perocheau D, et al. IRF5 controls both acute and chronic inflammation. Proc Natl Acad Sci U S A [Internet]. 2015 Sep 1 [cited 2016 Jun 10];112(35):11001–6. Available from: http://www.ncbi.nlm.nih.gov/pubmed/26283380

193. Oriss TB, Raundhal M, Morse C, Huff RE, Das S, Hannum R, et al. IRF5 distinguishes severe asthma in humans and drives Th1 phenotype and airway hyperreactivity in mice. JCI Insight [Internet]. 2017 May 18 [cited 2018 Mar 21];2(10). Available from: https://insight.jci.org/articles/view/91019

194. Jourdan T, Szanda G, Cinar R, Godlewski G, Holovac DJ, Park JK, et al.

Developmental Role of Macrophage Cannabinoid-1 Receptor Signaling in Type 2 Diabetes. Diabetes [Internet]. 2017 Apr [cited 2018 Mar 21];66(4):994–1007. Available from: http://www.ncbi.nlm.nih.gov/pubmed/28082458

195. Dalmas E, Toubal A, Alzaid F, Blazek K, Eames HL, Lebozec K, et al. Irf5 deficiency in macrophages promotes beneficial adipose tissue expansion and insulin sensitivity during obesity. Nat Med [Internet]. 2015 Jun [cited 2016 Jun 10];21(6):610–8. Available from: http://www.ncbi.nlm.nih.gov/pubmed/25939064

196. Alzaid F, Lagadec F, Albuquerque M, Ballaire R, Orliaguet L, Hainault I, et al. IRF5 governs liver macrophage activation that promotes hepatic fibrosis in mice and humans. JCI insight [Internet]. 2016 Dec 8 [cited 2018 Mar 21];1(20):e88689. Available from: http://www.ncbi.nlm.nih.gov/pubmed/27942586

197. Feng D, Yang L, Bi X, Stone RC, Patel P, Barnes BJ. Irf5-deficient mice are protected from pristane-induced lupus via increased Th2 cytokines and altered IgG class switching. Eur J Immunol [Internet]. 2012 Jun [cited 2016 Jun 10];42(6):1477–87. Available from: http://www.ncbi.nlm.nih.gov/pubmed/22678902

198. Kaufman RJ. Overview of Vector Design for Mammalian Gene Expression. Mol Biotechnol [Internet]. 2000 [cited 2020 Mar 1];16(2):151–60. Available from: http://link.springer.com/10.1385/MB:16:2:151

199. Twyman R. Gene Transfer to Animal Cells [Internet]. Taylor & Francis; 2004. (Advanced Methods). Available from: https://books.google.com.my/books?id=fSVQZUA9fwcC

200. Nayerossadat N, Maedeh T, Ali PA. Viral and nonviral delivery systems for gene delivery. Adv Biomed Res [Internet]. 2012 [cited 2020 Feb 26];1:27. Available from: http://www.ncbi.nlm.nih.gov/pubmed/23210086

201. Pereyra A, Hereñu C. Gene Delivery Systems. In: Romanowski V, editor. Current Issues in Molecular Virology [Internet]. Rijeka: IntechOpen; 2013. Available from: https://doi.org/10.5772/56869

202. Cevher E. Gene Delivery Systems: Recent Progress in Viral and Non-Viral Therapy. In: Sezer AD, editor. Rijeka: IntechOpen; 2012. p. Ch. 16. Available from: https://doi.org/10.5772/53392

203. Prelich G. Gene Overexpression: Uses, Mechanisms, and Interpretation. Genetics [Internet]. 2012 Mar 14 [cited 2020 Mar 17];190(3):841–54. Available from: http://www.ncbi.nlm.nih.gov/pubmed/22419077

204. Al-Hejin A, Bora R, Ahmed M. Plasmids for Optimizing Expression of Recombinant Proteins in E. coli. In 2019.

205. Doghaither H Al, Gull M. Plasmids as Genetic Tools and Their Applications in Ecology and Evolution. In: Gull M, editor. Plasmid [Internet]. Rijeka: IntechOpen; 2019. Available from: https://doi.org/10.5772/intechopen.85705

206. Keeney JB. Microorganisms: Applications in Molecular Biology. In: Encyclopedia of Life Sciences [Internet]. Chichester, UK: John Wiley & Sons, Ltd; 2007 [cited 2020 Feb 26]. Available from: http://doi.wiley.com/10.1002/9780470015902.a0000971.pub2

207. Carson S, Miller HB, Witherow DS, Carson S, Miller HB, Witherow DS. Purification and Digestion of Plasmid (Vector) DNA. In: Molecular Biology Techniques [Internet]. Academic Press; 2012 [cited 2020 Mar 1]. p. 11–20. Available from: https://www.sciencedirect.com/science/article/pii/B9780123855442000028

208. Carter M, Shieh J, Carter M, Shieh J. Molecular Cloning and Recombinant DNA Technology. In: Guide to Research Techniques in Neuroscience [Internet]. Academic Press; 2015 [cited 2020 Mar 1]. p. 219–37. Available from: https://www.sciencedirect.com/science/article/pii/B9780128005118000101

209. Idalia V-MN, Bernardo F. *Escherichia coli* as a Model Organism and Its Application in Biotechnology. In: Samie A, editor. *Escherichia coli* [Internet]. Rijeka: IntechOpen; 2017. Available from: https://doi.org/10.5772/67306

210. Wrenbeck EE, Klesmith JR, Stapleton JA, Adeniran A, Tyo KEJ, Whitehead TA. Plasmid-based one-pot saturation mutagenesis. Nat Methods [Internet]. 2016 Nov 10 [cited 2020 Feb 26];13(11):928–30. Available from: http://www.nature.com/articles/nmeth.4029

211. Nora LC, Westmann CA, Martins-Santana L, Alves L de F, Monteiro LMO, Guazzaroni M-E, et al. The art of vector engineering: towards the construction of next-generation genetic tools. Microb Biotechnol [Internet]. 2019 Jan [cited 2020 Feb 26];12(1):125–47. Available from: http://www.ncbi.nlm.nih.gov/pubmed/30259693

212. Hunter M, Yuan P, Vavilala D, Fox M. Optimization of Protein Expression in Mammalian Cells. Curr Protoc Protein Sci [Internet]. 2019 Feb 1 [cited 2020 Mar 1];95(1):e77. Available from: http://doi.wiley.com/10.1002/cpps.77

213. Julin D. Plasmid Cloning Vectors. In: Molecular Life Sciences [Internet]. New York, NY: Springer New York; 2014 [cited 2020 Feb 26]. p. 1–12. Available from: http://link.springer.com/10.1007/978-1-4614-6436-5_86-1

214. Khan KH. Gene expression in Mammalian cells and its applications. Adv Pharm Bull [Internet]. 2013 [cited 2020 Mar 1];3(2):257–63. Available from: http://www.ncbi.nlm.nih.gov/pubmed/24312845

215. Milone MC, O'Doherty U. Clinical use of lentiviral vectors. Leukemia [Internet]. 2018 Jul 22 [cited 2019 Dec 1];32(7):1529–41. Available from: http://www.nature.com/articles/s41375-018-0106-0

216. MJ B, FP M. Lentivirus Production and Purification. Methods Mol Biol [Internet]. 2016 [cited 2019 Dec 3];1382. Available from: https://pubmed.ncbi.nlm.nih.gov/26611582-lentivirus-production-and-purification/

217. Dull T, Zufferey R, Kelly M, Mandel RJ, Nguyen M, Trono D, et al. A third-generation lentivirus vector with a conditional packaging system. J Virol [Internet]. 1998 Nov [cited 2019 Dec 3];72(11):8463–71. Available from: http://www.ncbi.nlm.nih.gov/pubmed/9765382

218. Chang L-J, Zaiss A-K. Lentiviral Vectors: Preparation and Use. In: Gene Therapy Protocols [Internet]. New Jersey: Humana Press; 2002 [cited 2019 Dec 3]. p. 303–18. Available from: http://link.springer.com/10.1385/1-59259-

141-8:303

219. Rodrigues A. Production of Retroviral and Lentiviral Gene Therapy Vectors: Challenges in the Manufacturing of Lipid Enveloped Virus. In: Alves PM, editor. Rijeka: IntechOpen; 2011. p. Ch. 2. Available from: https://doi.org/10.5772/18615

220. Delenda C. Lentiviral vectors: optimization of packaging, transduction and gene expression. J Gene Med [Internet]. 2004 Feb [cited 2019 Dec 3];6 Suppl 1:S125-38. Available from: http://www.ncbi.nlm.nih.gov/pubmed/14978756

221. Durand S, Cimarelli A. The inside out of lentiviral vectors. Viruses [Internet]. 2011 Feb [cited 2019 Dec 1];3(2):132–59. Available from: http://www.ncbi.nlm.nih.gov/pubmed/22049307

222. Bryson PD, Wang P. Lentivector Vaccines. Gene Ther Cancer [Internet]. 2014 Jan 1 [cited 2019 Dec 1];345–61. Available from: https://www.sciencedirect.com/science/article/pii/B978012394295100024X

223. Graham FL, Smiley J, Russell WC, Nairn R. Characteristics of a Human Cell Line Transformed by DNA from Human Adenovirus Type 5. J Gen Virol [Internet]. 1977 Jul 1 [cited 2015 May 4];36(1):59–72. Available from: http://www.ncbi.nlm.nih.gov/pubmed/886304

224. DuBridge RB, Tang P, Hsia HC, Leong PM, Miller JH, Calos MP. Analysis of mutation in human cells by using an Epstein-Barr virus shuttle system. Mol Cell Biol [Internet]. 1987 Jan [cited 2015 Oct 1];7(1):379–87. Available from: http://www.pubmedcentral.nih.gov/articlerender.fcgi?artid=365079&tool=pmcentrez&rendertype=abstract

225. Ramezani A, Hawley RG. Generation of HIV-1-based lentiviral vector particles. Curr Protoc Mol Biol [Internet]. 2002 Nov [cited 2015 Jul 7];Chapter 16:Unit 16.22. Available from: http://www.ncbi.nlm.nih.gov/pubmed/18265303

226. Lin YC, Boone M, Meuris L, Lemmens I, Van Roy N, Soete A, et al. Genome dynamics of the human embryonic kidney 293 lineage in response to cell biology manipulations. Nat Commun [Internet]. 2014 Sep 3 [cited 2020 Aug 10];5(1):12. Available from: www.nature.com/naturecommunications

227. Thomas P, Smart TG. HEK293 cell line: A vehicle for the expression of recombinant proteins. J Pharmacol Toxicol Methods. 2005 May 1;51(3 SPEC. ISS.):187–200.

228. Ooi A, Wong A, Esau L, Lemtiri-Chlieh F, Gehring C. A guide to transient expression of membrane proteins in HEK-293 cells for functional characterization. Front Physiol [Internet]. 2016 Jul 19 [cited 2020 Aug 10];7(JUL). Available from: https://pubmed.ncbi.nlm.nih.gov/27486406/

229. Schneider U, Schwenk H -U, Bornkamm G. Characterization of EBV-genome negative "null" and "T" cell lines derived from children with acute lymphoblastic leukemia and leukemic transformed non-Hodgkin lymphoma. Int J Cancer. 1977;19(5).

230. Abraham RT, Weiss A. Jurkat T cells and development of the T-cell receptor signalling paradigm. Nat Rev Immunol [Internet]. 2004 Apr [cited 2015 Oct

1];4(4):301–8. Available from: http://www.nature.com/articles/nri1330

231. Lawrence CP, Chow SC. FADD deficiency sensitises Jurkat T cells to TNF-α-dependent necrosis during activation-induced cell death. FEBS Lett. 2005 Nov 21;579(28):6465–72.

232. Lhuillier C, Barjon C, Niki T, Gelin A, Praz F, Morales O, et al. Impact of Exogenous Galectin-9 on Human T Cells: CONTRIBUTION OF THE T CELL RECEPTOR COMPLEX TO ANTIGEN-INDEPENDENT ACTIVATION BUT NOT TO APOPTOSIS INDUCTION. J Biol Chem [Internet]. 2015 Jul 3 [cited 2016 Dec 21];290(27):16797–811. Available from: http://www.ncbi.nlm.nih.gov/pubmed/25947381

233. Takeuchi Y, McClure MO, Pizzato M. Identification of Gammaretroviruses Constitutively Released from Cell Lines Used for Human Immunodeficiency Virus Research. J Virol [Internet]. 2008 Dec 15 [cited 2021 May 18];82(24):12585–8. Available from: /pmc/articles/PMC2593302/

234. Bartelt RR, Cruz-Orcutt N, Collins M, Houtman JCD. Comparison of T cell receptor-induced proximal signaling and downstream functions in immortalized and primary T cells. PLoS One [Internet]. 2009 May 4 [cited 2020 Oct 6];4(5). Available from: /pmc/articles/PMC2673025/?report=abstract

235. Fonseca FN, Papanicolaou G, Lin H, Lau CBS, Kennelly EJ, Cassileth BR, et al. Echinacea purpurea (L.) Moench modulates human T-cell cytokine response. Int Immunopharmacol [Internet]. 2014 Mar [cited 2020 Oct 23];19(1):94–102. Available from: /pmc/articles/PMC4140398/?report=abstract

236. Gholijani N, Gharagozloo M, Kalantar F, Ramezani A, Amirghofran Z. Modulation of Cytokine Production and Transcription Factors Activities in Human Jurkat T Cells by Thymol and Carvacrol. Adv Pharm Bull [Internet]. 2015 Dec [cited 2017 Dec 4];5(Suppl 1):653–60. Available from: http://www.ncbi.nlm.nih.gov/pubmed/26793612

237. Aherne SA, O'Brien NM. Modulation of cytokine production by plant sterols in stimulated human Jurkat T cells. Mol Nutr Food Res [Internet]. 2008 Jun [cited 2017 Dec 7];52(6):664–73. Available from: http://www.ncbi.nlm.nih.gov/pubmed/18465778

238. Smeets RL, Fleuren WWM, He X, Vink PM, Wijnands F, Gorecka M, et al. Molecular pathway profiling of T lymphocyte signal transduction pathways; Th1 and Th2 genomic fingerprints are defined by TCR and CD28-mediated signaling. BMC Immunol [Internet]. 2012 [cited 2020 Oct 23];13:12. Available from: /pmc/articles/PMC3355027/?report=abstract

239. Pan Y, Wei X, Hao W. Trichloroethylene and Its Oxidative Metabolites Enhance the Activated State and Th1 Cytokine Gene Expression in Jurkat Cells. Int J Environ Res Public Health [Internet]. 2015 Aug 28 [cited 2017 Dec 4];12(9):10575–86. Available from: http://www.ncbi.nlm.nih.gov/pubmed/26343699

240. Verlengia R, Gorjão R, Kanunfre CC, Bordin S, Martins De Lima T, Martins EF, et al. Comparative effects of eicosapentaenoic acid and docosahexaenoic acid on proliferation, cytokine production, and pleiotropic gene expression in

Jurkat cells. J Nutr Biochem [Internet]. 2004 Nov [cited 2015 Jan 12];15(11):657–65. Available from: http://www.sciencedirect.com/science/article/pii/S0955286304001202

241. Houng J-Y, Tai T-S, Hsu S-C, Hsu H-F, Hwang T-S, Lin C-J, et al. Glossogyne tenuifolia (Hsiang-ju) extract suppresses T cell activation by inhibiting activation of c-Jun N-terminal kinase. Chin Med [Internet]. 2017 [cited 2017 Dec 4];12:9. Available from: http://www.ncbi.nlm.nih.gov/pubmed/28400856

242. Li J, Tu Y, Tong L, Zhang W, Zheng J, Wei Q. Immunosuppressive activity on the murine immune responses of glycyrol from *Glycyrrhiza uralensis* via inhibition of calcineurin activity. Pharm Biol [Internet]. 2010 Oct 16 [cited 2020 Oct 23];48(10):1177–84. Available from: http://www.tandfonline.com/doi/full/10.3109/13880200903573169

243. Levin R, Mhashilkar AM, Dorfman T, Bukovsky A, Zani C, Bagley J, et al. Inhibition of early and late events of the HIV-1 replication cycle by cytoplasmic Fab intrabodies against the matrix protein, p17. Mol Med [Internet]. 1997 Feb [cited 2015 Jul 5];3(2):96–110. Available from: http://www.pubmedcentral.nih.gov/articlerender.fcgi?artid=2230055&tool=pmcentrez&rendertype=abstract

244. Poznansky M, Lever A, Bergeron L, Haseltine W, Sodroski J. Gene transfer into human lymphocytes by a defective human immunodeficiency virus type 1 vector. J Virol [Internet]. 1991 Jan [cited 2015 Jul 5];65(1):532–6. Available from: http://www.pubmedcentral.nih.gov/articlerender.fcgi?artid=240552&tool=pmcentrez&rendertype=abstract

245. Nasri M, Karimi A, Allahbakhshian Farsani M. Production, purification and titration of a lentivirus-based vector for gene delivery purposes. Cytotechnology [Internet]. 2014 Dec [cited 2015 Feb 1];66(6):1031–8. Available from: http://www.ncbi.nlm.nih.gov/pubmed/24599752

246. Sambrook J, Russell DW. Molecular Cloning - Sambrook & Russel - Vol. 1, 2, 3. Cold Spring Harb Lab Press [Internet]. 2001;3th Editio. Available from: www.molecularcloning.com

247. Cribbs AP, Kennedy A, Gregory B, Brennan FM. Simplified production and concentration of lentiviral vectors to achieve high transduction in primary human T cells. BMC Biotechnol [Internet]. 2013 Jan 12 [cited 2015 May 21];13(1):98. Available from: https://bmcbiotechnol.biomedcentral.com/articles/10.1186/1472-6750-13-98

248. Wang D, Li G, Schauflinger M, Nguyen CC, Hall ED, Yurochko AD, et al. The ULb' region of the human cytomegalovirus genome confers an increased requirement for the viral protein kinase UL97. J Virol [Internet]. 2013 Jun 1 [cited 2015 Jul 6];87(11):6359–76. Available from: http://jvi.asm.org/content/87/11/6359#ref-list-1

249. O'Keefe EP. Nucleic Acid Delivery: Lentiviral and Retroviral Vectors. Mater Methods. 2013 Mar 22;3.

250. Derse D, Hill SA, Lloyd PA, Chung Hk, Morse BA. Examining human T-

lymphotropic virus type 1 infection and replication by cell-free infection with recombinant virus vectors. J Virol [Internet]. 2001 Sep [cited 2015 Jul 5];75(18):8461–8. Available from: http://www.pubmedcentral.nih.gov/articlerender.fcgi?artid=115091&tool=pmc entrez&rendertype=abstract

251. Lieber D. Generation of a Stable Cell Line for Constitutive miRNA Expression. In Humana Press, Totowa, NJ; 2013 [cited 2017 Dec 4]. p. 183–200. Available from: http://link.springer.com/10.1007/978-1-62703-601-6_13

252. Wang H, Cao F, Li X, Miao H, E J, Xing J, et al. miR-320b suppresses cell proliferation by targeting c-Myc in human colorectal cancer cells. BMC Cancer [Internet]. 2015 Oct 20 [cited 2020 Jul 9];15:748. Available from: http://www.ncbi.nlm.nih.gov/pubmed/26487644

253. Sgadari C, Angiolillo A, Tosato G. Inhibition of angiogenesis by interleukin-12 is mediated by the interferon-inducible protein 10. Blood [Internet]. 1996 May 1 [cited 2020 Jul 8];87(9):3877–82. Available from: https://ashpublications.org/blood/article/87/9/3877/124770/Inhibition-of-angiogenesis-by-interleukin12-is

254. Lorentz A, Schwengberg S, Sellge G, Manns MP, Bischoff SC. Human intestinal mast cells are capable of producing different cytokine profiles: role of IgE receptor cross-linking and IL-4. J Immunol [Internet]. 2000 Jan 1 [cited 2020 Jul 9];164(1):43–8. Available from: http://www.ncbi.nlm.nih.gov/pubmed/10604991

255. Ochensberger B, Daepp G, Rihs S, Dahinden C. Human blood basophils produce interleukin-13 in response to IgE- receptor-dependent and -independent activation. Blood [Internet]. 1996 Oct 15 [cited 2020 Jul 9];88(8):3028–37. Available from: https://ashpublications.org/blood/article/88/8/3028/125301/Human-blood-basophils-produce-interleukin13-in

256. Jutras BL, Verma A, Stevenson B. Identification of Novel DNA-Binding proteins Using DNA-Affinity Chromatography/Pull Down. Curr Protoc Microbiol [Internet]. 2012 Feb [cited 2020 Aug 18];CHAPTER(SUPPL.24):Unit1F.1. Available from: /pmc/articles/PMC3564586/?report=abstract

257. Chu C, Xin A, Zhou Y, Zhang Y. A simple protocol for producing high-titer lentivirus. Acta Biochim Biophys Sin (Shanghai) [Internet]. 2013 [cited 2020 Aug 18];45(12):1079–82. Available from: https://pubmed.ncbi.nlm.nih.gov/24113089/

258. Tang Y, Garson K, Li L, Vanderhyden BC. Optimization of lentiviral vector production using polyethylenimine-mediated transfection. Oncol Lett [Internet]. 2015 Jan 1 [cited 2020 Aug 18];9(1):55–62. Available from: https://pubmed.ncbi.nlm.nih.gov/25435933/

259. Ching Ngai S, Ramasamy R, Abdullah S. SCIENCE & TECHNOLOGY Production of Lentivirus Carrying Green fluorescent Protein with Different Promoters for in vitro Gene Transfermy (Syahril Abdullah) *Corresponding Author. Pertanika J Sci Technol [Internet]. 2012 [cited 2020 Aug

18];20(2):269–81. Available from: http://www.pertanika.upm.edu.my/

260. Khalil M, Gout I. Overexpression or downregulation of mTOR in mammalian cells. Methods Mol Biol [Internet]. 2012 [cited 2020 Aug 18];821:87–103. Available from: https://pubmed.ncbi.nlm.nih.gov/22125062/

261. Kutner RH, Zhang X-Y, Reiser J. Production, concentration and titration of pseudotyped HIV-1-based lentiviral vectors. Nat Protoc [Internet]. 2009 Jan [cited 2015 Jun 23];4(4):495–505. Available from: http://dx.doi.org/10.1038/nprot.2009.22

262. Klages N, Zufferey R, Trono D. A stable system for the high-titer production of multiply attenuated lentiviral vectors. Mol Ther [Internet]. 2000 Aug [cited 2015 Jul 5];2(2):170–6. Available from: http://www.ncbi.nlm.nih.gov/pubmed/10947945

263. Barde I, Salmon P, Trono D. Production and titration of lentiviral vectors. Curr Protoc Neurosci [Internet]. 2006 Nov [cited 2015 Jun 18];Chapter 4:Unit 4.21. Available from: http://www.ncbi.nlm.nih.gov/pubmed/18428637

264. Davis HE, Morgan JR, Yarmush ML. Polybrene increases retrovirus gene transfer efficiency by enhancing receptor-independent virus adsorption on target cell membranes. Biophys Chem [Internet]. 2002 Jun 19 [cited 2015 Jul 6];97(2–3):159–72. Available from: https://pubmed.ncbi.nlm.nih.gov/12050007/

265. Denning W, Das S, Guo S, Xu J, Kappes JC, Hel Z. Optimization of the transductional efficiency of lentiviral vectors: Effect of sera and polycations. Mol Biotechnol [Internet]. 2013 Mar [cited 2020 Aug 11];53(3):308–14. Available from: https://pubmed.ncbi.nlm.nih.gov/22407723/

266. Mora AL, Stephenson LM, Enerson B, Youn J, Keegan AD, Boothby M. New Programming of IL-4 Receptor Signal Transduction in Activated T Cells: Stat6 Induction and Th2 Differentiation Mediated by IL-4Rα Lacking Cytoplasmic Tyrosines. J Immunol [Internet]. 2003 Aug 15 [cited 2020 Aug 18];171(4):1891–900. Available from: http://www.jimmunol.org/content/171/4/1891http://www.jimmunol.org/content/171/4/1891.full#ref-list-1

267. Nencioni A, Hua F, Dillon CP, Yokoo R, Scheiermann C, Cardone MH, et al. Evidence for a protective role of Mcl-1 in proteasome inhibitor-induced apoptosis. Blood [Internet]. 2005 Apr 15 [cited 2020 Aug 18];105(8):3255–62. Available from: https://pubmed.ncbi.nlm.nih.gov/15613543/

268. Le Fourn V, Girod P-AA, Buceta M, Regamey A, Mermod N. CHO cell engineering to prevent polypeptide aggregation and improve therapeutic protein secretion. Metab Eng [Internet]. 2014 Jan [cited 2015 Jul 20];21:91–102. Available from: https://pubmed.ncbi.nlm.nih.gov/23380542/

269. Mamane Y, Grandvaux N, Hernandez E, Sharma S, Innocente SA, Lee JM, et al. Repression of IRF-4 target genes in human T cell leukemia virus-1 infection. Oncogene [Internet]. 2002 Oct 2 [cited 2020 Aug 18];21(44):6751–65. Available from: www.nature.com/onc

270. Favre N, Bordmann G, Rudin W. Comparison of cytokine measurements using ELISA, ELISPOT and semi-quantitative RT-PCR. J Immunol Methods

[Internet]. 1997 May 12 [cited 2020 Sep 30];204(1):57–66. Available from: https://pubmed.ncbi.nlm.nih.gov/9202710/

271. IOP Conference Series: Earth and Environmental Science.

272. Chwae Y-J, Chang MJ, Park SM, Yoon H, Park H-J, Kim SJ, et al. Molecular Mechanism of the Activation-Induced Cell Death Inhibition Mediated by a p70 Inhibitory Killer Cell Ig-Like Receptor in Jurkat T Cells. J Immunol [Internet]. 2002 Oct 1 [cited 2020 Oct 6];169(7):3726–35. Available from: https://pubmed.ncbi.nlm.nih.gov/12244166/

273. Doyle MC, Tremblay S, Dumais N. 15-Deoxy-Δ12,14-prostaglandin J2 inhibits IL-13 production in T cells via an NF-κB-dependent mechanism. Biochem Biophys Res Commun [Internet]. 2013 Feb 15 [cited 2020 Oct 22];431(3):472–7. Available from: https://pubmed.ncbi.nlm.nih.gov/23333326/

274. Rubenfeld J, Guo J, Sookrung N, Chen R, Chaicumpa W, Casolaro V, et al. Lysophosphatidic acid enhances interleukin-13 gene expression and promoter activity in T cells. Am J Physiol - Lung Cell Mol Physiol [Internet]. 2006 Jan [cited 2020 Oct 22];290(1):66–74. Available from: http://www.ajplung.orgl66

275. Treuter E, Fan R, Huang Z, Jakobsson T, Venteclef N. Transcriptional repression in macrophages-basic mechanisms and alterations in metabolic inflammatory diseases. FEBS Lett [Internet]. 2017 Oct 1 [cited 2019 Jun 2];591(19):2959–77. Available from: http://doi.wiley.com/10.1002/1873-3468.12850

276. Khoyratty TE, Udalova IA. Diverse mechanisms of IRF5 action in inflammatory responses. Int J Biochem Cell Biol [Internet]. 2018 Jun [cited 2019 May 24];99:38–42. Available from: http://www.ncbi.nlm.nih.gov/pubmed/29578052

277. Wu KK. Analysis of protein-DNA binding by streptavidin-agarose pulldown. Methods Mol Biol [Internet]. 2006 [cited 2020 Oct 23];338:281–90. Available from: https://pubmed.ncbi.nlm.nih.gov/16888365/

278. Kawai T, Akira S. Signaling to NF-κB by Toll-like receptors [Internet]. Vol. 13, Trends in Molecular Medicine. Elsevier; 2007 [cited 2020 Oct 21]. p. 460–9. Available from: www.sciencedirect.com

279. Pahl A, Zhang M, Kuss H, Szelenyi I, Brune K. Regulation of IL-13 synthesis in human lymphocytes: implications for asthma therapy. Br J Pharmacol [Internet]. 2002 Apr 1 [cited 2020 Oct 22];135(8):1915–26. Available from: http://doi.wiley.com/10.1038/sj.bjp.0704656

280. Ban T, Sato GR, Nishiyama A, Akiyama A, Takasuna M, Umehara M, et al. Lyn Kinase Suppresses the Transcriptional Activity of IRF5 in the TLR-MyD88 Pathway to Restrain the Development of Autoimmunity. Immunity [Internet]. 2016 Aug 16 [cited 2016 Oct 2];45(2):319–32. Available from: http://www.ncbi.nlm.nih.gov/pubmed/27521268

281. Gray P, Dagvadorj J, Michelsen KS, Brikos C, Rentsendorj A, Town T, et al. Myeloid Differentiation Factor-2 Interacts with Lyn Kinase and Is Tyrosine Phosphorylated Following Lipopolysaccharide-Induced Activation of the TLR4 Signaling Pathway. J Immunol [Internet]. 2011 Oct 15 [cited 2020 Oct 22];187(8):4331–7. Available from:

https://pubmed.ncbi.nlm.nih.gov/21918188/

282. Ni X, Ou C, Guo J, Liu B, Zhang J, Wu Z, et al. Lentiviral vector-mediated co-overexpression of VEGF and Bcl-2 improves mesenchymal stem cell survival and enhances paracrine effects in vitro. Int J Mol Med [Internet]. 2017 Aug 1 [cited 2020 Oct 6];40(2):418–26. Available from: http://www.spandidos-publications.com/10.3892/ijmm.2017.3019/abstract

283. Li L, Li B, Zhang H, Bai S, Wang Y, Zhao B, et al. Lentiviral vector-mediated PAX6 overexpression promotes growth and inhibits apoptosis of human retinoblastoma cells. Investig Ophthalmol Vis Sci. 2011 Oct 1;52(11):8393–400.

284. Campeau E, Ruhl VE, Rodier F, Smith CL, Rahmberg BL, Fuss JO, et al. A versatile viral system for expression and depletion of proteins in mammalian cells. PLoS One [Internet]. 2009 Jan [cited 2015 Jun 30];4(8):e6529. Available from: http://www.pubmedcentral.nih.gov/articlerender.fcgi?artid=2717805&tool=pmcentrez&rendertype=abstract

285. Merten OW, Hebben M, Bovolenta C. Production of lentiviral vectors [Internet]. Vol. 3, Molecular Therapy - Methods and Clinical Development. Elsevier Inc; 2016 [cited 2020 Oct 22]. p. 16017. Available from: www.nature.com/mtm

286. Bolton DL, Hahn B-I, Park EA, Lehnhoff LL, Hornung F, Lenardo MJ. Death of CD4(+) T-cell lines caused by human immunodeficiency virus type 1 does not depend on caspases or apoptosis. J Virol [Internet]. 2002 May [cited 2015 Jun 15];76(10):5094–107. Available from: http://www.pubmedcentral.nih.gov/articlerender.fcgi?artid=136143&tool=pmcentrez&rendertype=abstract

287. O'Doherty U, Swiggard WJ, Malim MH. Human immunodeficiency virus type 1 spinoculation enhances infection through virus binding. J Virol [Internet]. 2000 Nov [cited 2015 Jul 4];74(21):10074–80. Available from: http://www.pubmedcentral.nih.gov/articlerender.fcgi?artid=102046&tool=pmcentrez&rendertype=abstract

288. Geering B, Schmidt-Mende J, Federzoni E, Stoeckle C, Simon HU. Protein overexpression following lentiviral infection of primary mature neutrophils is due to pseudotransduction. J Immunol Methods. 2011 Oct 28;373(1–2):209–18.

289. de la Luna S, Ortín J. pac gene as efficient dominant marker and reporter gene in mammalian cells. Methods Enzymol [Internet]. 1992 [cited 2017 Dec 7];216:376–85. Available from: http://www.ncbi.nlm.nih.gov/pubmed/1479910

290. Vara J, Perez-Gonzalez JA, Jimenez A. Biosynthesis of puromycin by Streptomyces alboniger: characterization of puromycin N-acetyltransferase. Biochemistry [Internet]. 1985 Dec 31 [cited 2017 Dec 7];24(27):8074–81. Available from: http://www.ncbi.nlm.nih.gov/pubmed/4092057

291. Mok HP, Lever A. A method to estimate the efficiency of gene expression from an integrated retroviral vector. Retrovirology [Internet]. 2006 Aug 17 [cited 2020 Aug 18];3(1):51. Available from:

https://retrovirology.biomedcentral.com/articles/10.1186/1742-4690-3-51

292. M. Twyman R, Whitelaw B. Gene Expression in Recombinant Animal Cells and Transgenic Animals. In: Encyclopedia of Industrial Biotechnology [Internet]. Hoboken, NJ, USA: John Wiley & Sons, Inc.; 2010 [cited 2020 Oct 6]. p. 213–95. Available from: http://doi.wiley.com/10.1002/9780470054581.eib342

293. Froelich S, Tai A, Wang P. Lentiviral vectors for immune cells targeting [Internet]. Vol. 32, Immunopharmacology and Immunotoxicology. NIH Public Access; 2010 [cited 2020 Oct 6]. p. 208–18. Available from: /pmc/articles/PMC2864798/?report=abstract

294. Mori T, Anazawa Y, Iiizumi M, Fukuda S, Nakamura Y, Arakawa H. Identification of the interferon regulatory factor 5 gene (IRF-5) as a direct target for p53. Oncogene [Internet]. 2002 Apr 25 [cited 2020 Oct 24];21(18):2914–8. Available from: www.nature.com/onc

295. Yanai H, Chen H-M, Inuzuka T, Kondo S, Mak TW, Takaoka A, et al. Role of IFN regulatory factor 5 transcription factor in antiviral immunity and tumor suppression. Proc Natl Acad Sci U S A [Internet]. 2007 Feb 27 [cited 2016 Jun 10];104(9):3402–7. Available from: http://www.ncbi.nlm.nih.gov/pubmed/17360658

296. Gerolami R, Uch R, Jordier F, Chapel S, Bagnis C, Bréchot C, et al. Gene transfer to hepatocellular carcinoma: Transduction efficacy and transgene expression kinetics by using retroviral and lentiviral vectors [Internet]. Vol. 7, Cancer Gene Therapy. 2000 [cited 2020 Oct 6]. Available from: www.nature.com/cgt

297. Löser P, Jennings GS, Strauss M, Sandig V. Reactivation of the Previously Silenced Cytomegalovirus Major Immediate-Early Promoter in the Mouse Liver: Involvement of NFκB. J Virol [Internet]. 1998 Jan 1 [cited 2020 Oct 6];72(1):180–90. Available from: /pmc/articles/PMC109363/?report=abstract

298. Yamada A, Arakaki R, Saito M, Kudo Y, Ishimaru N. Dual role of Fas/FasL-mediated signal in peripheral immune tolerance [Internet]. Vol. 8, Frontiers in Immunology. Frontiers Research Foundation; 2017 [cited 2020 Oct 24]. p. 403. Available from: www.frontiersin.org

299. Hu G, Barnes BJ. IRF-5 is a mediator of the death receptor-induced apoptotic signaling pathway. J Biol Chem [Internet]. 2009 Jan 30 [cited 2020 Oct 22];284(5):2767–77. Available from: https://pubmed.ncbi.nlm.nih.gov/19028697/

300. Couzinet A, Tamura K, Chen HM, Nishimura K, Wang ZC, Morishita Y, et al. A cell-type-specific requirement for IFN regulatory factor 5 (IRF5) in Fas-induced apoptosis. Proc Natl Acad Sci U S A [Internet]. 2008 Feb 19 [cited 2020 Oct 22];105(7):2556–61. Available from: www.pnas.org/cgi/content/full/

301. Benbernou N, Esnault S, Shin HCK, Fekkar H, Guenounou M. Differential regulation of IFN-γ IL-10 and inducible nitric oxide synthase in human T cells by cyclic AMP-dependent signal transduction pathway. Immunology [Internet]. 1997 [cited 2021 May 17];91(3):361–8. Available from: https://pubmed.ncbi.nlm.nih.gov/9301524/

302. Jiang L, Cheng Z, Qiu S, Que Z, Bao W, Jiang C, et al. Altered let-7 expression in Myasthenia gravis and let-7c mediated regulation of IL-10 by directly targeting IL-10 in Jurkat cells. Int Immunopharmacol [Internet]. 2012 Oct [cited 2021 May 17];14(2):217–23. Available from: https://pubmed.ncbi.nlm.nih.gov/22835429/

303. Mordvinov VA, Peroni SE, De Boer ML, Kees UR, Sanderson CJ. A human T-cell line with inducible production of interleukins 5 and 4. A model for studies of gene expression. J Immunol Methods [Internet]. 1999 Aug 31 [cited 2020 Oct 6];228(1–2):163–8. Available from: https://pubmed.ncbi.nlm.nih.gov/10556553/

304. Chang WK, Yang KD, Chuang H, Jan JT, Shaio MF. Glutamine protects activated human T cells from apoptosis by up-regulating glutathione and Bcl-2 levels. Clin Immunol [Internet]. 2002 Aug 1 [cited 2020 Oct 6];104(2):151–60. Available from: https://pubmed.ncbi.nlm.nih.gov/12165276/

305. Watkins AA, Yasuda K, Wilson GE, Aprahamian T, Xie Y, Maganto-Garcia E, et al. IRF5 deficiency ameliorates lupus but promotes atherosclerosis and metabolic dysfunction in a mouse model of lupus-associated atherosclerosis. J Immunol [Internet]. 2015 Feb 15 [cited 2016 Oct 2];194(4):1467–79. Available from: http://www.ncbi.nlm.nih.gov/pubmed/25595782

306. Yan J, Pandey SP, Barnes BJ, Turner JR, Abraham C. T Cell-Intrinsic IRF5 Regulates T Cell Signaling, Migration, and Differentiation and Promotes Intestinal Inflammation. Cell Rep [Internet]. 2020 Jun 30 [cited 2020 Oct 6];31(13). Available from: https://pubmed.ncbi.nlm.nih.gov/32610123/

307. Kitamura N, Kitamura F, Kaminuma O, Miyatake S, Tatsumi H, Nemoto S, et al. IL-4 gene transcription in human T cells is suppressed by T-bet. In: International Archives of Allergy and Immunology [Internet]. Int Arch Allergy Immunol; 2007 [cited 2020 Oct 24]. p. 68–70. Available from: https://pubmed.ncbi.nlm.nih.gov/17541280/

308. Suzuki K, Kaminuma O, Hiroi T, Kitamura F, Miyatake S, Takaiwa F, et al. Downregulation of IL-13 gene transcription by T-bet in human T cells. Int Arch Allergy Immunol [Internet]. 2008 [cited 2020 Oct 24];146 Suppl 1:33–5. Available from: https://pubmed.ncbi.nlm.nih.gov/18504404/

309. Manni M, Gupta S, Ricker E, Chinenov Y, Park SH, Shi M, et al. Regulation of age-associated B cells by IRF5 in systemic autoimmunity. Nat Immunol [Internet]. 2018 Apr 1 [cited 2021 May 18];19(4):407–19. Available from: https://www.nature.com/articles/s41590-018-0056-8

310. Ng THS, Britton GJ, Hill E V., Verhagen J, Burton BR, Wraith DC. Regulation of adaptive immunity; the role of interleukin-10 [Internet]. Vol. 4, Frontiers in Immunology. Front Immunol; 2013 [cited 2021 May 18]. Available from: https://pubmed.ncbi.nlm.nih.gov/23755052/

311. Jankovic D, Kugler DG, Sher A. IL-10 production by CD4+ effector T cells: A mechanism for self-regulation [Internet]. Vol. 3, Mucosal Immunology. NIH Public Access; 2010 [cited 2021 May 17]. p. 239–46. Available from: /pmc/articles/PMC4105209/

312. Gour N, Wills-Karp M. IL-4 and IL-13 signaling in allergic airway disease

[Internet]. Vol. 75, Cytokine. Academic Press; 2015 [cited 2021 May 18]. p. 68–78. Available from: /pmc/articles/PMC4532591/

313. Rockwell CE, Qureshi N. Differential effects of lactacystin on cytokine production in activated Jurkat cells and murine splenocytes. Cytokine [Internet]. 2010 Jul [cited 2021 May 18];51(1):12–7. Available from: https://pubmed.ncbi.nlm.nih.gov/20427199/

314. Gioia L, Siddique A, Head SR, Salomon DR, Su AI. A genome-wide survey of mutations in the Jurkat cell line. BMC Genomics [Internet]. 2018 [cited 2020 Oct 6];19(1):334. Available from: https://doi.org/10.1186/s12864-018-4718-6

315. Ai W, Li H, Song N, Li L, Chen H. Optimal method to stimulate cytokine production and its use in immunotoxicity assessment. Int J Environ Res Public Health [Internet]. 2013 Aug 27 [cited 2021 May 18];10(9):3834–42. Available from: /pmc/articles/PMC3799516/

7 Appendix

1.1 Recipes of reagents

a) 10x TBE –adapted from Sigma Aldrich protocol

- Dissolve 108 g of Tris and 55 g Boric acid in 900 ml of distilled water
- Add 40 ml of 0.5 M Na_2EDTA (pH 8.0)
- Adjust volume to 1 liter.

b) LB medium/ agar preparation

- Dissolve 5 g of Nacl, 5 g of Tryptone and 2.5 g of yeast to 300 ml of distilled water
- For LB agar preparation, add 7.5 g of agar
- Adjust volume to 500 ml and autoclave

c) RIPA lysis buffer-adapted from Cold Spring Harbour Protocols

- Add 1.5 ml of NaCl (1M), 0.1 ml Nodidet P-40, 0.05 ml of Sodium deoxycholate, 0.01 ml of SDS and 5ml of Tris (50mM, pH 7.4)
- Adjust to 10 ml distilled water
- Store in 4^0C and use within 1 month

d) 1x SDS PAGE running buffer

- Dissolve 3.03g of Tris, 144.4 g of Glycine, 1 g of SDS in 1 liter of distilled water

e) Towbin transfer buffer

- Dissolve 3.03g of Tris, 14.4 g of Glycine in 800ml of distilled water
- Add 200 ml of methanol

f) Mild stripping buffer- adapted from Abcam protocol

- Dissolve 15 g of Glycine, 0.1 g of SDS in 80ml of ultrapure water
- Add 10 ml of Tween-20
- Adjust pH to 2.2 and bring volume to 1 litre

1.2 Steps for designing IRF5 primers for reverse transcriptase PCR (RT-PCR)

1. Open Bioedit sequence with IRF5v4 and IRF5v5 sequences obtained from sequencing

2. Press "Ctrl F" and find the sequences of primer sense and antisense (obtained from Journal). Only antisense sequence can be found on both IRF5v4 and IRF5v5. The length was recorded.

3. Next the sense primer sequence was Blast using NCBI Blast, with human + transcript being selected.

4. The blast results showed the similarity region 100% and all IRF5 mRNA transcript showed 100%. (This showed the primer used was to target the entire sequence of IRF5, so the primers used were consensus primers)

5. IRF5v5 mRNA was clicked and the FASTA sequence was copied and saved in Notepad.

6. The sequence was open in Bioedit. Open> choose file on desktop

7. Highlight the 3 sequences IRF5v4, IRF5v5 and IRF5v5 mRNA, click copy and paste into new alignment

8. Highlight the 3 sequences, click accessory application>ClustalW Multiple alignment>run>chose to colour the nucleotide (back colour view mode)

9. Check for the sequence length of antisense

10. For sense, click new alignment> open new sequence>copy and paste the sequence > name title as IRF-5 primer sense (RC)> DNA>apply and close

11. Click on the sequence on the "new alignment page">click nucleic acid>RC

12. Next click open RC sequence, copy and paste by finding Ctrl F"

13. Based on observation the sequence is towards the end of the IRF5v5 mRNA, hence the sequence was modified by taking the front 5 bases and leaving behind those 5 towards the end to make up 20 bases. The sequence lengths were recorded. The highest value minus lower value gives the length of base pair.

14. To check for the complement sequence of RC, Tm and GC content, the primer sequences were analysed through Oligo IDT website

15. To check back whether the complement sequence primer is correct, the sequence was RC and checked with the previous RC sequences.

16. The primers sequences were checked through NCBI Blast and the properties were checked in Oligo IDT and ordered.

2.1 Amplification of human IRF5cDNA at lower annealing temperatures were not clearly detected
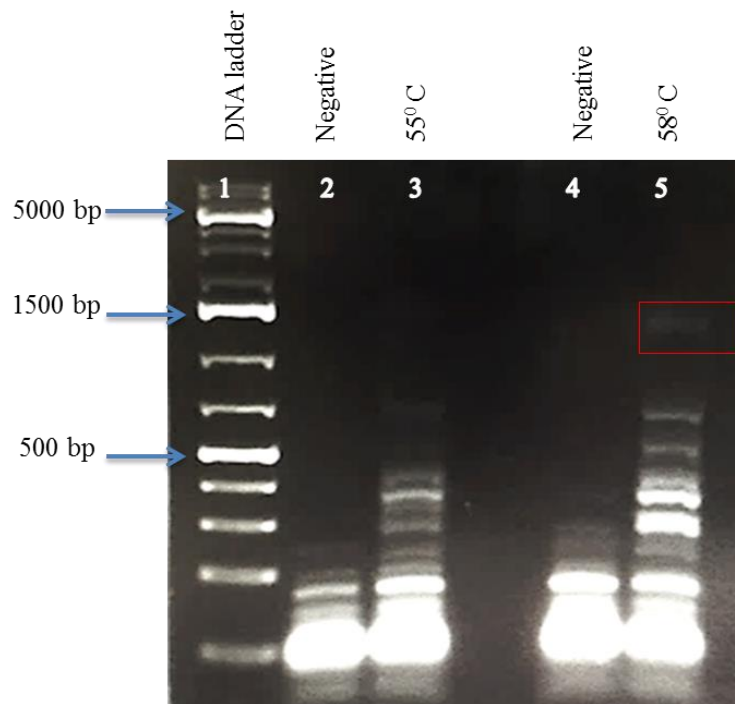
Figure 1 Amplification of IRF5 from cDNA of B cells. No amplification was detected at 55^0C. A light unclear band was seen at 58^0C.

2.2 (a)Full sequences of TOPO-IRF5v4 and TOPO-IRF5v5 with *Bam*HI *and Sal*I sequences

➢ Transformant 1(encoded IRF5v5)

```
ATGAACCAGTCCATCCCAGTGGCTCCCACCCCACCCCGCCGCGTGCGGCTGAAGCCCTGGCTGGTGGCCCAG
GTGAACAGCTGCCAGTACCCAGGGCTTCAATGGGTCAACGGGGAAAAGAAATTATTCTGCATCCCCTGGAGG
CATGCCACAAGGCATGGTCCCAGCCAGGACGGAGATAACACCATCTTCAAGGCCTGGGCCAAGGAGACAGGG
AAATACACCGAAGGCGTGGATGAAGCCGATCCGGCCAAGTGGAAGGCCAACCTGCGCTGTGCCCTTAACAAG
AGCCGGGACTTCCGCCTCATCTACGACGGGCCCCGGGACATGCCACCTCAGCCCTACAAGATCTACGAGGTC
TGCTCCAATGGCCCTGCTCCCACAGACTCCCAGCCCCCTGAGGATTACTCTTTTGGTGCAGGAGAGGAGGAG
GAAGAAGAGGAAGAGCTGCAGAGGATGTTGCCAAGCCTGAGCCTCACAGATGCAGTGCAGTCTGGCCCCCAC
ATGACACCCTATTCTTTACTCAAAGAGGATGTCAAGTGGCCGCCCACTCTGCAGCCGCCCACTCTGCAGCCG
CCCGTGGTGCTGGGTCCCCCTGCTCCAGACCCCAGCCCCCTGGCTCCTCCCCCTGGCAACCCTGCTGGCTTC
AGGGAGCTTCTCTCTGAGGTCCTGGAGCCTGGGCCCCTGCCTGCCAGCCTGCCCCCTGCAGGCGAACAGCTC
CTGCCAGACCTGCTGATCAGCCCCCACATGCTGCCTCTGACCGACCTGGAGATCAAGTTTCAGTACCGGGGG
CGGCCACCCCGGGCCCTCACCATCAGCAACCCCCATGGCTGCCGGCTCTTCTACAGCCAGCTGGAGGCCACC
CAGGAGCAGGTGGAACTCTTCGGCCCCATAAGCCTGGAGCAAGTGCGCTTCCCCAGCCCTGAGGACATCCCC
AGTGACAAGCAGCGCTTCTACACGAACCAGCTGCTGGATGTCCTGGACCGCGGGCTCATCCTCCAGCTACAG
GGCCAGGACCTTTATGCCATCCGCCTGTGTCAGTGCAAGGTGTTCTGGAGCGGGCCTTGTGCCTCAGCCCAT
GACTCATGCCCCAACCCCATCCAGCGGGAGGTCAAGACCAAGCTTTTCAGCCTGGAGCATTTTCTCAATGAG
CTCATCCTGTTCCAAAAGGGCCAGACCAACACCCCACCACCCTTCGAGATCTTCTTCTGCTTTGGGGAAGAA
TGGCCTGACCGCAAACCCCGAGAGAAGAAGCTCATTACTGTACAGGTGGTGCCTGTAGCAGCTCGACTGCTG
CTGGAGATGTTCTCAGGGGAGCTATCTTGGTCAGCTGATAGTATCCGGCTACAGATCTCAAACCCAGACCTC
AAAGACCGCATGGTGGAGCAATTCAAGGAGCTCCATCACATCTGGCAGTCCCAGCAGCGGTTGCAGCCTGTG
GCCCAGGCCCCTCCTGGAGCAGGCCTTGGTGTTGGCCAGGGGCCCTGGCCTATGCACCCAGCTGGCATGCAA
TAA
```

➤ Transformant 3 (encoded IRF5v4)

```
ATGAACCAGTCCATCCCAGTGGCTCCCACCCCACCCCGCCGCGTGCGGCTGAAGCCCTGGCTGGTGGCCCAG
GTGAACAGCTGCCAGTACCCAGGGCTTCAATGGGTCAACGGGGAAAAGAAATTATTCTGCATCCCCTGGAGG
CATGCCACAAGGCATGGTCCCAGCCAGGACGGAGATAACACCATCTTCAAGGCCTGGGCCAAGGAGACAGGG
AAATACACCGAAGGCGTGGATGAAGCCGATCCGGCCAAGTGGAAGGCCAACCTGCGCTGTGCCCTTAACAAG
AGCCGGGACTTCCGCCTCATCTACGACGGGCCCCGGGACATGCCACCTCAGCCCTACAAGATCTACGAGGTC
TGCTCCAATGGCCCTGCTCCCACAGACTCCCAGCCCCCTGAGGATTACTCTTTTGGTGCAGGAGAGGAGGAG
GAAGAAGAGGAAGAGCTGCAGAGGATGTTGCCAAGCCTGAGCCTCACAGAGGATGTCAAGTGGCCGCCCACT
CTGCAGCCGCCCACTCTGCAGCCGCCCGTGGTGCTGGGTCCCCCTGCTCCAGACCCCAGCCCCCTGGCTCCT
CCCCCTGGCAACCCTGCTGGCTTCAGGGAGCTTCTCTCTGAGGTCCTGGAGCCTGGGCCCCTGCCTGCCAGC
CTGCCCCCTGCAGGCGAACAGCTCCTGCCAGACCTGCTGATCAGCCCCCACATGCTGCCTCTGACCGACCTG
GAGATCAAGTTTCAGTACCGGGGGCGGCCACCCCGGGCCCTCACCATCAGCAACCCCCATGGCTGCCGGCTC
TTCTACAGCCAGCTGGAGGCCACCCAGGAGCAGGTGGAACTCTTCGGCCCCATAAGCCTGGAGCAAGTGCGC
TTCCCCAGCCCTGAGGACATCCCCAGTGACAAGCAGCGCTTCTACACGAACCAGCTGCTGGATGTCCTGGAC
CGCGGGCTCATCCTCCAGCTACAGGGCCAGGACCTTTATGCCATCCGCCTGTGTCAGTGCAAGGTGTTCTGG
AGCGGGCCTTGTGCCTCAGCCCATGACTCATGCCCCAACCCCATCCAGCGGGAGGTCAAGACCAAGCTTTTC
AGCCTGGAGCATTTTCTCAATGAGCTCATCCTGTTCCAAAAGGGCCAGACCAACACCCCACCACCCTTCGAG
ATCTTCTTCTGCTTTGGGGAAGAATGGCCTGACCGCAAACCCCGAGAGAAGAAGCTCATTACTGTACAGGTG
GTGCCTGTAGCAGCTCGACTGCTGCTGGAGATGTTCTCAGGGGAGCTATCTTGGTCAGCTGATAGTATCCGG
CTACAGATCTCAAACCCAGACCTCAAAGACCGCATGGTGGAGCAATTCAAGGAGCTCCATCACATCTGGCAG
TCCCAGCAGCGGTTGCAGCCTGTGGCCCAGGCCCCTCCTGGAGCAGGCCTTGGTGTTGGCCAGGGGCCCTGG
CCTATGCACCCAGCTGGCATGCAATAA
```

260

2.2 (b) Full sequences of TOPO-IRF5v4 and TOPO-IRF5v5 with *Bam*HI and *Xba*I sequences

➢ Transformant 1 (encoded IRF5v4)

```
GCTGGAATTCGCCCTTTCGGATCCATGAACCAGTCCATCCCAGTGGCTCCCACCCCACCCCGCCGCGTGCGG
CTGAAGCCCTGGCTGGTGGCCCAGGTGAACAGCTGCCAGTACCCAGGGCTTCAATGGGTCAACGGGGAAAAG
AAATTATTCTGCATCCCCTGGAGGCATGCCACAAGGCATGGTCCCAGCCAGGACGGAGATAACACCATCTTC
AAGGCCTGGGCCAAGGAGACAGGGAAATACACCGAAGGCGTGGATGAAGCCGATCCGGCCAAGTGGAAGGCC
AACCTGCGCTGTGCCCTTAACAAGAGCCGGGACTTCCGCCTCATCTACGACGGGCCCCGGGACATGCCACCT
CAGCCCTACAAGATCTACGAGGTCTGCTCCAATGGCCCTGCTCCCACAGACTCCCAGCCCCCTGAGGATTAC
TCTTTTGGTGCAGGAGAGGAGGAGGAAGAAGAGGAAGAGCTGCAGAGGATGTTGCCAAGCCTGAGCCTCACA
GAGGATGTCAAGTGGCCGCCCACTCTGCAGCCGCCCACTCTGCAGCCGCCCGTGGTGCTGGGTCCCCCTGCT
CCAGACCCCAGCCCCCTGGCTCCTCCCCCTGGCAACCCTGCTGGCTTCAGGGAGCTTCTCTCTGAGGTCCTG
GAGCCTGGGCCCCTGCCTGCCAGCCTGCCCCCTGCAGGCGAACAGCTCCTGCCAGACCTGCTGATCAGCCCC
CACATGCTGCCTCTGACCGACCTGGAGATCAAGTTTCAGTACCGGGGGCGGCCACCCCGGGCCCTCACCATC
AGCAACCCCCATGGCTGCCGGCTCTTCTACAGCCAGCTGGAGGCCACCCAGGAGCAGGTGGAACTCTTCGGC
CCCATAAGCCTGGAGCAAGTGCGCTTCCCCAGCCCTGAGGACATCCCCAGTGACAAGCAGCGCTTCTACACG
AACCAGCTGCTGGATGTCCTGGACCGCGGGCTCATCCTCCAGCTACAGGGCCAGGACCTTTATGCCATCCGC
CTGTGTCAGTGCAAGGTGTTCTGGAGCGGGCCTTGTGCCTCAGCCCATGACTCATGCCCCAACCCCATCCAG
CGGGAGGTCAAGACCAAGCTTTTCAGCCTGGAGCATTTTCTCAATGAGCTCATCCTGTTCCAAAAGGGCCAG
ACCAACACCCCACCACCCTTCGAGATCTTCTTCTGCTTTGGGGAAGAATGGCCTGACCGCAAACCCCGAGAG
AAGAAGCTCATTACTGTACAGGTGGTGCCTGTAGCAGCTCGACTGCTGCTGGAGATGTTCTCAGGGGAGCTA
TCTTGGTCAGCTGATAGTATCCGGCTACAGATCTCAAACCCAGACCTCAAAGACCGCATGGTGGAGCAATTC
AAGGAGCTCCATCACATCTGGCAGTCCCAGCAGCGGTTGCAGCCTGTGGCCCAGGCCCCTCCTGGAGCAGGC
CTTGGTGTTGGCCAGGGGCCCTGGCCTATGCACCCAGCTGGCATGCAATAACAAGGCTTCTAGAAAGGGCGA
ATTCTGCAGA
```

➢ Transformant 2 (encoded IRF5v5)

```
GCTGGAATTCGCCCTTTCGGATCCATGAACCAGTCCATCCCAGTGGCTCCCACCCCACCCCGCCGCGTGCGG
CTGAAGCCCTGGCTGGTGGCCCAGGTGAACAGCTGCCAGTACCCAGGGCTTCAATGGGTCAACGGGGAAAAG
AAATTATTCTGCATCCCCTGGAGGCATGCCACAAGGCATGGTCCCAGCCAGGACGGAGATAACACCATCTTC
AAGGCCTGGGCCAAGGAGACAGGGAAATACACCGAAGGCGTGGATGAAGCCGATCCGGCCAAGTGGAAGGCC
AACCTGCGCTGTGCCCTTAACAAGAGCCGGGACTTCCGCCTCATCTACGACGGGCCCCGGGACATGCCACCT
CAGCCCTACAAGATCTACGAGGTCTGCTCCAATGGCCCTGCTCCCACAGACTCCCAGCCCCCTGAGGATTAC
TCTTTTGGTGCAGGAGAGGAGGAGGAAGAAGAGGAAGAGCTGCAGAGGATGTTGCCAAGCCTGAGCCTCACA
GAGGATGTCAAGTGGCCGCCCACTCTGCAGCCGCCCACTCTGCAGCCGCCCGTGGTGCTGGGTCCCCCTGCT
CCAGACCCCAGCCCCCTGGCTCCTCCCCCTGGCAACCCTGCTGGCTTCAGGGAGCTTCTCTCTGAGGTCCTG
GAGCCTGGGCCCCTGCCTGCCAGCCTGCCCCCTGCAGGCGAACAGCTCCTGCCAGACCTGCTGATCAGCCCC
CACATGCTGCCTCTGACCGACCTGGAGATCAAGTTTCAGTACCGGGGGCGGCCACCCCGGGCCCTCACCATC
AGCAACCCCCATGGCTGCCGGCTCTTCTACAGCCAGCTGGAGGCCACCCAGGAGCAGGTGGAACTCTTCGGC
CCCATAAGCCTGGAGCAAGTGCGCTTCCCCAGCCCTGAGGACATCCCCAGTGACAAGCAGCGCTTCTACACG
AACCAGCTGCTGGATGTCCTGGACCGCGGGCTCATCCTCCAGCTACAGGGCCAGGACCTTTATGCCATCCGC
CTGTGTCAGTGCAAGGTGTTCTGGAGCGGGCCTTGTGCCTCAGCCCATGACTCATGCCCCAACCCCATCCAG
CGGGAGGTCAAGACCAAGCTTTTCAGCCTGGAGCATTTTCTCAATGAGCTCATCCTGTTCCAAAAGGGCCAG
ACCAACACCCCACCACCCTTCGAGATCTTCTTCTGCTTTGGGGAAGAATGGCCTGACCGCAAACCCCGAGAG
AAGAAGCTCATTACTGTACAGGTGGTGCCTGTAGCAGCTCGACTGCTGCTGGAGATGTTCTCAGGGGAGCTA
TCTTGGTCAGCTGATAGTATCCGGCTACAGATCTCAAACCCAGACCTCAAAGACCGCATGGTGGAGCAATTC
AAGGAGCTCCATCACATCTGGCAGTCCCAGCAGCGGTTGCAGCCTGTGGCCCAGGCCCCTCCTGGAGCAGGC
CTTGGTGTTGGCCAGGGGCCCTGGCCTATGCACCCAGCTGGCATGCAATAACAAGGCTTCTAGAAAGGGCGA
ATTCTGCAGA
```

2.3 Results of Luciferase assay responding to *Il13* promoter activity (data from controls included)
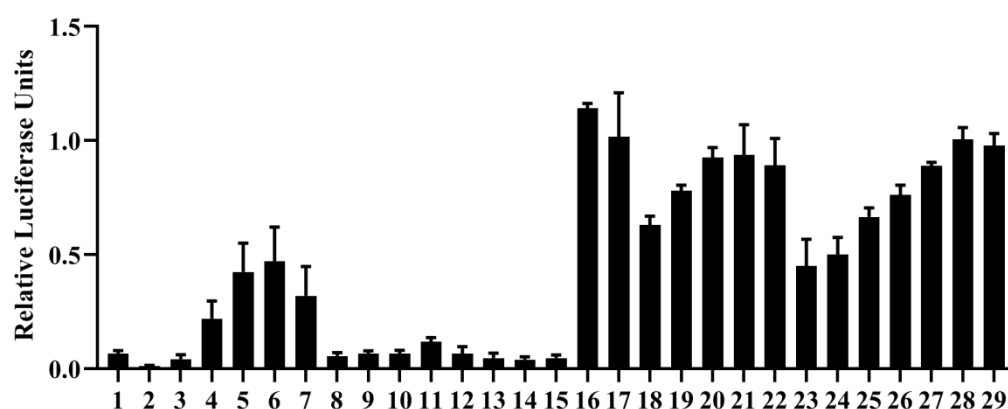
Figure 2 Relative expression (RE) of IL13 promoter in HEK293T cells co-transfected with IRF5-v4 or IRF5-v5 with MyD88.
Bar 1:IL13 promoter luciferase (IL-13L)
Bar 2: T4 Renilla luciferase (T4R)
Bar 3: IL13L+T4R
Bar 4-7 : increasing MyD88 concentration (25, 50, 75 and 100 ng)
Bar 8-11: increasing IRF5v4 concentration (25, 50, 75 and 100 ng)
Bar 12-15: increasing IRF5v5 concentration (25, 50, 75 and 100 ng)
Bar 16-19: increasing IRF5v4 concentration (MyD88 constant 100 ng)
Bar 20-22 : increasing MyD88 concentration (IRF5v4 constant 100 ng)
Bar 23-26 : increasing IRF5v5 concentration (MyD88 constant 100 ng)
Bar 27-29 : increasing MyD88 concentration (IRF5v5 constant 100 ng)

2.4 Confirmation of plasmids produced by large scale of isolation by restriction digestion
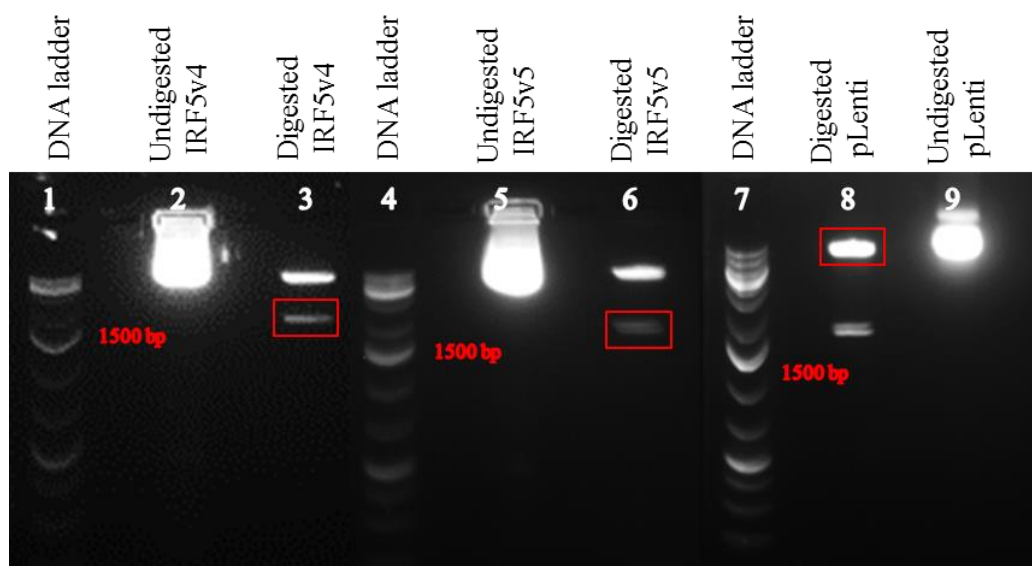
Figure 3 Restriction digestion of extracted plasmids of pLenti, TOPO-IRF5v4 and TOPO-IRF5v5 using *Bam*HI and *Sal*I.
Digestion of IRF5v4 and IRF5v5 gave fragment of 1500bp and pLenti gave a fragment of about 7000bp. The indicated red boxes are the desired bands used for ligation.

2.5 Sloughing of cells and low titer of recombinant lentivirus during optimization of protocol, showing the importance of proper seeding number and confluency

a)

b)

c)
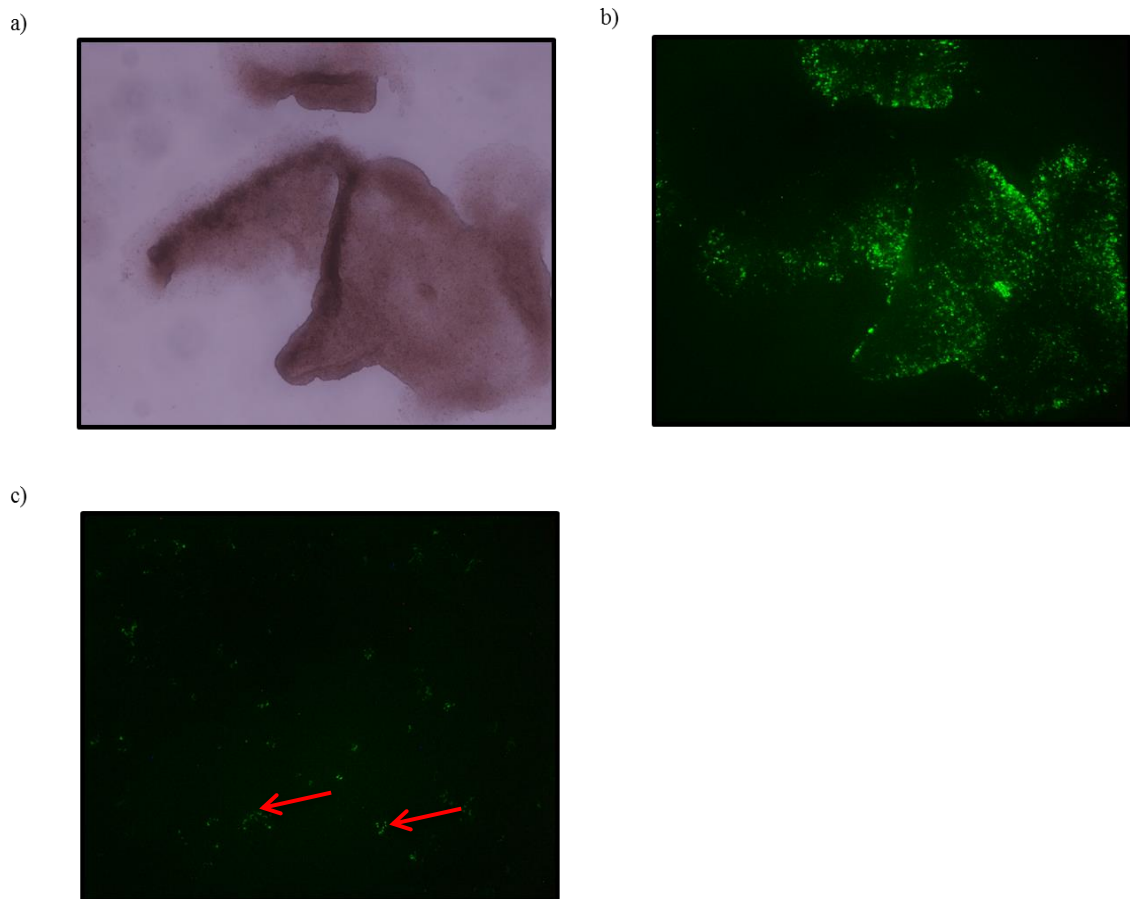
Figure 4 Visualisation of GFP expression during trial experiment. (a) Bright-field of sloughed HEK 293 T cells observed at day 3 post-transfection, (b) GFP expression of sloughed HEK 293 T cells observed at day 3 post-transfection, (c) GFP expression of transduced HEK 293 T cells observed at day 3 post-transduction. Photos were taken under Nikon Upright Microscope Eclipse Ei under fluorescent light (x100 magnification). The exposure time of fluorescent photos were 600 milliseconds. The red indicator is showing some weak signal of GFP.

2.6 Gradient PCR of IRF5 primers using isolated IRF5v5 plasmid as template
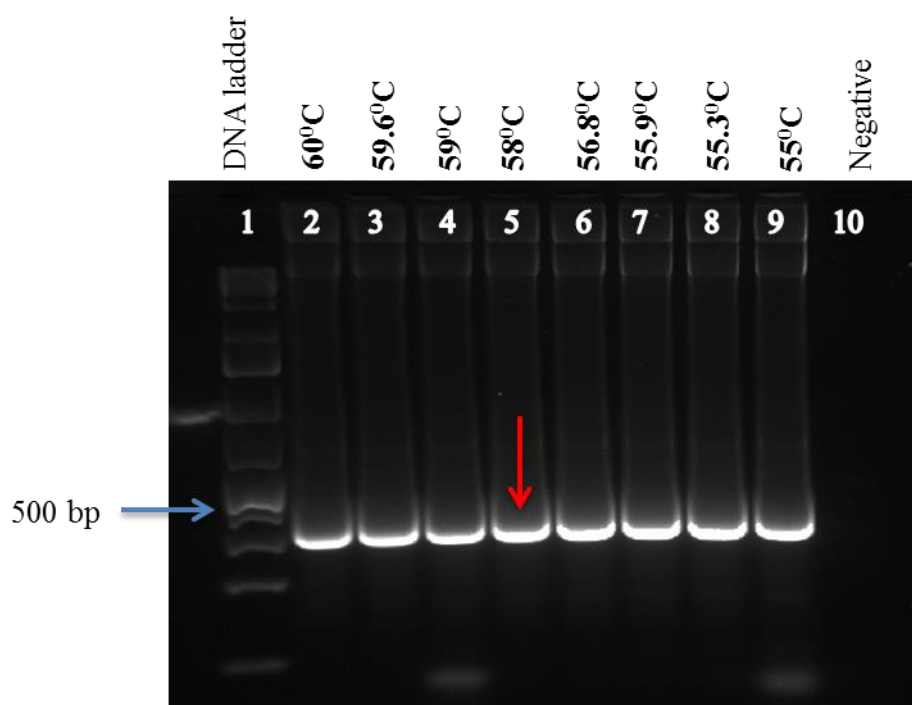
Figure 5 Determination of optimal annealing temperature for the amplification of IRF5v5 by gradient PCR.

TOPO-IRF5v5 plasmid was used as template. Thirty cycles of gradient PCR were carried out at the indicated annealing temperature. The red arrowhead marks the chosen annealing temperature that gave clear band of expected size of 482 bp.
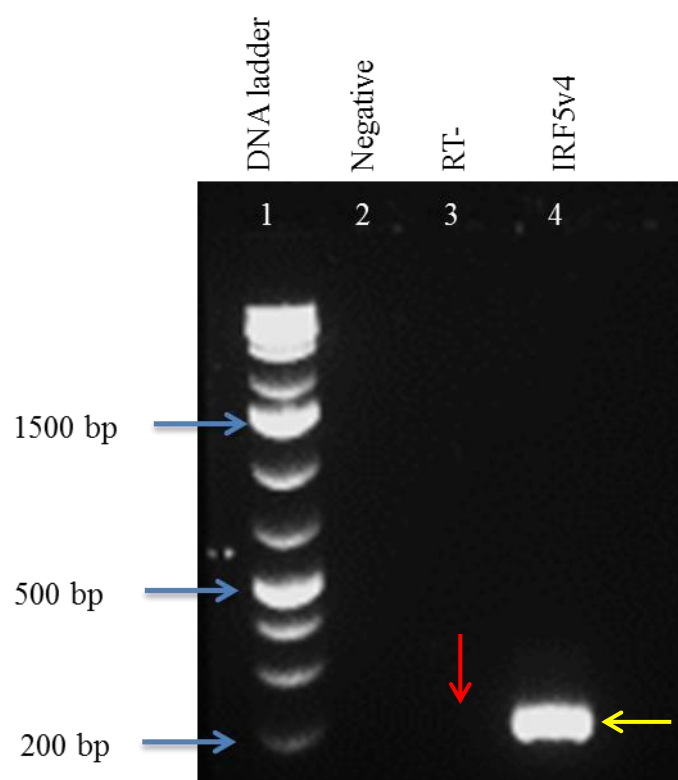
2.7 Confirmation of optimal genomic DNA elimination protocol

Figure 6 Confirmation of optimal genomic DNA elimination protocol assessed through gel electrophoresis.
The red arrow head shows no band was seen in RT- sample, meanwhile yellow arrowhead shows 182 bp corresponding to β-actin detected in PCR product amplified from IRF5v4 cDNA sample.

2.8 Silencing of IRF5v4 or IRF5v5 under CMV promoter were restored upon PMA and Ionomycin stimulation
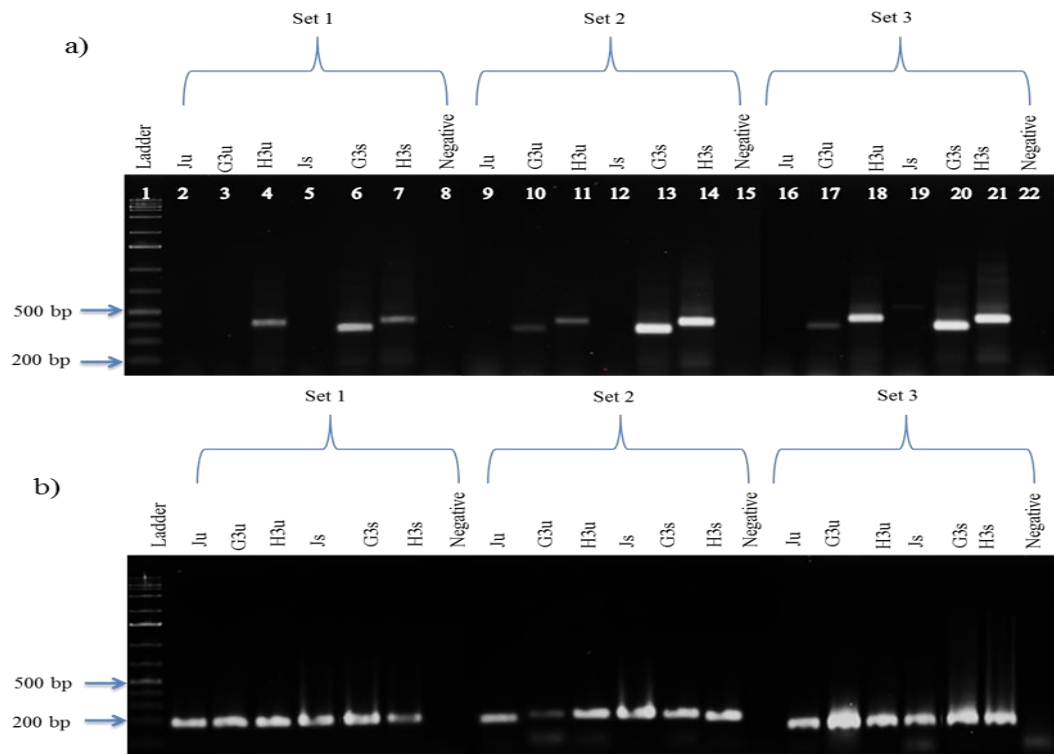
Figure 7 Demonstration of silencing of IRF5v4 (G3) and IRFv5 (H3) gene under CMV promoter were restored upon PMA and Ionomcyin stimulation.
Unstimulated cells are indicated as Ju (Jurkat-control), G3u (IRF5v4) and H3u (IRF5v5). Stimulated cells are indicated as Js (Jurkat-control), G3s (IRF5v4), H3s (IRF5v5). a) IRF5v4 (314 bp) and IRF5v5 (382 bp) mRNA levels were determined by reverse transcription PCR. b) housekeeping gene, β-actin as the loading control (182bp).

2.9 Gradient PCR to determine optimal annealing temperature for amplification of cytokine transcripts
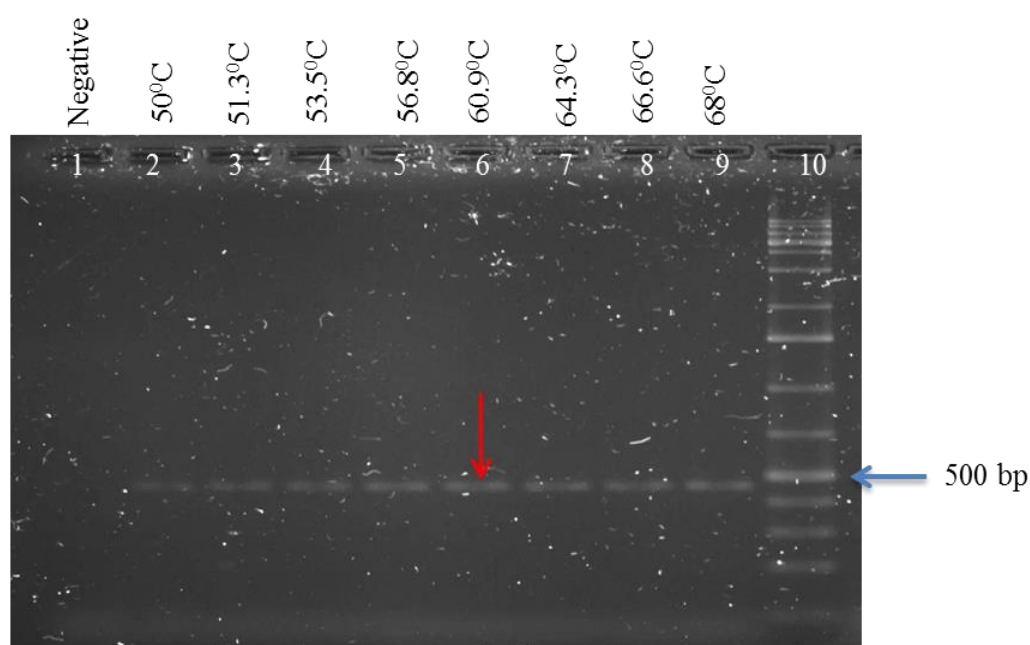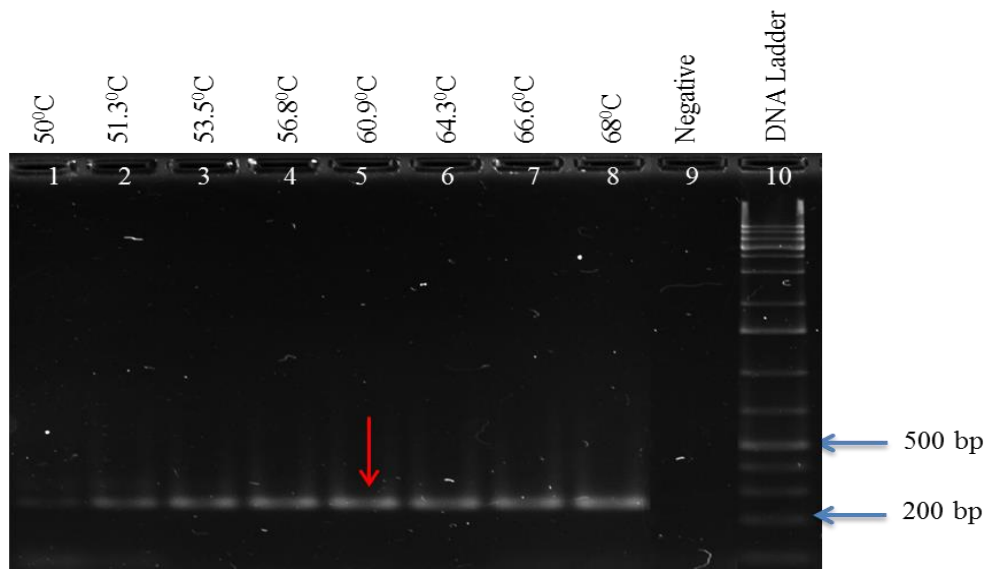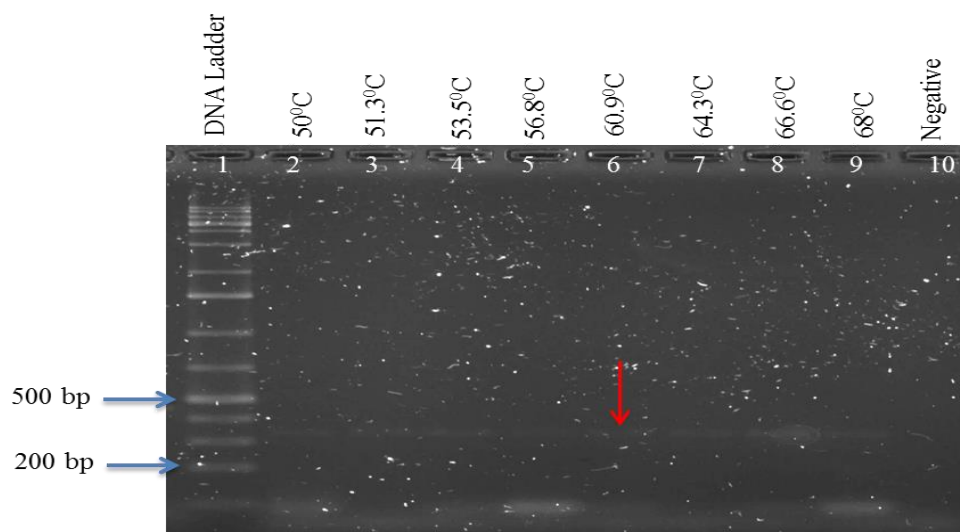

Figure 8 Determination of optimal annealing temperature for the amplification of IFNγ by gradient PCR.
PMA/Ionomycin stimulated Jurkat cells for 6 hours were used as template. Thirty cycles of gradient PCR were carried out at the indicated annealing temperature. The red arrowhead marks the chosen annealing temperature that gave clear band of expected size of 453 bp.

Figure 9 Determination of optimal annealing temperature for the amplification of IL-2 by gradient PCR.

PMA/Ionomycin stimulated Jurkat cells for 6 hours were used as template. Thirty cycles of gradient PCR were carried out at the indicated annealing temperature. The arrowhead marks the chosen annealing temperature that gave clear band of expected size of 250bp.
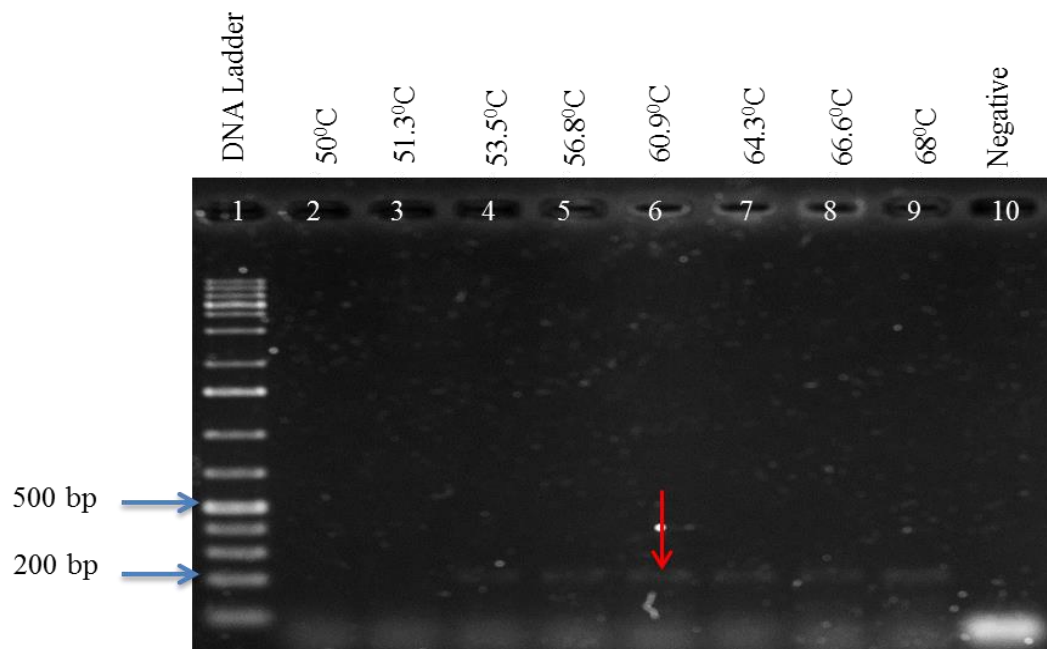
Figure 10 Determination of optimal annealing temperature for the amplification of IL-4 by gradient PCR.

PMA/Ionomycin stimulated Jurkat cells for 6 hours were used as template. Thirty cycles of gradient PCR were carried out at the indicated annealing temperature. The arrowhead marks the chosen annealing temperature that gave clear band of expected size of 331 bp.

Figure 11 Determination of optimal annealing temperature for the amplification of IL-13 by gradient PCR.

PMA/Ionomycin stimulated Jurkat cells for 6 hours were used as template. Thirty cycles of gradient PCR were carried out at the indicated annealing temperature. The arrowhead marks the chosen annealing temperature that gave clear band of expected size of 253 bp.
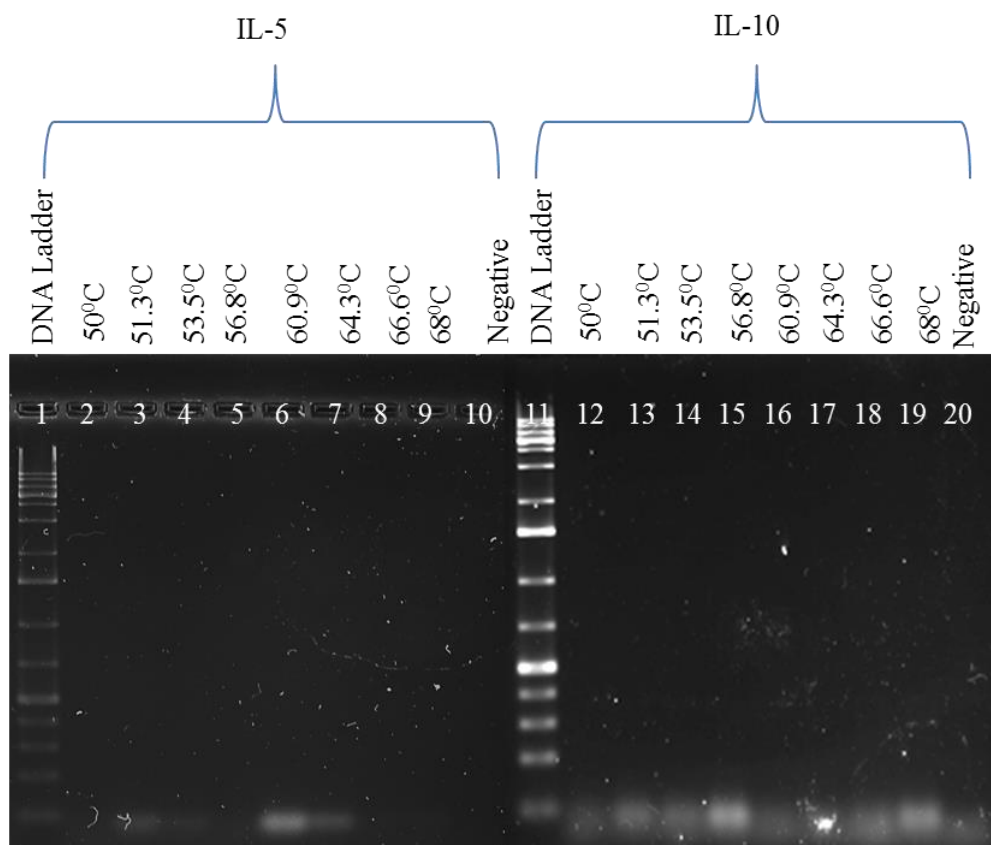
Figure 12 Determination of optimal annealing temperatures for the amplification of IL-5 and IL-10 by gradient PCR.

PMA/Ionomycin stimulated Jurkat cells for 6 hours were used as template. Thirty cycles of gradient PCR were carried out at the indicated annealing temperature. No amplication was detected.
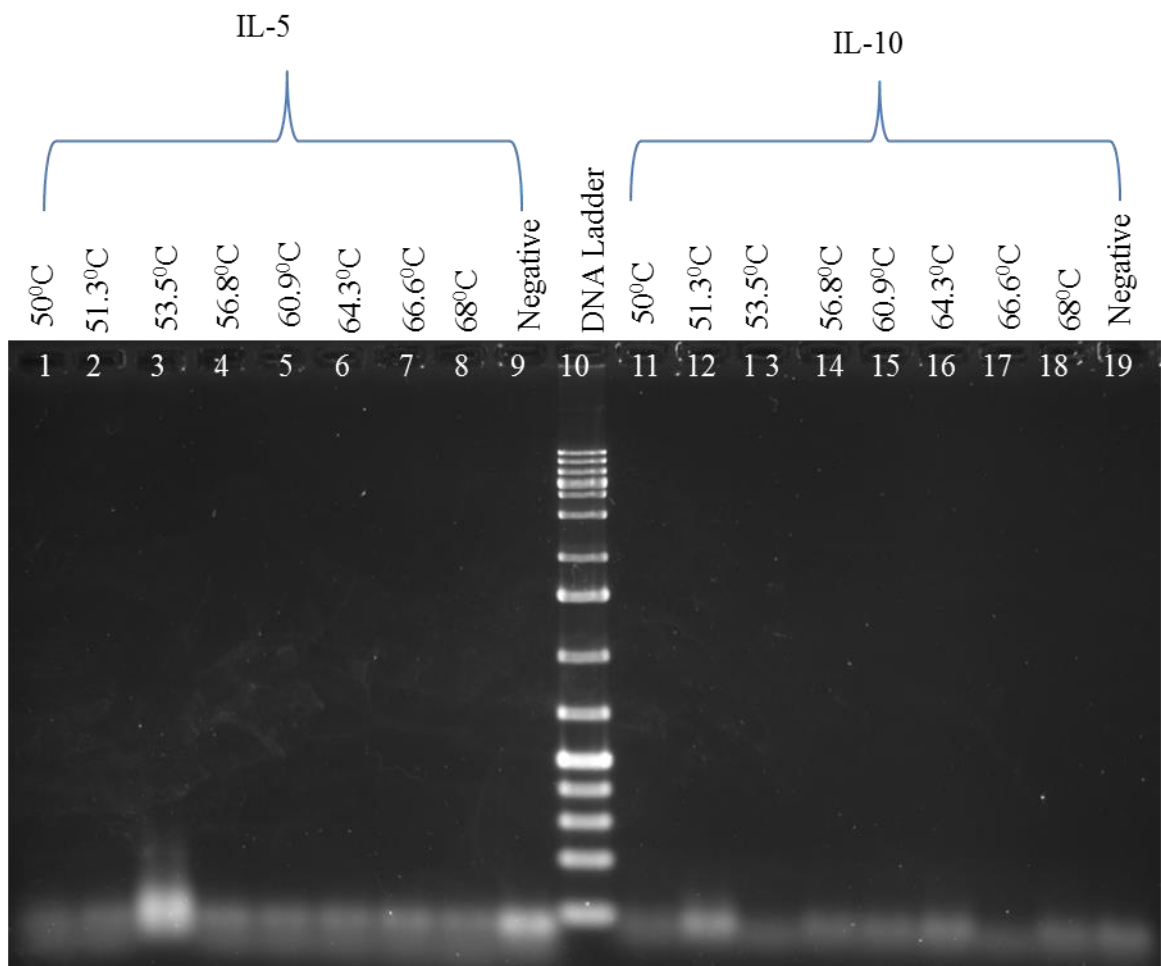
Figure 13 Determination of optimal annealing temperature for the amplification of IL-5 and IL-10 by gradient PCR.

PMA/Ionomycin stimulated IRF5v5 cells for 6 hours were used as template. Thirty cycles of gradient PCR were carried out at the indicated annealing temperature. a) Analysis of PCR products for amplification of IL-5. b) Analysis of PCR products for amplification of IL-10.

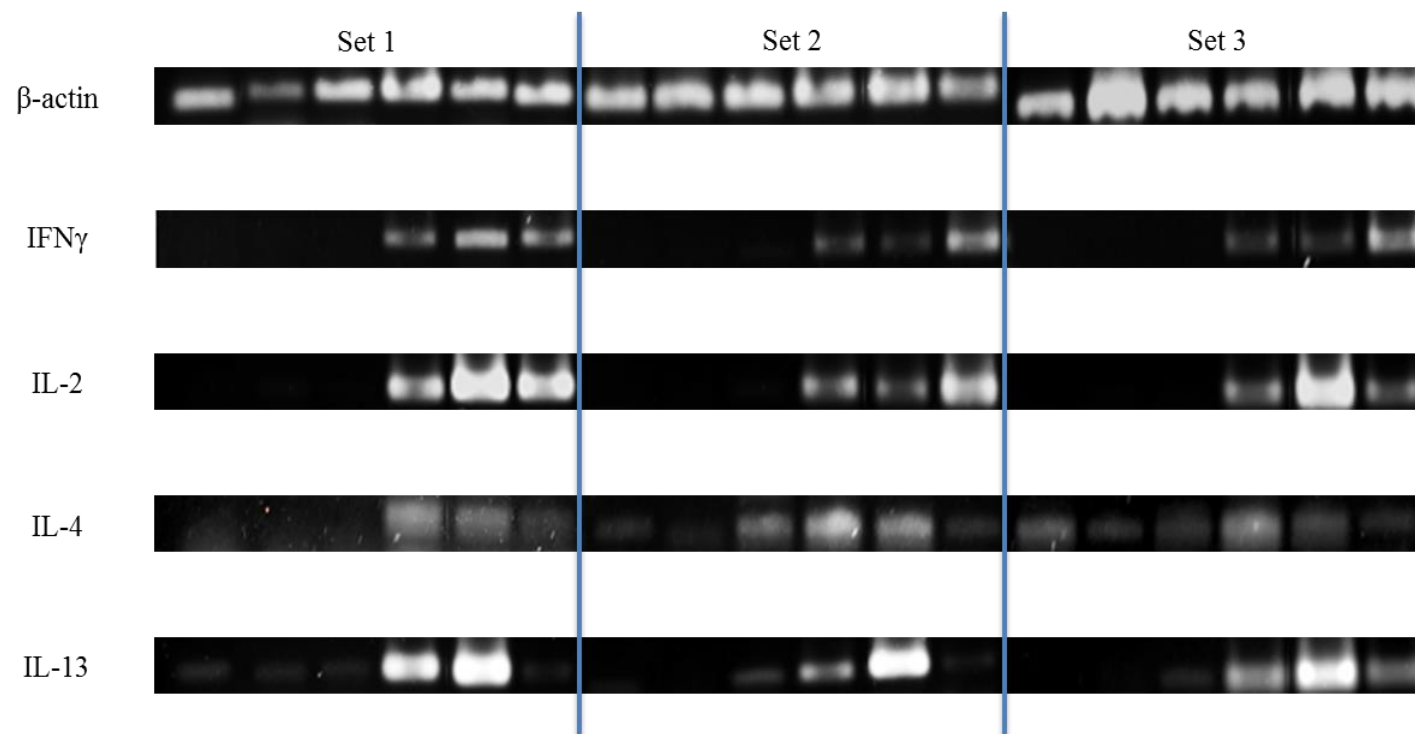**2.10 Analysis of cytokines transcripts by gel electrophoresis**

Figure 14 Visualisation of transcripts in unstimulated cells or cells stimulated with PMA-Ionomycin for 6 hours. Amplification of products sizes for IFNγ (453 bp), IL-2 (250 bp), IL-4 (331 bp) and IL-13 (253 bp). Housekeeping gene, β-actin was included as the loading control (182bp). Samples were arranged as unstimulated Jurkat cells, IRF5v4 and IRF5v5 cells, followed by stimulated Jurkat, IRF5v4 and IRF5v5 cells, respectively. Three individual experiments were conducted, represented as set 1, 2 and 3.

Publication

Kaur A, Lee L-HL-H, Chow S-CS-C, Fang C-MC-M. IRF5-mediated immune responses and its implications in immunological disorders. Int Rev Immunol [Internet]. 2018 Jul 9; 37 (5): 1-20. Available from: https://www.tandfonline.com/doi/full/10.1080/08830185.2018.1469629

Kaur A, Fang C-M. An overview of the human immune system and the role of interferon regulatory factors (IRFs). Prog Microbes Mol Bio [Internet]. 2020 Nov 4. Available from: https://journals.hh-publisher.com/index.php/pmmb/article/view/338

Kaur A, Fang C-M. Generation of stably expressing IRF5 spliced isoform in Jurkat cells. Prog Microbes Mol Biol [Internet]. 2020 Nov 4. Available from: https://journals.hh-publisher.com/index.php/pmmb/article/view/337

Poster Presentation

ASHWINDER KAUR, CHENG- FOH LE, LEARN-HAN LEE, SEK-CHUEN CHOW, CHEE-MUN FANG. Role of Interferon Regulatory Factor 5 (IRF5) in the regulation of Interleukin (IL)-13, a key mediator of allergic asthma. International Conference on Biochemistry, Molecular Biology and Biotechnology.15&16 August 2018, Selangor, Malaysia. (Winner)